Cosmic rays: propagation in theory and practice

Andy Strong,

MPE Garching

Erice School on Cosmic Rays
August 1-7 2016

Lecture 1 : Basic ideas and context

Lecture 2: Practical computations and further topics

Two useful references

Strong, Moskalenko, Ptuskin: Annual Review of Nuclear and Particles Physics 57, 2007

Grenier, Black, Strong: Annual Review of Astronomy and Astrophysics, 53, 2015

Lecture 1

Cosmic-ray propagation: basic ideas and context

Orientation, context.

Cosmic-rays: roughly starting from kinetic energy = mass of electron i.e. MeV
(thermal gas: few Kelvin to keV energies)
Up to TeV and beyond (10^{21} eV)
Here cover only to TeV, focus on Galactic CR.

Species:
Nuclei: Z= +1 to >64 protons, Helium.... to Ni and beyond
Z= -1 antiprotons

Isotopes essential!
Primary CR: produced in sources
Secondary CR: produced by spallation on interstellar gas

Leptons: electrons, positrons (primary and secondary)

Related to magnetic fields, synchroton, gamma rays: *CR astronomy*

Basics: Units

Mass m
Kinetic energy T
Total energy E = T + m
Momentum p
Velocity/c β, β= p/E

Normally use eV, MeV, GeV etc (hence no c in formulae)

$$E^2 = p^2 + m^2$$

Momentum is fundamental quantity for propagation, although kinetic energy is more commonly used by experimenters. Diffusive shock acceleration gives power-law in p not T.

Flux I(T) $cm^{-2}\ sr^{-1}\ s^{-1}\ MeV^{-1}$ **most commonly used by experimenters**
Density n(p) cm^{-3} MeV^{-1} **is more physically appropriate for propagation**
[cf phase space also used e.g. shock acceleration, $p^2 n(p)$ **]**

I(T) = βc n(p) dp/dT / 4π **dp/dT = E/p =** $1/\beta$

$$n(p) = (4\pi/c)\ I(T)$$ **very convenient!**

NB T= K.E. ***per nucleon*** **usually**

Rigidity p/Ze controls propagation via

$$d\mathbf{p}/dt = Ze\ \mathbf{v} \times \mathbf{B}$$

Secondary production example:

C Z=6 A=12 → **B** Z=5 A=10,11

(Cross-section includes prompt decays e.g. 11C ->11B)

Partial cross-section e.g. $^{12}C \rightarrow {}^{11}B$ ~ few mb

Total destruction cross-section ~100 mb

(Cross-section plot)

Also $^{16}O \rightarrow {}^{11}B$ and heavier primaries contribute

Back-of-envelope estimate:

Cross-section ~ 30 mbarn = $30\ 10^{-27}$ cm^2

Gas density ~ 1 cm^{-3}

Time in Galaxy ~ 10^7 years = $3\ 10^{14}$ s

B/C = cross-section X gas density X c X time

$30\ 10^{-27}$ X 1 X $3\ 10^{10}$ X $3\ 10^{14}$

~ 0.3

Lucky! **C** is mainly primary (but significant destruction),
B is all secondary, and an informative ratio
is produced! (not too small, and not too large otherwise information would be lost).
Allows CR propagation to be probed.

Since we measure the actual C spectrum, *the source spectrum of B can be computed*
hence allowing a unique diagnostic of CR propagation as function of energy!

Primary source abundances depend on allowing for secondary production.

Cross-sections are major uncertainty (recent DRAGON paper using FLUKA)
Measured in lab + theoretical models to complete.

Radioactive CR and the propagation region.

^{10}Be decays to ^{10}B in 1.4 Myr, ^{9}Be is stable. Ratio sensitive to propagation time (halo size)
^{10}Be/^{9}Be ~ 0.1 hence time >> 1 Myr

CR residence time in Galaxy = 10^{7}-10^{8} years

Also ^{26}Al, ^{36}Cl, ^{54}Mn but shorter lifetime, harder to measure.
Pity that ^{10}Be data insufficient, need new experiments!
Relativistic lifetime increase → more sensitive to long times at higher energies

Leaky Box model (constant gas density) + "surviving decay fraction" gives misleading results:
time ~ 10^{6} yr too small

Random walk distance d ~ sqrt(Dt)
D~3 10^{28} cm^{2} s^{-1}
t=10^{8} yr d=sqrt(Dt) = 3 kpc: size of containment region, CR "halo boundary" z_h

B/C and ^{10}Be/^{9}Be determine D and z_h

Remark: K-capture isotopes generally stable in CR since stripped (e.g. ^{59}Ni, ^{57}Co, ^{56} Ni),
but possible probe of acceleration delay and reacceleration (^{51}V etc).

Cosmic-ray propagation

$$\partial \psi (\underline{r} , p) / \partial t = q (\underline{r} , p)$$

cosmic-ray sources (primary and secondary)

$$+ \nabla \cdot (D_{xx} \nabla \psi - v \psi)$$

diffusion convection

$$+ \partial / \partial p \; [p^2 D_{pp} \partial / \partial p \; \psi / p^2]$$

$D_{pp} D_{xx} \sim p^2 v_A^2$

diffusive reacceleration (diffusion in p)

$$- \partial / \partial p \; [d p / d t \; \psi - p / 3 \; (\nabla \cdot v) \; \psi]$$

momentum loss adiabatic momentum loss

ionization, bremsstrahlung

$- \psi / \tau_f$ nuclear fragmentation

$- \psi / \tau_r$ radioactive decay

Main propagation processes

Spatial Diffusion

Convection

Diffusive Reacceleration

NB the equation is linear (easy!) but reality is non-linear e.g.

Streaming instability
CR-driven winds

Spatial Diffusion

Random walk along B-field lines.
Caused by pitch-angle scattering relative to field lines.
Resonant with MHD waves of interstellar turbulence.
$D_{xx} \sim (1/3)\, \lambda^2/\tau = (1/3)\, \lambda\, v = (1/3)\, v^2\, \tau$ λ=mean-free-path τ = time between scatterings

Larmor radius $r_g = pc/ZeB \sim$ A.U. at **1 GeV** for B~μG i.e. tiny cf parsec-scales of Galaxy
v=c, λ=A.U. $\sim 10^{13}$ cm $D_{xx} \sim 10^{23}$ cm^2 s^{-1} Bohm diffusion
$\lambda = 1$ pc $= 3\ 10^{18}$ cm $D_{xx} \sim 10^{28}$ cm^2 s^{-1} from secondary/primary ratios
r_g=100 pc @ 10^{15} eV, change from diffusion to trajectories in B-field
(unified model for both cases desirable but not yet done)

"Quasi-linear theory (QLT)" predicts diffusive transport
$D_{xx} = (\delta B_{res}/B)^{-2}\, v\, r_g/3$
$k_{res} = 1/r_g$ $\omega(k) \sim k^{-2+a}$, a ~1/3 – 1/2 (Kolmogorov, Kraichnan turbulence) 10^8-10^{20} cm

$$D(p) \sim \beta\, p^{\delta}$$

β because speed determines distance, random walk refers to number of steps.
Velocity-dependence Important at non-relativistic energies.

Spatial Diffusion

Random walk along B-field lines.
Caused by pitch-angle scattering relative to field lines.
Resonant with MHD waves of interstellar turbulence.
$D_{xx} \sim (1/3)\, \lambda^2/\tau = (1/3)\, \lambda\, v = (1/3)\, v^2\, \tau$ λ=mean-free-path τ = time between scatterings

"Quasi-linear theory (QLT)" predicts diffusive transport
$D_{xx} = (\delta B_{res}/B)^{-2}\, v\, r_g/3$
$k_{res}=1/r_g$ $\omega(k)\sim k^{-2+\delta}$, $\delta \sim 1/3 - 1/2$ (Kolmogorov, Kraichnan turbulence) 10^8-10^{20} cm

$$D_{xx}(p) \sim \beta\, p^{\delta}$$

β because speed determines distance, random walk refers to number of steps.
Important at non-relativistic energies.

Anisotropic – diffusion tensor, parallel and perpendicular to B-field $D_{perp} << D_{par}$
$D_{perp} \sim D_{par}/10$ from numerical simulations. But usually assume isotropic.

Propagation term $\partial\psi/\partial t = \nabla \cdot (D_{xx} \nabla\psi)$ (ψ = CR density)

B/C demonstrates increase of D with p

Affects primary spectra: propagated spectrum steeper by δ relative to injection

Spatial Diffusion

General approach – direct numerical integration of particle trajectories in turbulent **B** with wave spectrum.
Jokipii, Giacalone, Schalchi … (solar wind)

Confirms diffusive nature of propagation
Studies of e.g. cross-field diffusion.
Active topic.

THE ASTROPHYSICAL JOURNAL, 520:204–214, 1999 July 20

THE TRANSPORT OF COSMIC RAYS ACROSS A TURBULENT MAGNETIC FIELD

J. GIACALONE AND J. R. JOKIPII[1]

We present a new analysis of the transport of cosmic rays in a turbulent magnetic field that varies in all three spatial dimensions. The analysis utilizes a numerical simulation that integrates the trajectories of an ensemble of test particles from which we obtain diffusion coefficients based on the particle motions.

The trajectories of the cosmic rays are computed by numerically integrating the Lorentz force on each particle given by

$$\frac{d\boldsymbol{v}}{dt} = \frac{q}{mc}\,\boldsymbol{v}\times\boldsymbol{B}\,, \qquad (9)$$

Book: Nonlinear Cosmic Ray Diffusion Theories, Andreas Shalchi (Uni. Bochum), Springer, 2009

Global diffusion of cosmic rays in random magnetic fields

A. P. Snodin,[1,2] ⋆ A. Shukurov,[3] G. R. Sarson,[3] P. J. Bushby[3] and L. F. S. Rodrigues[3]

MNRAS 457, 3975 (2016)

Galactic propagation

$$\kappa_{xx}(t) = \frac{1}{2}\frac{\mathrm{d}}{\mathrm{d}t}\langle(\Delta x)^2\rangle = \langle v_x(t)\Delta x\rangle$$

The fit has a non-zero intercept,

$$\kappa_0|_{R_\mathrm{L}\to 0} \approx 3\times 10^{-3} v_0 L\,, \qquad (21)$$

corresponding to a part of the diffusivity independent of the Larmor radius (i.e., the particle energy). For $v_0 = c$, and $L \simeq 100$ pc for the outer turbulent scale, we obtain $\kappa_0 \simeq 3\times 10^{28}$ cm^2 s^{-1}. We

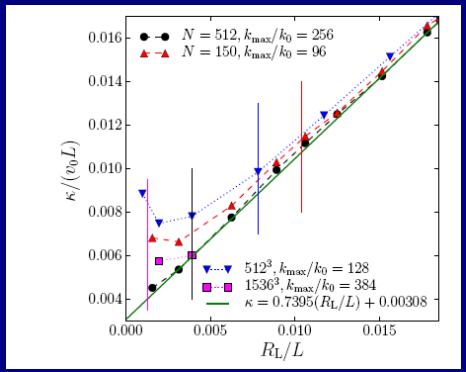

Diffusive Reacceleration

If diffusion occurs in the ISM and particles gain or lose momentum on moving scatterers then some diffusion in momentum is inevitable.

Thornbury & Drury MNRAS 442 3010 (2014)
Simple derivation of diffusion coefficient in momentum D_{pp}

$D_{xx} \sim (1/3)\ \lambda^2/\tau = (1/3)\ \lambda\ v = (1/3)\ v^2\ \tau$ λ=mean-free-path τ = time between scatterings

At each scattering the particle undergoes momentum change

$\Delta p \sim V_A / v$ (taking V_A as typical of speed of scatterers)

$D_{pp} \sim (1/3)\ (\Delta p)^2/\tau = (1/3)\ p^2\ V_A^{\ 2} / (v^2\ \tau)$

Hence

$$\mathbf{D_{xx}\, D_{pp} \sim (1/9)\ p^2 V_A^{\ 2}}$$

More precise calculations: depends on turbulence spectral index δ, factor is

$1 / [\delta(4-\delta)(4-\delta^2)]$ ($=1/9$ for $\delta=1$, 0.2 for Kolmogorov $\delta=1/3$)

Term in propagation equation $\mathbf{\partial\psi/\partial t =}\ \partial/\partial p\ [p^{-2} D_{pp}\ \partial/\partial p\ (\psi / p^{-2})]$

Reacceleration is a popular explanation of peak in B/C without ad-hoc break in D_{xx}

Compatible with Kolmogorov diffusion, helps with anisotropy.

But does it really occur?

Large energy transfer from ISM to CR, is that physical?

For $V_A \sim 30$ km s^{-1} (to explain B/C)

~30% of energy at GeV comes from reacceleration! Drury& Strong 2015 *arXiv:1508.02675*

If so then CR not just from SNR but from ISM!

Convection

Galactic wind – observational fact e.g. from X-ray observations

Convection velocity $v_c = 10 – 100$ km s^{-1}

Momentum-independent transport, hence dominates at small p where diffusion is small. Typically below 1 GeV.

Also adiabatic energy losses: if v_c increases with z, relativistic gas expands, $\gamma = 4/3$

Terms in propagation equation

$$\partial\psi/\partial t = \nabla \cdot (v_c \psi) + \partial/\partial p \; [\, p/3 \; (\nabla \cdot v_c) \, \psi \;]$$

Physical wind models are available, including CR-driven winds.

CR Streaming

Convection at Alfven speed

Self-generated waves: streaming instability

See e.g. D'Angelo, Blasi & Amato 2016 arXiv:1512.05000

Highly non-linear

Requires CR gradient, hence mainly important near CR sources

$$D(p,z,t) = \frac{1}{3} r_L(p) v(p) \frac{1}{\mathcal{F}(k,z,t)}\bigg|_{k=1/r_L(p)}, \qquad (3)$$

where the spectrum of the self-generated waves $\mathcal{F}(k,z,t)$ satisfies the differential equation:

$$\frac{\partial \mathcal{F}}{\partial t} + v_A \frac{\partial \mathcal{F}}{\partial z} = (\Gamma_{CR} - \Gamma_D)\mathcal{F} \ . \qquad (4)$$

In the latter equation, damping rate $\Gamma_D = \Gamma_{IN} + \Gamma_{NL}$ contains both the effects of ion-neutral damping (IND) at rate Γ_{IN} [15] and non-linear Landau damping (NLLD) [16]. For the

$$\Gamma_{\rm CR}(k) = \frac{16\pi^2}{3} \frac{v_{\rm A}}{\mathcal{F} B_0^2} \left[p^4 v(p) \frac{\partial f}{\partial z} \right]_{p=qB_0/kc} \qquad (5)$$

is the growth rate of the resonant streaming instability associated with CRs moving at superalfvènic speed [13],

CR Streaming

Not included in most CR-propagation models but exceptions:
Ptuskin etal DRD model with self-consistent treatment of self-generated waves

CR Interactions

Energy losses

Nuclei	medium		
ionization/Coulomb	gas	< 1 GeV	
Inelastic – pion-production	gas	> 1 GeV, small effect	

Electrons + positrons			dE/dt ~
Ionization	gas	< 1 GeV	const
Bremsstrahlung	gas	< 1 GeV	E
Synchrotron	B-field	> 1 GeV	E^2
Inverse Compton	ISRF	> 1 GeV	E^2

Spallation : total = loss of particle
partial = gain secondary particle
Assume that energy/nucleon is conserved: approximation!
Better treatments are coming (Mazziota, FLUKA) MC cascade with physics
More on this.
Secondary, tertiary protons.

Radioactive decay: ^{10}Be, ^{26}Al, ^{36}Cl, ^{54}Mn timescale Myr
^{10}Be->^{10}B source of ^{10}B

Production of secondary particles and nuclei in cosmic rays collisions with the interstellar gas using the FLUKA code

M. N. Mazziotta[a,*], F. Cerutti[b], A. Ferrari[b], D. Gaggero[c,d,1], F. Loparco[a,e], P. R. Sala[f]

[a]Istituto Nazionale di Fisica Nucleare, Sezione di Bari, 70126 Bari, Italy
[b]CERN, Geneva, Switzerland
[c]SISSA, via Bonomea 265, 34136 Trieste, Italy
[d]INFN, Sezione di Trieste, via Valerio 2, 34127 Trieste, Italy
[e]Dipartimento di Fisica "M. Merlin" dell'Università e del Politecnico di Bari, I-70126 Bari, Italy
[f]Istituto Nazionale di Fisica Nucleare, Sezione di Milano, 20133 Milano, Italy

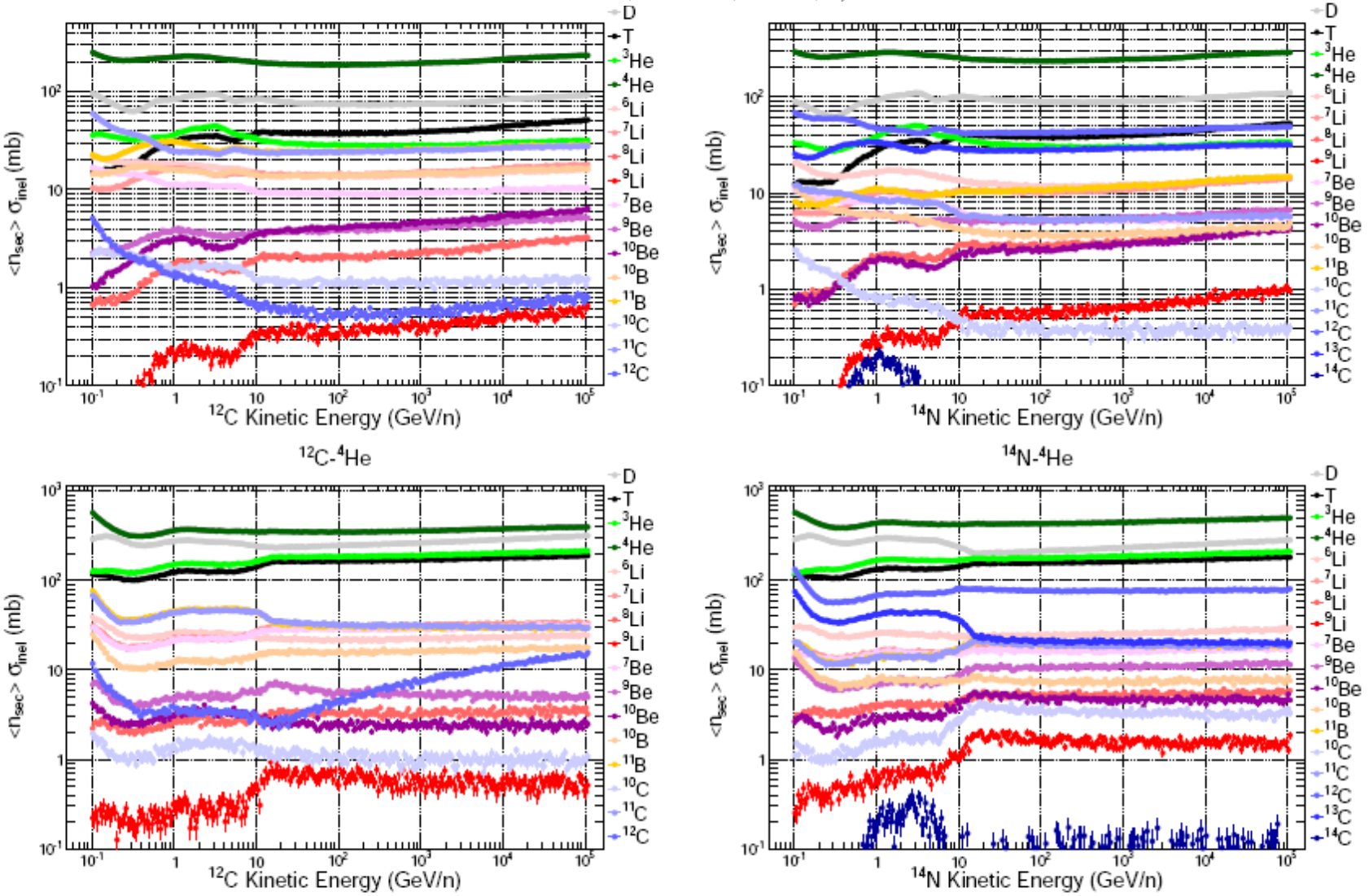

Figure 7: Inclusive cross sections for the production of spallation nuclei in collisions of ^{12}C and ^{14}N with p and ^{4}He nuclei. The plots show the cross sections for the production of Deuteron (gray markers), Triton (black markers) and for the isotopes of He (^{3}He and ^{4}He, green markers), Li (^{6}Li, ^{7}Li, ^{8}Li and ^{9}Li, red markers), Be (^{7}Be and ^{9}Be, magenta markers), B (^{10}B and ^{11}B, orange markers) and C (^{10}C, ^{11}C, ^{12}C, ^{13}C and ^{14}C, blue markers). Lighter (darker) color shades correspond to lighter (heavier) isotopes.

Anisotropy

Small, order 10^{-3} up to 10^{14} eV

CR isotropized by scattering

$\delta \sim 3 D (\text{grad } f) / f$

$D \sim p^{0.5}$ (from simple B/C) leads to larger δ than observed at high energies

$D \sim p^{1/3}$ (Kolmogorov) helps to resolve the problem, hence preference for reacceleration models with this index

But the formula for δ is too simple, in reality depends on local sources, Galactic structure etc.

So much for theory
Now some examples

Source abundances corrected for propagation

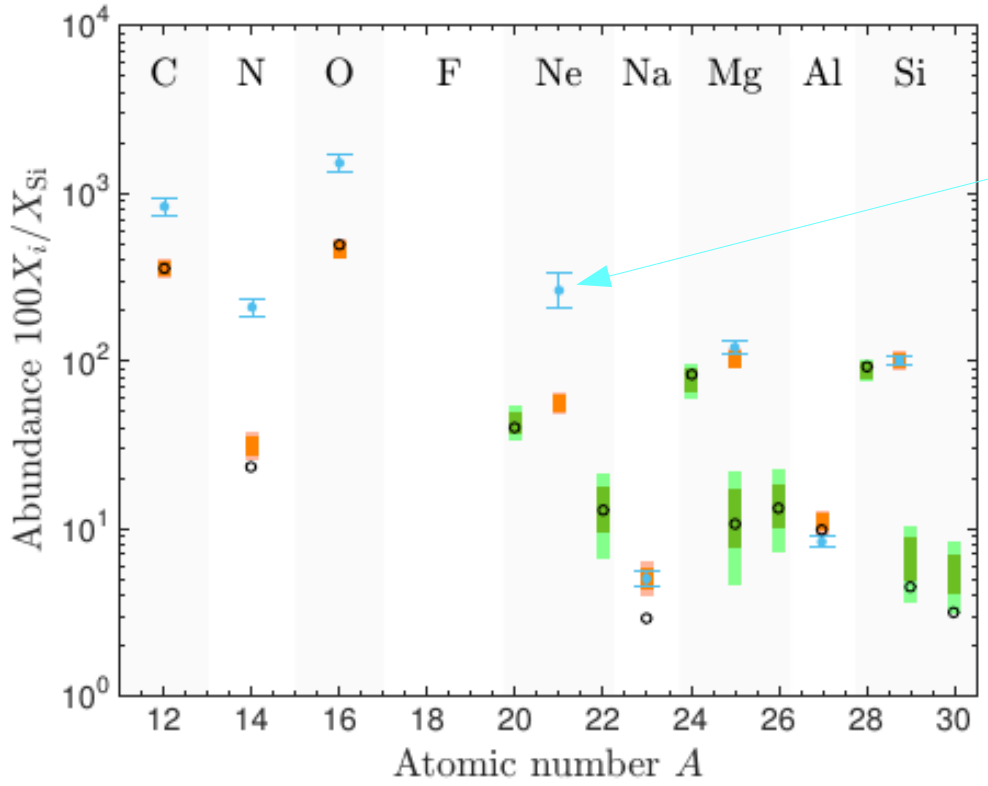

Photospheric abundances

FIG. 2.— 95% (light bars) and 68% (dark bars) posterior intervals from our final abundance study. Total elemental abundances are in orange, while individual isotopes are in green. We show the latest determination of the solar photospheric (blue dots) elemental abundances and errors from Asplund et al. (2009), with updated heavier (A $\geq$ 23) elemental abundances from Scott et al. (2015). We also show previously-used values from GALPROP (Moskalenko et al. 2008) with open black circles.

Johannesson etal 2016: Bayesian analysis

Source abundances corrected for propagation

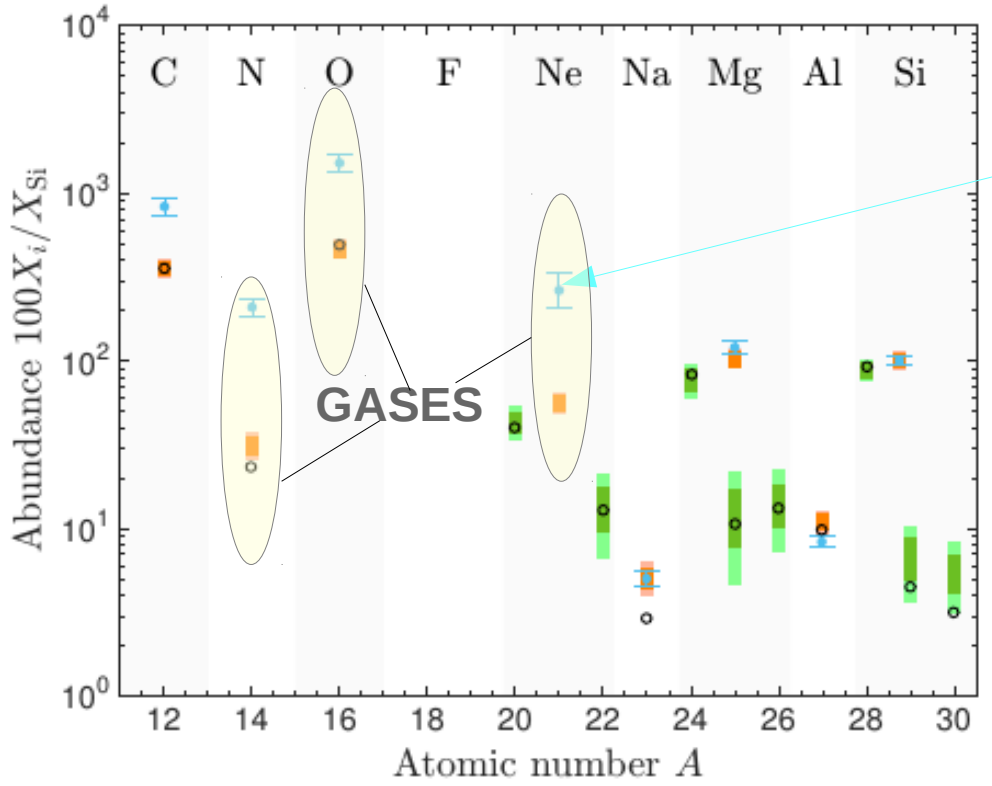

Photospheric abundances

FIG. 2.— 95% (light bars) and 68% (dark bars) posterior intervals from our final abundance study. Total elemental abundances are in orange, while individual isotopes are in green. We show the latest determination of the solar photospheric (blue dots) elemental abundances and errors from Asplund et al. (2009), with updated heavier (A $\geq$ 23) elemental abundances from Scott et al. (2015). We also show previously-used values from GALPROP (Moskalenko et al. 2008) with open black circles.

Johannesson etal 2016: Bayesian analysis
Well-known volatile/refractory (or FIP) trend. e.g. acceleration of grains.

AMS results on the fluxes of elementary particles

Stefan Schael
Gamma2016, Heidelberg

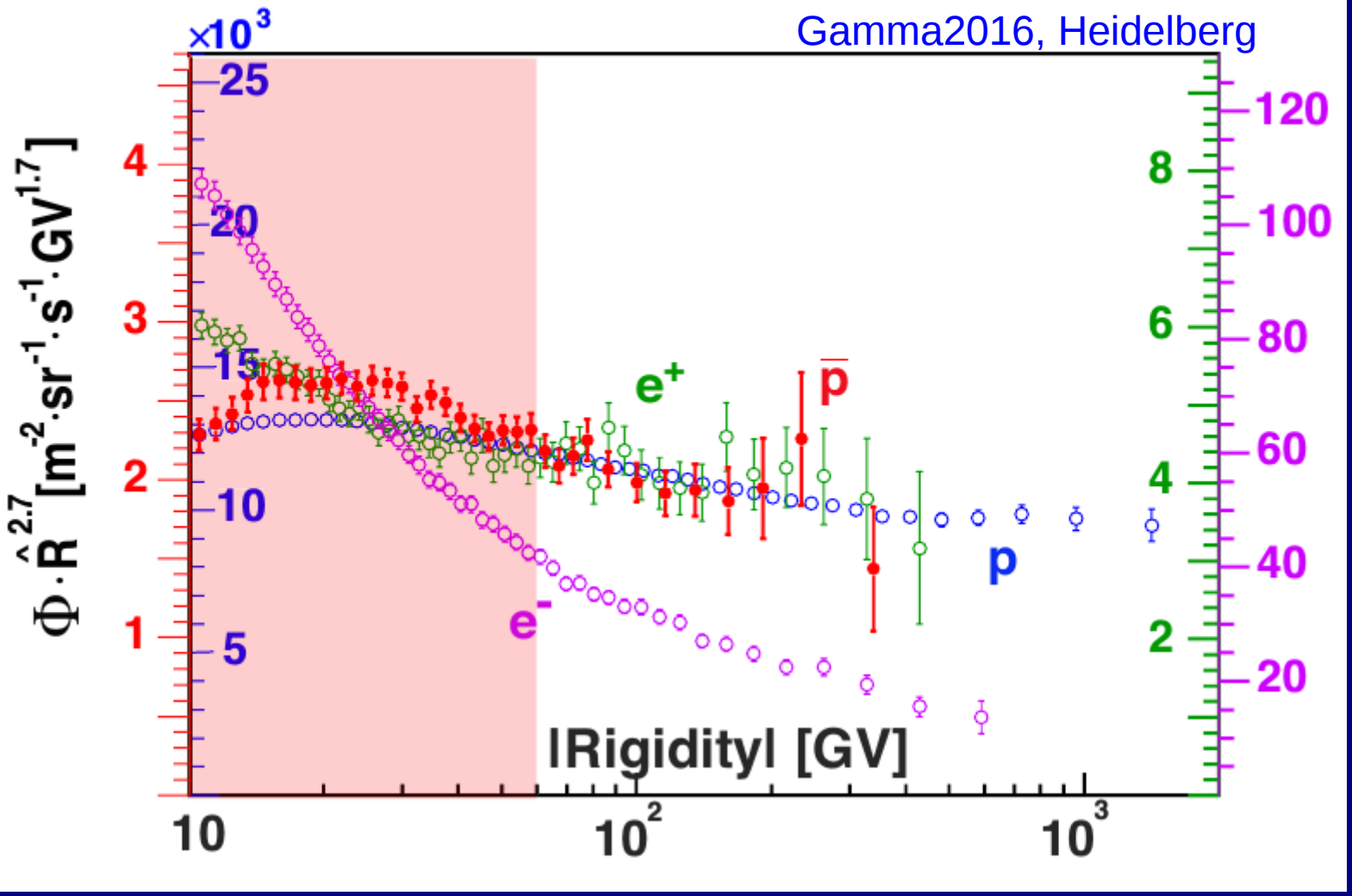

Fit Solar Modulation Potential:
Fit AMS Proton data with model from AMS Hawaii group

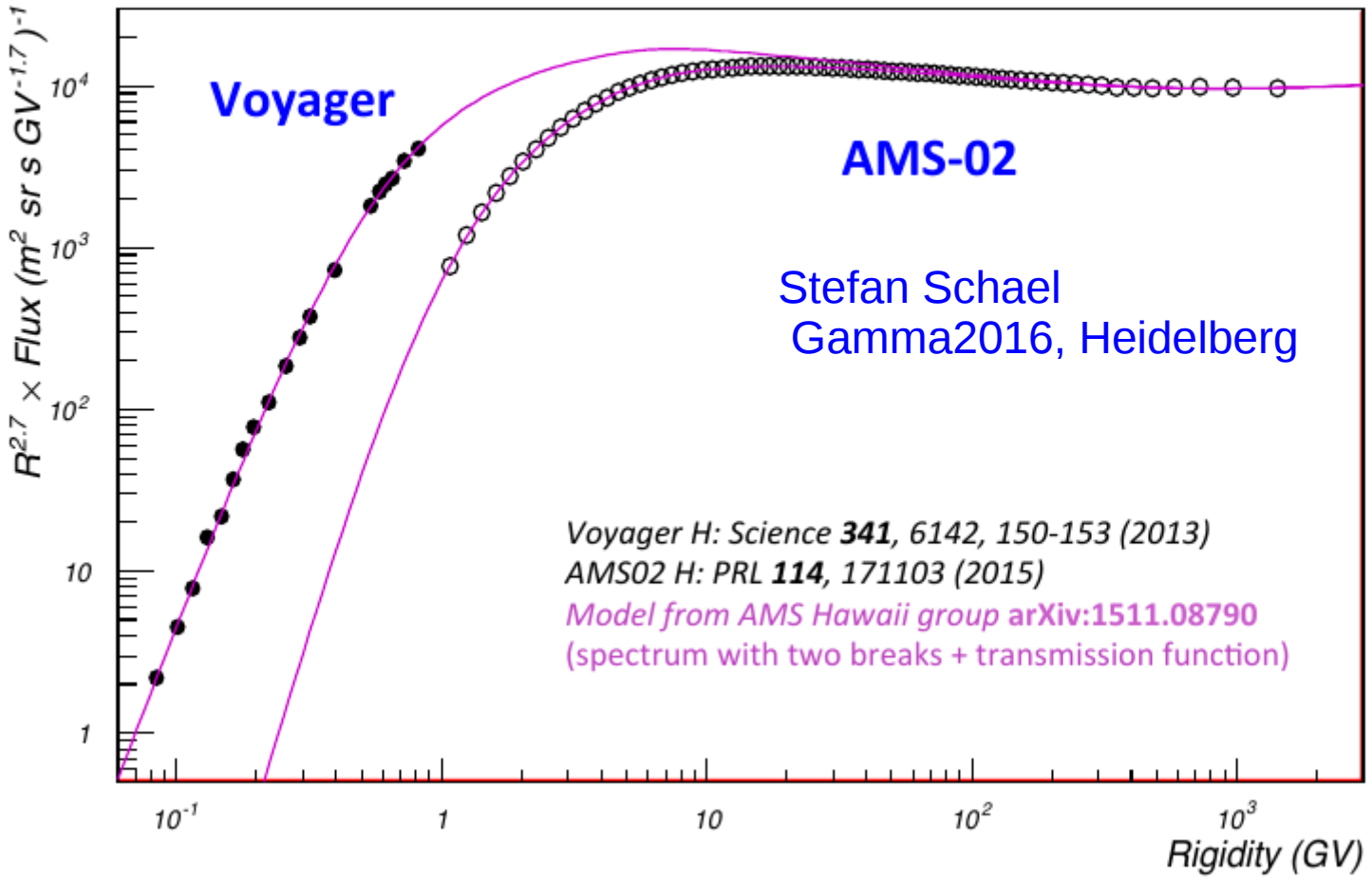

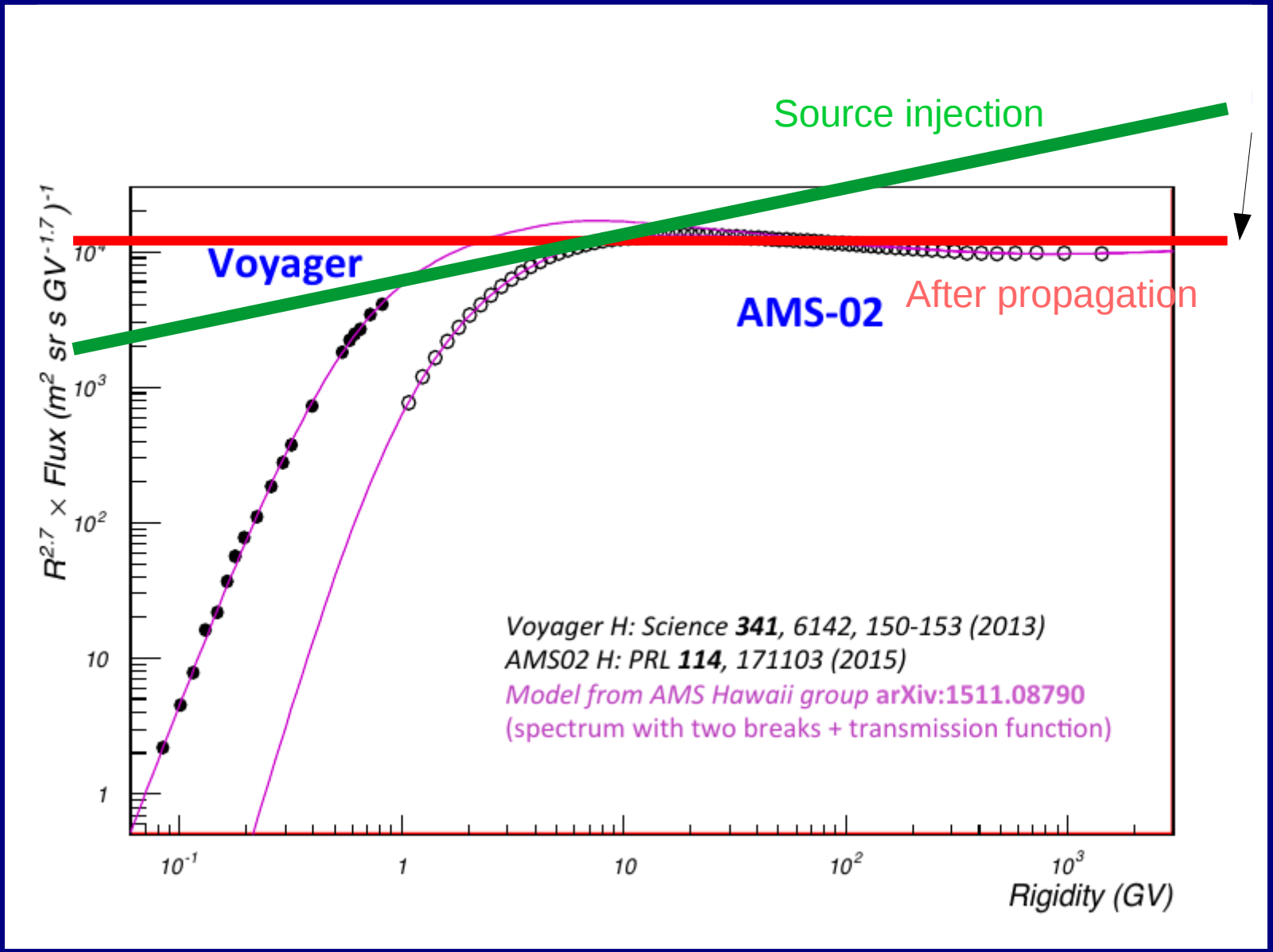

Sketch of effect of propagation on protons: injection index 2.3, propagated 2.8

Cosmic-ray secondary/primary ratios: e.g. Boron/Carbon probes *cosmic-ray propagation*

Boron / Carbon

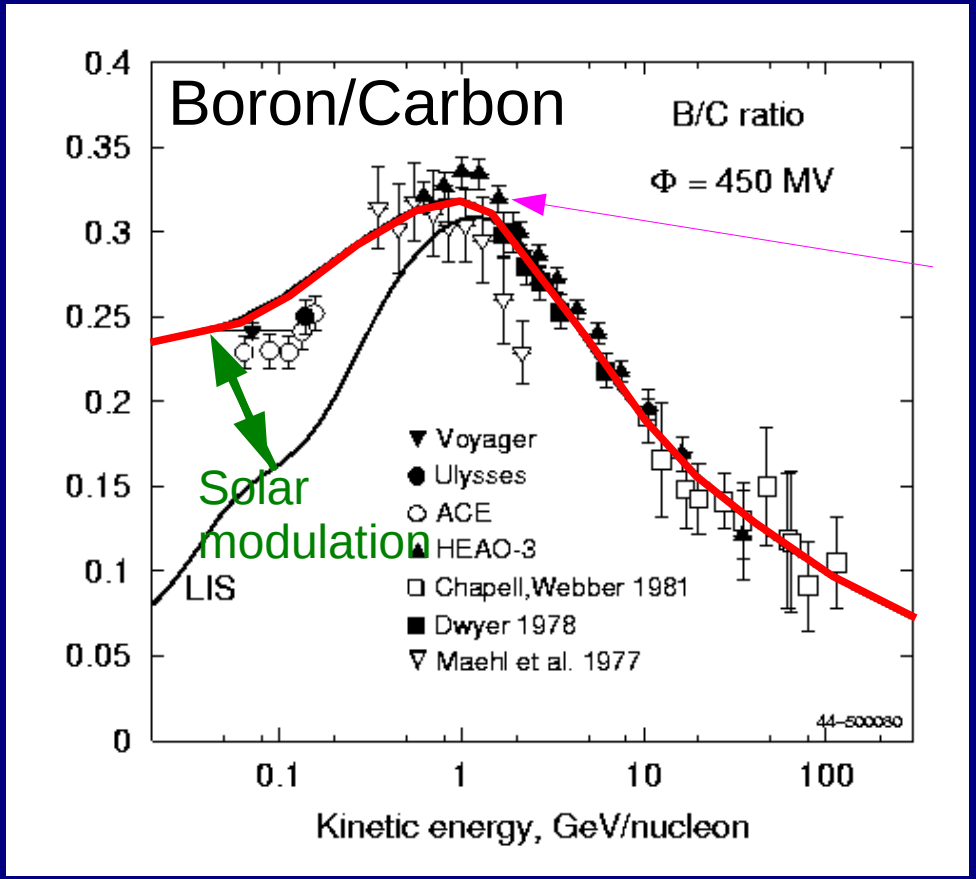

Peak in Boron/Carbon could be explained by **diffusive reacceleration** with Kolmogorov spectrum giving momentum-dependence of diffusion coefficient

Spatial diffusion

$D_{xx} \sim p^{1/3}$

Momentum space diffusion

$D_{pp} \sim 1 / D_{xx}$

However reacceleration not proven, maybe does not happen

→ 'pure diffusion' model: $D_{xx}(p) \sim p^{0.5}$, constant < 3 GeV.

Cosmic-ray secondary/primary ratios: e.g. Boron/Carbon probes *cosmic-ray propagation*

Boron / Carbon

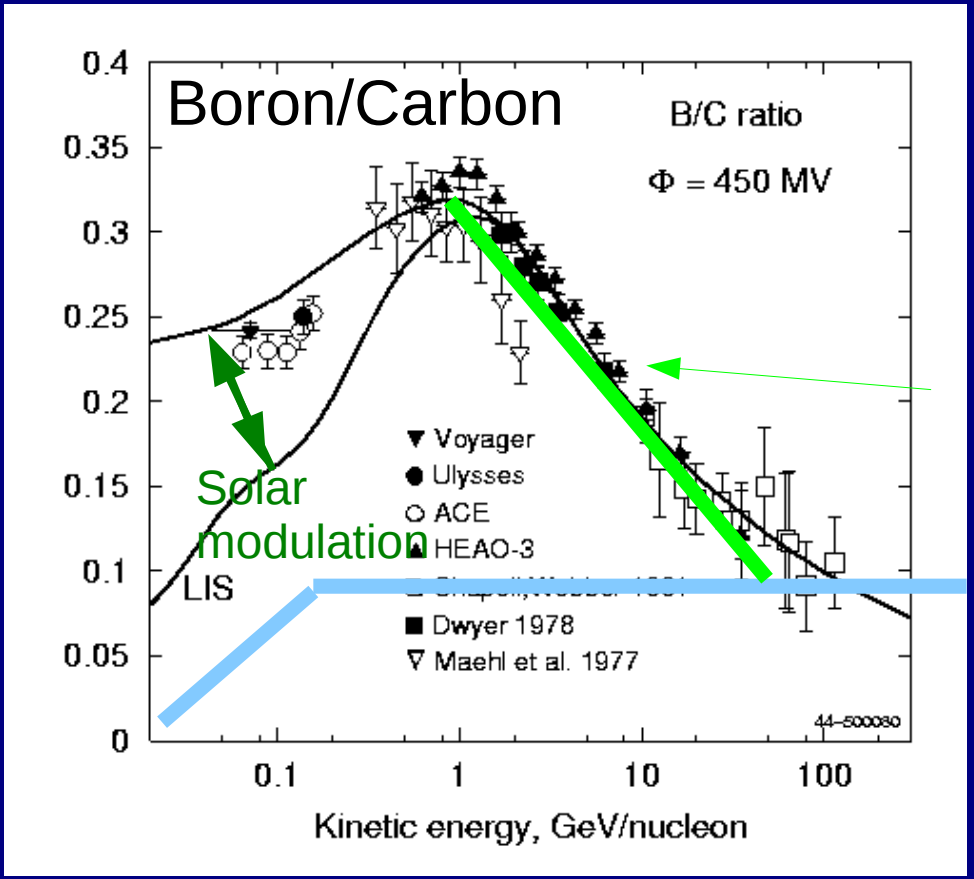

Peak in Boron/Carbon could also be explained by convection and decreasing velocity of particles

Spatial diffusion

$D_{xx} \sim p^{½} \rightarrow B/C \sim p^{-1/2}$

Convection B/C ~ const * v

Cosmic-ray secondary/primary ratios: e.g. Boron/Carbon probes *cosmic-ray propagation*

Boron / Carbon

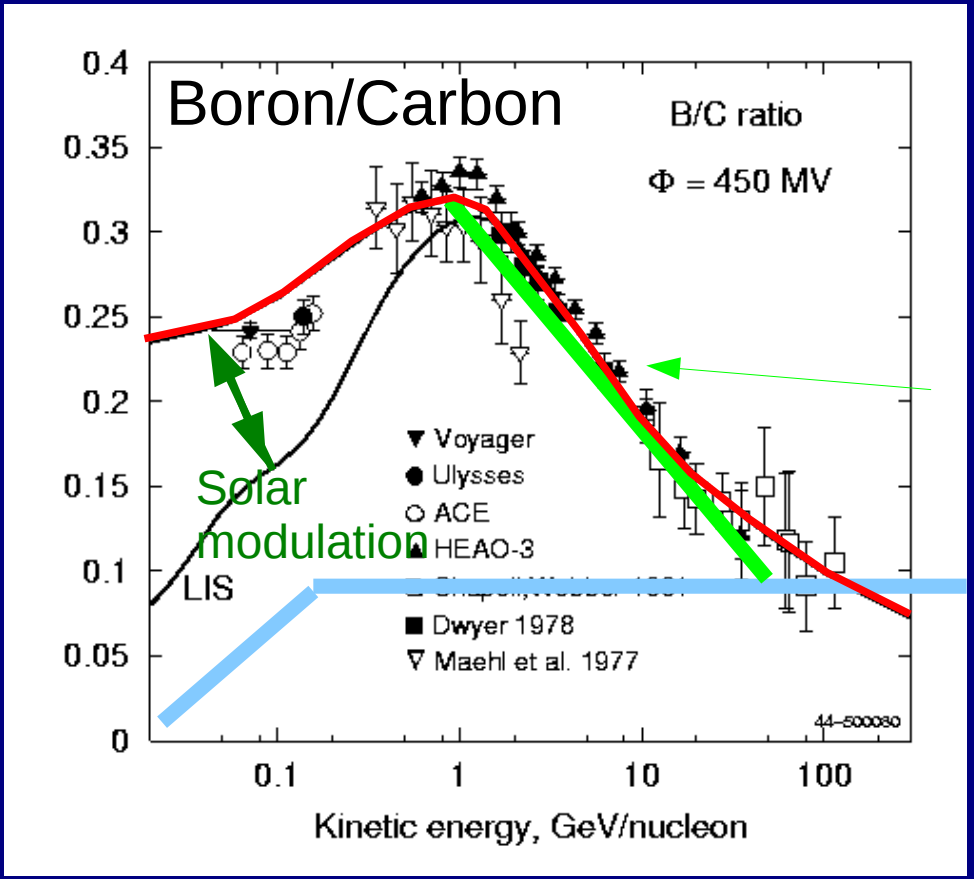

Peak in Boron/Carbon could also be explained by convection and decreasing velocity of particles

Spatial diffusion

$D_{xx} \sim p^{½} \rightarrow B/C \sim p^{-1/2}$

Convection B/C ~ const * v

B/C Ratio

Stefan Schael
Gamma2016, Heidelberg

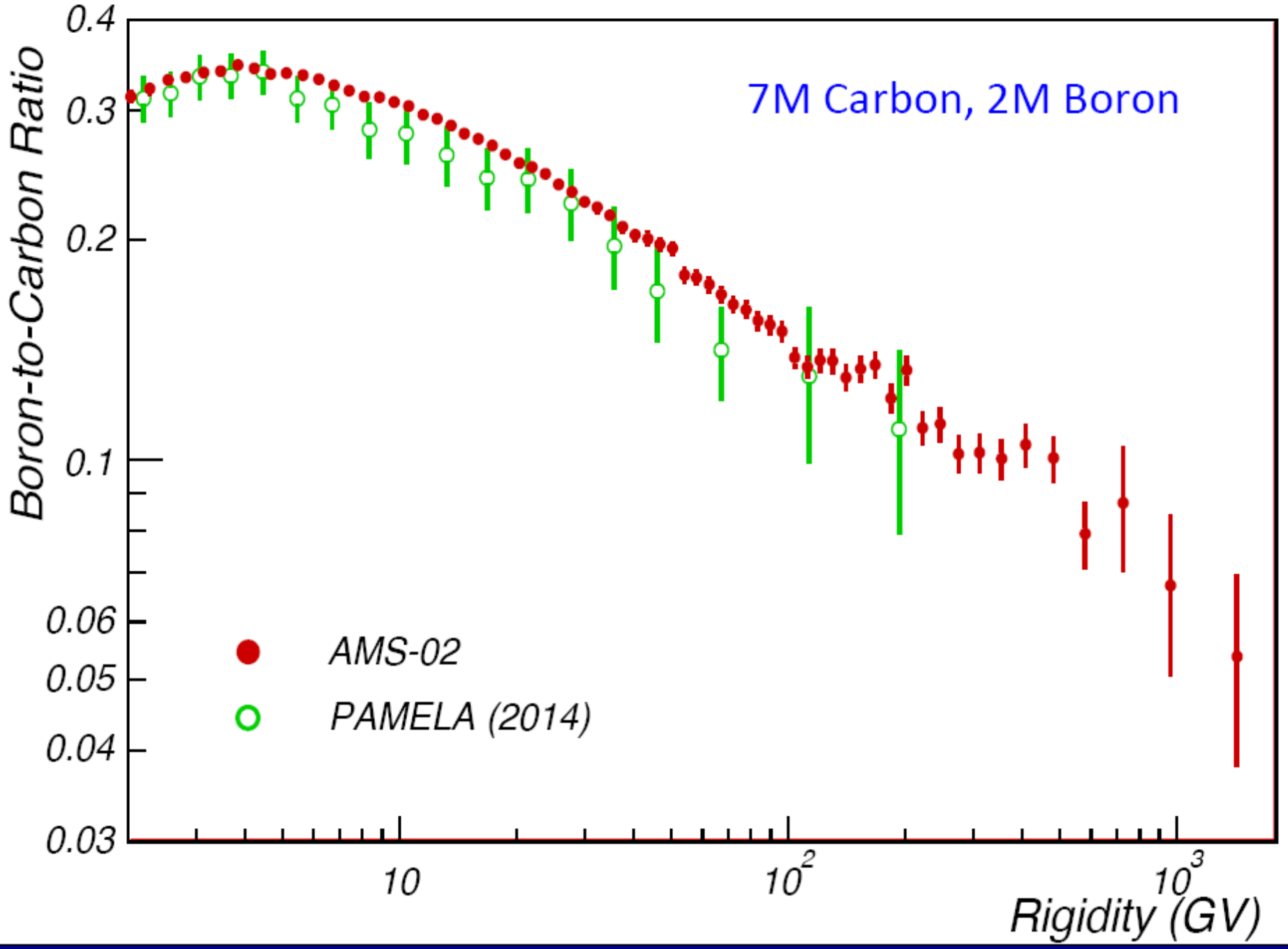

be

B/C Ratio

Stefan Schael
Gamma2016, Heidelberg

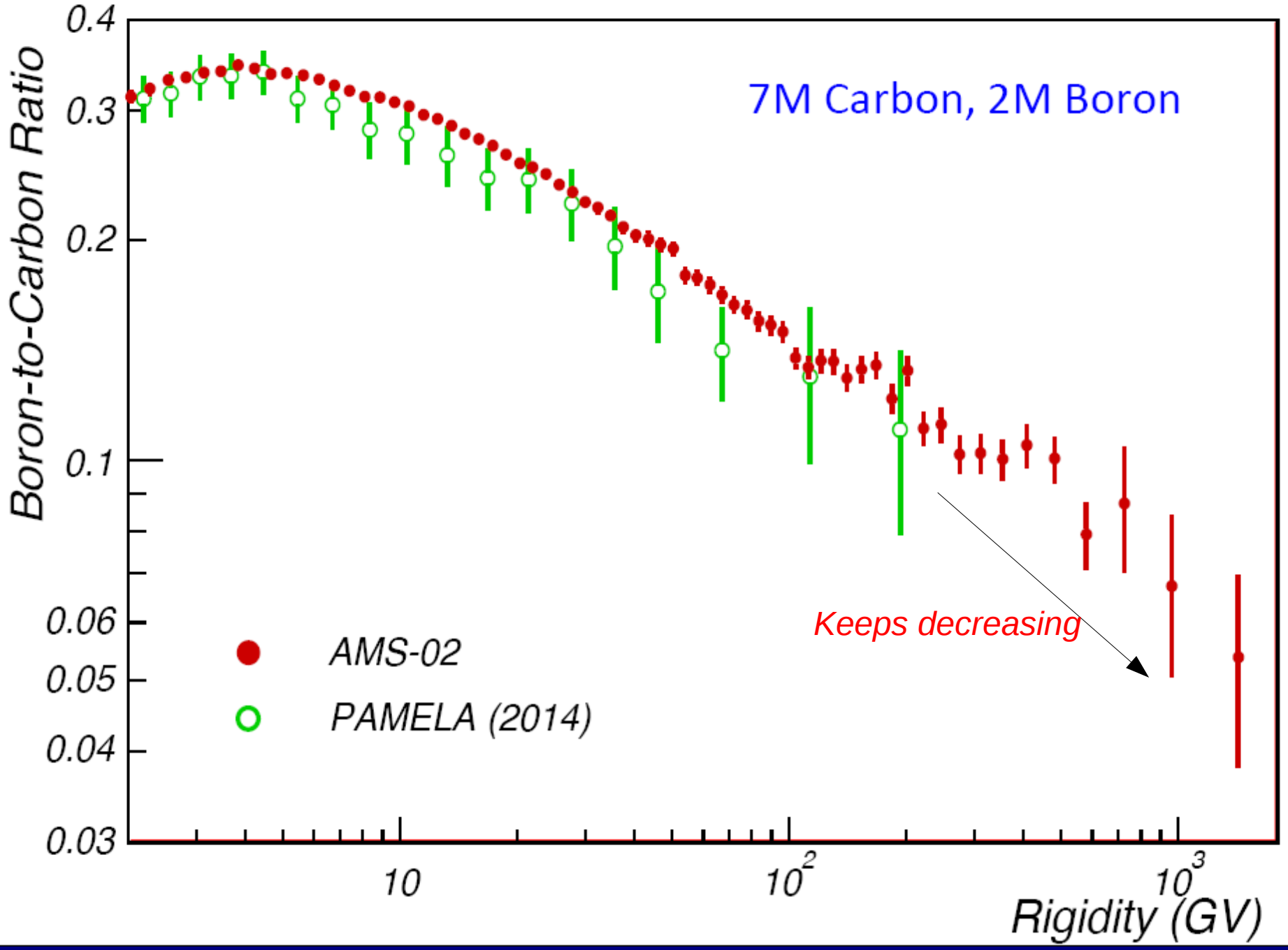

B/C Ratio converted in Kinetic Energy

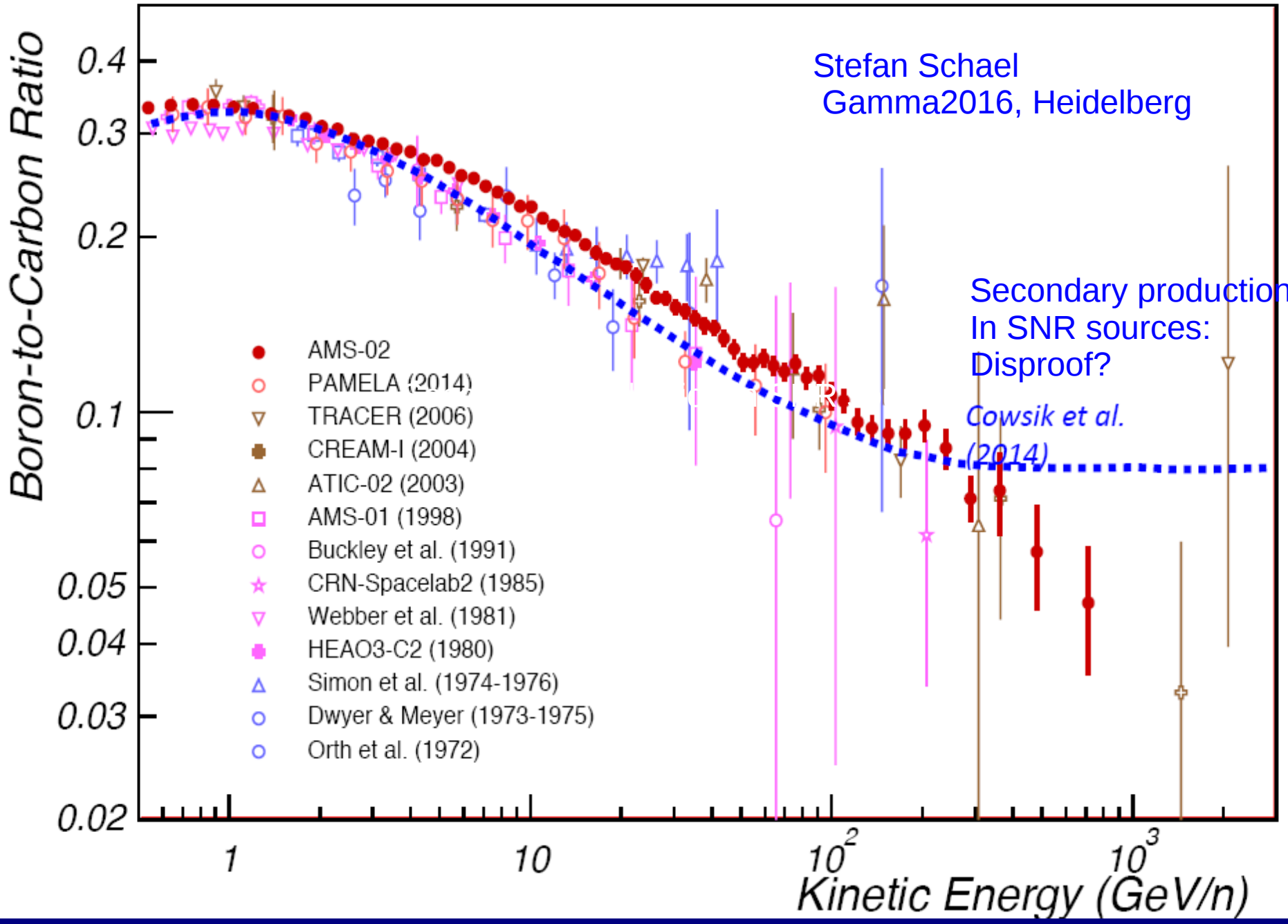

Cosmic-ray secondary/primary ratios: e.g. Boron/Carbon probes *cosmic-ray propagation*

Boron / Carbon

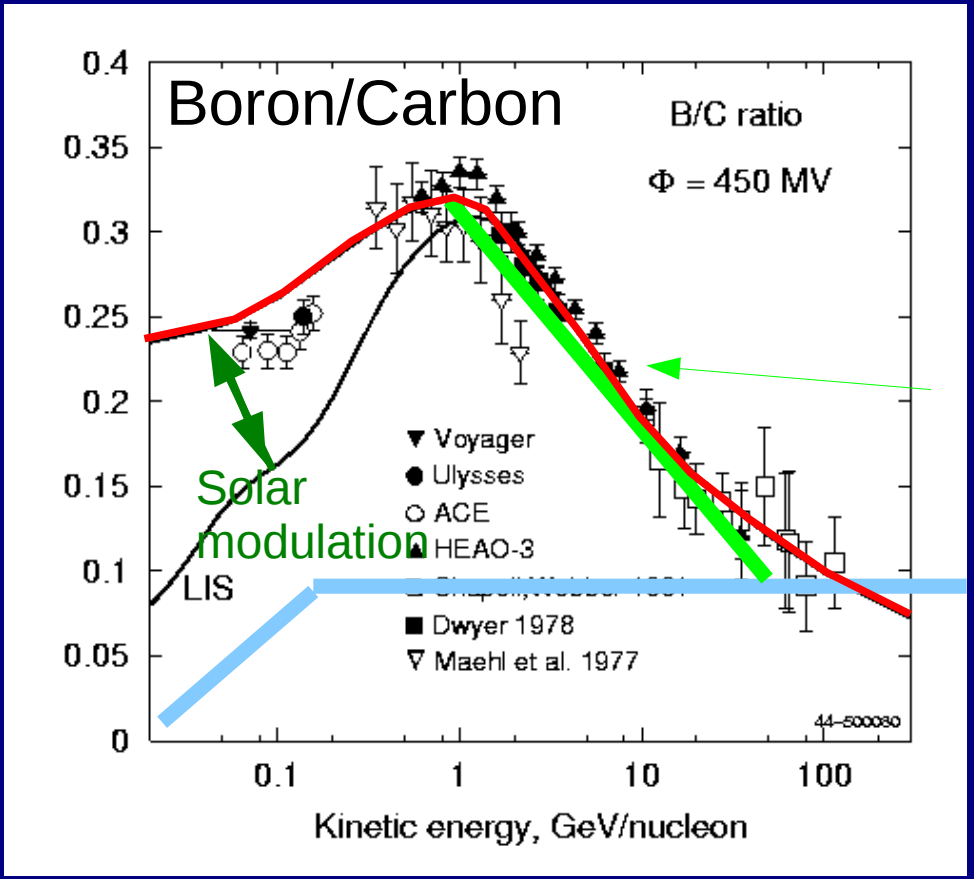

Convection B/C ~ const * v

Keeps decreasing

plain diffusion

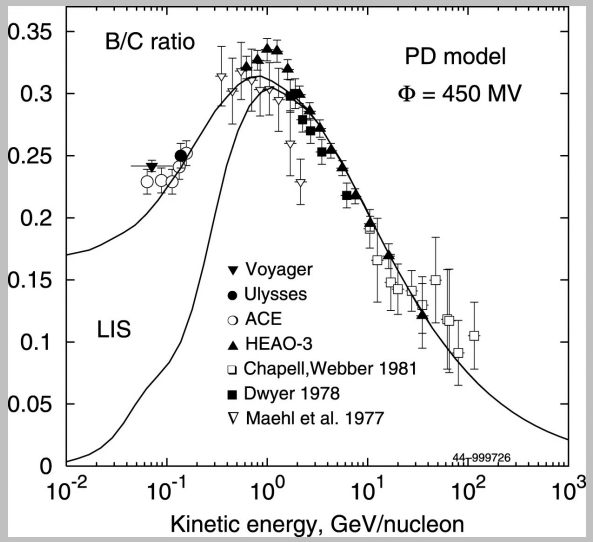

diffusive reacceleration

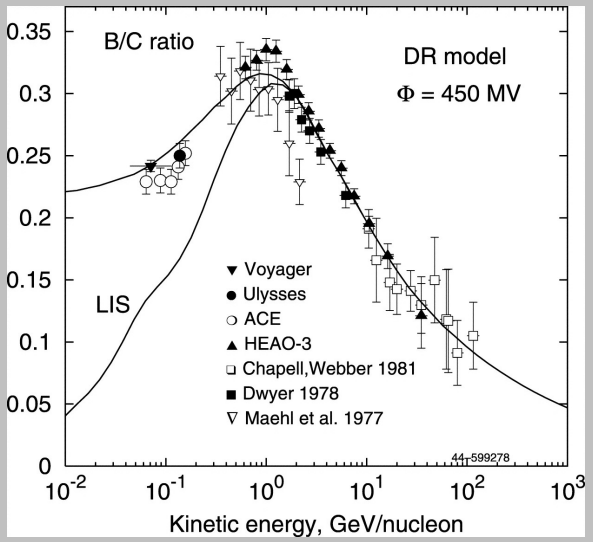

wave damping

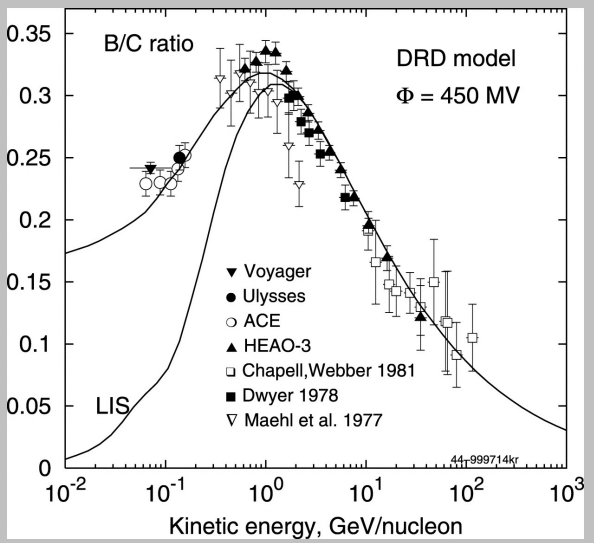

For any model, first adjust parameters to fit Boron/Carbon

Ptuskin et al. 2006 ApJ 642, 902

plain diffusion

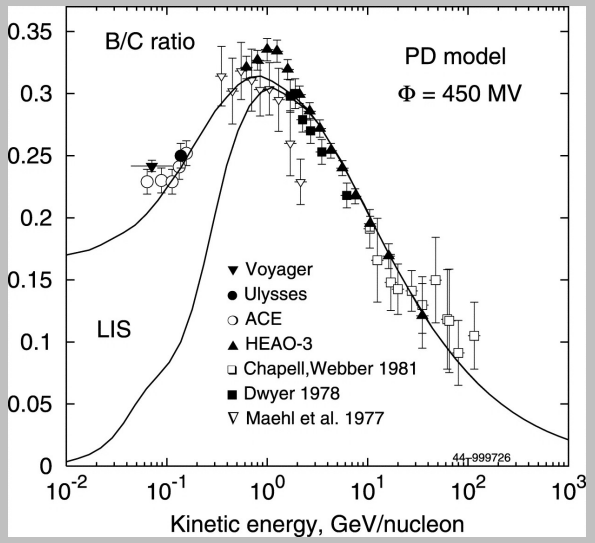

diffusive reacceleration

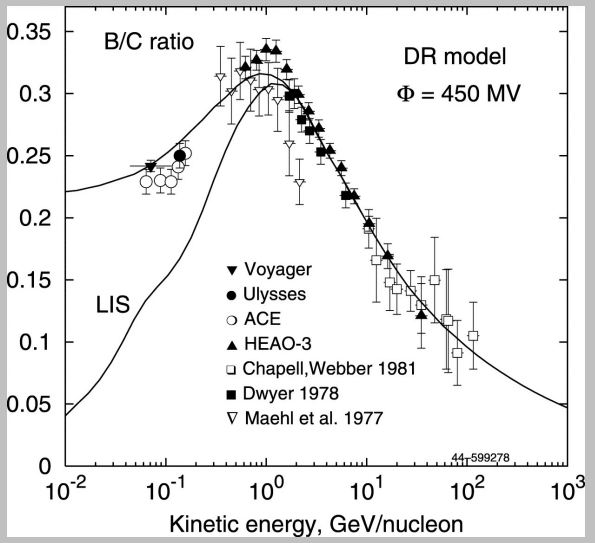

wave damping

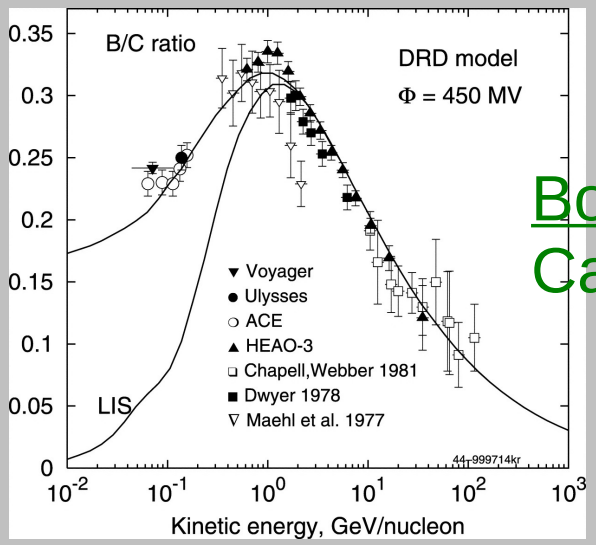

Boron/ Carbon

then predict the other cosmic-ray spectra

antiprotons

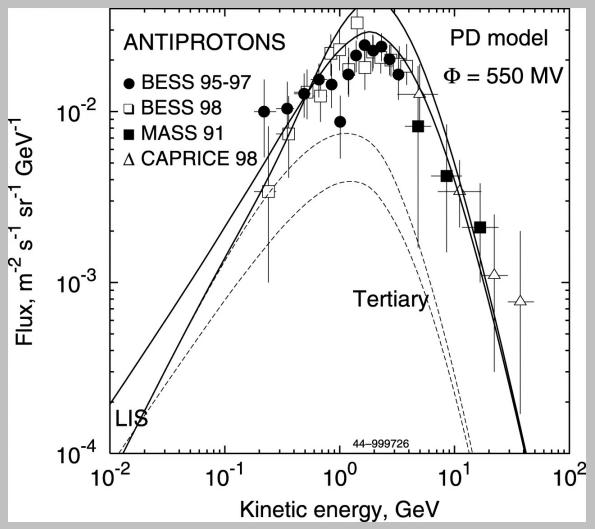

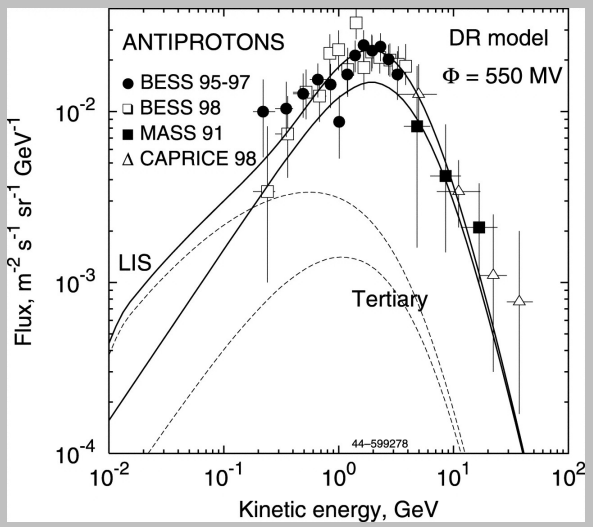

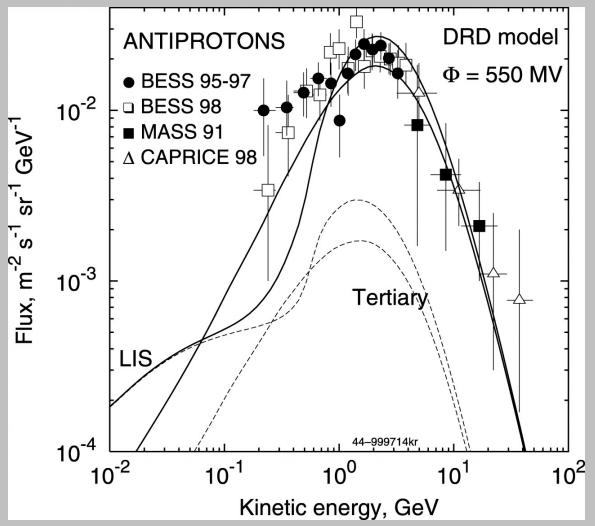

Ptuskin et al. 2006 ApJ 642, 902

plain diffusion

diffusive reacceleration

wave damping

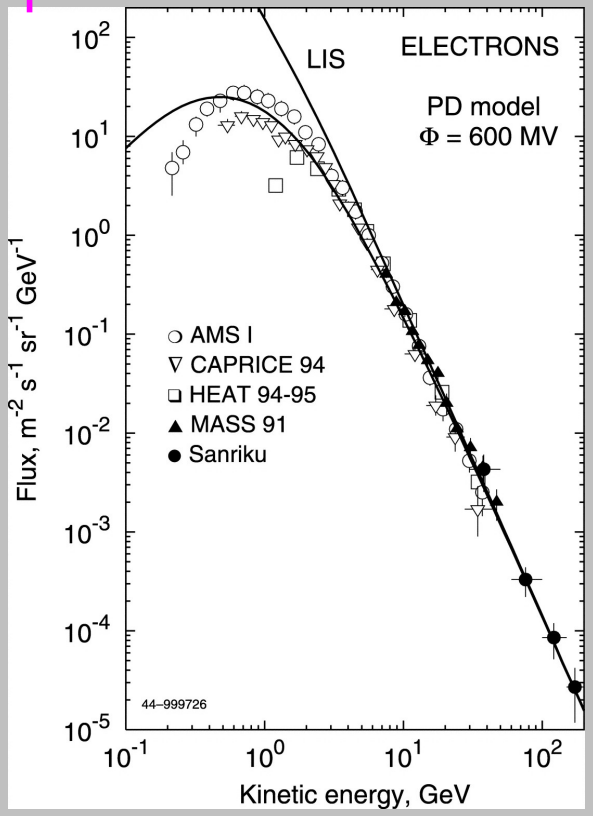

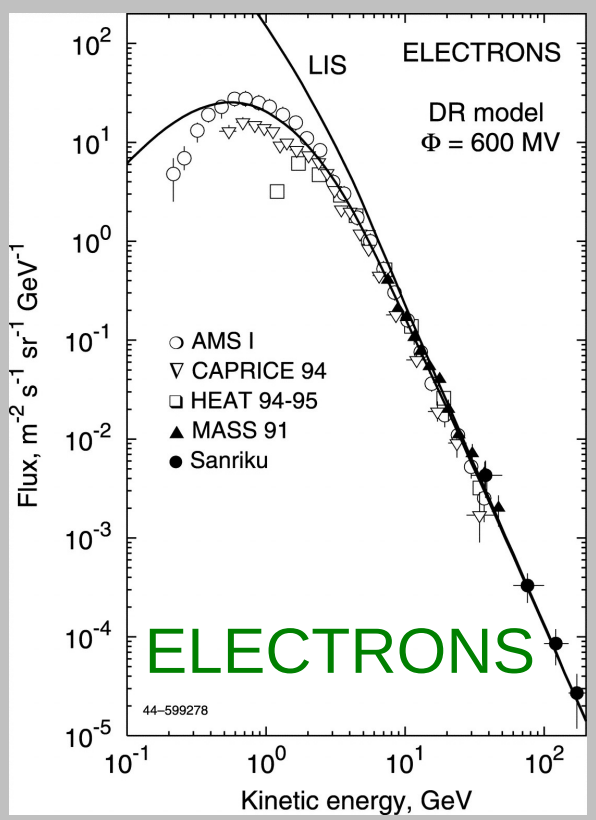

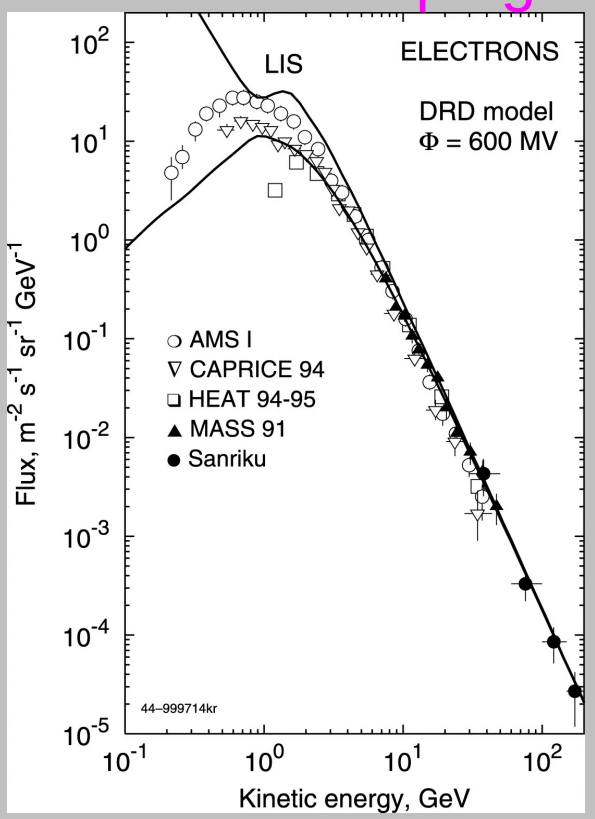

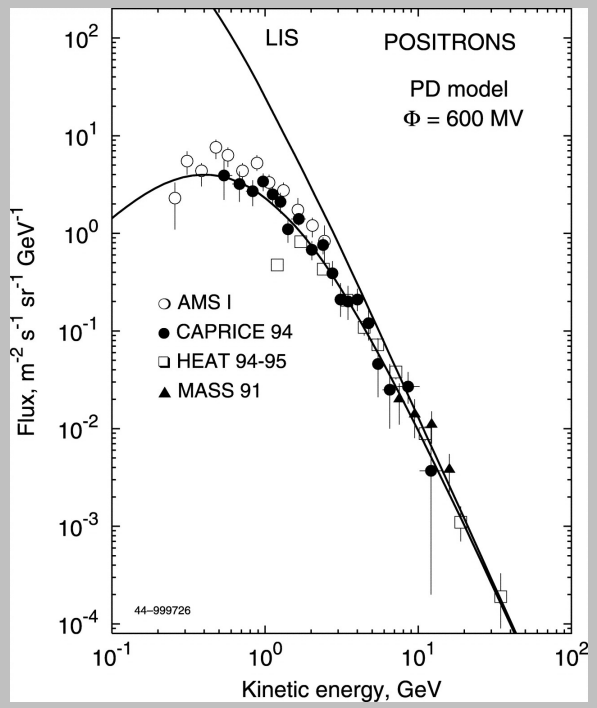

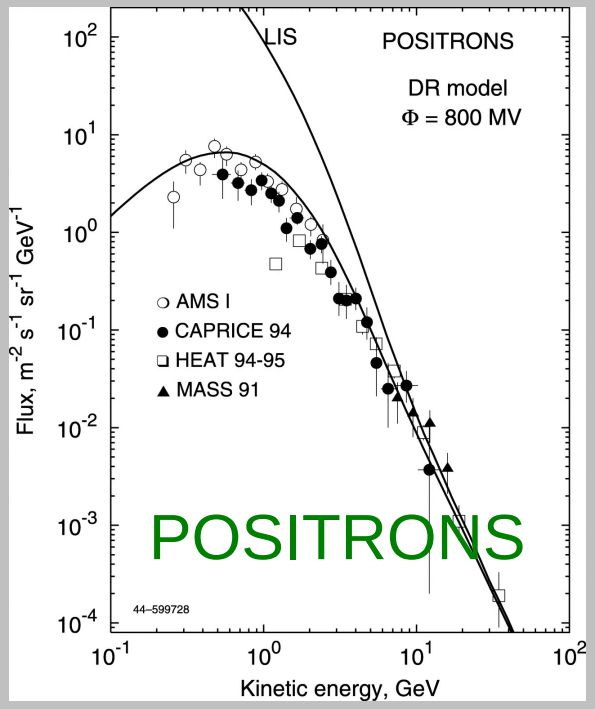

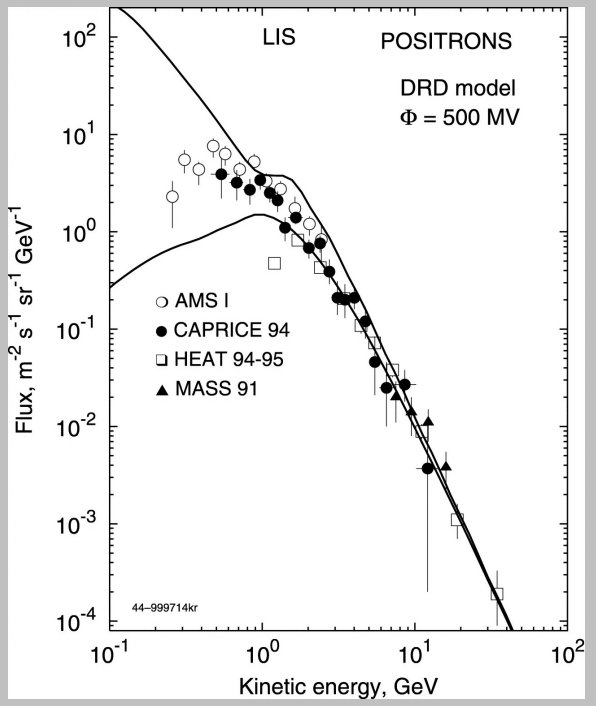

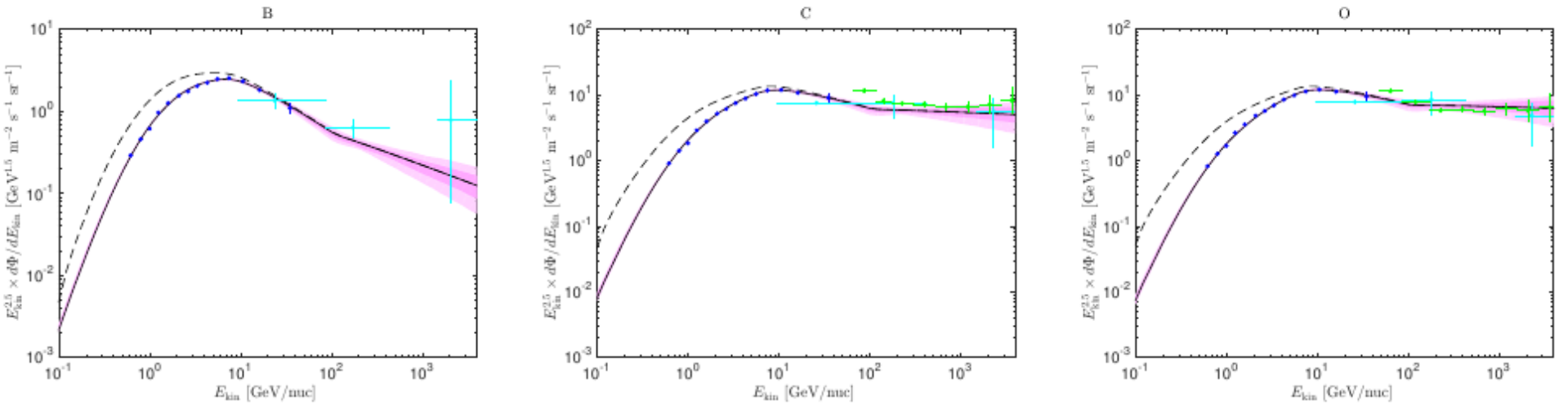

FIG. 5.— Spectral fluxes with 68% and 95% posterior regions from the posteriors of our light element (Be–Si) scan, shown in magenta in Figure 3, and using the HEAO modulation posteriors, . Data shown are HEAO (blue), CREAM (green) and TRACER (cyan). The best fit is shown as a black line, and the dashed lines correspond to the LIS (umodulated) spectra.

G. JÓHANNESSON[1], R. RUIZ DE AUSTRI[2], A.C. VINCENT[3], I. V. MOSKALENKO[4,5], E. ORLANDO[4,5], T. A. PORTER[4], A. W. STRONG[6], R. TROTTA[7,8], F. FEROZ, P. GRAFF[9], AND M.P. HOBSON[10]

ApJ 824, 16 (2016)

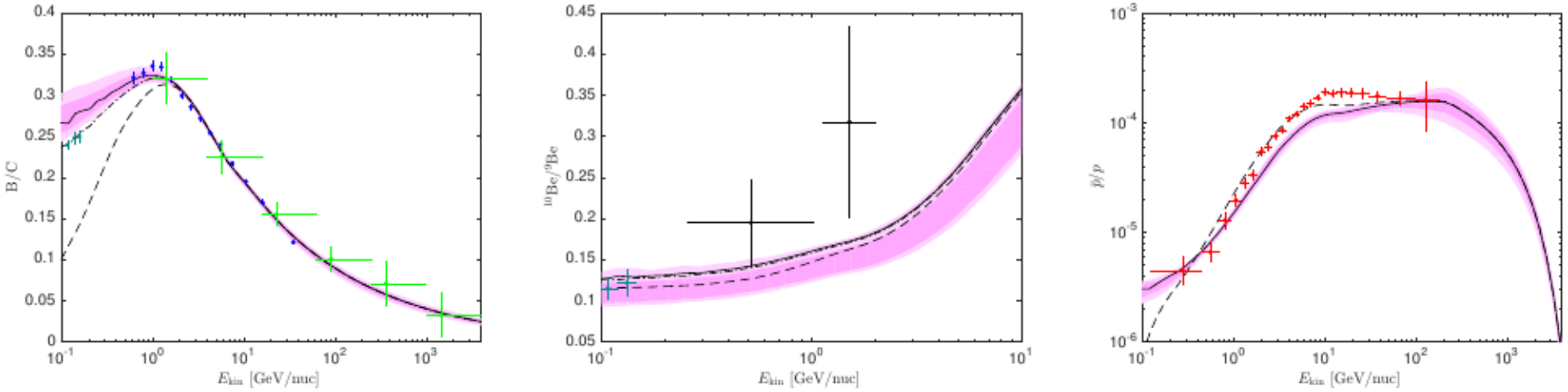

FIG. 6.— Secondary-to-primary ratio 68% and 95% posterior bands from our light element (Be–Si) scan, shown in magenta in Fig. 3. The $\bar{p}/p$ ratio is shown to indicate that using the same propagation parameters for hydrogen yields a very bad fit to the data. Data shown are HEAO (blue), CREAM (green), ACE (light blue), ISOMAX (black) and PAMELA (red). The best fit is shown as a black line, and the dashed lines correspond to the LIS (umodulated) ratios. In the left-hand panel we use the HEAO modulation posterior, and the solid line uses the HEAO best fit modulation potential. The dash-dotted line is the modulated spectrum using the best fit to the ACE-CRIS modulation potential; for clarity we do not show the posterior intervals for this case. Correspondingly, the central plot uses the ACE modulation (BF in black), and we show the best fit using the ISOMAX best fit modulation potential with a dash-dotted line.

G. JÓHANNESSON[1], R. RUIZ DE AUSTRI[2], A.C. VINCENT[3], I. V. MOSKALENKO[4,5], E. ORLANDO[4,5], T. A. PORTER[4], A. W. STRONG[6], R. TROTTA[7,8], F. FEROZ, P. GRAFF[9], AND M.P. HOBSON[10]

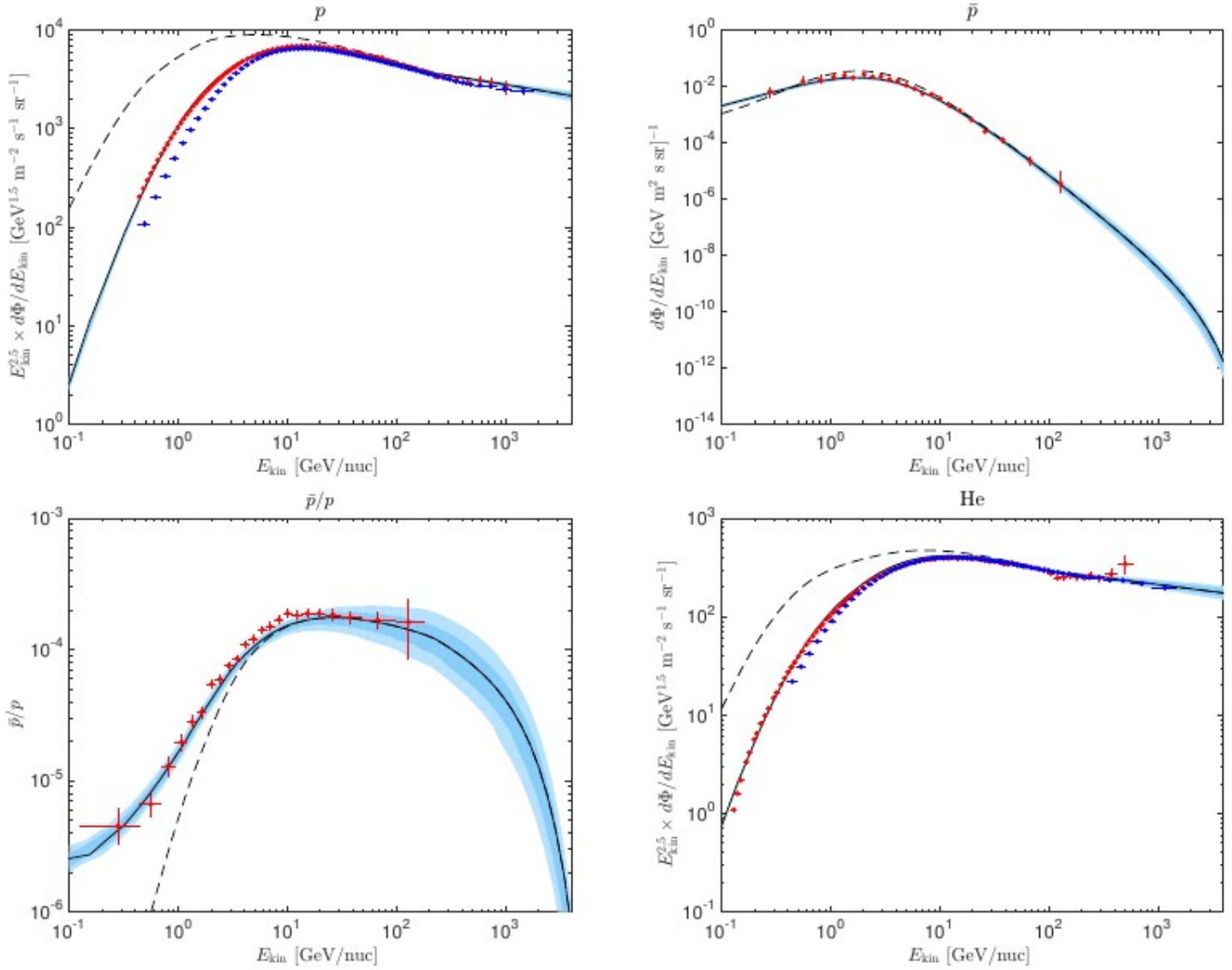

FIG. 7.— Spectra and $\bar{p}/p$ ratio 68% and 95% posterior bands of our $\bar{p}, p$ He scan, shown in blue in Fig. 3. The best fit is plotted in black, and the dashed lines correspond to the LIS (umodulated) spectra. PAMELA data are shown in red. We also show recent AMS-02 (Aguilar et al. 2015b,a, blue) for the available proton and helium flux data, which were not available at the time of our analysis (and hence are not included in the likelihood).

G. JÓHANNESSON[1], R. RUIZ DE AUSTRI[2], A.C. VINCENT[3], I. V. MOSKALENKO[4,5], E. ORLANDO[4,5], T. A. PORTER[4], A. W. STRONG[6], R. TROTTA[7,8], F. FEROZ, P. GRAFF[9], AND M.P. HOBSON[10]

TABLE 3
SUMMARY OF CONSTRAINTS ON ALL PROPAGATION PARAMETERS

	$p, \bar{p}$, He scan			Light element (B, ..., Si) scan		
Quantity	Best fit value	Posterior mean and standard deviation	Posterior 95% range	Best fit value	Posterior mean and standard deviation	Posterior 95% range
DIFFUSION MODEL PARAMETERS Θ_P						
D_0 (10^{28} cm^2 s^{-1})	6.330	6.102±1.662	[2.138,8.205]	6.188	9.030±1.610	[5.743,11.256]
δ	0.466	0.461±0.065	[0.343,0.586]	0.375	0.380±0.018	[0.349,0.412]
v_{Alf} (km/s)	8.922	8.970±1.244	[7.036,11.254]	32.573	30.017±2.461	[25.484,34.465]
z_h (kpc)	9.507	10.358±4.861	[2.461,19.034]	4.900	10.351±4.202	[4.544,19.078]
ρ_{br} (GV)	2.486	2.345±0.344	[1.870,2.739]	15.782	16.687±1.498	[14.051,19.849]
ν_0	1.854	1.765±0.229	[1.230,2.133]	2.012	2.025±0.073	[1.885,2.155]
ν_1	2.352	2.358±0.063	[2.230,2.468]	2.549	2.548±0.050	[2.452,2.642]
ν_2	2.182	2.186±0.068	[2.062,2.308]	2.195	2.197±0.088	[2.042,2.374]
$10^9 N_p$ (cm^{-2} sr^{-1} s^{-1} MeV^{-1})	4.798	4.791±0.066	[4.672,4.913]	4.511	4.482±0.220	[4.055,4.884]
δ_ν	0.045	0.047±0.009	[0.030,0.064]	–	–	–
$X_{\rm He} \times 10^{-4}$	10.261	10.294±0.505	[9.416,11.240]	–	–	–

G. JÓHANNESSON[1], R. RUIZ DE AUSTRI[2], A.C. VINCENT[3], I. V. MOSKALENKO[4,5], E. ORLANDO[4,5], T. A. PORTER[4], A. W. STRONG[6], R. TROTTA[7,8], F. FEROZ, P. GRAFF[9], AND M.P. HOBSON[10]

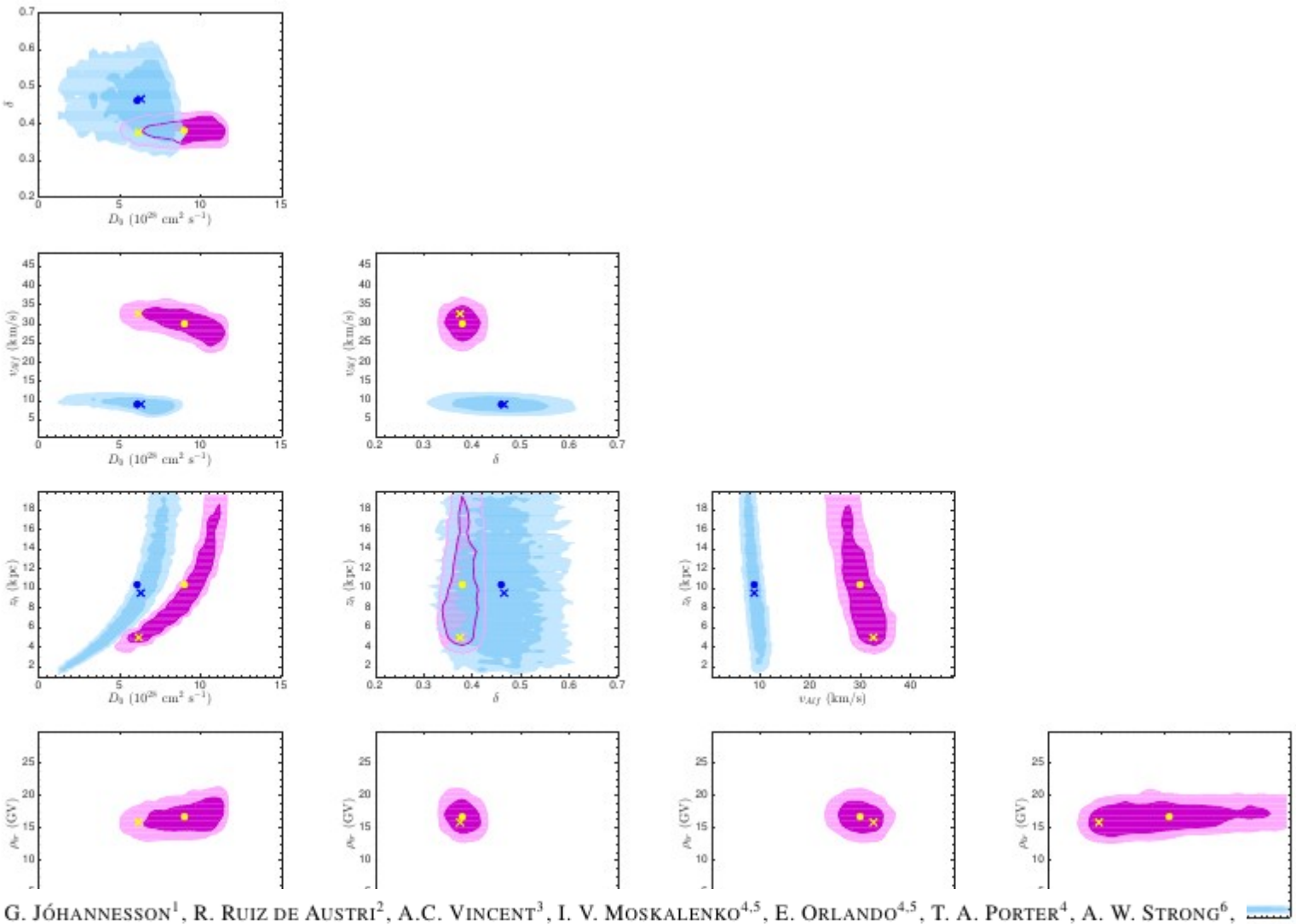

G. JÓHANNESSON[1], R. RUIZ DE AUSTRI[2], A.C. VINCENT[3], I. V. MOSKALENKO[4,5], E. ORLANDO[4,5], T. A. PORTER[4], A. W. STRONG[6], R. TROTTA[7,8], F. FEROZ, P. GRAFF[9], AND M.P. HOBSON[10]

FIG. 4.— Two-dimensional posterior distributions, showing 1 and 2-sigma credible intervals for the p, $\bar{p}$ and He scan (blue), and for the light element (Be–Si, magenta). The posterior mean in each case is shown as a dot and the best fit as a cross.

G. JÓHANNESSON[1], R. RUIZ DE AUSTRI[2], A.C. VINCENT[3], I. V. MOSKALENKO[4,5], E. ORLANDO[4,5], T. A. PORTER[4], A. W. STRONG[6], R. TROTTA[7,8], F. FEROZ, P. GRAFF[9], AND M.P. HOBSON[10]

CR Streaming

Secondary production in SNR sources

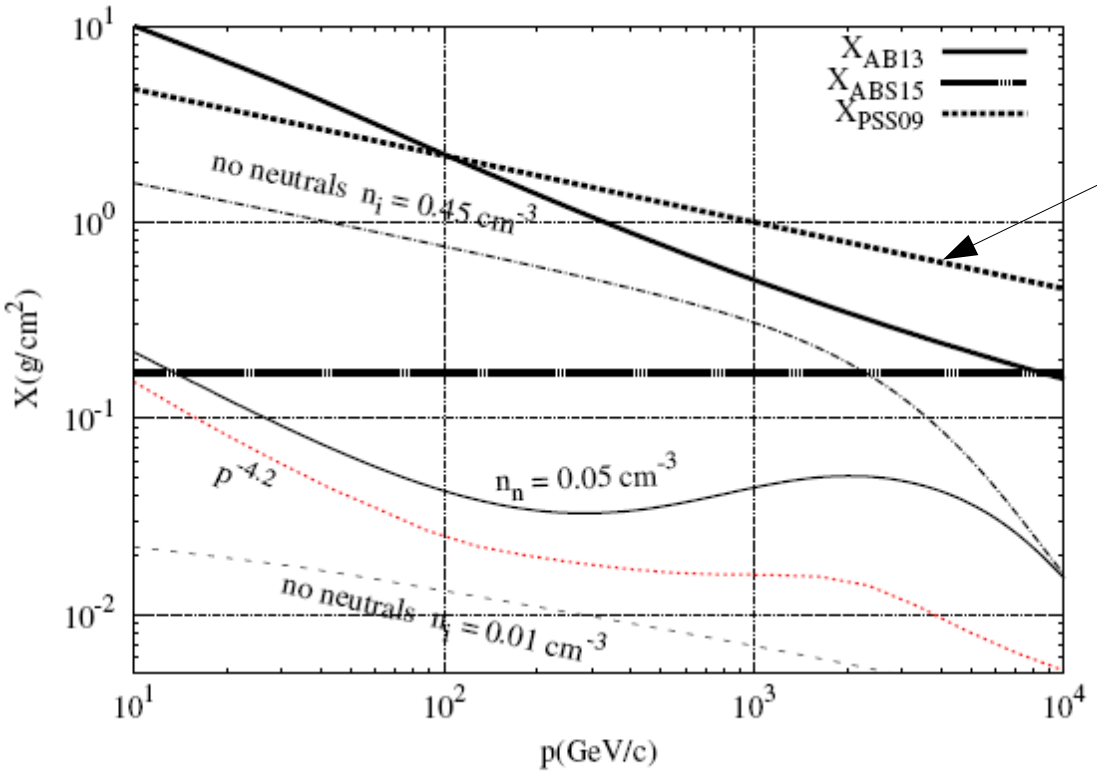

From secondary/primary ratios

FIG. 1: Grammage accumulated by CRs in the near-source region for $L_c = 100$ pc in the three cases: (1) $n_n = 0$, $n_i = 0.45\text{cm}^{-3}$; (2) $n_i = 0.45\text{cm}^{-3}$ and $n_n = 0.05\text{cm}^{-3}$; (3) $n_n = 0$, $n_i = 0.01\text{cm}^{-3}$, as labelled. The thin dotted (red) line corresponds to case (2) but with slope of the injection spectrum 4.2. The thick dashed line (labelled as X_{PSS09}) shows the grammage inferred from the measured B/C ratio [11], while the thick solid line (labelled as X_{AB13}) shows the results of the non-linear propagation of Ref. [8]. The horizontal (thick dotted) line (labelled as X_{ABS15}) is the source grammage, as estimated in Ref. [20].

D'Angelo, Blasi & Amato 2016
arXiv:1512.05000

c.f. AMS B/C...

Testable with gamma-rays:
Look for halos around SNR
D'Angelo, Heidelberg Gamma2016.

Flux Ratios $\bar{p}/e^+$ and p/e^+ are also energy independent in the interval 60–450 GV

Stefan Schael
Gamma2016, Heidelberg

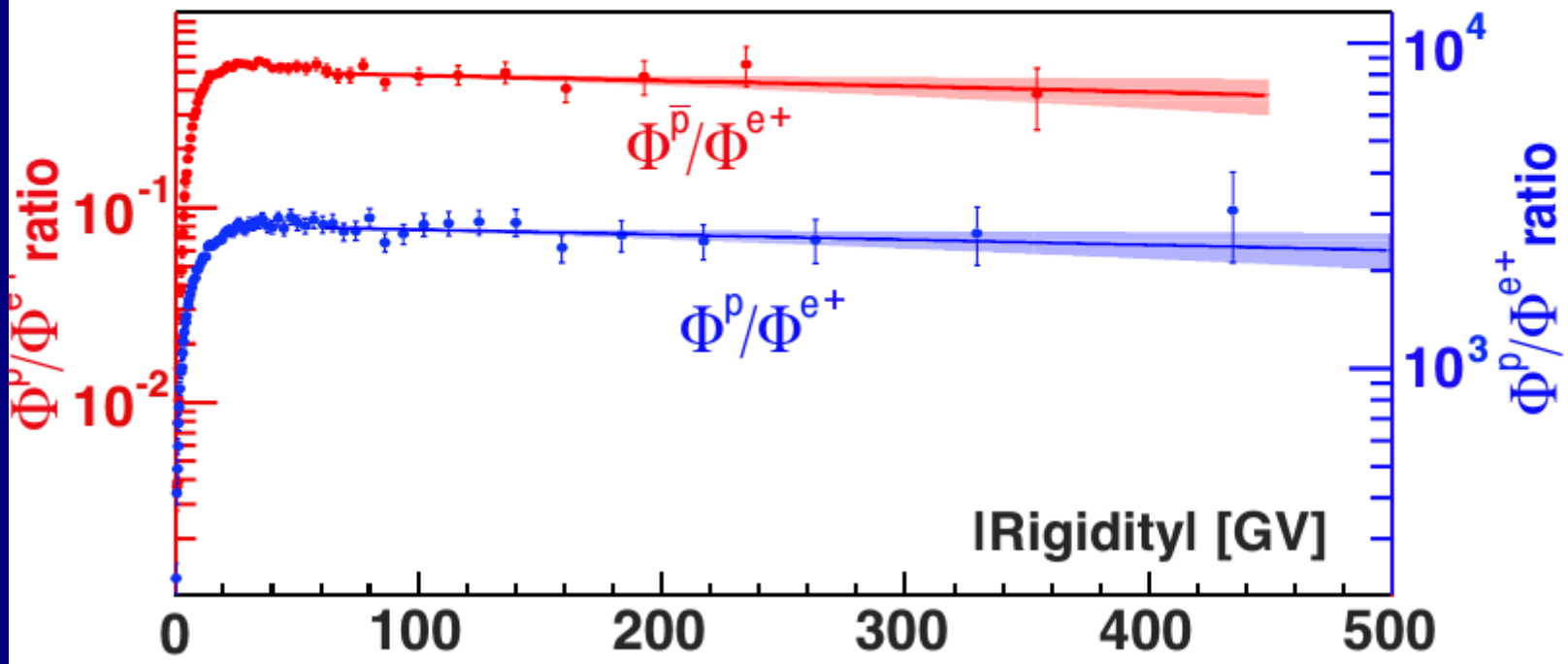

pbar and e+ production have similar spectra since hadronic interactions
But e+ are supposed to lose energy and steepen !
A mean conspiracy – a concidence? Or a challenge to standard models?

PAUSE FOR REFLECTION

Only sure things are the observations.
Rest is theory.

Sure about: what are primaries, what are secondaries
Not sure about: where secondaries are produced
Do we really know it is in ISM, could be in sources
Diffusion: standard assumption but no absolute proof.
Convection can be essential too.
Diffusive reacceleration: nice fits to B/C but no proof

Antiprotons have same slope as positrons, quite different from standard picture (see later)

Many other standard assumptions but need to take critical stance,
Challenge the tradional assumptions (especially younger people).

CR Beyond the Standard Model, San Vito di Cadore, Sept 18-24 2016

END OF PART 1

Lecture 2
Practical computations of Galactic Cosmic-Ray Propagation

Cosmic Rays and Galactic Dynamics

Lecture 1

Intro: first lecture just about the physics, second one about practical computations.
CR propagation only: not origin!
Species, nuclei, leptons: standard pics
isotopes, source abundances, reaction chain from Ni down (and >Ni too)
cross-sections, total and partial, K-capture, actinides, radioactive isotopes
LB as basic paradigm
secondaries as probe of propagation because can compute production
synchrotron gammas gas tracers
Emissivities → protons
propagation equation, each effect
Reacceleration ala Drury
units momentum KE flux density
multimessengers
external galaxies, radio. recognition of halo.
LECR Voyager ionization chemistry protoplanetary discs
CO destruction
CR becoming mainstream as people realize

Lecture 2
About practical computations, packages.
Usual things for intro: quotation, obvious idea, surprising not done before, now good that several.
MHD winds CR-driven dynamos – quest for realistic models

GALPROP

Origins

Shortcomings

'Competitors'

Future desiderata

More physical approaches

Potpourri of relevant topics

Lecture 2
Practical computations of cosmic-ray propagation

The original motivation :

- to escape from the leaky-box

into the Galaxy

The original motivation :

- to escape from the leaky-box

into the Galaxy

but now...

precision experiments e.g.
Fermi, PAMELA, ACE, AMS02, Planck
and now also Voyager beyond the heliosphere

require correspondingly *detailed* – 'realistic' - models to do them justice

Annual Reviews of Nuclear and Particle Science, 2007

Cosmic-Ray Propagation and Interactions in the Galaxy

Andrew W. Strong,[1] Igor V. Moskalenko,[2] and Vladimir S. Ptuskin[3]

[1]Max-Planck-Institut für extraterrestrische Physik, 85741 Garching, Germany; email: aws@mpe.mpg.de

[2]Hansen Experimental Physics Laboratory and Kavli Institute for Particle Astrophysics and Cosmology, Stanford University, Stanford, California 94305; email: imos@stanford.edu

[3]Institute for Terrestrial Magnetism, Ionosphere and Radiowave Propagation of the Russian Academy of Sciences (IZMIRAN), Troitsk, Moscow region 142190, Russia; email: vptuskin@izmiran.ru

Annu. Rev. Nucl. Part. Sci. 2007. 57:285–327

The *Annual Review of Nuclear and Particle Science* is online at http://nucl.annualreviews.org

This article's doi:
10.1146/annurev.nucl.57.090506.123011

0163-8998/07/1123-0285$20.00

Key Words

energetic particles, gamma rays, interstellar medium, magnetic fields, plasmas

Abstract

We survey the theory and experimental tests for the propagation of cosmic rays in the Galaxy up to energies of 10^{15} eV. A guide to the previous reviews and essential literature is given, followed by an exposition of basic principles. The basic ideas of cosmic-ray propagation are described, and the physical origin of its processes is explained. The various techniques for computing the observational consequences of the theory are described and contrasted. These include analytical and numerical techniques. We present the comparison of models with data, including direct and indirect—especially γ-ray—observations, and indicate what we can learn about cosmic-ray propagation. Some important topics, including electron and antiparticle propagation, are chosen for discussion.

Quote.....

It is unclear whether one would wish to go much beyond the generalizations discussed here for an analytically soluble diffusion model. The added insight from any analytic solution of a purely numerical approaches is quickly cancelled by the growing complexity of the formulae. With rapidly developing computational capabilities, one could profitably employ numerical solutions....

Quote.....

It is unclear whether one would wish to go much beyond the generalizations discussed here for an analytically soluble diffusion model. The added insight from any analytic solution of a purely numerical approaches is quickly cancelled by the growing complexity of the formulae. With rapidly developing computational capabilities, one could profitably employ numerical solutions....

---------- J.M. Wallace, ApJ, 1981

Quote.....

It is unclear whether one would wish to go much beyond the generalizations discussed here for an analytically soluble diffusion model. The added insight from any analytic solution of a purely numerical approaches is quickly cancelled by the growing complexity of the formulae. With rapidly developing computational capabilities, one could profitably employ numerical solutions....

---------- J.M. Wallace, ApJ, 1981

34 years ago!

Leaky-box, path-length distribution models
these are numerical 0-D models

not discussed here since we regard them as outdated.

But it is a well-known fact that for stable nuclei without energy losses, these methods can be designed to produce the same results as propagation models,

So OK for for cosmic-ray source composition studies.

For unstable nuclei, electrons, positrons, gamma rays.... not realistic enough to be useful

Leaky-box, path-length distribution models
these are numerical 0-D models

not discussed here since we regard them as outdated.

But it is a well-known fact that for stable nuclei without energy losses, these methods can be designed to produce the same results as propagation models,
So OK for for cosmic-ray source composition studies.
For unstable nuclei, electrons, positrons, gamma rays.... not realistic enough to be useful

Spatial Propagation models

Advantage is the physical interpretation in terms of diffusion, convection etc.
related to the real Galaxy. Intuitive understanding of meaning of terms.

Both analytical and numerical, and hybrids, all have their proponents.

Workshop
“Tango in Paris” 2009 session
on
cosmic-ray programmes

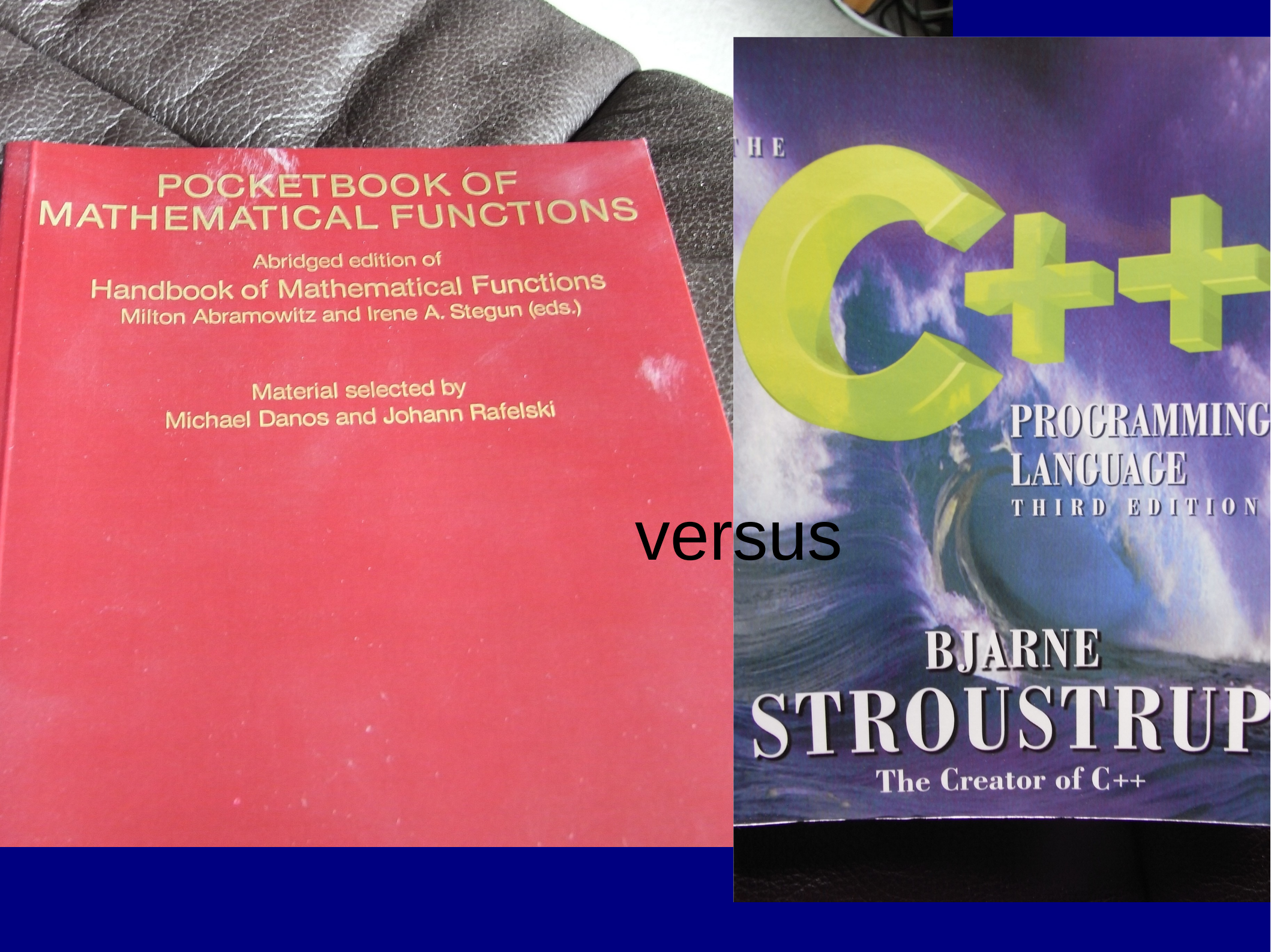
POCKETBOOK OF
MATHEMATICAL FUNCTIONS
Abridged edition of
Handbook of Mathematical Functions
Milton Abramowitz and Irene A. Stegun (eds.)
Material selected by
Michael Danos and Johann Rafelski
versus
THE
C++
PROGRAMMING
LANGUAGE
THIRD EDITION
BJARNE
STROUSTRUP
The Creator of C++

Propagation models

A main advantage is the physical interpretation in terms of diffusion, convection etc. related to the real Galaxy. Intuitive understanding of meaning of terms.

1D, 2D, or 3D
Both analytical and numerical, and hybrids, all have their proponents.

Analytical	**Numerical**
Mainly 1D, some 2D	2D or 3D
complex (but impressive) formulae	simple formulae (computer does the work)
simplified energy losses	full energy losses
simplified gas distribution	gas based on HI, CO surveys in 3D
simplified magnetic field	any magnetic field model
gamma rays only in simple way	full gamma ray calculation
synchrotron only in simple way	full synchrotron calculation

High energy particles and radiation in the Galaxy

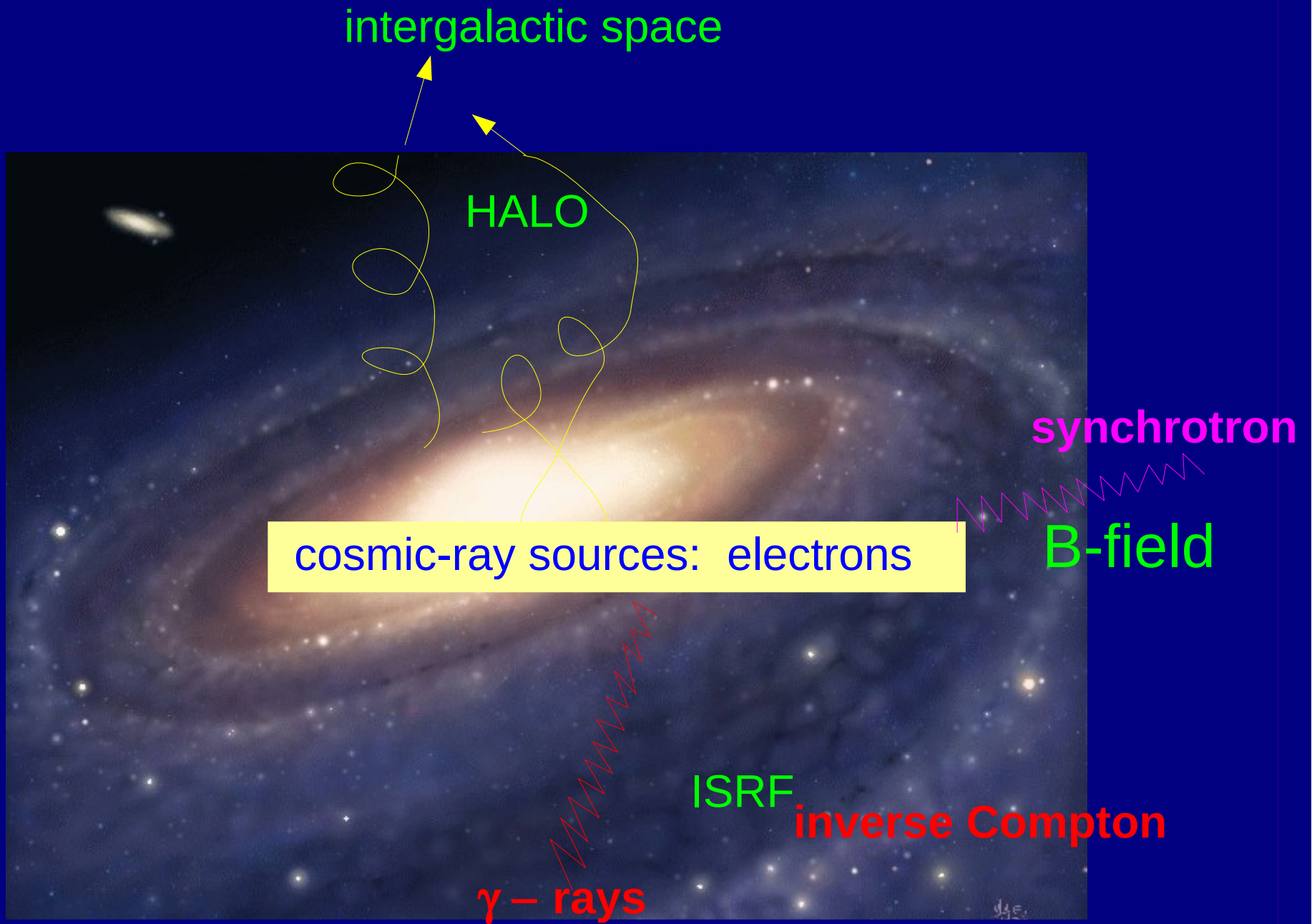
intergalactic space
HALO
synchrotron
B-field
cosmic-ray sources: electrons
ISRF
inverse Compton
γ – rays

COSMIC RAYS produce many observables

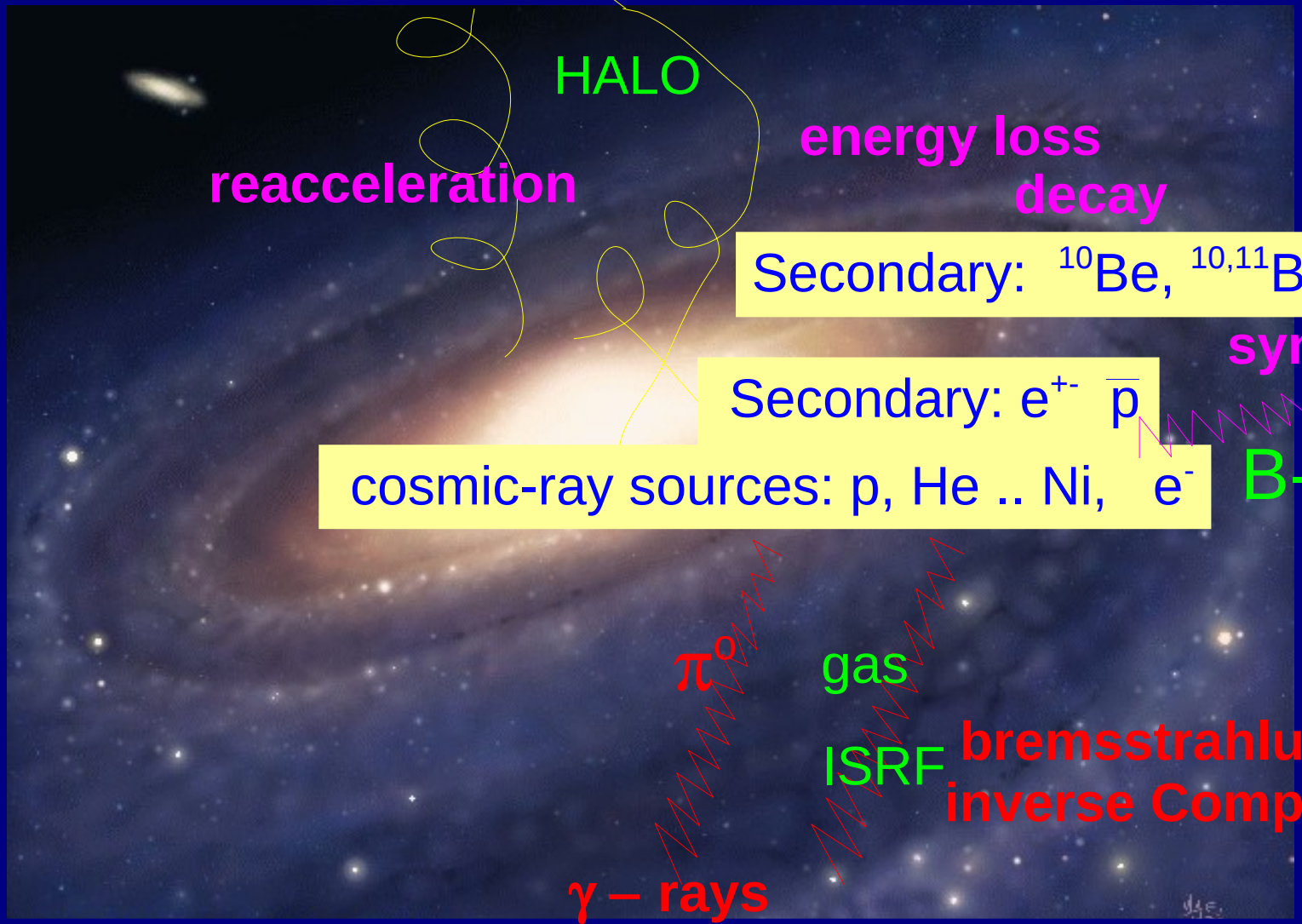

GALPROP model

The **goal** : use *all* types of data in self-consistent way to test models of cosmic-ray propagation.

Observed *directly, near Sun:*

primary spectra (p, He ... Fe; e^-)

secondary/primary (B/C etc)

secondary e^+ , antiprotons...

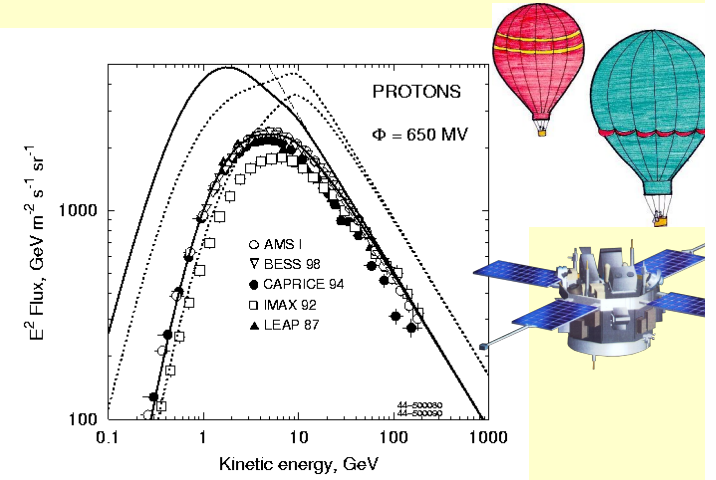

Observed *from whole Galaxy:*

γ - rays

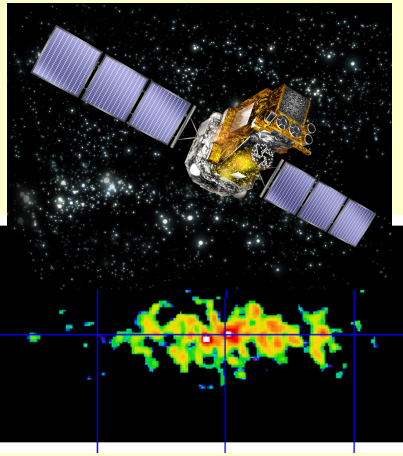

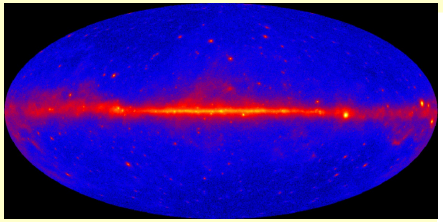

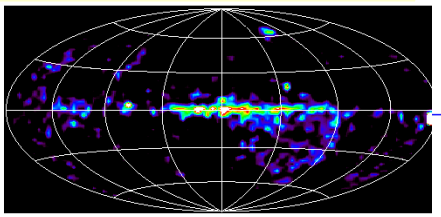

synchrotron

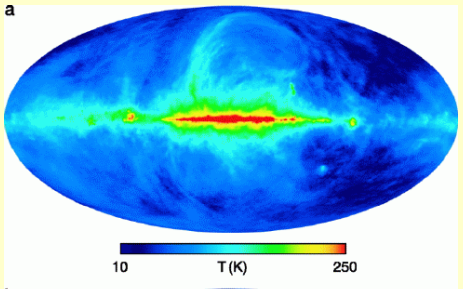

TeV

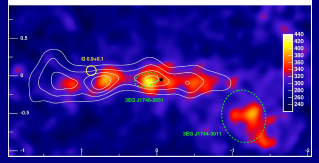

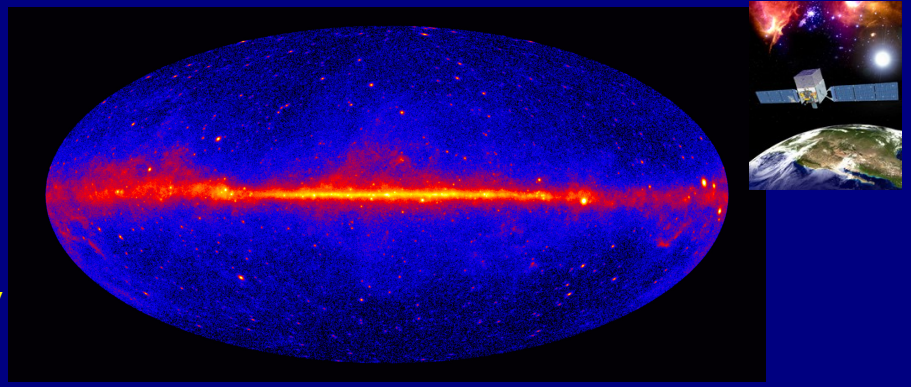

GeV

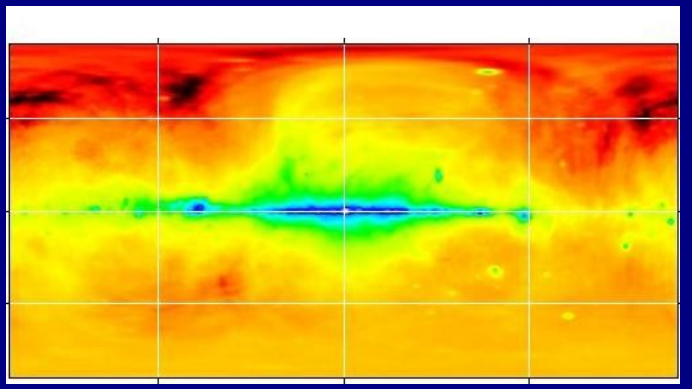

µeV

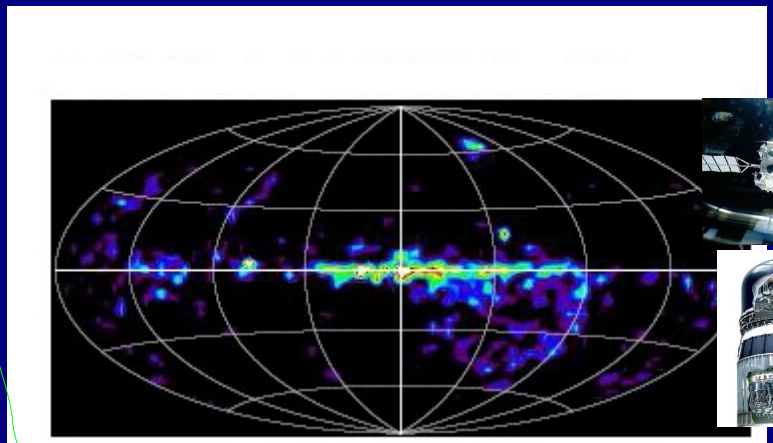

Cosmic-ray interactions
probed
by their photon emission

GHz

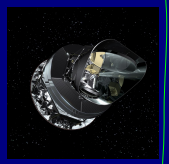

MeV

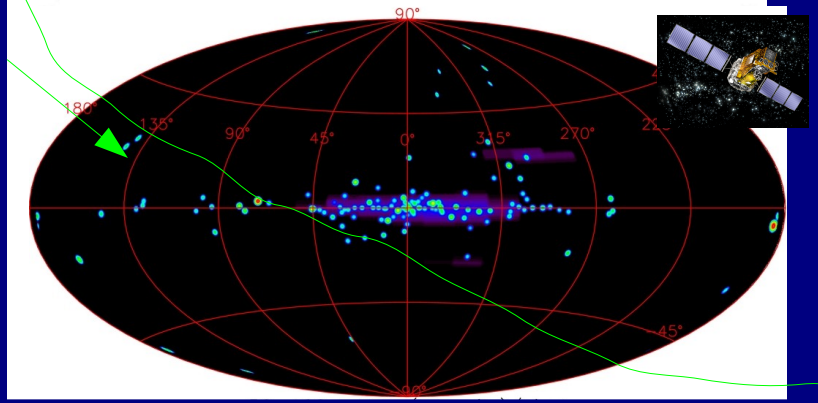

meV

THz

Cosmic-ray propagation

$$\partial \psi (\underline{r} , p) / \partial t = q (\underline{r} , p)$$

cosmic-ray sources (primary and secondary)

$$+ \nabla \cdot (D_{xx} \nabla \psi - v \psi)$$

diffusion convection

$$+ \partial / \partial p \; [p^2 D_{pp} \partial / \partial p \; \psi / p^2]$$

$D_{pp} D_{xx} \sim p^2 v_A^2$

diffusive reacceleration (diffusion in p)

$$- \partial / \partial p \; [d p / d t \; \psi - p / 3 \; (\nabla \cdot v) \; \psi]$$

momentum loss adiabatic momentum loss

ionization, bremsstrahlung

$- \psi / \tau_f$ nuclear fragmentation

$- \psi / \tau_r$ radioactive decay

Solving CR propagation numerically

GALPROP *Explanatory Supplement*

Andrew W. Strong[*]
Max-Planck-Institut für extraterrestrische Physik,
Postfach 1312, 85741 Garching, Germany

Igor V. Moskalenko[†]
Hansen Experimental Physics Laboratory,
Stanford University, Stanford, CA 94305, U.S.A.

Troy A. Porter[‡]
Hansen Experimental Physics Laboratory,
Stanford University, Stanford, CA 94305, U.S.A.

Gudlaugur Jóhannesson[§]
Science Institute, University of Iceland Dunhaga 5 IS-107 Reykjavk, Iceland

Elena Orlando[¶]
Hansen Experimental Physics Laboratory,
Stanford University, Stanford, CA 94305, U.S.A.

Seth W. Digel [‖]
SLAC National Accelerator Laboratory,
2575 Sand Hill Road,
Menlo Park, CA 94025, USA

Andrey E. Vladimirov[**]
Hansen Experimental Physics Laboratory,
Stanford University, Stanford, CA 94305, U.S.A.

April 16, 2015

Abstract
This document provides a description of the *GALPROP* cosmic ray propagation code.

Solving CR propagation numerically

$$\frac{\partial \psi}{\partial t} = q(\vec{r},p) + \vec{\nabla}\cdot(D_{xx}\vec{\nabla}\psi - \vec{V}\psi) + \frac{\partial}{\partial p}p^2 D_{pp}\frac{\partial}{\partial p}\frac{1}{p^2}\psi - \frac{\partial}{\partial p}\left[\dot{p}\psi - \frac{p}{3}(\vec{\nabla}\cdot\vec{V})\psi\right] - \frac{1}{\tau_f}\psi - \frac{1}{\tau_r}\psi$$

Crank-Nicolson method Alternatively, the propagation equation can be finite-differenced in the form

$$\frac{\partial \psi_i}{\partial t} = \frac{\psi_i^{t+\Delta t} - \psi_i^t}{\Delta t} = \frac{\alpha_1\psi_{i-1}^{t+\Delta t} - \alpha_2\psi_i^{t+\Delta t} + \alpha_3\psi_{i+1}^{t+\Delta t}}{2\Delta t} + \frac{\alpha_1\psi_{i-1}^{t} - \alpha_2\psi_i^{t} + \alpha_3\psi_{i+1}^{t}}{2\Delta t} + q_i \qquad (27)$$

This is the *Crank-Nicolson method* (34) where the updating scheme is

$$\psi_i^{t+\Delta t} = \psi_i^t + \frac{\alpha_1}{2}\psi_{i-1}^{t+\Delta t} - \frac{\alpha_2}{2}\psi_i^{t+\Delta t} + \frac{\alpha_3}{2}\psi_{i+1}^{t+\Delta t} + \frac{\alpha_1}{2}\psi_{i-1}^{t} - \frac{\alpha_2}{2}\psi_i^{t} + \frac{\alpha_3}{2}\psi_{i+1}^{t} + q_i\Delta t\ . \qquad (28)$$

It thus uses a combination of implicit and explicit terms, forming the time-average of the differentials. Like the fully implicit method, this method is unconditionally stable for all α and Δt, but is 2nd-order accurate in time, so that larger time-steps are possible than with the 1st-order scheme.

The tridiagonal system of equations

$$-\frac{\alpha_1}{2}\psi_{i-1}^{t+\Delta t} + (1+\frac{\alpha_2}{2})\psi_i^{t+\Delta t} - \frac{\alpha_3}{2}\psi_{i+1}^{t+\Delta t} = \psi_i^t + q_i\Delta t + \frac{\alpha_1}{2}\psi_{i-1}^{t} - \frac{\alpha_2}{2}\psi_i^{t} + \frac{\alpha_3}{2}\psi_{i+1}^{t} \qquad (29)$$

or

$$-\frac{\alpha_1}{2}\psi_{i-1}^{t+\Delta t} + (1+\frac{\alpha_2}{2})\psi_i^{t+\Delta t} - \frac{\alpha_3}{2}\psi_{i+1}^{t+\Delta t} = \frac{\alpha_1}{2}\psi_{i-1}^{t} + (1-\frac{\alpha_2}{2})\psi_i^{t} + \frac{\alpha_3}{2}\psi_{i+1}^{t} + q_i\Delta t \qquad (30)$$

is again solved for the $\psi_i^{t+\Delta t}$ by the standard method. Note that the RHS has all known quantities from the current time-step.

Unconditionally stable for all timesteps.
Straight out of Numerical Recipes!

Table 1: Coefficients for the finite-differencing scheme in 2 spatial dimensions and one momentum dimension.

Process	Coordinate	$\alpha_1/\Delta t$	$\alpha_2/\Delta t$	$\alpha_3/\Delta t$
Diffusion	R	$D_{xx}\frac{2R_i-\Delta R}{2R_i(\Delta R)^2}$	$D_{xx}\frac{2R_i}{R_i(\Delta R)^2}$	$D_{xx}\frac{2R_i+\Delta R}{2R_i(\Delta R)^2}$
	z	$D_{xx}/(\Delta z)^2$	$2D_{xx}/(\Delta z)^2$	$D_{xx}/(\Delta z)^2$
Convection[a]	$z>0$ $(V>0)$	$V(z_{i-1})/\Delta z$	$V(z_i)/\Delta z$	0
	$z<0$ $(V<0)$	0	$-V(z_i)/\Delta z$	$-V(z_{i+1})/\Delta z$
	p $(\frac{dV}{dz}>0)$	0	$\frac{1}{3}\frac{dV}{dz}\frac{p_i}{P_i^{i+1}}$	$\frac{1}{3}\frac{dV}{dz}\frac{p_{i+1}}{P_i^{i+1}}$
Diffusive reacceleration[a]	p	$-\frac{D_{pp,i}-D_{pp,i-1}}{P_{i-1}^{i\,2}}$ $+\frac{2}{P_{i-1}^{i}}\left(\frac{D_{pp,i}}{P_{i-1}^{i+1}}+\frac{D_{pp,i-1}}{p_{i-1}}\right)$	$-\frac{D_{pp,i}-D_{pp,i-1}}{P_{i-1}^{i\,2}}$ $+\frac{2D_{pp,i}}{P_{i-1}^{i+1}}\left(\frac{1}{P_i^{i+1}}+\frac{1}{P_{i-1}^{i}}\right)$ $+\frac{2D_{pp,i}}{P_{i-1}^{i}p_i}$	$\frac{2D_{pp,i+1}}{P_{i-1}^{i+1}P_i^{i+1}}$
Energy loss[a]	p	0	$-\dot{p}_i/P_i^{i+1}$	$-\dot{p}_{i+1}/P_i^{i+1}$
Fragmentation	R,z,p	0	$1/3\tau_f$	0
Radioactive decay	R,z,p	0	$1/3\tau_r$	0

[a] $P_j^i \equiv p_i - p_j$

Solving CR propagation numerically

$$\frac{\partial \psi}{\partial t} = q(\vec{r},p) + \vec{\nabla}\cdot(D_{xx}\vec{\nabla}\psi - \vec{V}\psi) + \frac{\partial}{\partial p}p^2 D_{pp}\frac{\partial}{\partial p}\frac{1}{p^2}\psi - \frac{\partial}{\partial p}\left[\dot{p}\psi - \frac{p}{3}(\vec{\nabla}\cdot\vec{V})\psi\right] - \frac{1}{\tau_f}\psi - \frac{1}{\tau_r}\psi$$

Dimensions (R,z,p) or (x,y,z,p): use implicit scheme with operator splitting

Each dimension stepped in turn.
Propagate until steady-state: RHS = 0.
Start with very large time-steps and reduce to small value: converges.

Operator splitting not strictly accurate.
Accurate method without operator splitting implemented
but slow since small time-step needed for stability.

GALPROP Parameters
Well over 100 of them! In a file 'galdef_nnnn'
Explained in Explanatory Supplement

Grid options for Galaxy and spectra

```
n_spatial_dimensions = 2
```

Specifies whether 2 or 3 spatial dimensions. 2D is cylindrically symmetric (R,z), 3D is (x,y,z) and may be fully asymmetric or with symmetry in x,y,z as specified by the parameter use_symmetry.

```
r_min                =00.0    min r
```

Minimum galactocentric radius (R) for 2D case, in kpc. Normally 0. Ignored for 3D.

```
r_max                =30.00   max r
```

Maximum galactocentric radius (R) for 2D case, in kpc.

```
dr                   = 1.0    delta r
```

Cell size in galactocentric radius (R) for 2D case, in kpc.

```
z_min                =-04.0   min z
```

Minimum height for 2D and 3D case, in kpc. In 3D case with use_symmetry $= 1$ it must be 0, since in this case only $z > 0$ is explicitly computed.

```
z_max                =+04.0   max z
```

Maximum height for 2D and 3D case, in kpc.

```
dz                   =  0.1   delta z
```

Cell size in z for 2D and 3D case, in kpc.

```
x_min                = 00.0   min x
```

Minimum x for 3D case, in kpc. In 3D case with use_symmetry $= 1$ it must be 0, since in this case only $x > 0$ is explicitly computed. Ignored for 2D.

```
x_max                =+20.0   max x
```

Maximum x for 3D case, in kpc. Ignored for 2D.

```
dx                   =  0.2   delta x
```

Cell size in x for 3D case, in kpc. Ignored for 2D.

```
y_min                = 00.0   min y
```

See x_min, but now for y-axis.

```
y_max                =+20.0   max y
```

See x_max, but now for y-axis.

```
dy                   =  0.2   delta y
```

See dx, but now for y-axis.

```
iso_abundance_01_001 = 1.430e6        H  Source ELEM.abund.: Meyer,Dr
```

abundance of $Z = 1A = 1$.

```
iso_abundance_02_004 = 1.350e5        He   was 0.069e6   // So
```

abundance of $Z = 2A = 4$, and so on:

```
iso_abundance_03_006 =    0.          Li
iso_abundance_04_009 =    0.          Be
iso_abundance_05_010 =    0.          B
iso_abundance_06_012 = 2548.   (2573) C =3000
iso_abundance_06_013 =   25.
iso_abundance_07_014 =  175.          N  =137.
iso_abundance_08_016 = 3673.          O
iso_abundance_09_019 =    0.          F
iso_abundance_10_020 =  310.   (403)  Ne =???
iso_abundance_10_022 =   93.             22/20 =0.3 in source
iso_abundance_11_023 =   21.          Na
iso_abundance_12_024 =  626.          Mg =734 *1.1
iso_abundance_12_025 =   80.7
iso_abundance_12_026 =  100.5
iso_abundance_13_027 =   45.          Al
iso_abundance_14_028 =  680.   (760)  Si =707        Source ab
iso_abundance_14_029 =   60.
iso_abundance_14_030 =   20.
iso_abundance_15_031 =    8.          P  =4.92
iso_abundance_16_032 =   97.0  (105)  S  =92.4       Source ab
iso_abundance_16_033 =    2.1
iso_abundance_16_034 =    6.3
iso_abundance_17_035 =    0.9         Cl
iso_abundance_17_037 =    3.2
iso_abundance_18_036 =   20.0         Ar =15.2
iso_abundance_18_038 =    4.0            -introduced by imos
iso_abundance_19_039 =    0.          K  -introduced by imos
iso_abundance_20_040 =   39.0         Ca =42.
```

GALPROP Output
All as FITS files

CR spectra for all species (throughout Galaxy)
Gamma-ray skymaps (pion-decay, inverse Compton etc) as spectra, HEALPix
Also in Galactocentric rings.

Gamma-ray emissivities

Synchrotron skymaps as spectra, HEALPix, included polarization
Synchrotron emissivities

And many more.

Files tagged with same name as parameter file for traceabilty/reproduceability

parameter file e.g.

galdef_54_andys_model
produces
pion_decay_skymap_healpix_54_andys_model
etc

Cosmic-ray secondary/primary ratios: e.g. Boron/Carbon probes *cosmic-ray propagation*

Boron / Carbon

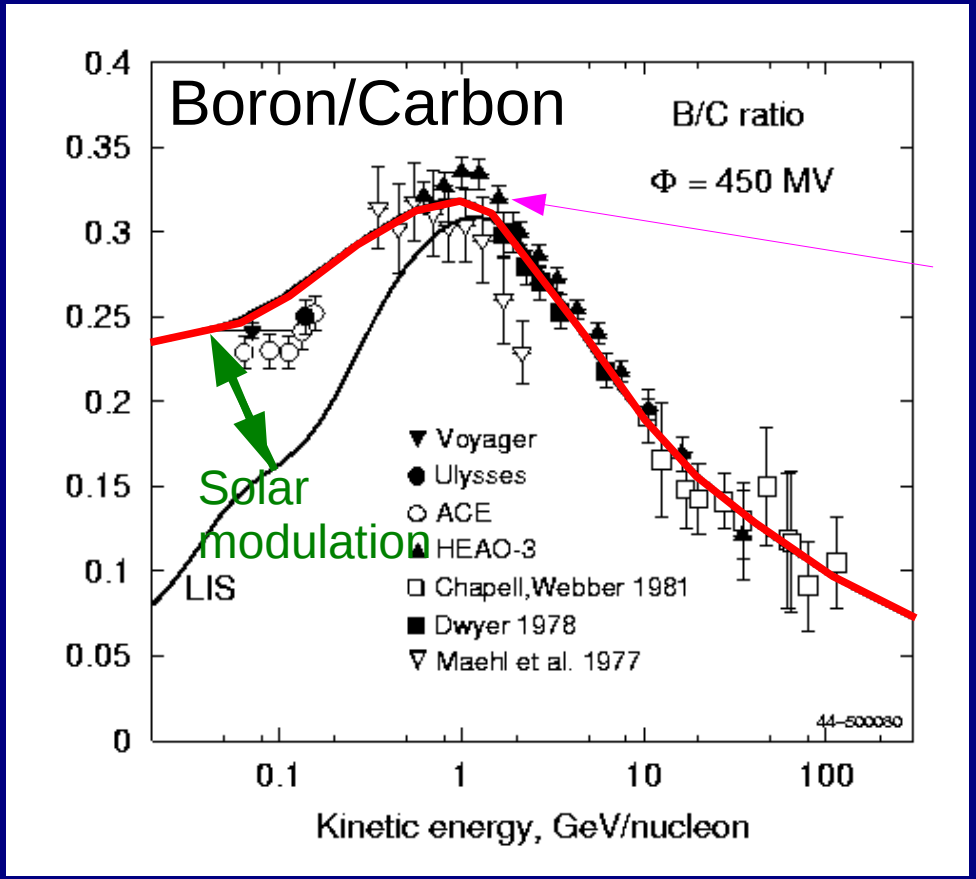

Peak in Boron/Carbon could be explained by **diffusive reacceleration** with Kolmogorov spectrum giving momentum-dependence of diffusion coefficient

Spatial diffusion

$D_{xx} \sim p^{1/3}$

Momentum space diffusion

$D_{pp} \sim 1 / D_{xx}$

However reacceleration not proven, maybe does not happen

→ 'pure diffusion' model: $D_{xx}(p) \sim p^{0.5}$, constant < 3 GeV.

plain diffusion

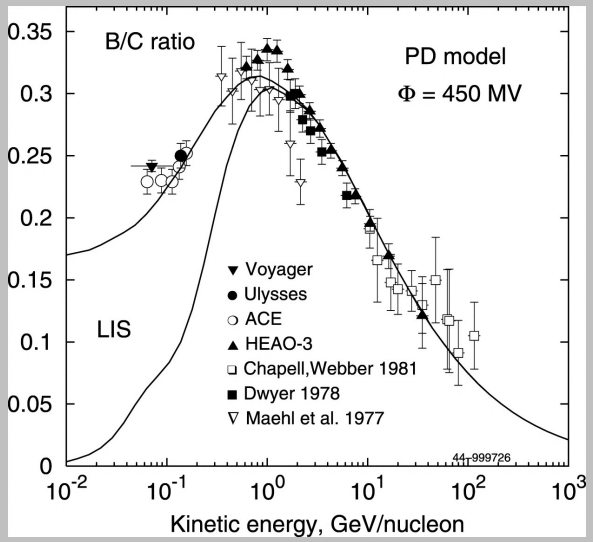

diffusive reacceleration

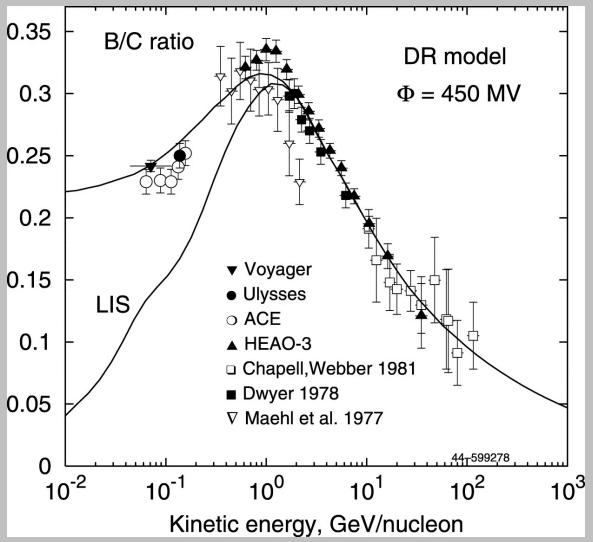

wave damping

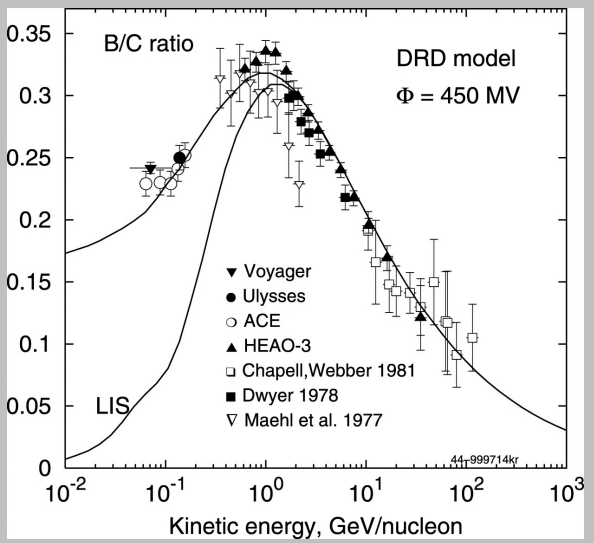

For any model, first adjust parameters to fit Boron/Carbon

Ptuskin et al. 2006 ApJ 642, 902

plain diffusion

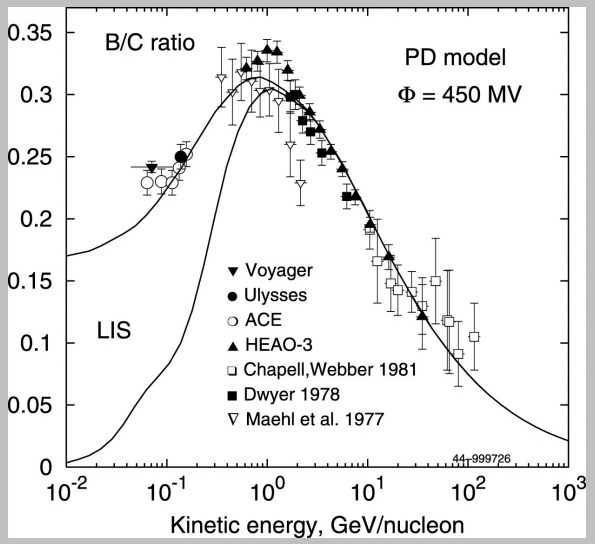

diffusive reacceleration

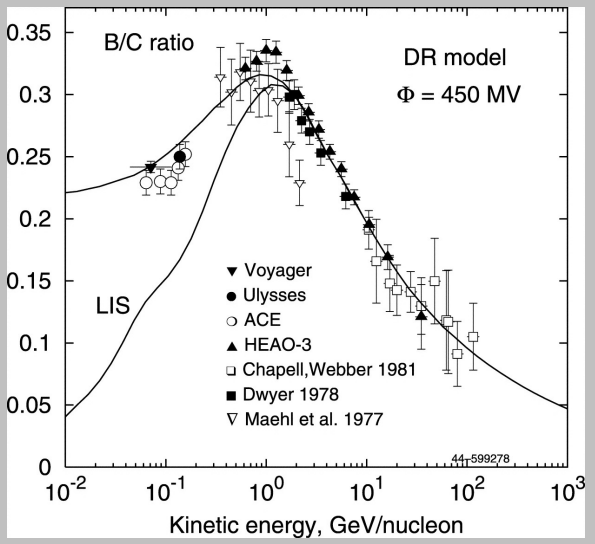

wave damping

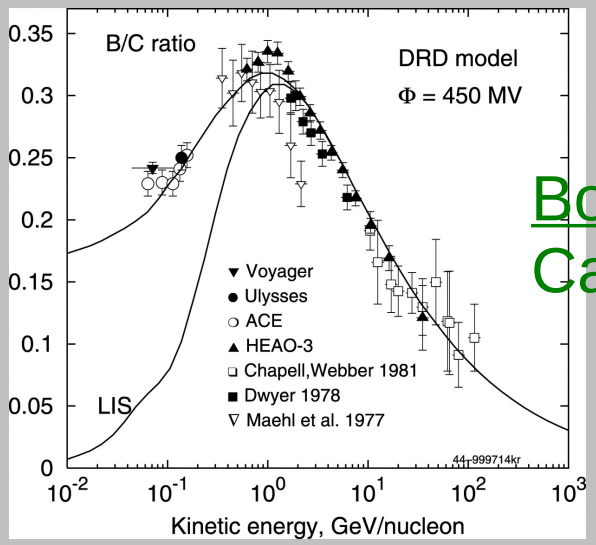

Boron/ Carbon

then predict the other cosmic-ray spectra

antiprotons

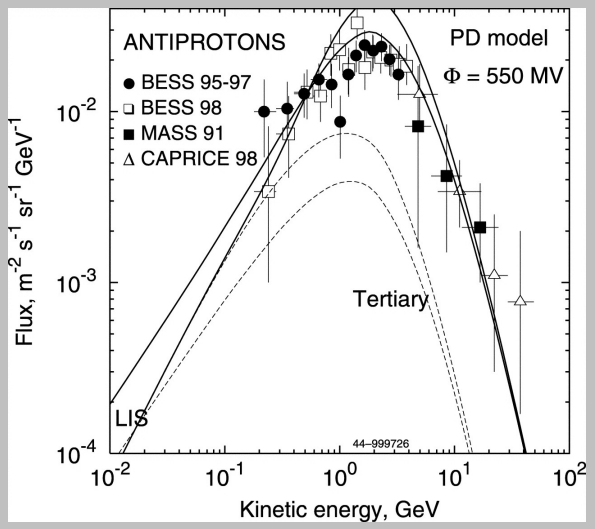

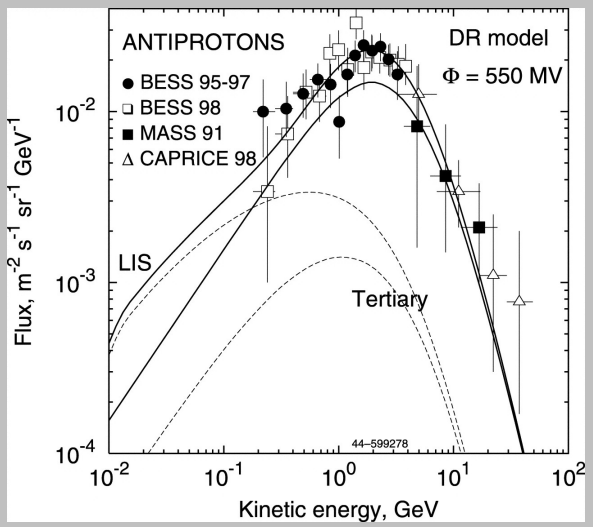

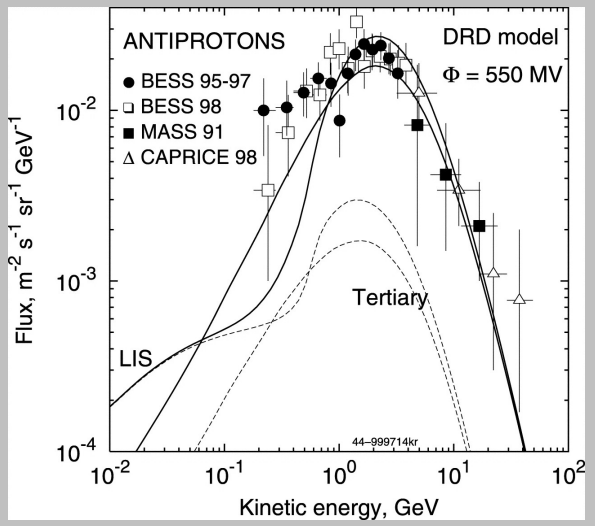

Ptuskin et al. 2006 ApJ 642, 902

plain diffusion

diffusive reacceleration

wave damping

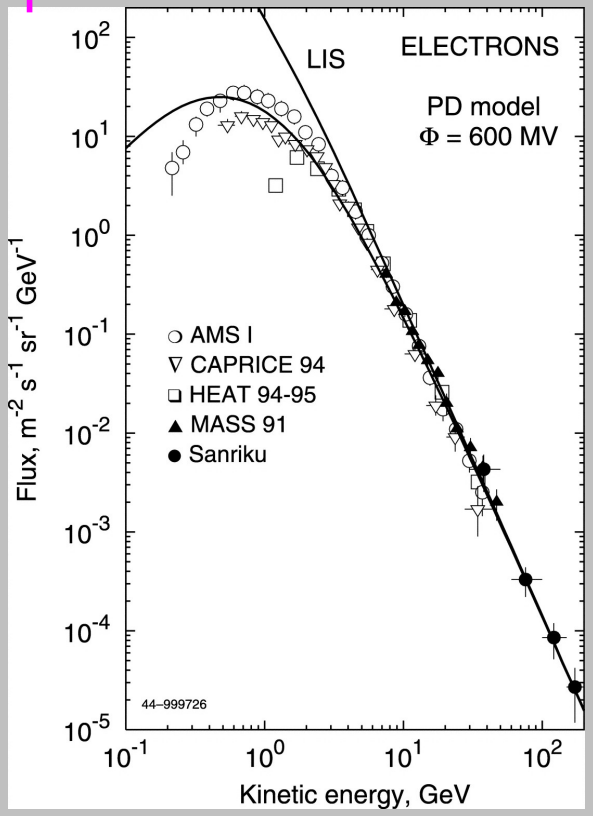

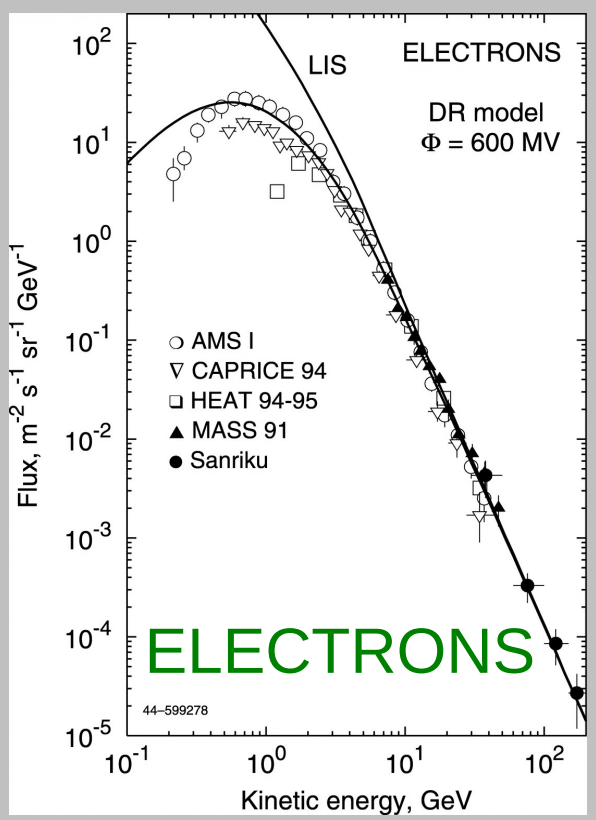

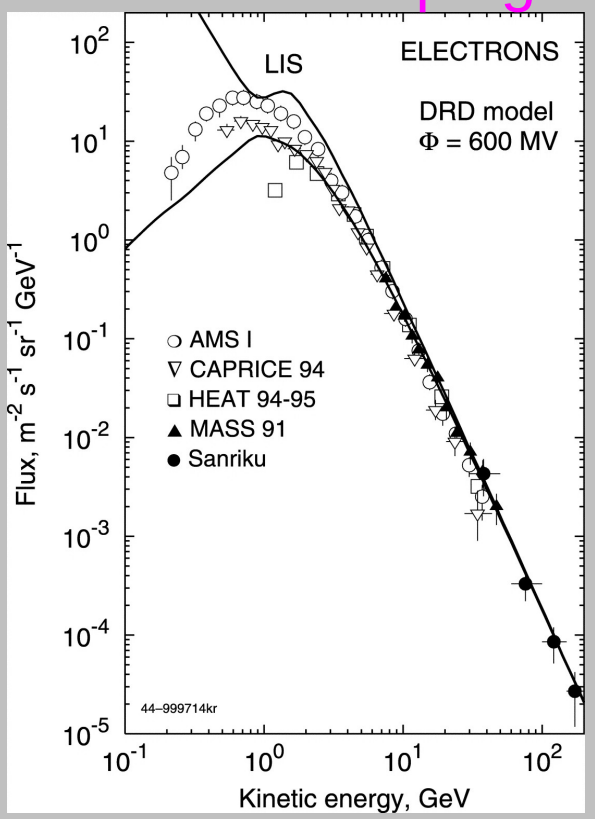

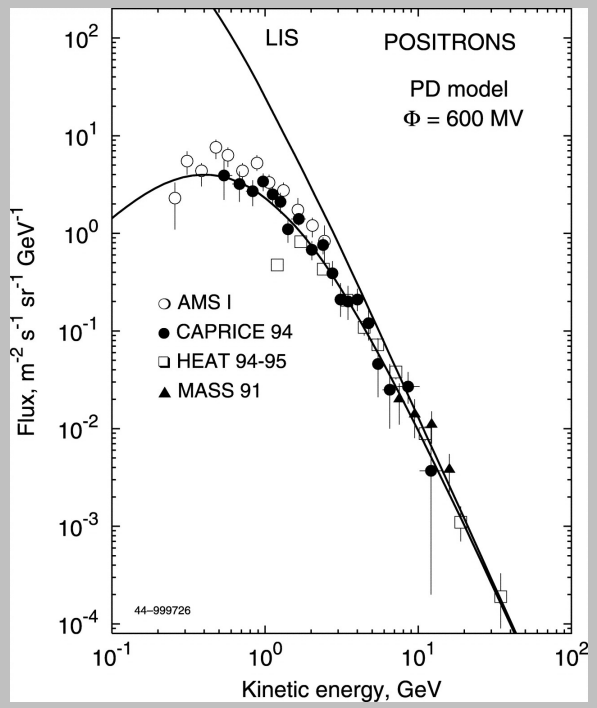

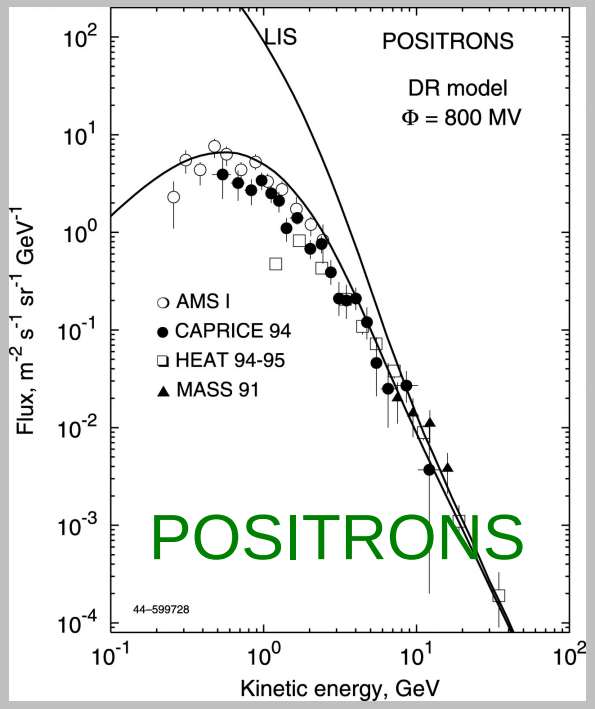

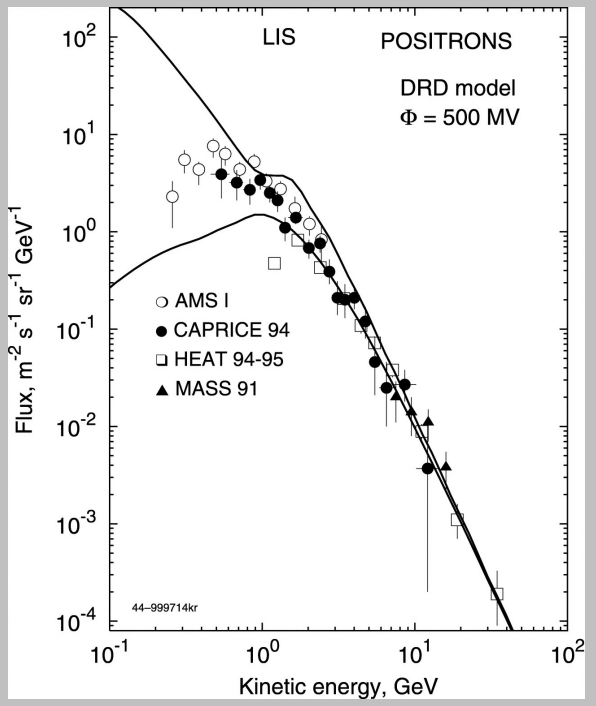

GALPROP retrospective

1993 start with student PhD idl
1995 fortran90 AWS + Igor Moskalenko
2000 c++ version
Troy Porter, Seth Digel, Gulli Johannesson, Elena Orlando
joined in following years

GALPROP owes part of success to long-term stable base over 20 years

Continuity is important!

Seemed an obvious idea in retrospect, why was it not done before?
Why so long before others followed?
Surprising that it is still the most-used programme on the market.

GALPROP developments 2013-2015 by AWS

Based on the 2011 public version 54,
(which was not followed by further releases by GALPROP team)

Available from sourceforge
ICRC 2015, arXiv:1507.05020 and updated Explanatory Supplement

>700 downloads so far

Enhancements:

Physical processes

Hadronic production cross sections QGSJET; Dermer for low energies
Hadronic energy losses via pion-production (were not included!)
Deuterium production by p-p fusion
Synchrotron radiation: polarization and new magnetic field models
Free-free emission in radio
Free-free absorption (radio low frequencies)

Cosmic-ray propagation

Accurate solution option. Avoids operator splitting and time-step fix.
Advantage: demonstrably steady-state solution, disadvantage: slow!
Anisotropic diffusion – perpendicular and parallel D can differ
Convective transport – more physical variation of velocity with z
Boundary condition: avoid forcing to zero at halo boundary. Not free escape!
Primary positrons; since now experimentally required.
spectrum and distribution independent from electrons

Formats:

HealPIX skymaps with energy in columns, compatible with CDS Aladin plotting package

Galactic cosmic-ray propagation in the light of AMS-02: I. Analysis of protons, helium, and antiprotons

Michael Korsmeier* and Alessandro Cuoco†
Institute for Theoretical Particle Physics and Cosmology, RWTH Aachen University, 52056 Aachen, Germany

arXiv:1607.06093 August 2016
GALPROP + MultiNest Bayesian analysis

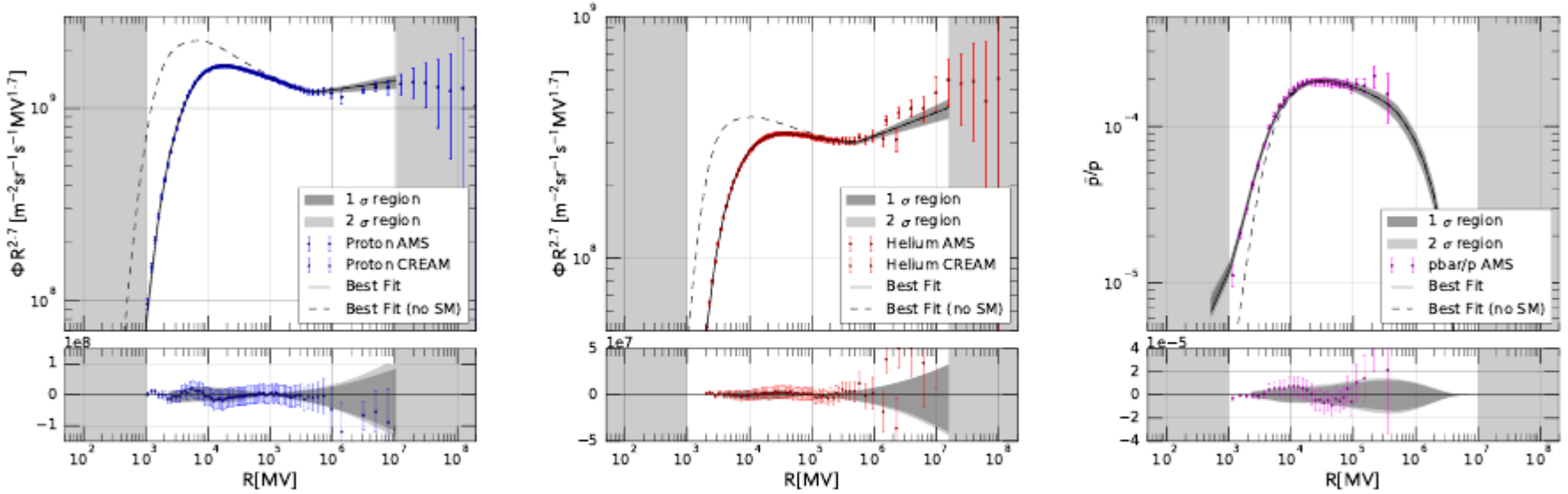

(a) Proton (b) Helium (c) $\bar{p}/p$

FIG. 11: Comparison between data and best-fit model for the global analysis including proton, helium, and antiprotons down to 1 GV (1GV).

Galactic cosmic-ray propagation in the light of AMS-02: I. Analysis of protons, helium, and antiprotons

Michael Korsmeier* and Alessandro Cuoco†
Institute for Theoretical Particle Physics and Cosmology, RWTH Aachen University, 52056 Aachen, Germany

arXiv:1607.06093 August 2016
GALPROP + MultiNest Bayesian analysis

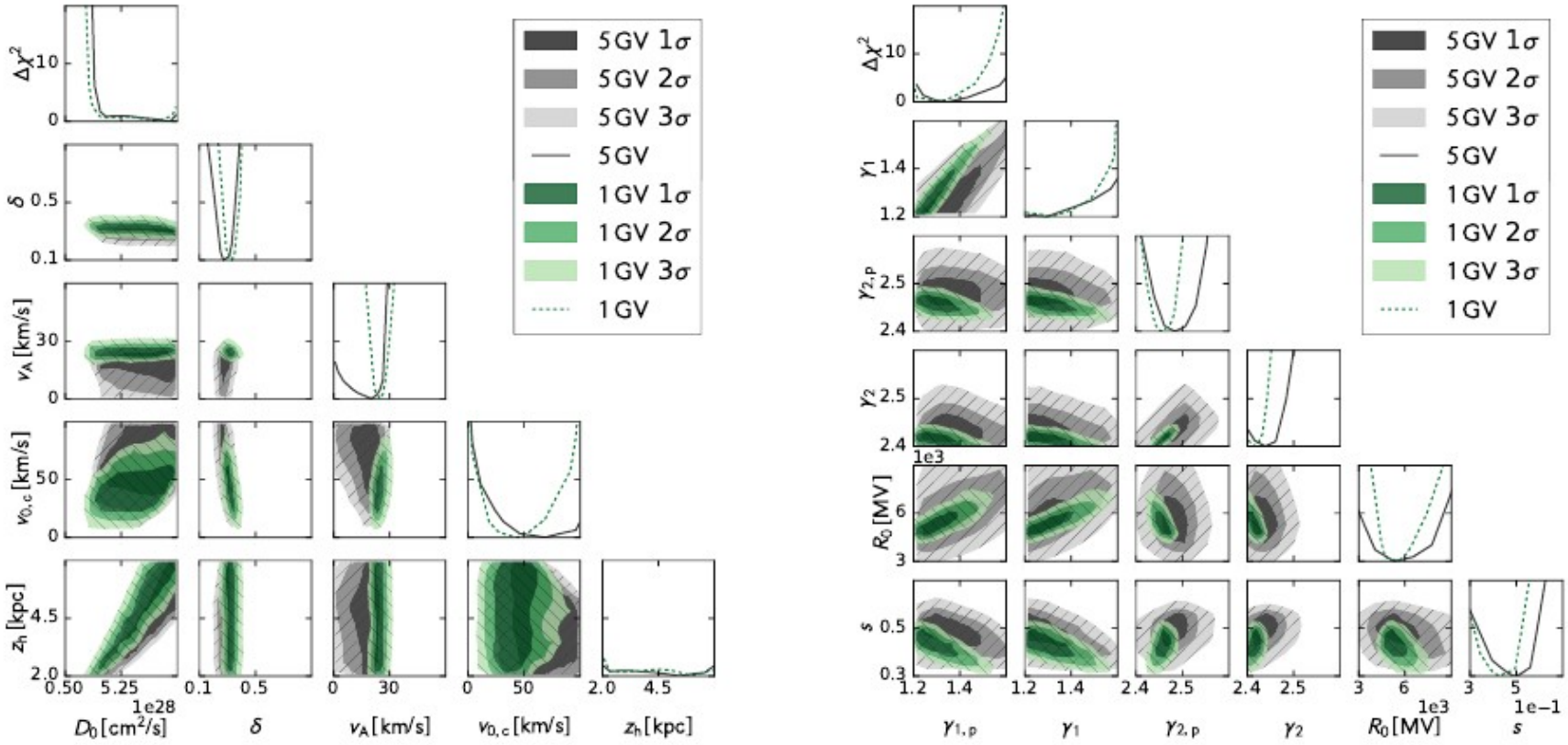

(a) Propagation parameters.

(b) Injection parameters

FIG. 10: Comparison of the baseline fit (main) to a fit including data down to 1 GV (1GV)for (a) propagation and (b) injection parameters.

GALPROP desiderata:

Update spallation cross-sections (e.g. DRAGON has FLUKA-based cross-sections)
Further improve hadronic production of gammas and e+-
Spiral and other structures
Replace old Fortran routines (!)
Free-escape at boundary: implement correctly

Keep improving/updating!
More involvement of other groups?

Combine forces with MHD Galactic modellers (see later).

In addition:

GALPLOT plotting package compatible with GALPROP
Cosmic-ray spectra, ratios, gamma rays, synchroton
Cosmic-ray database, compatible with Maurin's CRDB.
Fermi and other data, radio surveys
Publicly available

Various other tools:

Inverse Compton routines

Heliospheric and stellar inverse Compton: StellarICS package
(used by Fermi-LAT for diffuse emission model)

Synchrotron routines

More CR Propagation schemes

Evoli/ Gaggero/ Grasso/ di Bernardo+	**DRAGON, DRAGON2** PUBLIC
Ralf Kissman (Innsbruck)	**PICARD** **3D, not yet public**
David Maurin (Grenoble)	**USINE**: semi-analytical PUBLIC (?)
Büsching/Pohl	Green's function approach
DeMarco, Blasi, Stanev	Trajectory approach, for > 1 PeV
Philipp Girichidis (Munich)	MHD with CR = fluid
Michal Hanasz (Torun)	**PIERNIK** code: MHD, CR= fluid. CR-driven dynamo
Benyamin etal	Monte Carlo particle propagation
Tess Jaffe (Tououse)	**Hammurabi:** synchrotron/magnetic fields PUBLIC

DRAGON Cosmic-ray propagation package

Concept same as GALPROP

Newly written, improved structure

Extras w.r.t GALPROP:

Spatial dependence of diffusion coefficient
Full anisotropic diffusion tensor
Spatial grid size variation
FLUKA-based spallation cross-sections (Nicola Mazziotta, Bari)
Spiral structure

Public: used for various papers apart from DRAGON team.

DRAGON Cosmic-ray propagation package

Concept same as GALPROP

Newly written, improved structure

Extras w.r.t GALPROP:

Spatial dependence of diffusion coefficient
Full anisotropic diffusion tensor
Spatial grid size variation
FLUKA-based spallation cross-sections (Nicola Mazziotta, Bari)
Spiral structure

Public: used for various papers apart from DRAGON team.

Cosmic-ray propagation with DRAGON2: I. numerical solver and astrophysical ingredients

Carmelo Evoli[a] Daniele Gaggero[b] Andrea Vittino[c] Giuseppe Di Bernardo[d] Mattia Di Mauro[e] Arianna Ligorini[f] Piero Ullio[g] Dario Grasso[h]

[a]Gran Sasso Science Institute, viale Francesco Crispi 7, 67100 L'Aquila (AQ), Italy

[b]GRAPPA Institute, University of Amsterdam, Science Park 904, 1090 GL Amsterdam, The Netherlands

[c]Physik-Department T30d, Technische Universität München, James-Franck-Straße 1, D-85748 Garching, Germany

[d]Max-Planck-Institut für Astrophysik, Karl-Schwarzschild-Straße 1, 85740 Garching bei München, Germany

[e]W. W. Hansen Experimental Physics Laboratory, Kavli Institute for Particle Astrophysics and Cosmology, Department of Physics and SLAC National Accelerator Laboratory, Stanford University, Stanford, CA 94305, USA

[f]Institut Fizyky Jądrowej - PAN, ul. Radzikowskiego 152, 31-342 Kraków, Poland

[g]Scuola Internazionale di Studi Superiori Avanzati, via Bonomea 265, 34136 Trieste, Italy

[h]INFN and Dipartimento di Fisica "E. Fermi", Pisa University, Largo B. Pontecorvo 3, I-56127 Pisa, Italy

28 July 2016 arXiv:1607.07886 Very extensive exposition.

DRAGON2
New version, released July 2016.

Extensive rewrite of DRAGON.

Main extensions in DRAGON2

Non-separable in space and momentum diffusion and source term
Anisotropic diffusion
More advection models
Hadronic momentum losses for all nuclei
2nd order discretization for momentum losses
Alternative boundary conditions for momentum diffusion
New modular C++ structure with class inheritance to easily add user-provider models

DRAGON2: example with spatially varying anisotropic diffusion coefficient

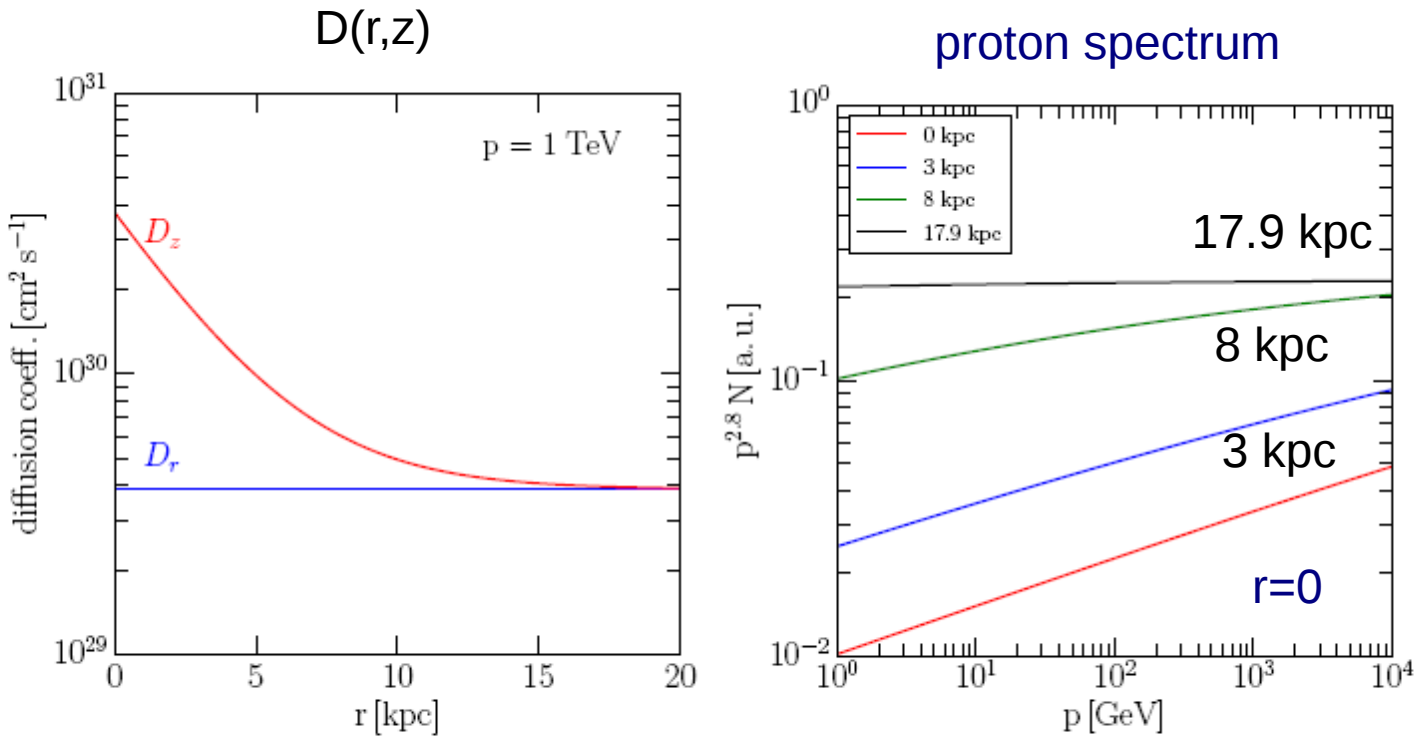

Figure 12. *Left panel:* profiles of the diffusion coefficients along r and z for particles with $p = 1TeV$ are shown. *Right panel:* energy spectrum computed at different radial distances from the Galactic Centre.

DRAGON2: example with single CR source and anisotropic diffusion coefficient

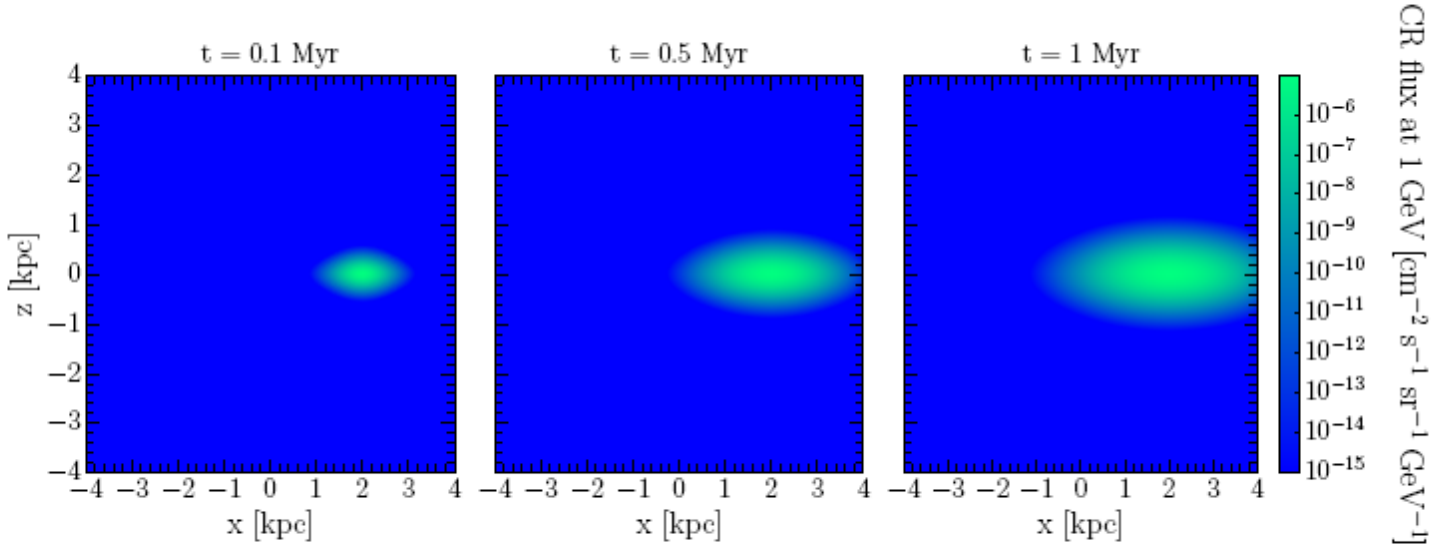

Figure 13. CR density in the x-z plane at different times; CRs are propagating anisotropically, with slower diffusion in the z direction.

PICARD Cosmic-ray propagation package.

Uni Innsbruck: Ralf Kissmann, (Michael Werner), Olaf Reimer with AWS@MPE
New student now working on PICARD at Innsbruck.

Fully 3D from outset.
Modern numerical techniques for solving cosmic-ray propagation.
Accurate and fast. Full MPI parallelization.
This allows fine 3D spatial resolution with reasonable CPU resources.
Spiral structure incorporated.
Uses *hdf5* for model storage (more flexible than *FITS* for 3D models)

Werner, M. et al. 2015, Astroparticle Physics 64, 18 : CR protons, electrons and spiral arms
Kissmann, R. et al. 2015, Astroparticle Physics 70, 39 : secondary/primary ratios

Synchrotron, B-fields: not yet, but foreseen. Fits well into 3D scheme.
Will allow all components to be accurately included.

A public version is planned sometime in the future.

Probably PICARD will replace GALPROP in the long term.

Anyway good to have multiple CR propagation packages:
e.g. GALPROP, DRAGON, PICARD
for cross-checks and healthy competition.

Propagation in 3D spiral-arm cosmic-ray source distribution models and secondary particle production using PICARD

R. Kissmann [a,*], M. Werner [a], O. Reimer [a], A.W. Strong [b]

[a] Institut für Astro- und Teilchenphysik, Leopold-Franzens-Universität Innsbruck, A-6020 Innsbruck, Austria
[b] Max Planck Institut für extraterrestrische Physik, Postfach 1312, D-85741 Garching, Germany

Kissmann, R. et al. 2015, Astroparticle Physics 70, 39

Features of Picard

Solver

- Steady-state solution
- Explicit time integrator
- MPI-parallel
- Improved nuclear network
- Speed

Example Resolution

- Standard CR simulation (e.g., Fermi Diffuse Paper)
  - 2D (1 kpc $\times$ 100 pc)
- Picard
  - 3D (up to $\sim$75 pc^3)

Example Simulation Results

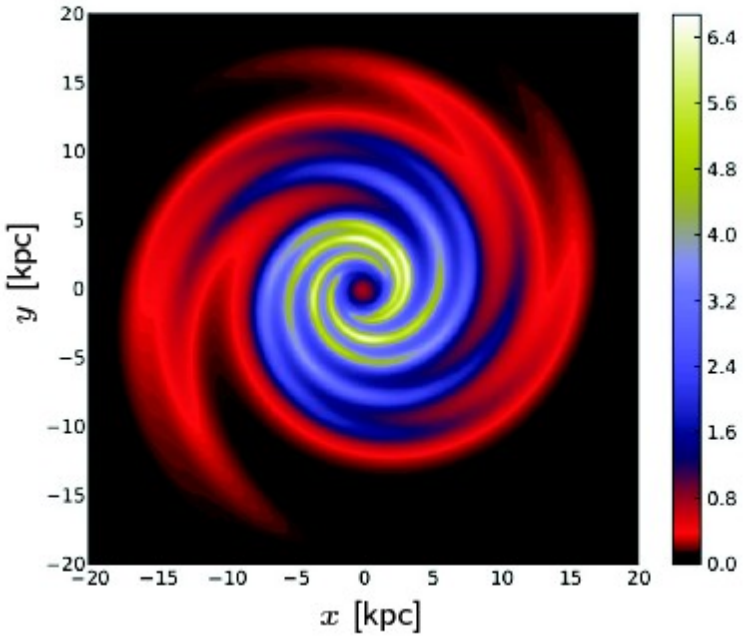

(RK et al. (2014))

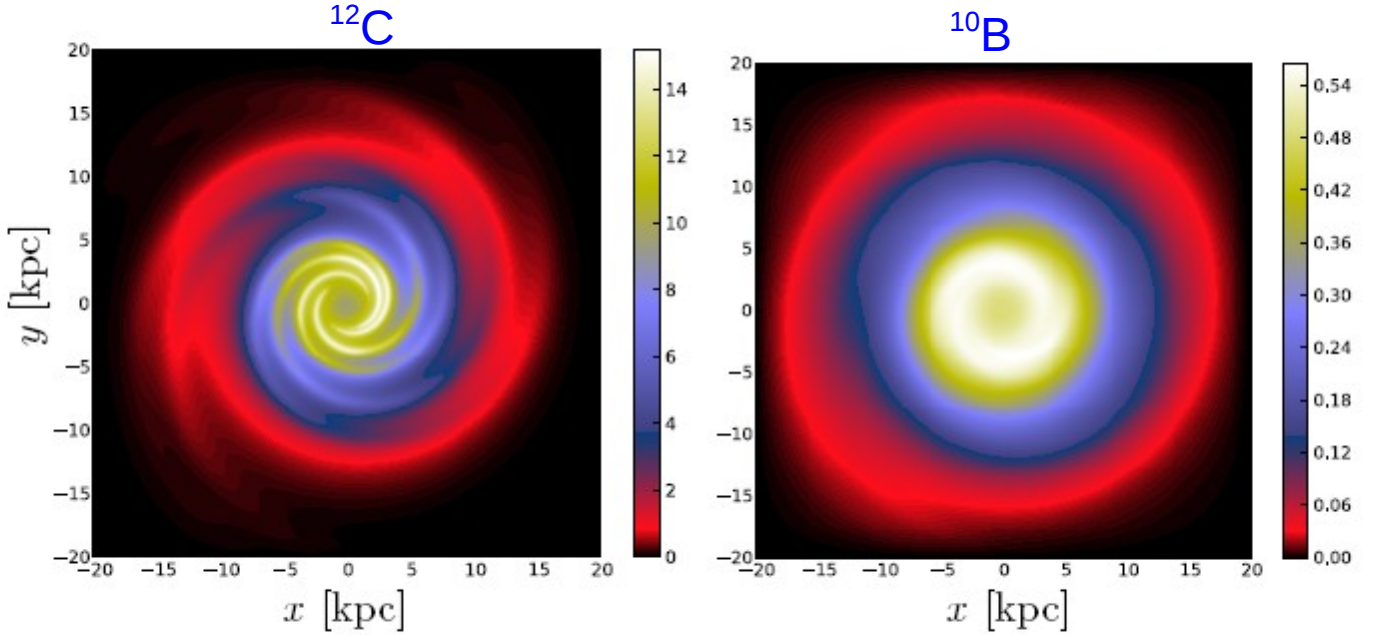

secondaries smoother than primaries

Fig. 2. Cosmic-ray flux in the Galactic plane at an energy of ~10 GeV/nucleon for the Steiman source distribution in model z4R20. Data are given in units of GeV/nucleon/m^{2}s sr. On the left the flux for ^{12}C as a standard primary is shown and on the right the flux for ^{10}B as a standard secondary.

R. Kissmann et al./Astroparticle Physics 70 (2015) 39–53

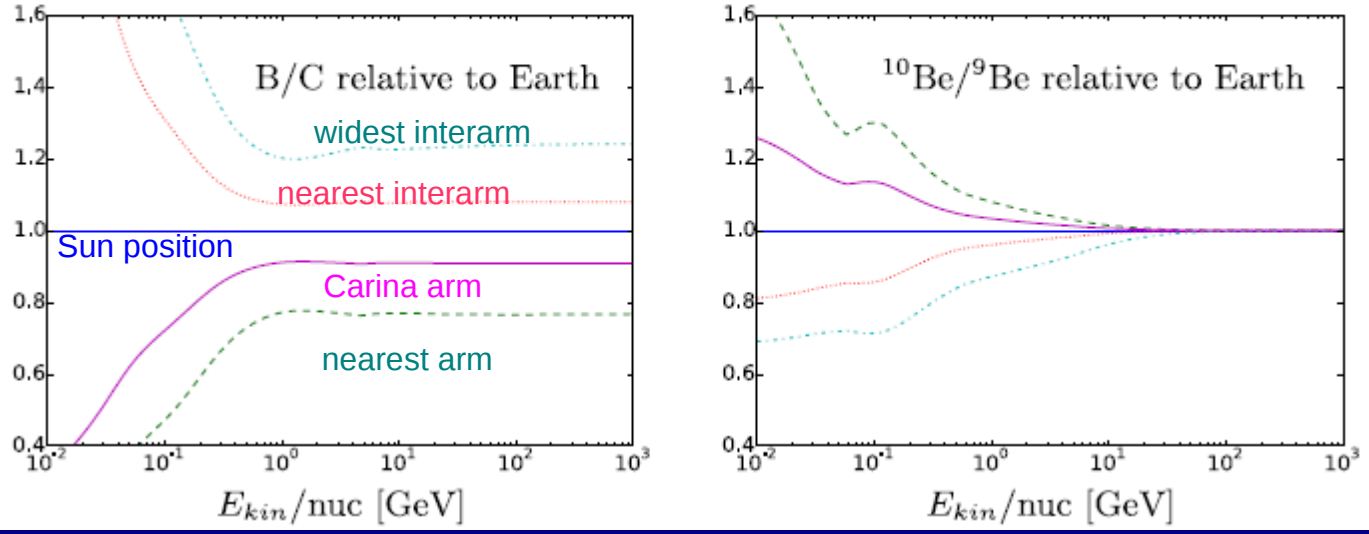

Deviations relative to the spectrum at the nominal position of Earth (solid blue line) are shown for the nearest spiral arm (green dashed line), the nearest inter-arm position (red dotted line), the widest inter-arm region (cyan dash-dotted line), and an intermediate position in the direction of the Carina arm (solid magenta line). (For interpretation

PICARD Cosmic-ray propagation package.

Werner, M. et al. 2015, Astroparticle Physics 64, 18 : CR and spiral arms

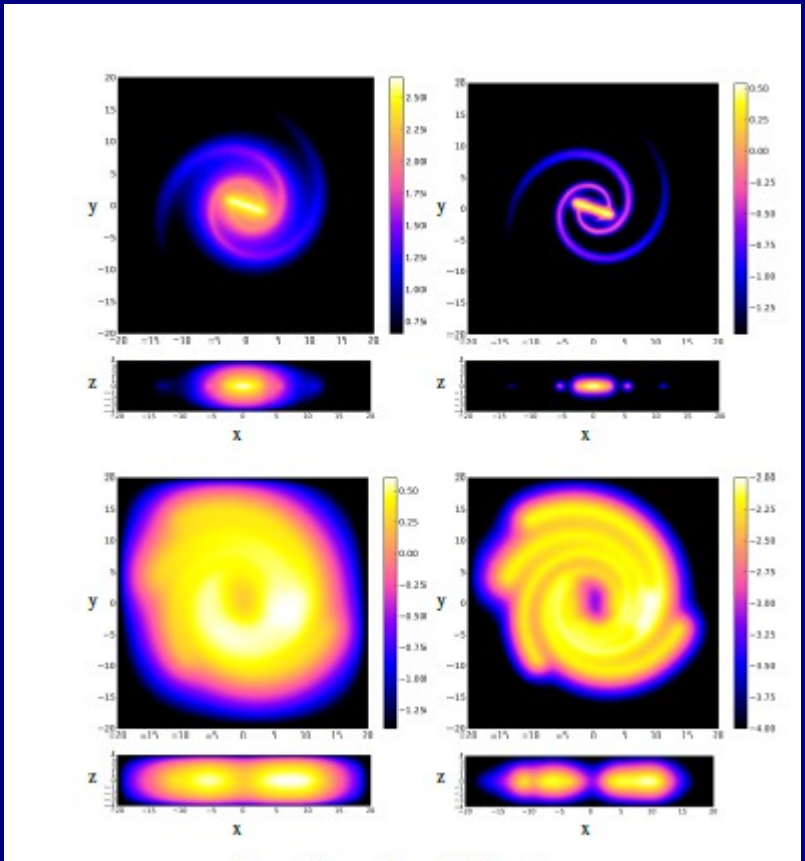

Figure 4: Same as Figure 3, but for electrons.

Cosmic-ray electrons, for 4 different spiral-arm source distributions

Future of modelling cosmic rays in the Galaxy.

GALPROP & co are phenomelogical i.e. just propagation equation with given parameters.

e.g. halo is just region with ad-hoc boundary, no physics.

But cosmic rays have dynamical effects.

Example from Philipp Girichidis (MPA Garching) et al.

Cosmic-ray driven wind from supernovae

includes chemistry.

Cosmic rays treated as relativistic gas, no energy spectrum.

Future: put in energy-dependence, secondary production etc.

Test against cosmic-ray, gamma-ray data.

The Astrophysical Journal Letters, 816:L19 (6pp), 2016 January 10 doi:10.3847/2041-8205/816/2/L19

LAUNCHING COSMIC-RAY-DRIVEN OUTFLOWS FROM THE MAGNETIZED INTERSTELLAR MEDIUM

Philipp Girichidis[1], Thorsten Naab[1], Stefanie Walch[2], Michał Hanasz[3], Mordecai-Mark Mac Low[4,5], Jeremiah P. Ostriker[6], Andrea Gatto[1], Thomas Peters[1], Richard Wünsch[7], Simon C. O. Glover[5], Ralf S. Klessen[5], Paul C. Clark[8], and Christian Baczynski[5]
[1] Max-Planck-Institut für Astrophysik, Karl-Schwarzschild-Str. 1, D-85741 Garching, Germany
[2] Physikalisches Institut, Universität zu Köln, Zülpicher Str. 77, D-50937 Köln, Germany
[3] Centre for Astronomy, Nicolaus Copernicus University, Faculty of Physics, Astronomy and Informatics, Grudziadzka 5, PL-87100 Toruń, Poland
[4] Department of Astrophysics, American Museum of Natural History, 79th Street at Central Park West, New York, NY 10024, USA
[5] Universität Heidelberg, Zentrum für Astronomie, Institut für Theoretische Astrophysik, Albert-Ueberle-Str. 2, D-69120 Heidelberg, Germany
[6] Department of Astronomy, Columbia University, 1328 Pupin Hall, 550 West 120th Street, New York, NY 10027, USA
[7] Astronomical Institute, Academy of Sciences of the Czech Republic, Bocni II 1401, 141 31 Prague, Czech Republic
[8] School of Physics & Astronomy, Cardiff University, 5 The Parade, Cardiff CF24 3AA, Wales, UK

$$\frac{\partial \rho}{\partial t} + \nabla \cdot (\rho \boldsymbol{v}) = 0$$

$$\frac{\partial \rho \boldsymbol{v}}{\partial t} + \nabla \cdot \left(\rho \boldsymbol{v}\boldsymbol{v}^{\mathrm{T}} - \frac{\boldsymbol{B}\boldsymbol{B}^{\mathrm{T}}}{4\pi} \right) + \nabla p_{\mathrm{tot}} = \rho \boldsymbol{g}$$

$$\frac{\partial e}{\partial t} + \nabla \cdot \left[(e + p_{\mathrm{tot}})\boldsymbol{v} - \frac{\boldsymbol{B}(\boldsymbol{B} \cdot \boldsymbol{v})}{4\pi} \right] = \rho \boldsymbol{v} \cdot \boldsymbol{g} + \nabla \cdot \mathsf{K} \nabla e_{\mathrm{CR}} + \dot{u}_{\mathrm{chem}} + \dot{u}_{\mathrm{inj}}$$

$$\frac{\partial \boldsymbol{B}}{\partial t} - \nabla \times (\boldsymbol{v} \times \boldsymbol{B}) = 0$$

$$\frac{\partial e_{\mathrm{CR}}}{\partial t} + \nabla \cdot (e_{\mathrm{CR}} \boldsymbol{v}) = -p_{\mathrm{CR}} \nabla \cdot \boldsymbol{v} + \nabla \cdot (\mathsf{K} \nabla e_{\mathrm{CR}}) + Q_{\mathrm{CR}}.$$

The Astrophysical Journal Letters, 816:L19 (6pp), 2016 January 10 doi:10.3847/2041-8205/816/2/L19

LAUNCHING COSMIC-RAY-DRIVEN OUTFLOWS FROM THE MAGNETIZED INTERSTELLAR MEDIUM

Philipp Girichidis[1], Thorsten Naab[1], Stefanie Walch[2], Michał Hanasz[3], Mordecai-Mark Mac Low[4,5], Jeremiah P. Ostriker[6], Andrea Gatto[1], Thomas Peters[1], Richard Wünsch[7], Simon C. O. Glover[5], Ralf S. Klessen[5], Paul C. Clark[8], and Christian Baczynski[5]
[1] Max-Planck-Institut für Astrophysik, Karl-Schwarzschild-Str. 1, D-85741 Garching, Germany
[2] Physikalisches Institut, Universität zu Köln, Zülpicher Str. 77, D-50937 Köln, Germany
[3] Centre for Astronomy, Nicolaus Copernicus University, Faculty of Physics, Astronomy and Informatics, Grudziadzka 5, PL-87100 Toruń, Poland
[4] Department of Astrophysics, American Museum of Natural History, 79th Street at Central Park West, New York, NY 10024, USA
[5] Universität Heidelberg, Zentrum für Astronomie, Institut für Theoretische Astrophysik, Albert-Ueberle-Str. 2, D-69120 Heidelberg, Germany
[6] Department of Astronomy, Columbia University, 1328 Pupin Hall, 550 West 120th Street, New York, NY 10027, USA
[7] Astronomical Institute, Academy of Sciences of the Czech Republic, Bocni II 1401, 141 31 Prague, Czech Republic
[8] School of Physics & Astronomy, Cardiff University, 5 The Parade, Cardiff CF24 3AA, Wales, UK

Modified FLASH code

$$\frac{\partial \rho}{\partial t} + \nabla \cdot (\rho \boldsymbol{v}) = 0$$

$$\frac{\partial \rho \boldsymbol{v}}{\partial t} + \nabla \cdot \left(\rho \boldsymbol{v}\boldsymbol{v}^{\mathrm{T}} - \frac{\boldsymbol{B}\boldsymbol{B}^{\mathrm{T}}}{4\pi} \right) + \nabla p_{\mathrm{tot}} = \rho \boldsymbol{g}$$

$$\frac{\partial e}{\partial t} + \nabla \cdot \left[(e + p_{\mathrm{tot}})\boldsymbol{v} - \frac{\boldsymbol{B}(\boldsymbol{B} \cdot \boldsymbol{v})}{4\pi} \right] = \rho \boldsymbol{v} \cdot \boldsymbol{g} + \dot{u}_{\mathrm{chem}} + \dot{u}_{\mathrm{inj}}$$

$$\frac{\partial \boldsymbol{B}}{\partial t} - \nabla \times (\boldsymbol{v} \times \boldsymbol{B}) = 0$$

$$p_{\mathrm{tot}} = p_{\mathrm{th}} + p_{\mathrm{mag}}$$

$$e = \rho v^2/2 + e_{\mathrm{th}} + B^2/8\pi$$

The Astrophysical Journal Letters, 816:L19 (6pp), 2016 January 10 doi:10.3847/2041-8205/816/2/L19

LAUNCHING COSMIC-RAY-DRIVEN OUTFLOWS FROM THE MAGNETIZED INTERSTELLAR MEDIUM

Philipp Girichidis[1], Thorsten Naab[1], Stefanie Walch[2], Michał Hanasz[3], Mordecai-Mark Mac Low[4,5], Jeremiah P. Ostriker[6], Andrea Gatto[1], Thomas Peters[1], Richard Wünsch[7], Simon C. O. Glover[5], Ralf S. Klessen[5], Paul C. Clark[8], and Christian Baczynski[5]
[1] Max-Planck-Institut für Astrophysik, Karl-Schwarzschild-Str. 1, D-85741 Garching, Germany
[2] Physikalisches Institut, Universität zu Köln, Zülpicher Str. 77, D-50937 Köln, Germany
[3] Centre for Astronomy, Nicolaus Copernicus University, Faculty of Physics, Astronomy and Informatics, Grudziadzka 5, PL-87100 Toruń, Poland
[4] Department of Astrophysics, American Museum of Natural History, 79th Street at Central Park West, New York, NY 10024, USA
[5] Universität Heidelberg, Zentrum für Astronomie, Institut für Theoretische Astrophysik, Albert-Ueberle-Str. 2, D-69120 Heidelberg, Germany
[6] Department of Astronomy, Columbia University, 1328 Pupin Hall, 550 West 120th Street, New York, NY 10027, USA
[7] Astronomical Institute, Academy of Sciences of the Czech Republic, Bocni II 1401, 141 31 Prague, Czech Republic
[8] School of Physics & Astronomy, Cardiff University, 5 The Parade, Cardiff CF24 3AA, Wales, UK

Modified FLASH code

$$\frac{\partial \rho}{\partial t} + \nabla \cdot (\rho \boldsymbol{v}) = 0$$

$$\frac{\partial \rho \boldsymbol{v}}{\partial t} + \nabla \cdot \left(\rho \boldsymbol{v}\boldsymbol{v}^{\mathrm{T}} - \frac{\boldsymbol{B}\boldsymbol{B}^{\mathrm{T}}}{4\pi} \right) + \nabla p_{\mathrm{tot}} = \rho \boldsymbol{g}$$

$$\frac{\partial e}{\partial t} + \nabla \cdot \left[(e + p_{\mathrm{tot}})\boldsymbol{v} - \frac{\boldsymbol{B}(\boldsymbol{B} \cdot \boldsymbol{v})}{4\pi} \right] = \rho \boldsymbol{v} \cdot \boldsymbol{g} + \nabla \cdot \mathsf{K} \nabla e_{\mathrm{CR}} + \dot{u}_{\mathrm{chem}} + \dot{u}_{\mathrm{inj}}$$

$$\frac{\partial \boldsymbol{B}}{\partial t} - \nabla \times (\boldsymbol{v} \times \boldsymbol{B}) = 0$$

$$\frac{\partial e_{\mathrm{CR}}}{\partial t} + \nabla \cdot (e_{\mathrm{CR}} \boldsymbol{v}) = -p_{\mathrm{CR}} \nabla \cdot \boldsymbol{v} + \nabla \cdot (\mathsf{K} \nabla e_{\mathrm{CR}}) + Q_{\mathrm{CR}}.$$

$$p_{\mathrm{tot}} = p_{\mathrm{th}} + p_{\mathrm{CR}} + p_{\mathrm{mag}}$$

$$e = \rho v^2/2 + e_{\mathrm{th}} + e_{\mathrm{CR}} + B^2/8\pi$$

Supernovae energy input

only thermal only cosmic rays both

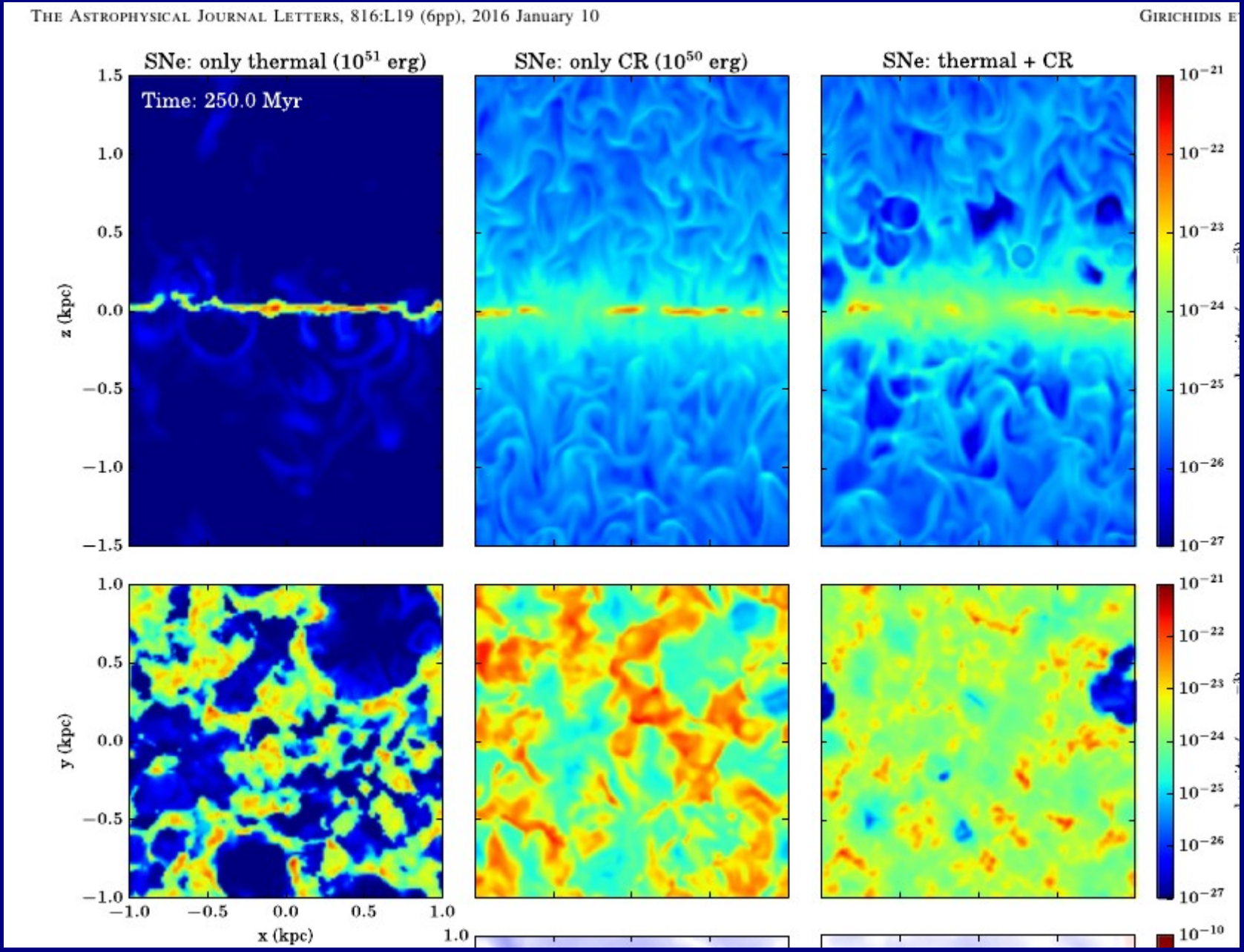

Time-dependent simulations avaiable for download

Cosmic rays increase vertical gas scale

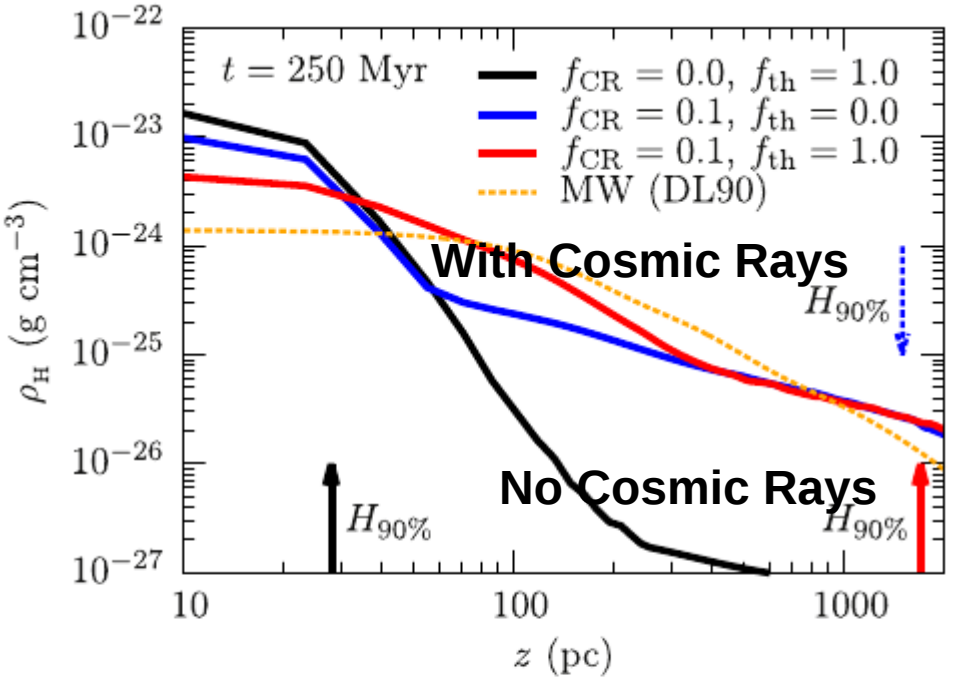

Figure 2. Vertical profiles of the total gas density for all simulations. The arrows indicate the height of 90% enclosed mass. A fit to the observed density profile of the solar neighborhood (Dickey & Lockman 1990) are shown in yellow. Thermal energy injection alone leads to a compact atomic gas distribution. Including CR feedback results in very extended distributions, which are much closer to the observed extent of the gas. The profiles indicate that CRs have their main impact at larger altitudes.

1. Including CRs thickens the galactic disk. The height of 90% enclosed total mass is found to be ∼1.5 kpc in the case of 10% CR energy injection per SN after 250 Myr and to increase continuously. Comparison with the vertical density distribution in the MW indicates good agreement.
2. We find that CRs quickly lead to the formation of a warm and neutral galactic atmosphere providing a mass reservoir for galactic winds and outflows. Whereas the thermal contribution of the SNe mainly shapes the disk close to the midplane, the additional CR energy shows the strongest impact above the disk and in the halo.
3. All simulations drive gas out of the midplane with little variation over time. For purely thermal SN feedback, the outflows are hot and composed of mainly ionized hydrogen with rates below the star formation rate. They are fast (up to $\sim$ a few 100 km s^{-1}) with low densities ($\rho \lesssim 10^{-27}$ g cm^{-3}). CRs alone can drive outflows with mass loading factors of order unity, which are warm (10^4 K) and mainly composed of atomic hydrogen. They are a factor of a few slower ($\sim$10–50 km s^{-1}) and 1–2 orders of magnitude denser ($\rho \sim 10^{-26}$–10^{-25} g cm^{-3}) compare to their thermally driven counterparts.

Future work in context of cosmic-ray physics:

* Test such cosmic-ray-driven wind models against cosmic-ray and gamma-ray data.
* Extend models to include energy spectrum of cosmic rays (at present just a single fluid)
* Use to make GALPROP-like approaches more physical for convection and halo structure instead of simple pre-defined forms.

Exploiting gamma rays

1 – 10 GeV

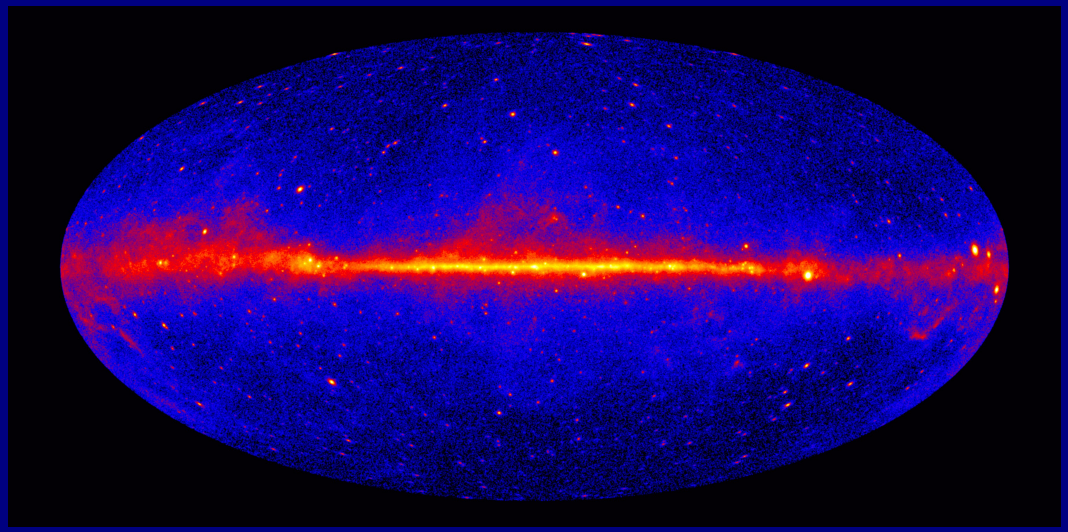

Cosmic-ray protons interacting with gas : hadronic (pion-decay)

Cosmic-ray electrons and positrons interacting with gas : bremsstrahlung

interacting with interstellar radiation : inverse Compton

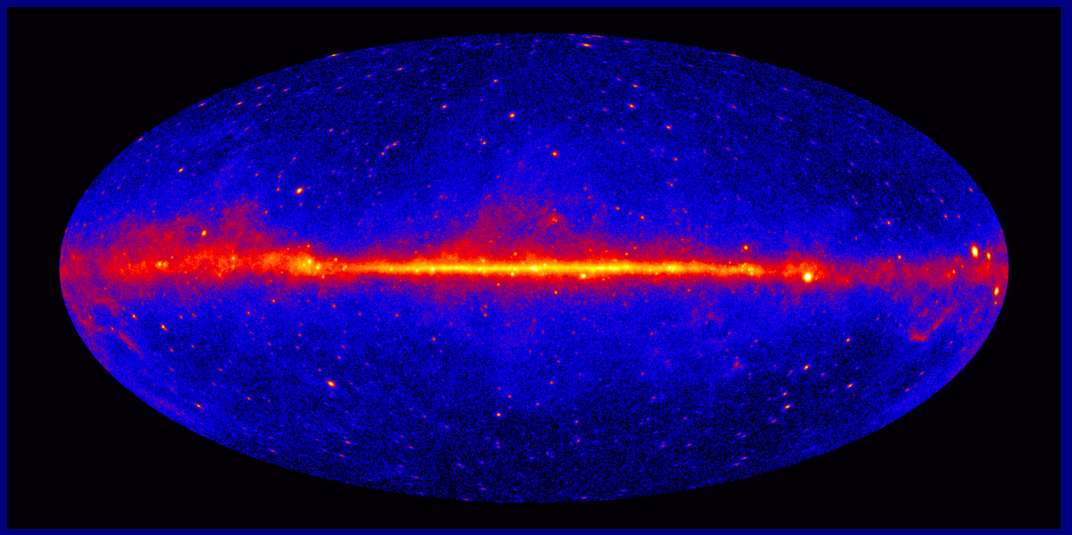

2 years

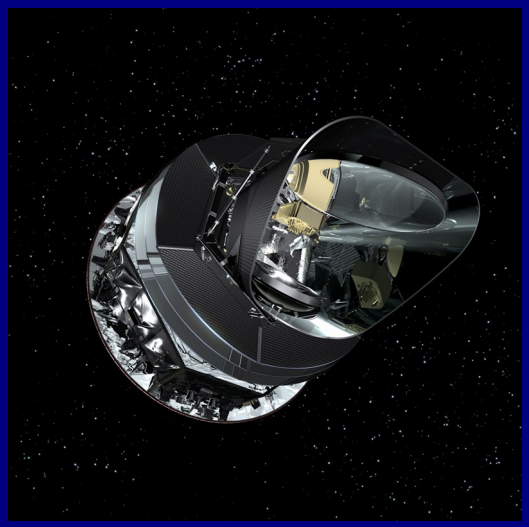

1 year

A lot of common astrophysics, cosmic rays, gas, magnetic fields !

Fermi-LAT
Inner Galaxy Gamma Ray Spectrum

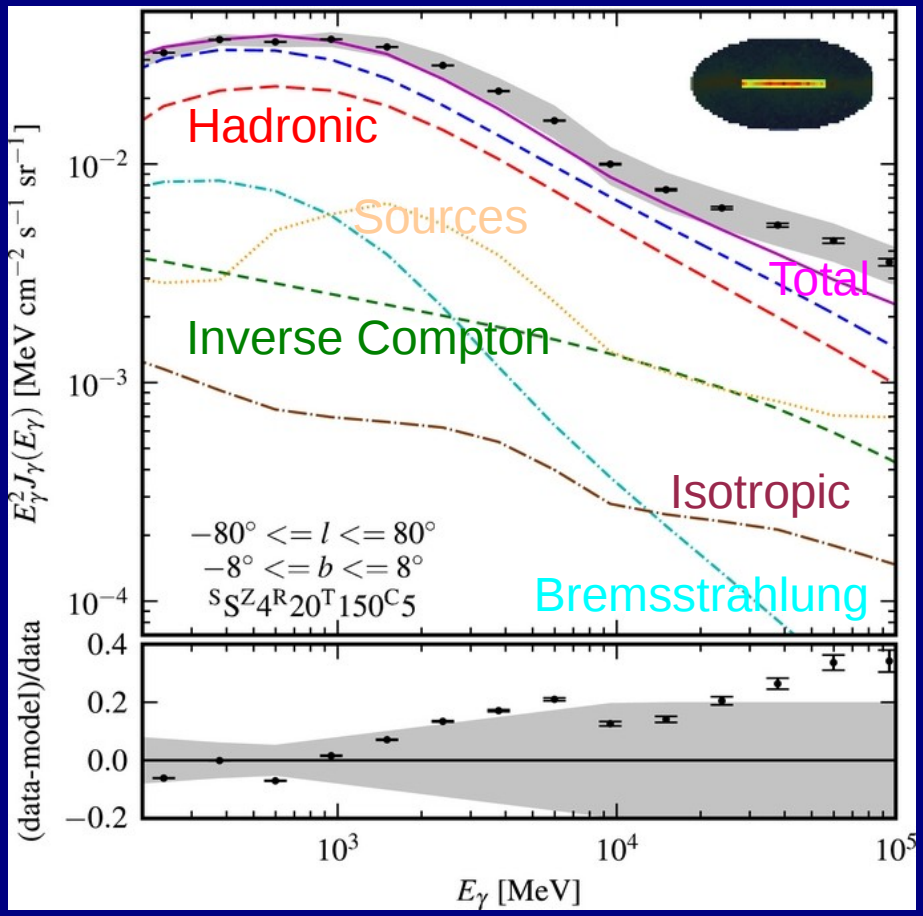

Ackermann et al. ApJ 750, 3 (2012)

Gamma-ray sky points to radial gradients in cosmic-ray transport

Daniele Gaggero,[1,2,*] Alfredo Urbano,[1,†] Mauro Valli,[1,2,‡] and Piero Ullio[1,2,§]

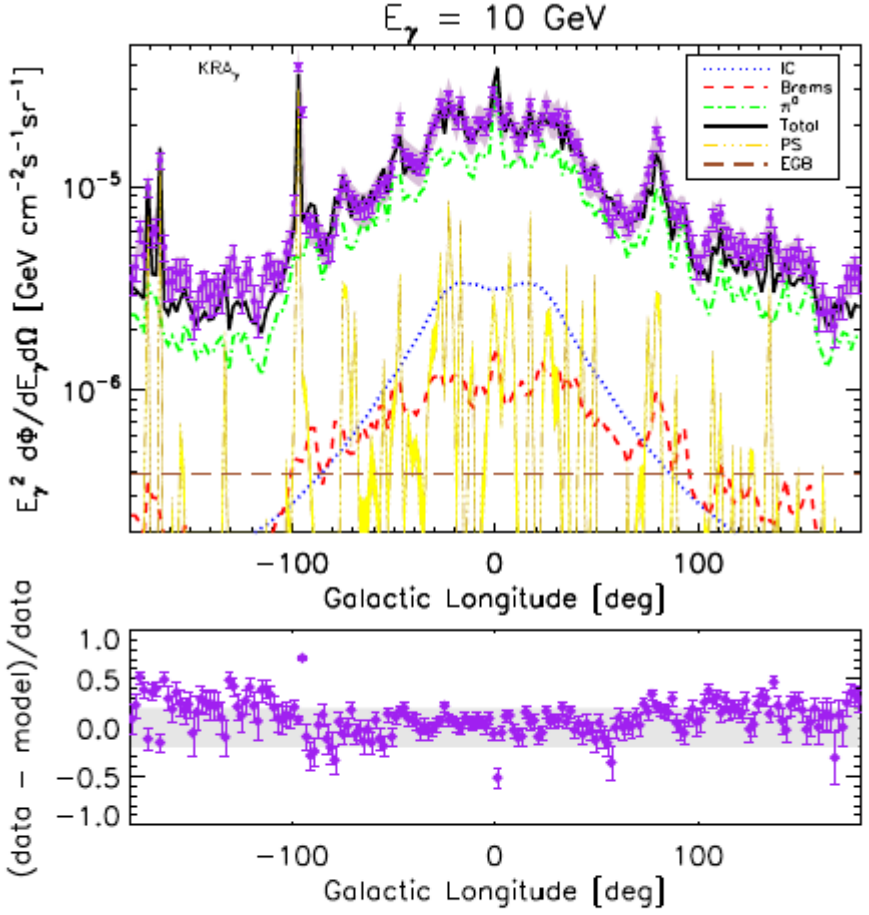

FIG. 8. *Longitudinal profile at fixed energy* $E_\gamma = 10$ *GeV. We average in latitude over the interval* $|b| < 5^\circ$.

Gamma-ray sky points to radial gradients in cosmic-ray transport

Daniele Gaggero,[1,2,*] Alfredo Urbano,[1,†] Mauro Valli,[1,2,‡] and Piero Ullio[1,2,§]

Phys. Rev. D 91, 083012 (2015)

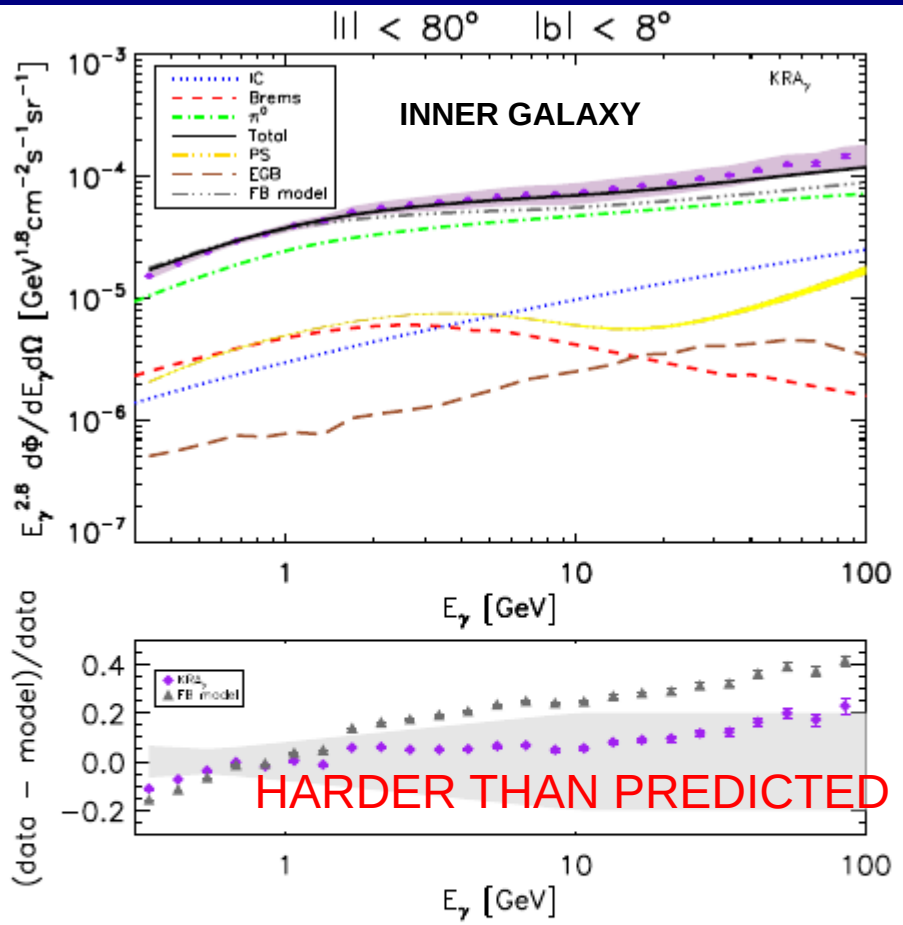

FIG. 1. *Upper panel. Comparison between the γ-ray flux computed with the CR propagation model proposed in this Letter (KRA$_\gamma$ total flux: solid black line; individual components shown) and the* Fermi-LAT *data (purple dots, including both statistic and systematic errors) in the Galactic disk. For comparison, we also show the total flux for the FB model defined in ref. [1] (double dot-dashed gray line). Lower panel. Residuals computed for the KRA$_\gamma$ and FB models.*

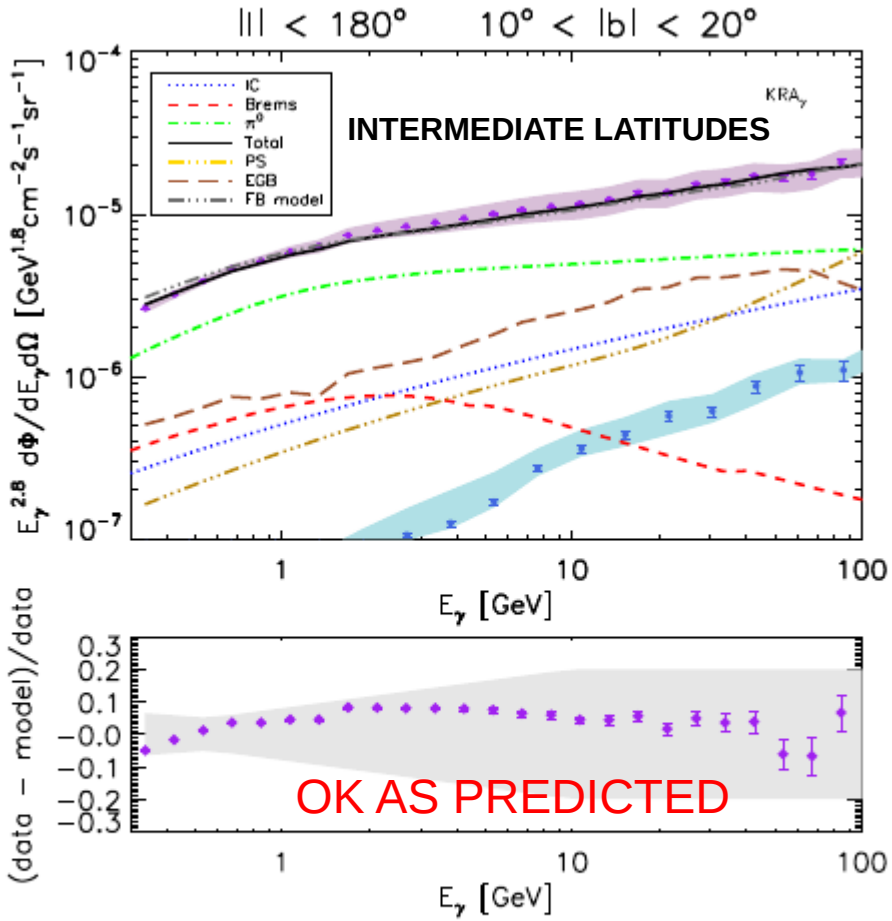

FIG. 7. *The same as in fig. [1] but considering the strip $|l| < 180°$, $10° < |b| < 20°$. The azure band represents the contribution of the Fermi bubbles according to ref. [37].*

Interstellar gamma-ray spectrum

Harder gamma-ray spectrum in Galactic plane than expected from local cosmic-ray proton spectrum via pion-decay

Gaggero etal. 2015 invoke spatially varying momentum-dependence of diffusion coeffiicient.

But since Galactic plane spectrum is harder than local, can be just a local CR source

Then spectral index in the plane is the “normal” one!

THIS IS A BIG EFFECT AND DESERVES MORE ATTENTION!

Potpourri of related topics to mention

David Maurin etal CR database: wonderful facility!
CRDB lpsc.in2p3.fr/cosmic-rays-db

Sample plot: Carbon

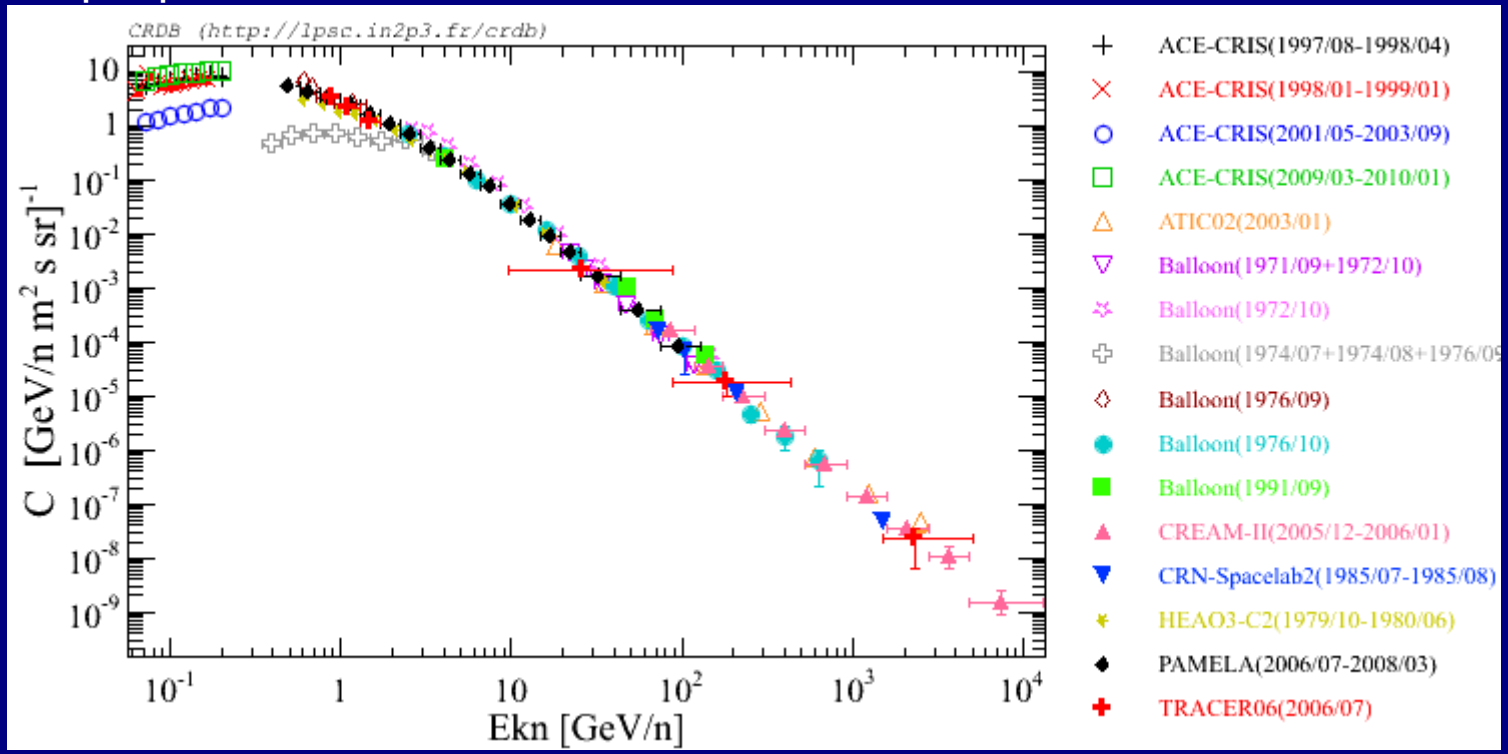

Enhances value of experiments, surprising little attention devoted to this before.
Replaces earlier compilation by Strong & Moskalenko.
Live demo can be performed.

Galaxy luminosity over 20 decades of energy

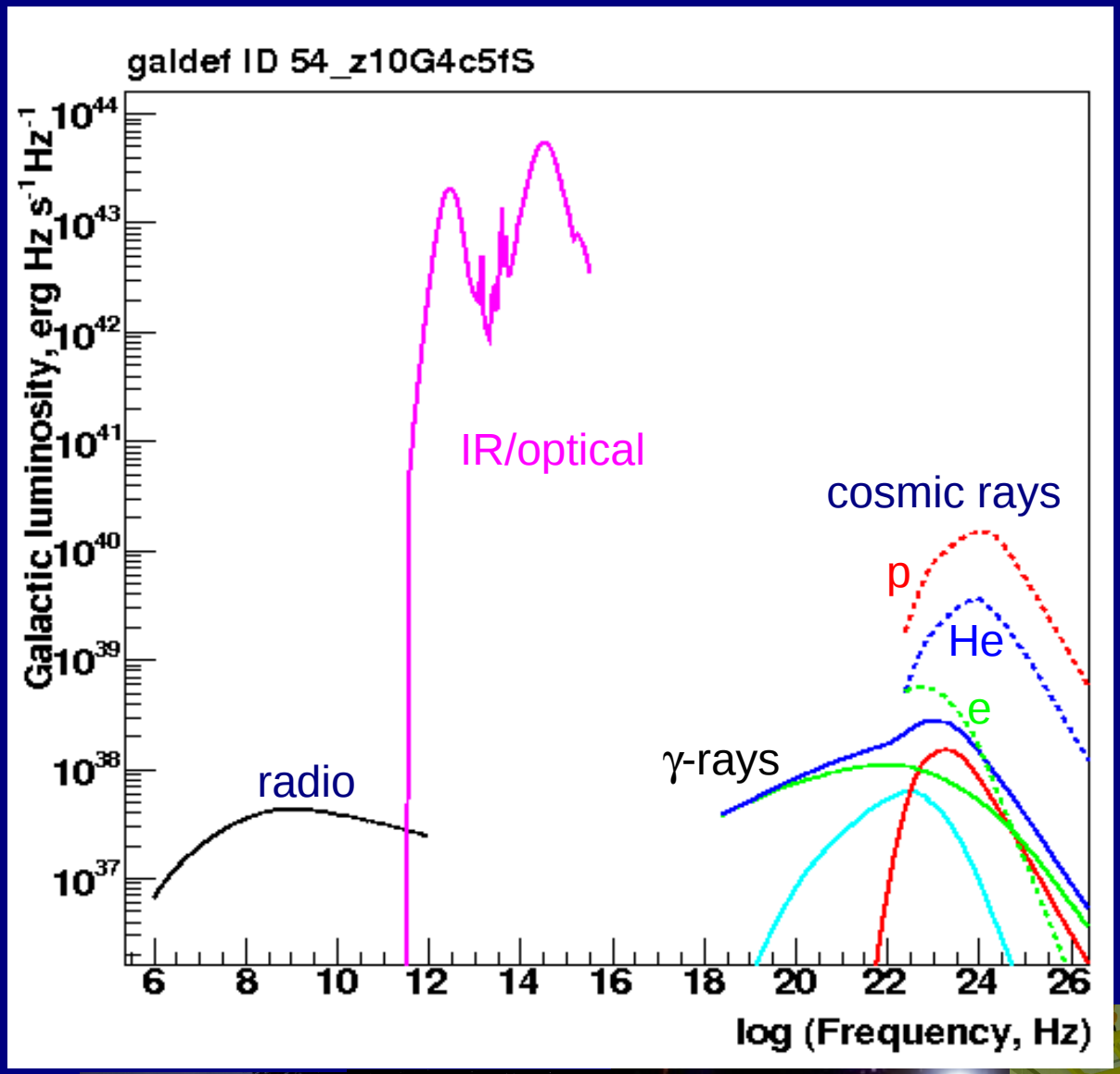

Strong et al. (2010), ApJL 722, L58

Interstellar Cosmic ray spectra derived from gamma rays

Method : Bayesian analysis (Strong etal arXiv:1507.05006)

Gamma-ray gas emissivity *used to derive* Cosmic-ray protons via pion-decay

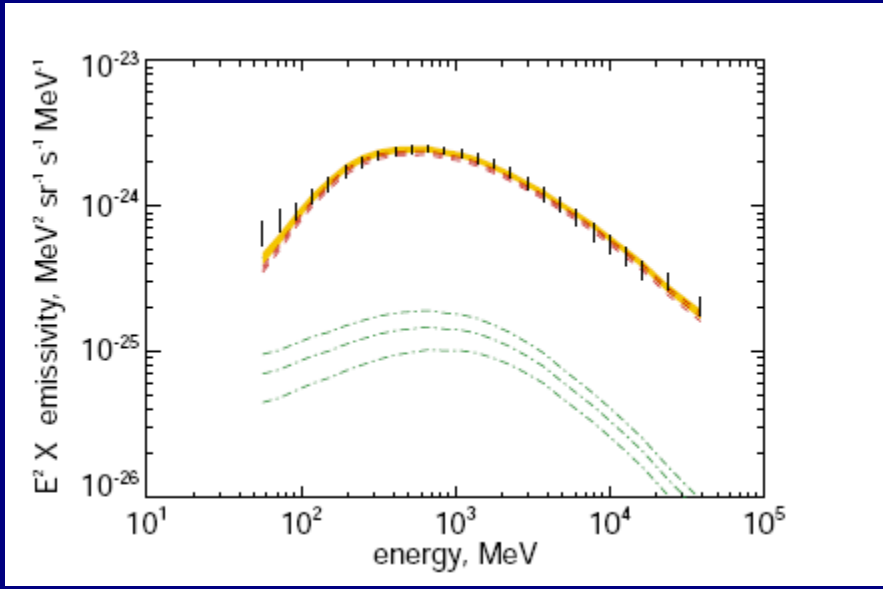

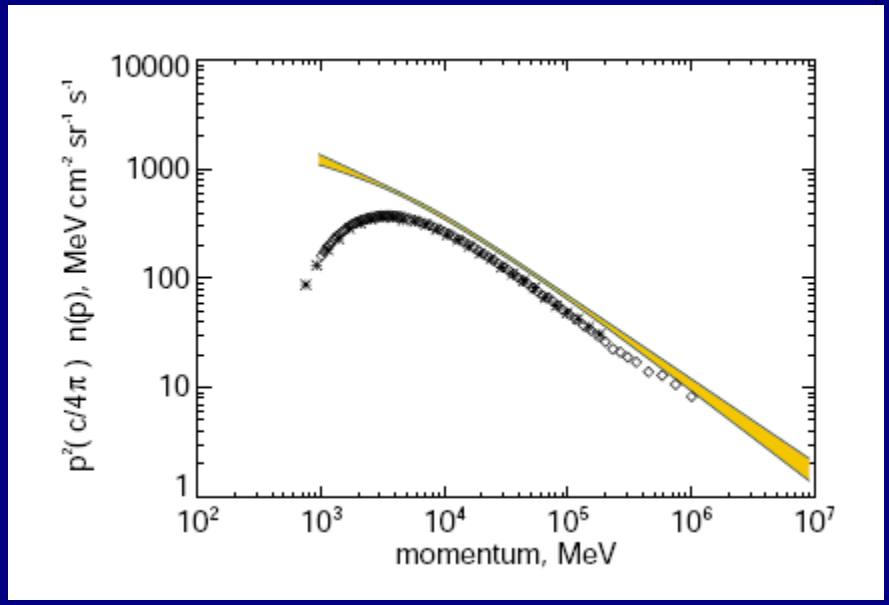

Below 10 GeV affected by solar modulation, but gamma rays probe the **interstellar** spectrum.

Emissivity of local interstellar gas – Jean-Marc Casandjian (Fermi-LAT Collab).

Power-law in momentum overall, but low-energy break
e.g. from power-law injection and interstellar propagation (diffusion = f(E))

Interstellar spectrum essential to test heliospheric modulation models.

CR spectrum modelled as smoothly broken power-law in momentum

$$n(p) \propto 1 \,/\, [(\frac{p}{p_{br}})^{\alpha_1/\delta} + (\frac{p}{p_{br}})^{\alpha_2/\delta}]^{\delta}$$

form used is $n(p) \propto 1 \,/\, [(\frac{p}{p_{br}})^{\alpha_1/\delta} + (\frac{p}{p_{br}})^{\alpha_2/\delta}]^{\delta}$ where α_1, α_2 are the indices below and above the break respectively for $\alpha_1 < \alpha_2$, and the spectrum breaks around a momentum centred on p_{br}; the parameter δ controls the sharpness of the break: smaller δ produces a sharper break, typical values are δ =0.5 – 1.5. It converges to the given power-laws at low and high p, with a smooth transition.

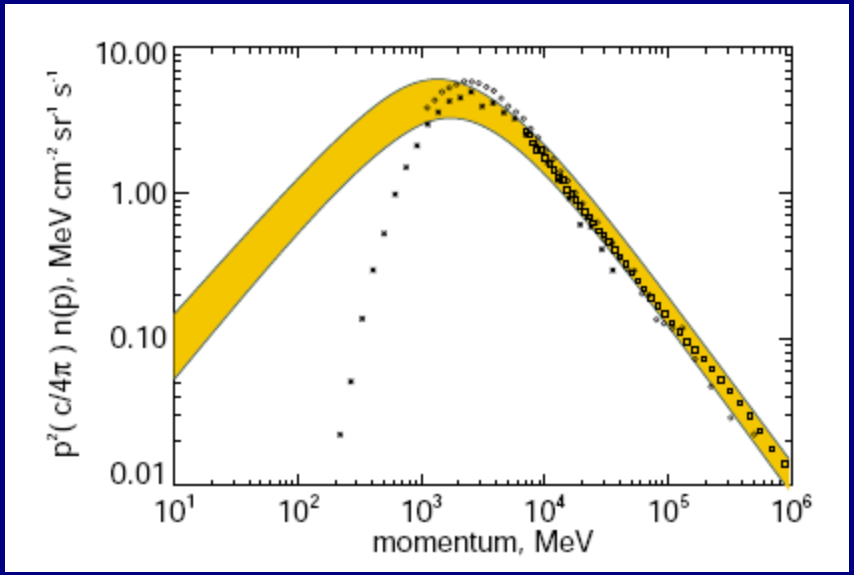

Method: Bayesian, MultiNest package implementing Nested Sampling algorithm
10 parameters
Posterior chains used to sample the resulting spectra.

Table 1: Summary of model fits to equation 6.1. Entries are prior range, posterior mean and standard deviation. The proton parameters are constrained by the γ-ray emissivities, while the lepton parameters reflect mainly the prior from synchrotron and direct measurements. The parameters are highly correlated and degenerate, so the resulting spectrum derived from the full posterior (Fig 1) is preferred to the individual parameters. The CR density n_{ref} is multiplied by $(c/4\pi)$ to give a flux in the usual units quoted in experiments. p_{ref}= 10^5 MeV for protons, 2×10^4 MeV for leptons.

Parameter	range: min	max	mean	std	units
Protons					
$(c/4\pi)n_{ref}$	1×10^{-9}	20×10^{-9}	6.4×10^{-9}	0.3×10^{-9}	$cm^{-2}\ sr^{-1}\ s^{-1}\ MeV^{-1}$
α_1	2.2	2.7	2.37	0.09	
α_2	2.6	3.5	2.82	0.05	
δ	0.05	1.0	0.5	0.1	
p_{br}	1000	10000	5870	2200	MeV
Leptons					
$(c/4\pi)n_{ref}$	1×10^{-9}	3×10^{-9}	2.2×10^{-9}	0.5×10^{-9}	$cm^{-2}\ sr^{-1}\ s^{-1}\ MeV^{-1}$
α_1	1.8	2.2	2.0	0.1	
α_2	3.1	3.2	3.15	0.03	
δ	0.05	1	0.47	0.25	
p_{br}	500	2000	1130	4067	MeV

Interstellar Cosmic ray spectra derived from gamma rays

Method : Bayesian analysis

Gamma-ray gas emissivity

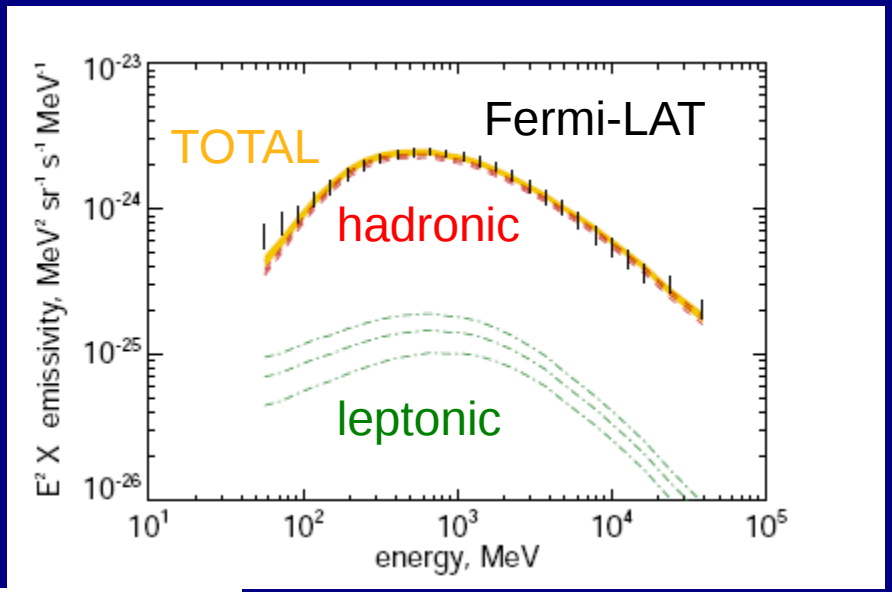

+ constraints
from synchtrotron

Cosmic-ray protons

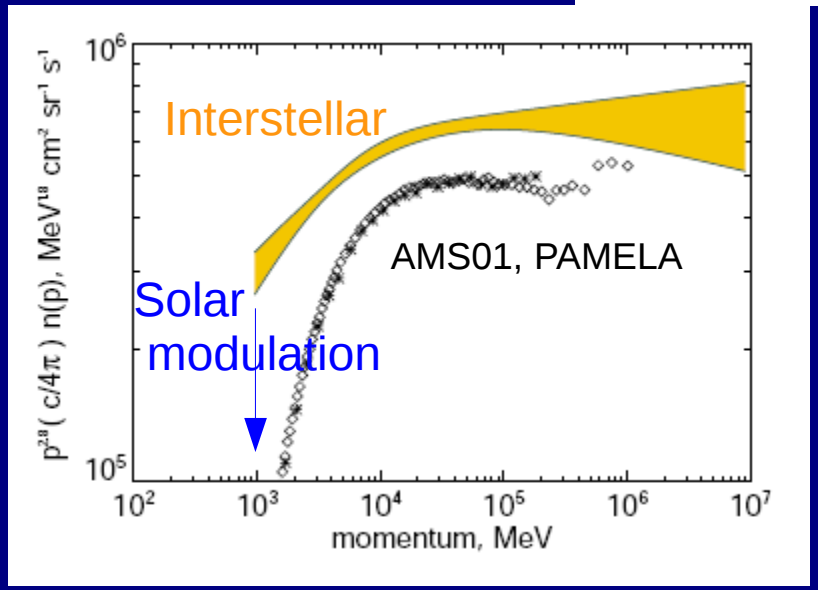

Cosmic-ray leptons

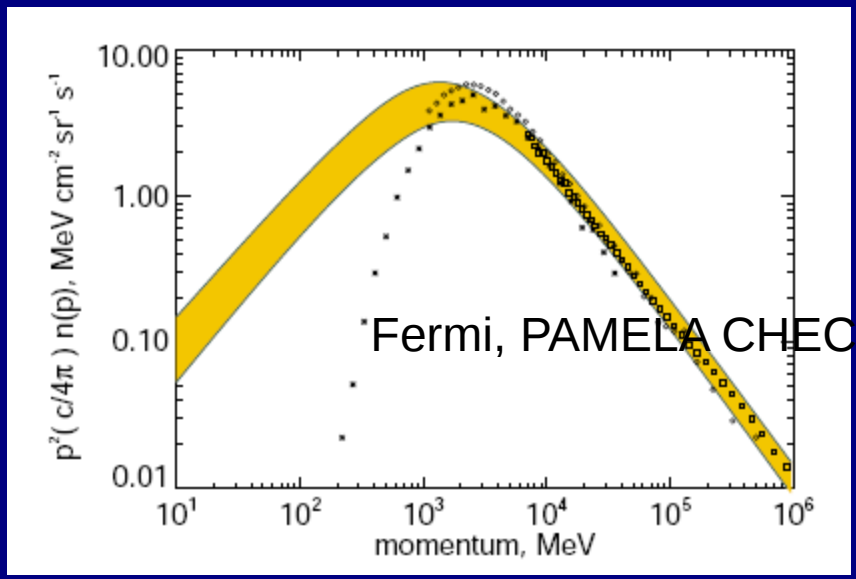

Technical note

Use momentum, not kinetic energy!
Momentum is physically appropriate for acceleration mechanisms
e.g. diffusive shock acceleration gives power-law in momentum.

Kinetic energy power-law has a break break when plotted in momentum

Originally pointed out by Chuck Dermer, see e.g. Strong etal ICRC2015

Also: use density $n(p)$ not flux $I(p)$
More physical, $n(p)$ are the units used by GALPROP etc.
We don't want the velocity!

Observers usually use $I(E_k)$ which is convenient since

$n(p) = (4\pi/c)\, I(E_k)$

Low energy Gamma rays

Fermi low-energy extension with Pass8 event processing.
Down to 20 MeV, difficult because of broad PSF, energy dispersion and earth emission
But coming along.

COMPTEL (1-30 MeV) heritage, still only available mission in this range.
Good news: Werner Collmar (MPE Garching) still working on this (only he can!)
Example: LS5039 microquasar periodicity
New point-source catalogue, eventually all-sky maps on the horizon.

(INTEGRAL/SPI: only 20 keV - 1 MeV)

New missions unfortunately slow in coming but e.g. AstroGam initiative
Large interest in the community.

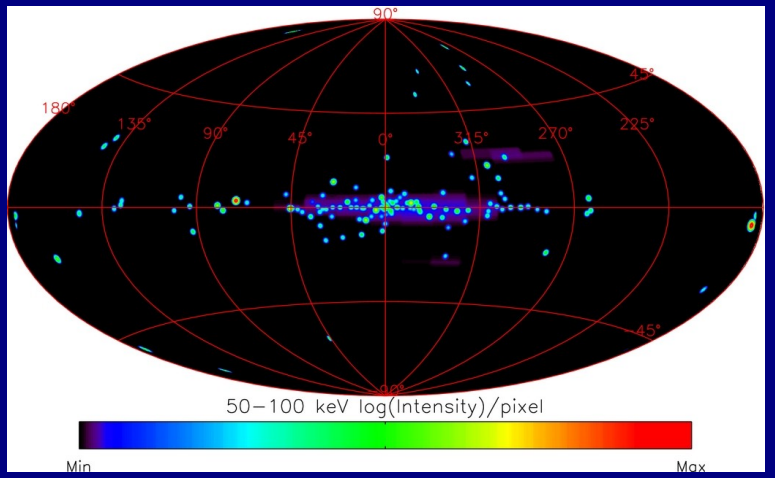

INTEGRAL / SPI
Continuum skymaps

Bouchet et al.
ApJ 739, 29 (2011)

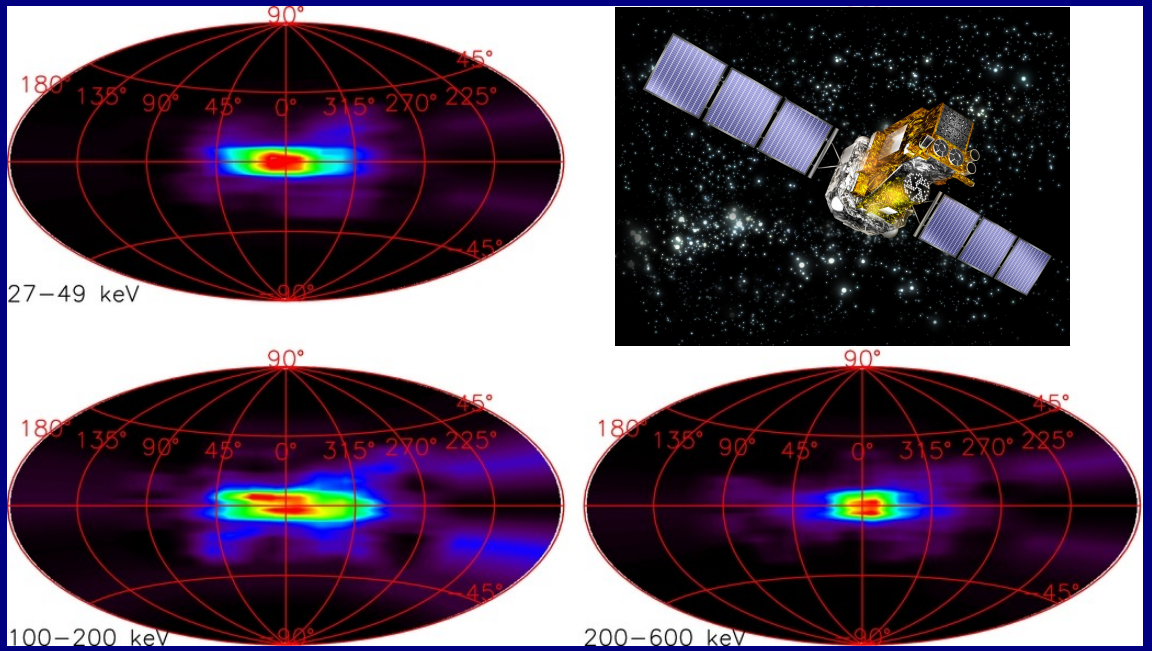

A real mix of processes !

Inner Galaxy
INTEGRAL / SPI
Bouchet et al. ApJ 739, 29 (2011)

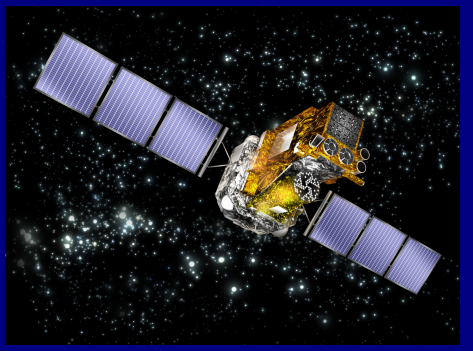

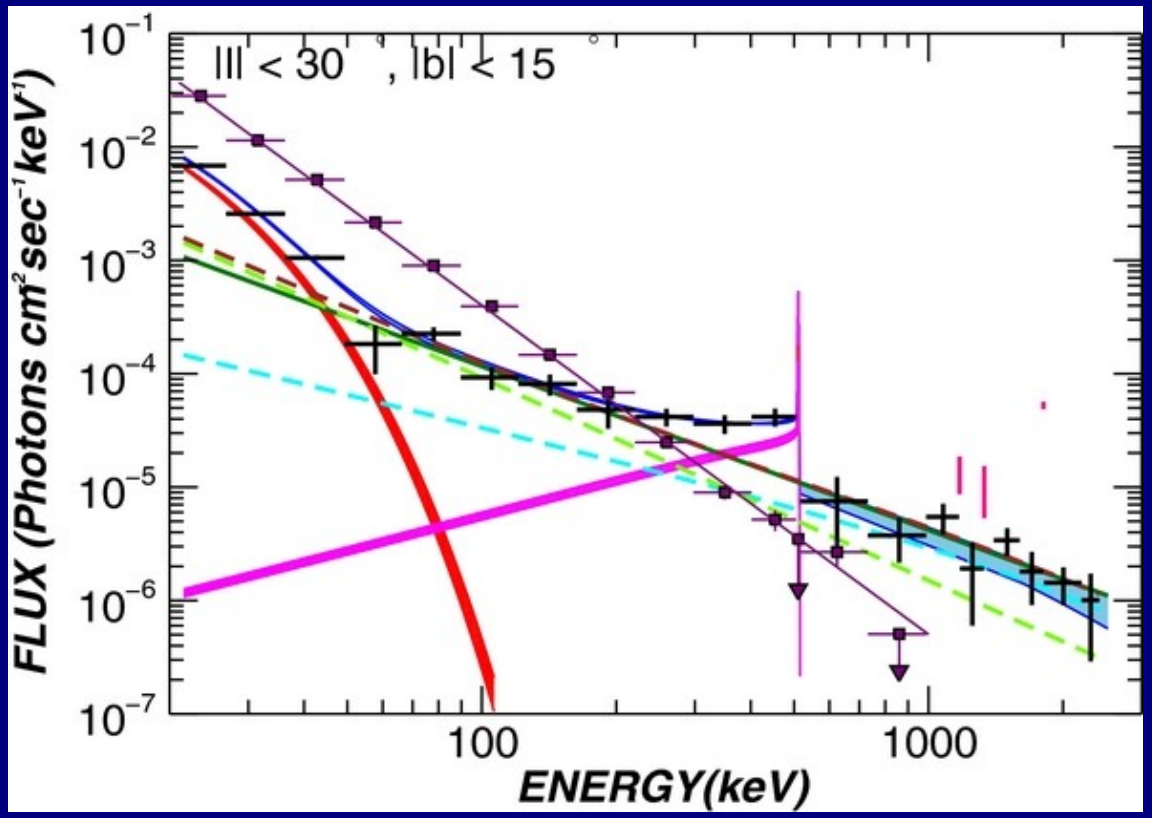

Inner Galaxy: keV to TeV

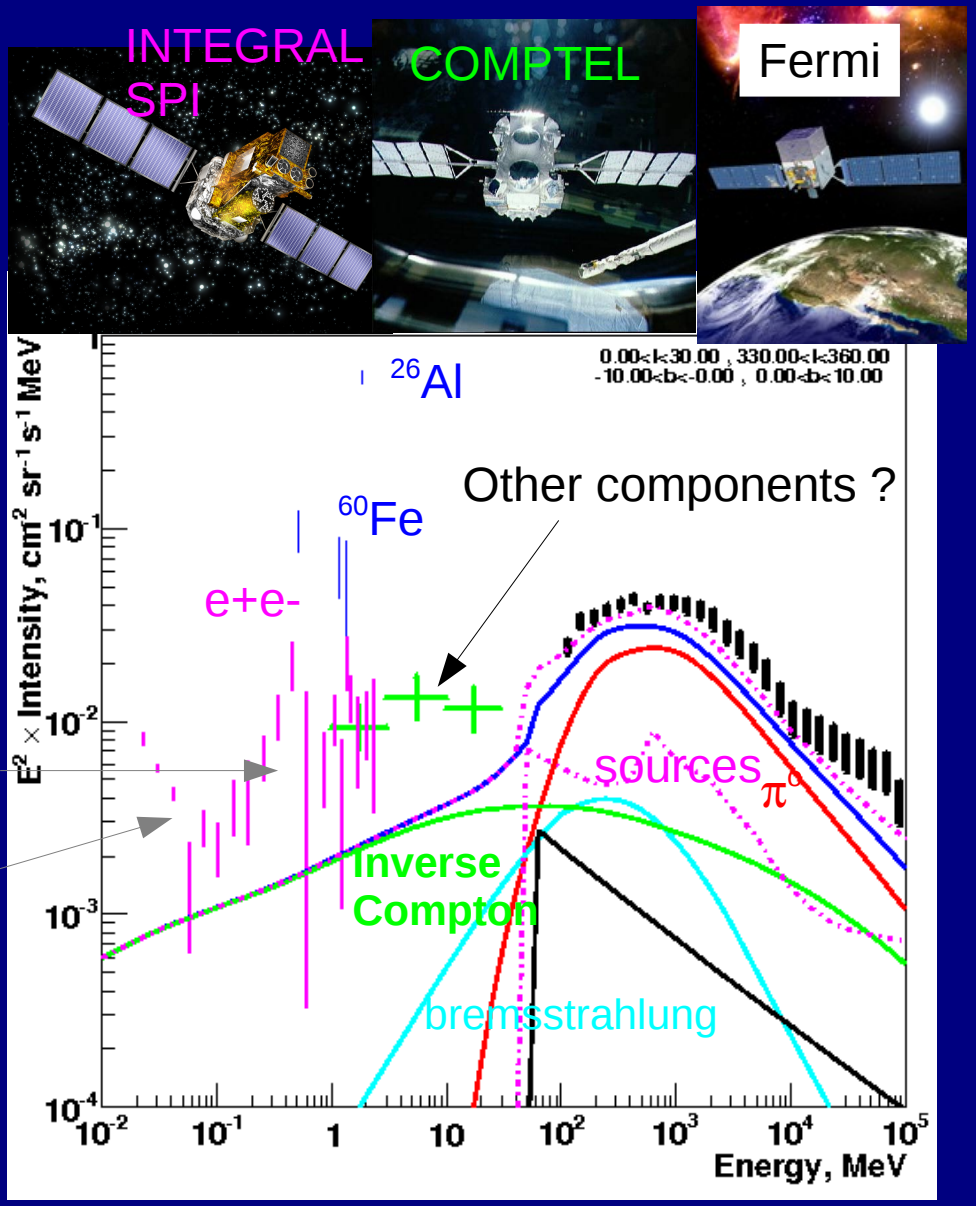

GeV electrons – inverse Compton - important for MeV gamma rays !

Fermi-LAT 25 – 40 MeV

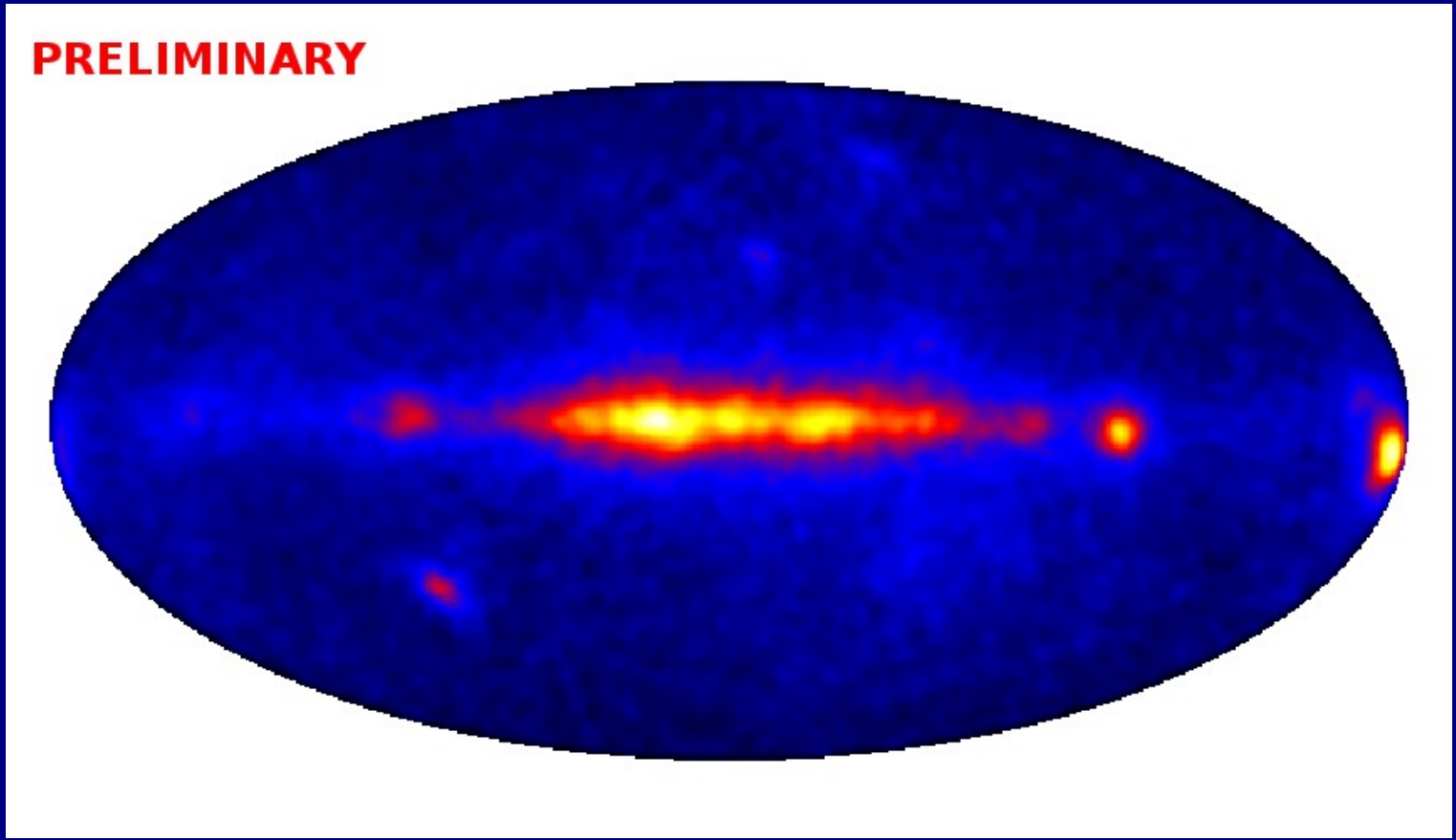

NB low angular and energy resolution !
Nominal energy range: photons may originate from range 10 to <100 MeV.
But valuable to bridge the MeV gap.

Fermi-LAT 25-40 MeV

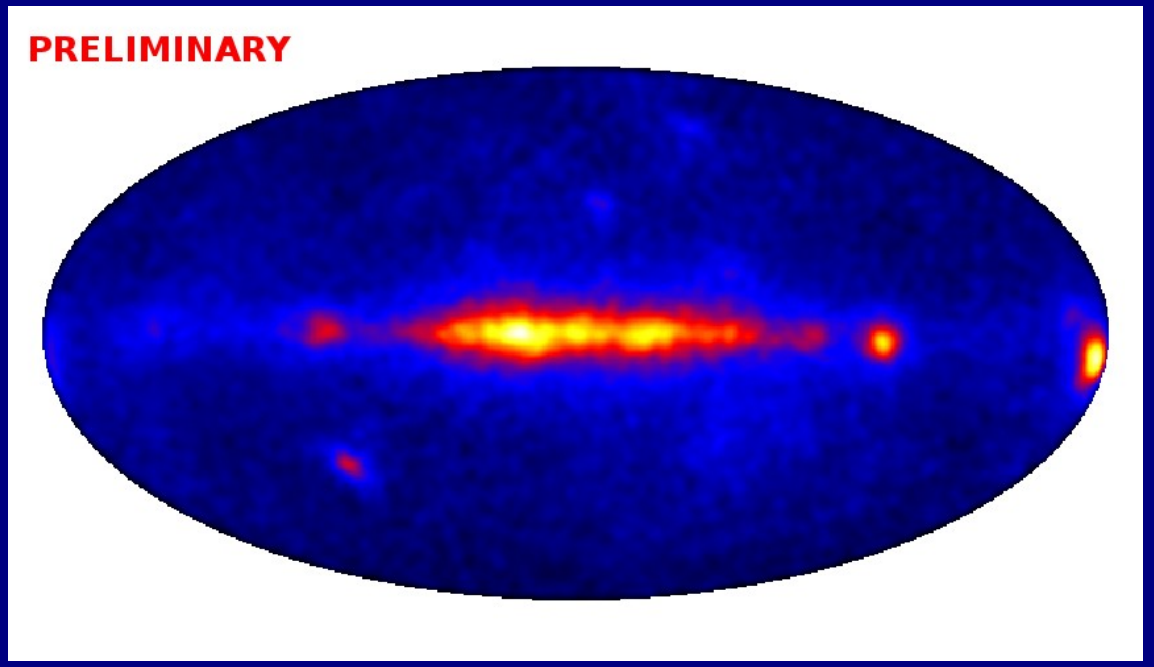

meets

COMPTEL 10-30 MeV

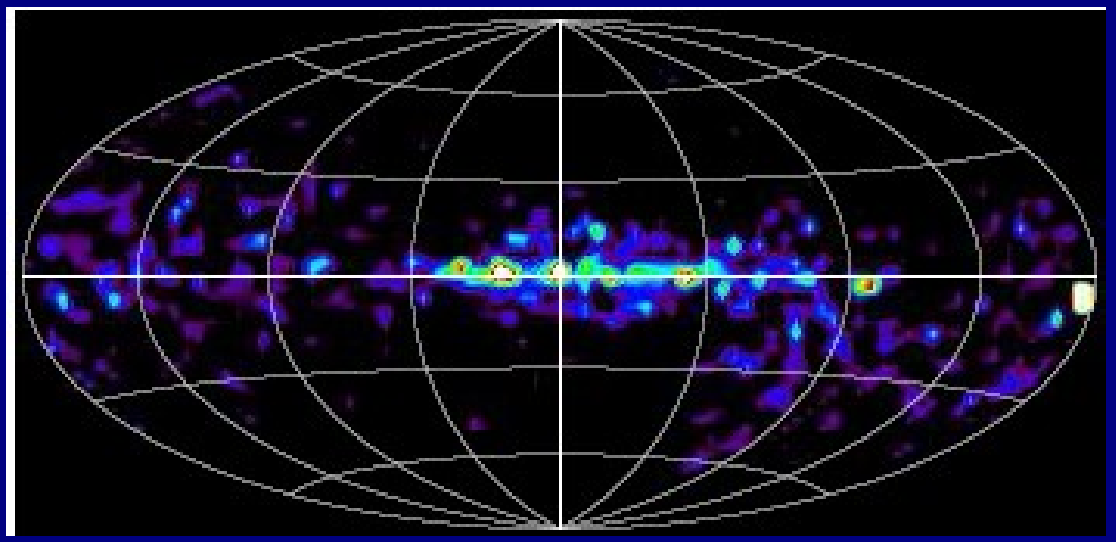

New COMPTEL analysis underway (poster at Heidelberg Gamma2016)

The Nine Lives of Cosmic Rays in Galaxies

Isabelle A. Grenier,[1] John H. Black,[2] and Andrew W. Strong[3]

[1]Laboratoire AIM Paris-Saclay, CEA/Irfu, CNRS, Université Paris Diderot, F-91191 Gif-sur-Yvette Cedex, France; email: isabelle.grenier@cea.fr

[2]Department of Earth & Space Sciences, Chalmers University of Technology, Onsala Space Observatory, SE-439 92 Onsala, Sweden; email: john.black@chalmers.se

[3]Max-Planck-Institut für extraterrestrische Physik, 85741 Garching, Germany; email: aws@mpe.mpg.de

Annual Review of Astronomy and Astrophysics, Vol 53, 2015


THE
END IS
NEAR

Diffusive reacceleration called into question

Diffusive reacceleration = diffusion in momentum
Spatial diffusion will be accompanied by momentum diffusion if the scattering medium is moving.
Standard formula : $D_{pp} = p^2 V_A^2 / (9 D_{xx})$

Popular since explains peak in B/C energy-dependence without
ad-hoc break in $D_{xx}(p)$ and more consistent with Kolmogorov diffusion index 1/3

Avoids high-energy anisotropy problem

BUT it is not proved!
In reacceleration models,
a large fraction of the energy in cosmic rays (up to 30%) comes from reacceleration i.e.
in the interstellar medium. So SNR are not the only major source of CR!

Is this physically plausible, and where does the energy come from?

Other ways to get B/C: convection is a natural mechanism.
Needs much more work.

See Drury & Strong ICRC 2015 arXiv:1508.02675

Low energy cosmic rays: 1-100 MeV

Important for interstellar chemistry: ionization. Traced by H_3^+
Hot topic!

Voyager 1 enters interstellar space, measures MeV protons unmodulated

For cosmic-ray propagation and modulation a new era starting.

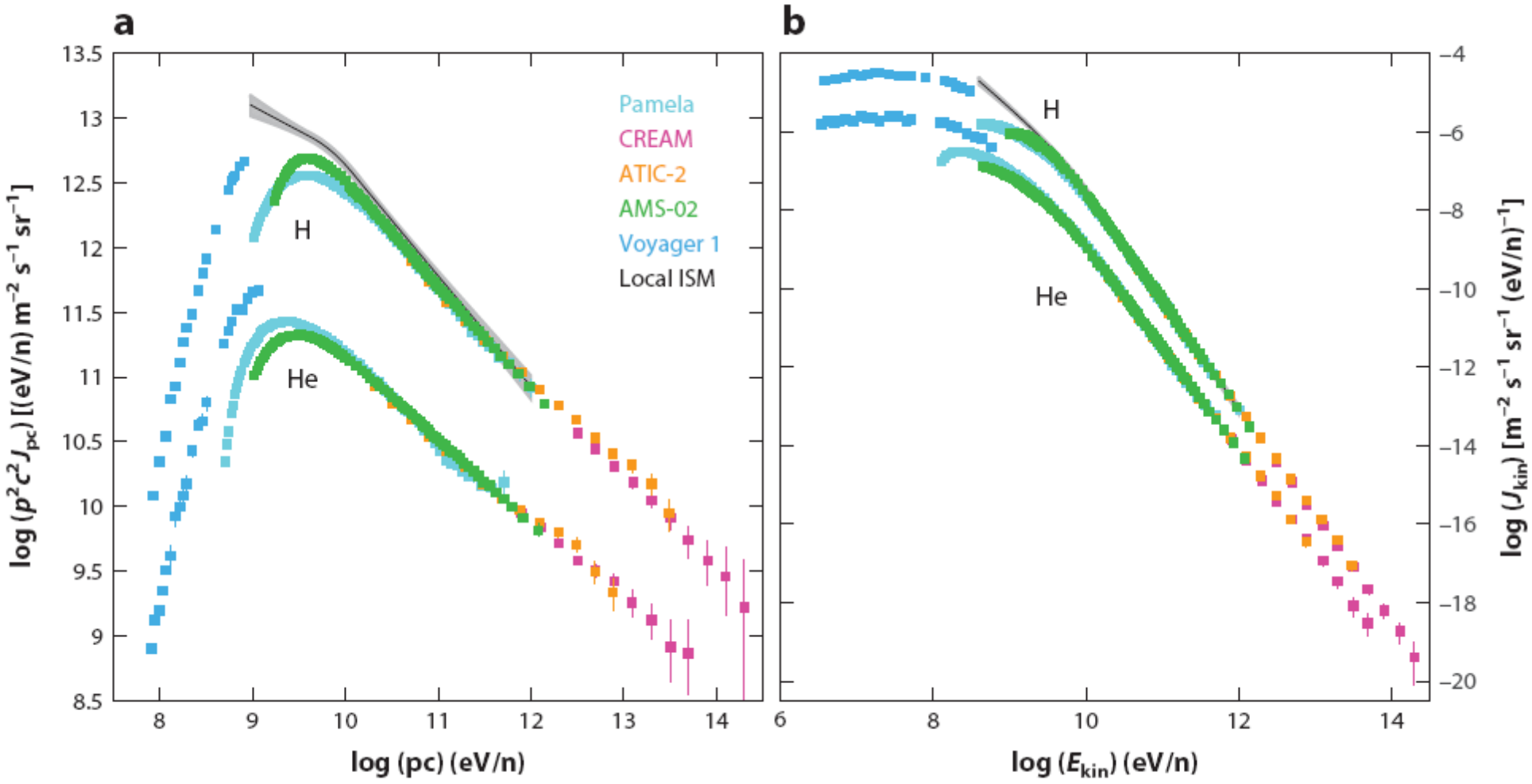

Figure 1

Local spectra of cosmic-ray protons and helium, as measured near the Earth and heliopause (Panov et al. 2009, Adriani et al. 2011, Yoon et al. 2011, Choutko et al. 2013, Stone et al. 2013, Consolandi et al. 2014), and displayed without solar demodulation (*a*) in momentum distributions and (*b*) in particle spectra in kinetic energy. They indicate proton hardening and He enrichment above a few hundred GeV. The gray band marks the range of proton spectra inferred in the local ISM from the average γ-ray emissivity of the interstellar gas, given the current uncertainties in the hadronic cross sections (data from Dermer et al. 2013b).

Grenier, Black & Strong, ARAA 53, 2015

New local interstellar spectra for protons, Helium and Carbon derived from PAMELA and Voyager 1 observations

D. Bisschoff • M.S. Potgieter

arXiv:1512.04836 Dec 2015

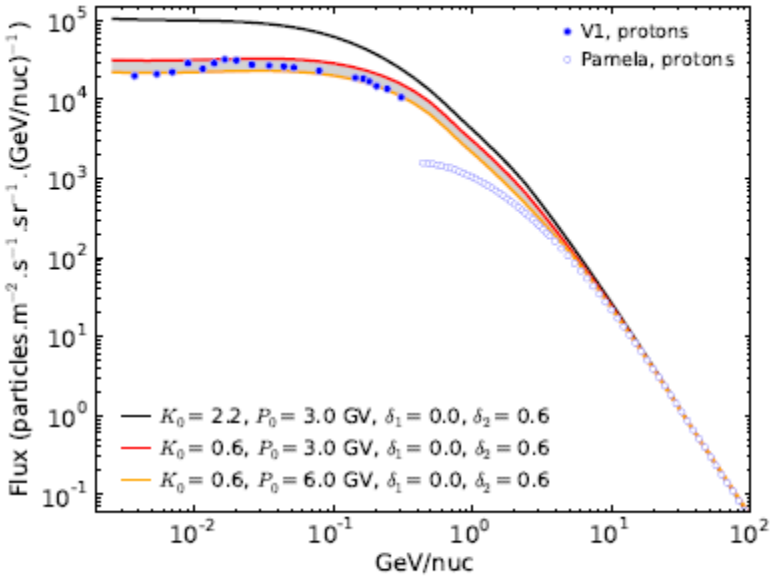

Fig. 3 The computed proton LIS band bounded by the parameters listed in Fig. 2, upper value given by the red curve and lower value by the yellow curve. These two LIS's, together with the reference LIS (black curve), are compared to the V1 and PAMELA proton data. A computed LIS reproducing the V1 data should ideally lie inside this band, given the spread in the observations. The PAMELA observations above 20 GeV are clearly reproduced well where solar modulation becomes negligible

GALPROP model
Fitted to Voyager 1

Gamma rays as gas tracer, dark gas

Gamma rays detect ALL gas independent of phase, via pion-decay.

Led to first detection of CO-dark molecular hydrogen (Grenier 2005)

Meanwhile confirmed e.g. by Planck thermal dust analyses.

Gas models for GALPROP etc have to address this.

See Strong, Black & Grenier ARAA 53 (2015) for recent review.

Also
C+ line emission (Herschel) REF
Radio recombination line survey (Jodrell Bank) HII, with kinematic info
HII is important for gammas too.

Source populations: how much of 'diffuse Galactic emission' is really sources?

Fermi-LAT 3rd Catalogue has ~3000 sources, about 300 Galactic.
The Galaxy contains perhaps 50000 sources, *most below detection threshold*.
They make a contribution to the 'diffuse' emission from the Galaxy.
Source population modelling: 5-10% contribution, energy-dependent.
Hence essential to account for this in analyses of 'diffuse' emission.

Source population synthesis in Fermi 3FGL paper.

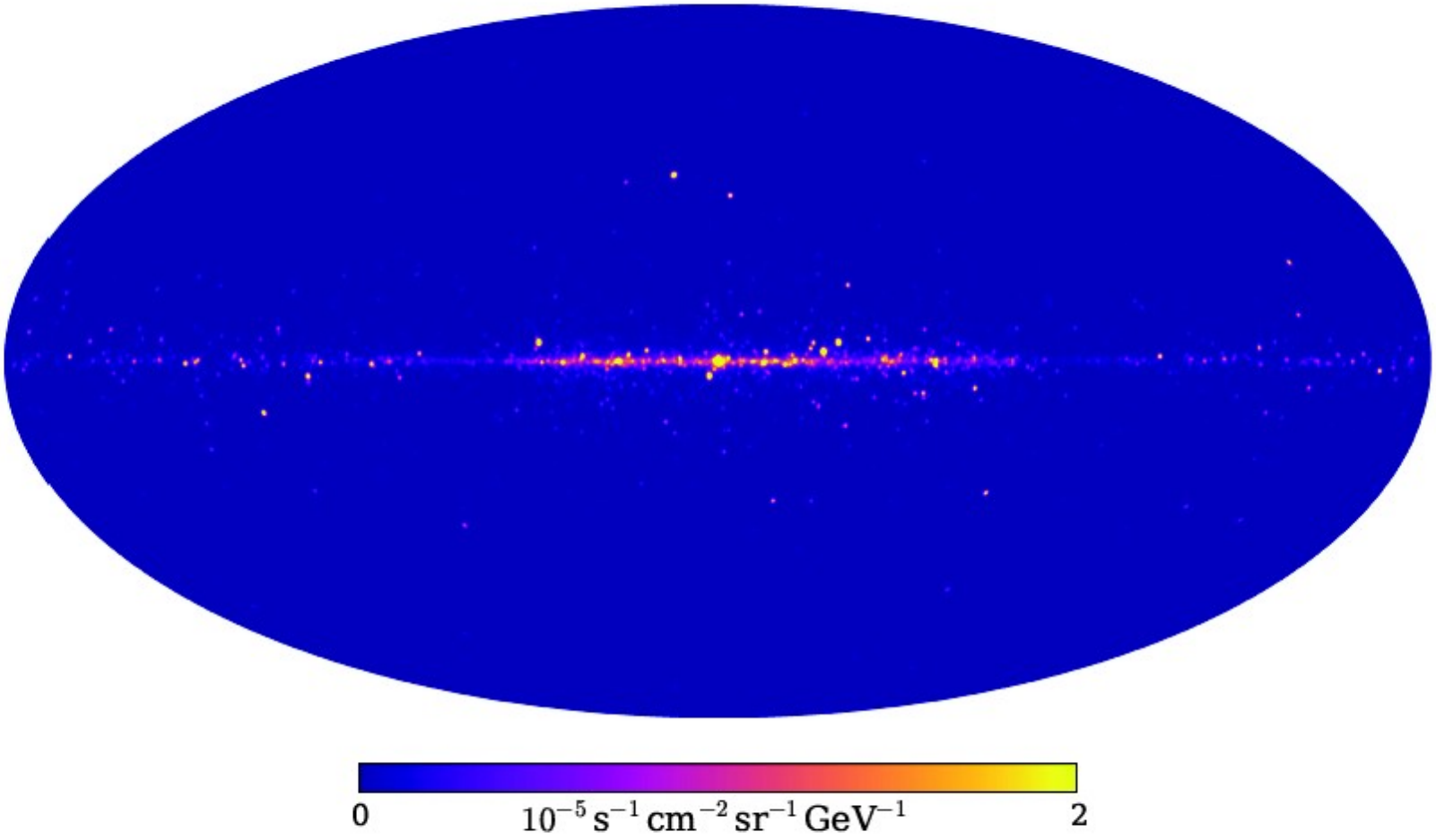

FIG. 1: All-sky model of the gamma-ray flux (dN/dE) from young pulsars in the Milky Way (MW) at 2 GeV, as discussed in § V. The bright peak in the center results from young pulsars arising in the Central Molecular Zone (CMZ) of the Galactic Center (GC). We have set the maximum flux at $2 \times 10^{-5}\mathrm{s}^{-1}\mathrm{cm}^{-2}\mathrm{sr}^{-1}\mathrm{GeV}^{-1}$ in order to enhance the visibility of the diffuse plane emission.

New paper on populations of pulsars and MSPs: O'Leary arXiv:1601.05797

Interstellar Radiation Field

Essential for leptons: energy losses, inverse Compton

New ISRF from Richard Tuffs (Bonn)
See talk at Obergurgl 2015 Workshop, Poster at Gamma2016 Heidelberg

Specialist for such calculations, up to now for external galaxies
Now for Milky Way
Will be public soon.

Differs from standard GALPROP ISRF.

Need to implement it in GALPROP etc
and compare with standard GALPROP ISRF

New analysis methods

Torsten Ensslin group at MPA Garching

IFT: Information Field Theory: Bayesian technique for data analysis on fields
NIFTY: package implementing IFT for general use

Example application:
D^3PO
Gamma rays: source detection with data-driven diffuse emission (no “diffuse model”)

Denoising, Deconvolving, and Decomposing Photon Observations

Selig et al. (2014)
www.mpa-garching.mpg.de/ift/d3po

D³PO

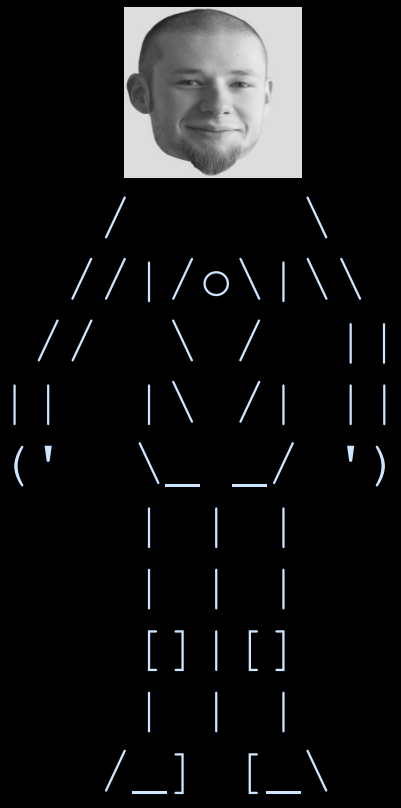

D³PO – challenges & assumptions

Selig & Enßlin (2013)
arXiv:

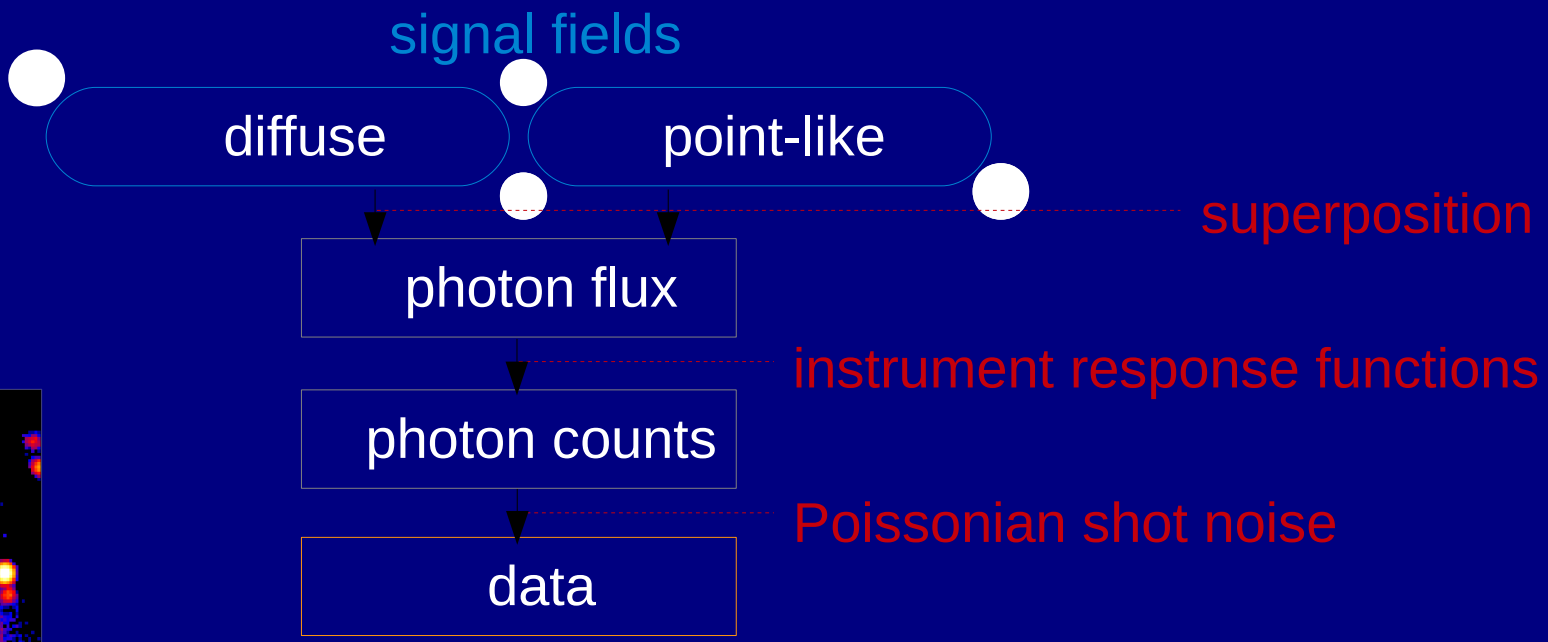

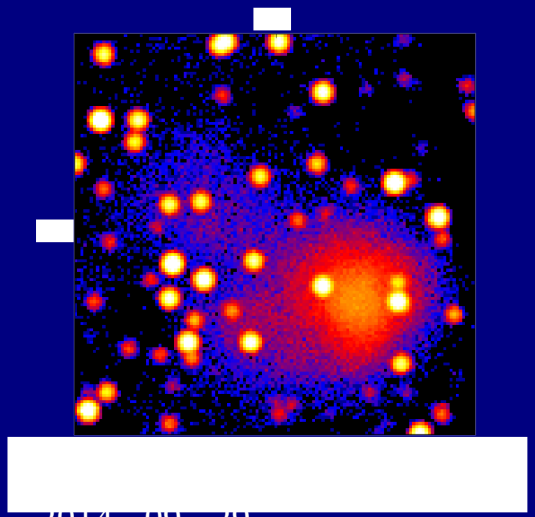

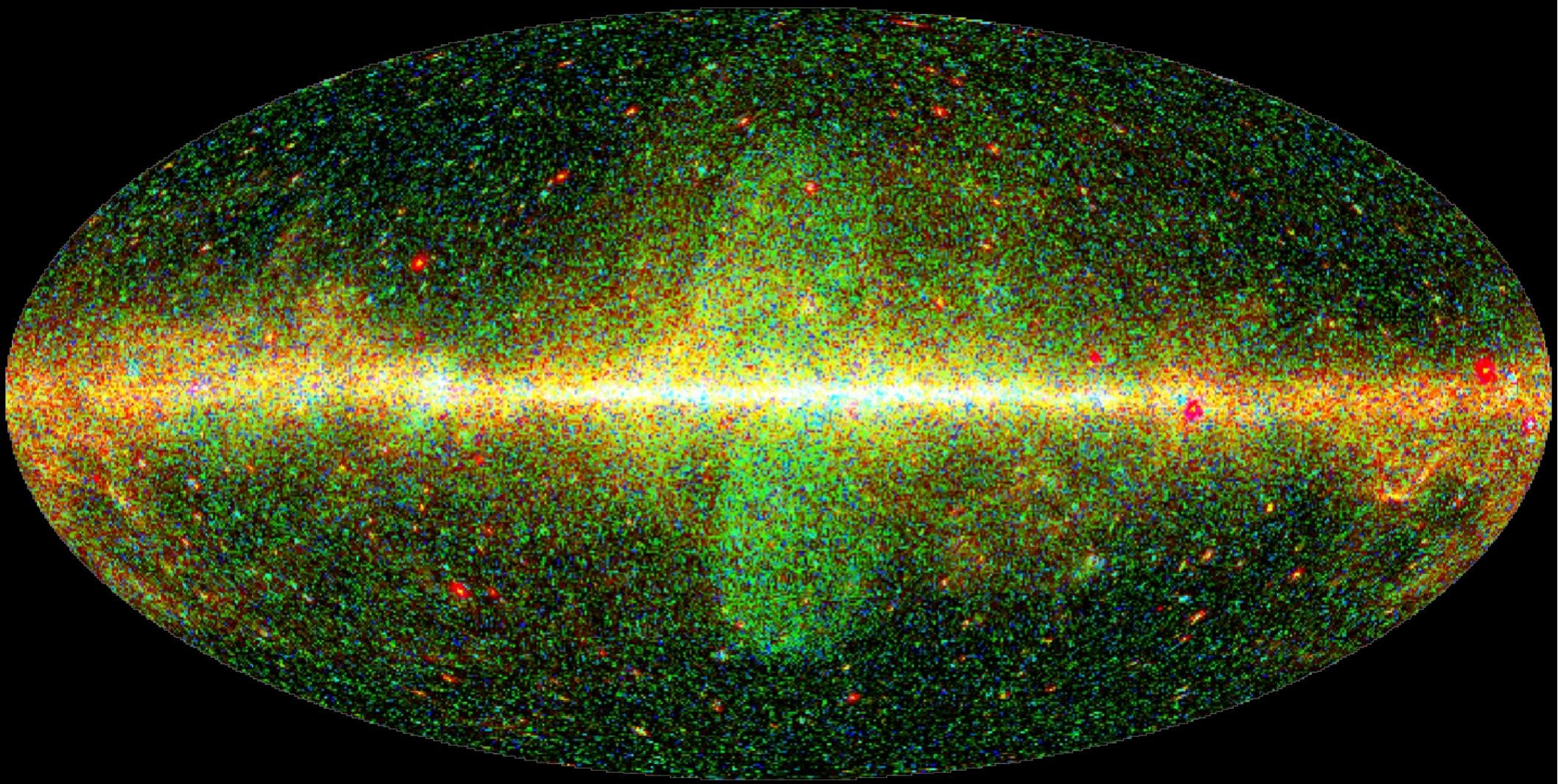

log-data

elig

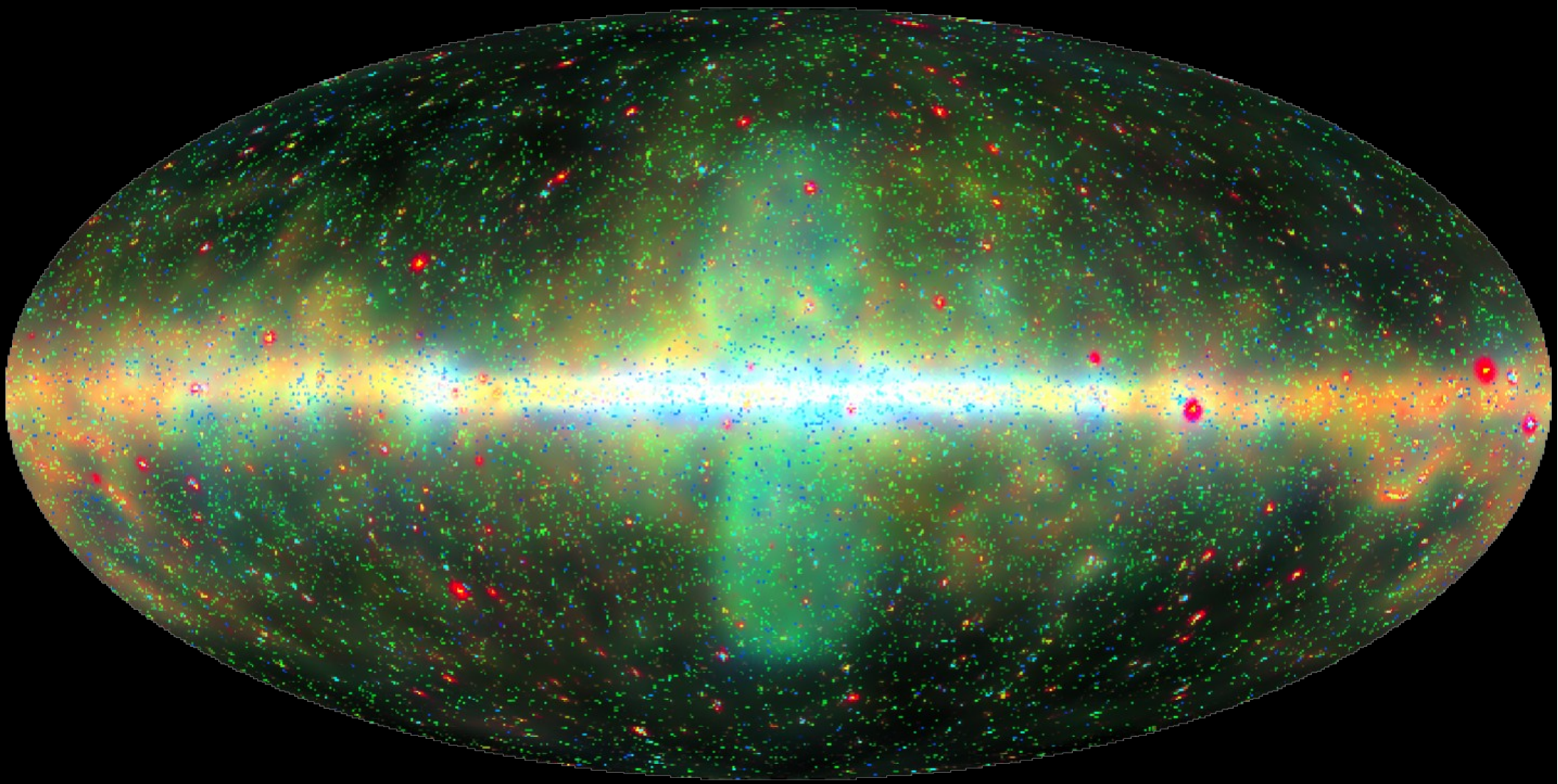

log-data … denoised

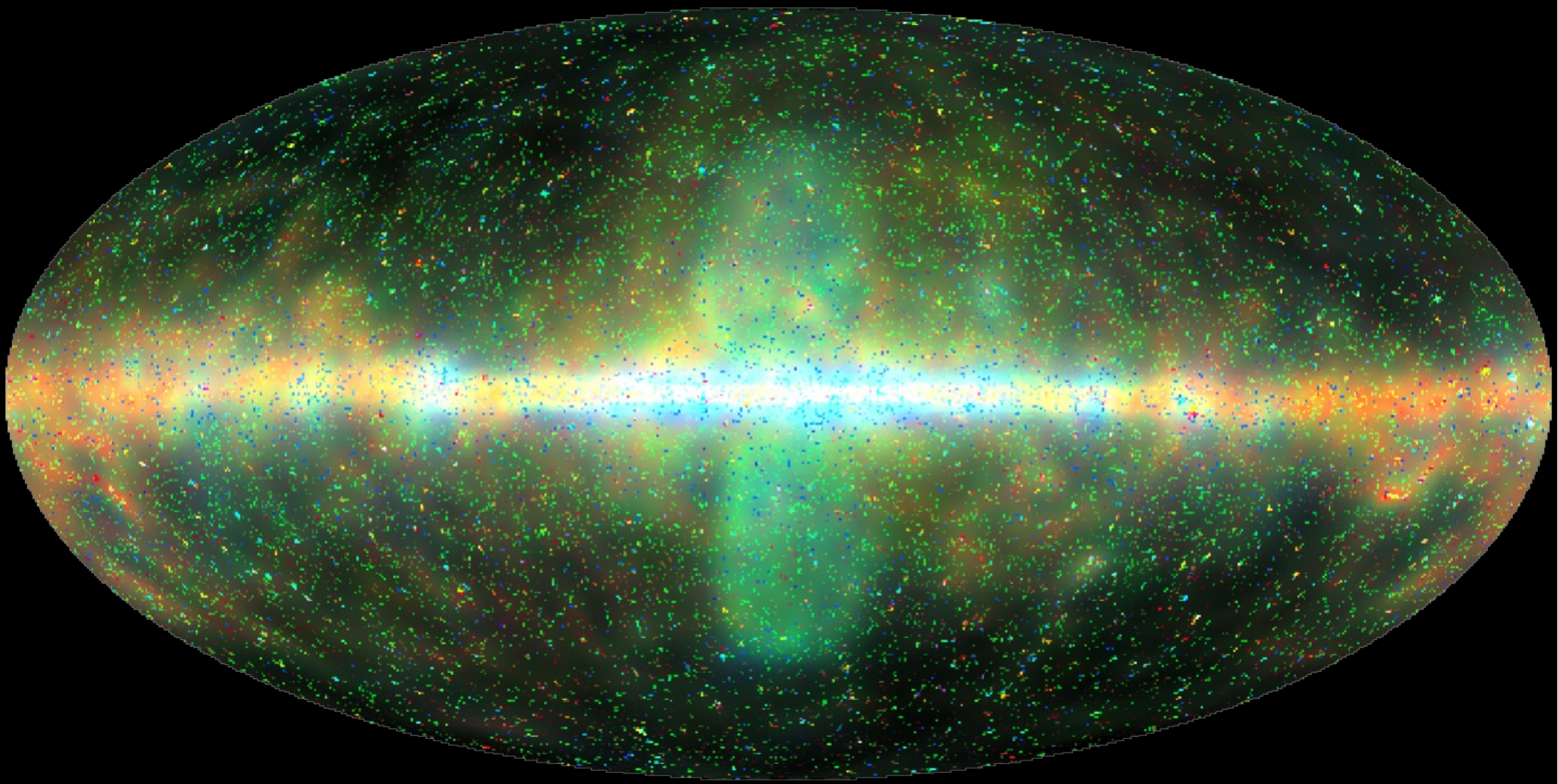

log-data … denoised … deconvolved

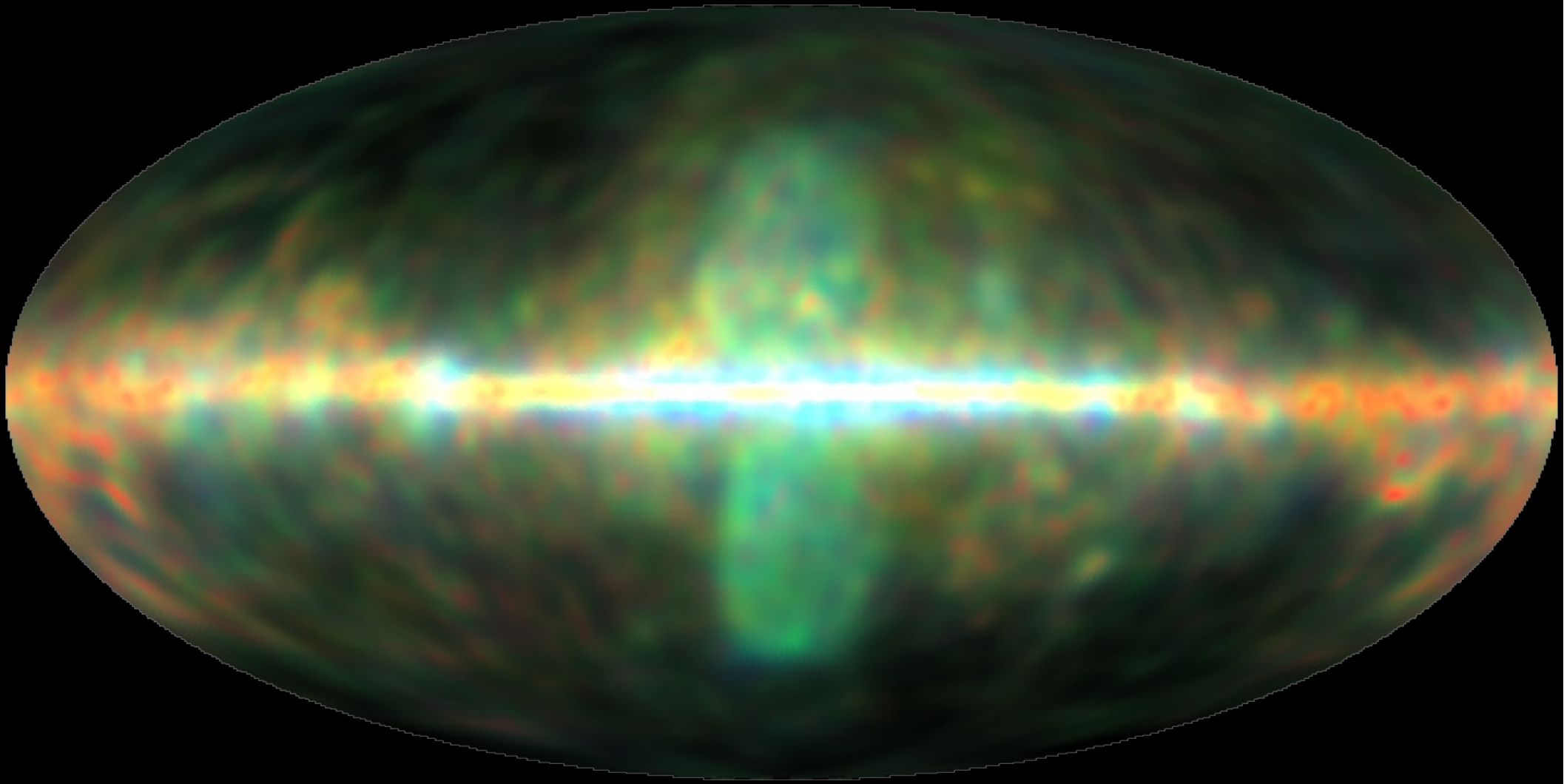

log-data … denoised … deconvolved … decomposed

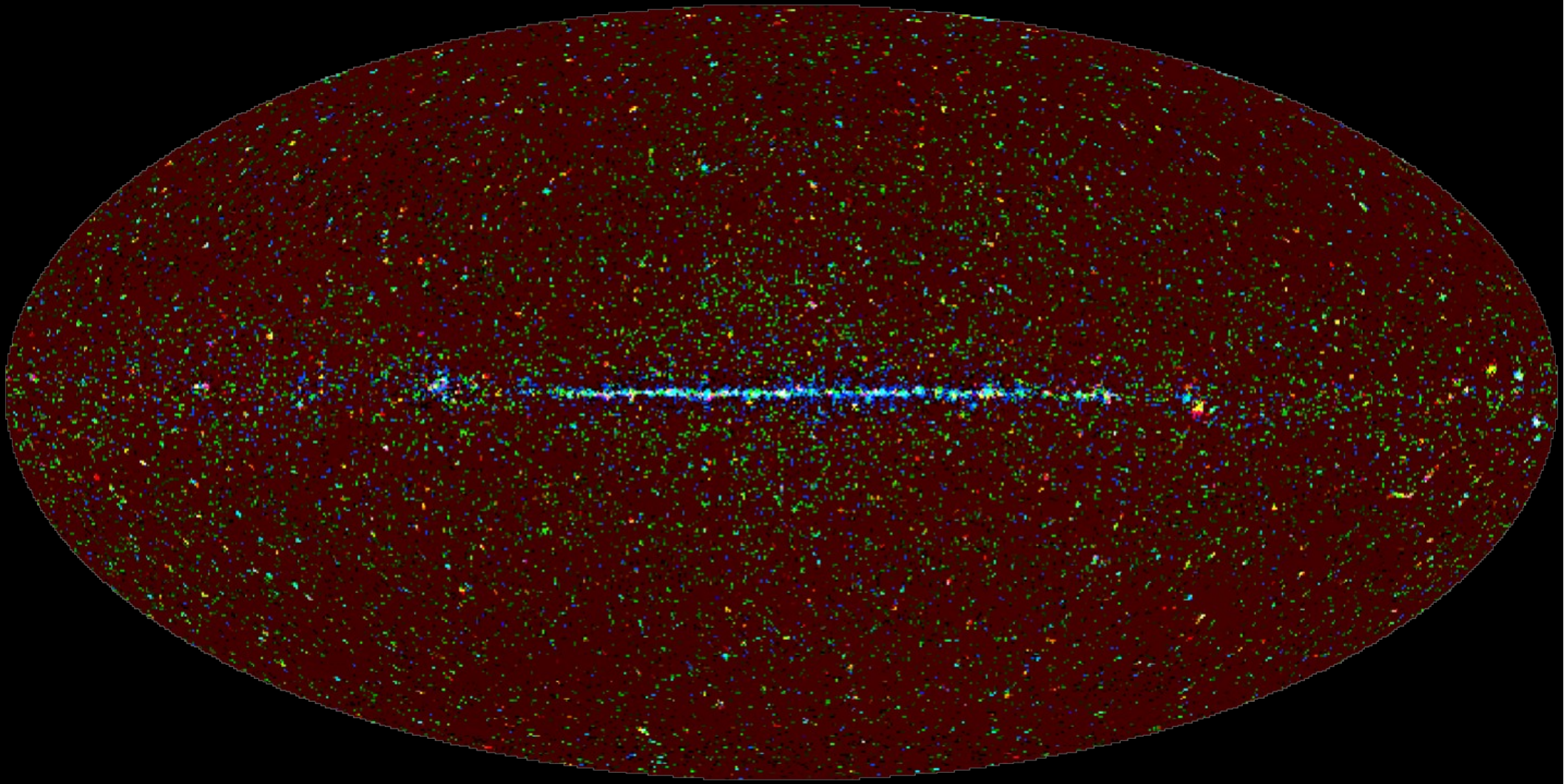

Eng

First D³PO Fermi Point Source Candidates Catalog (1DF)

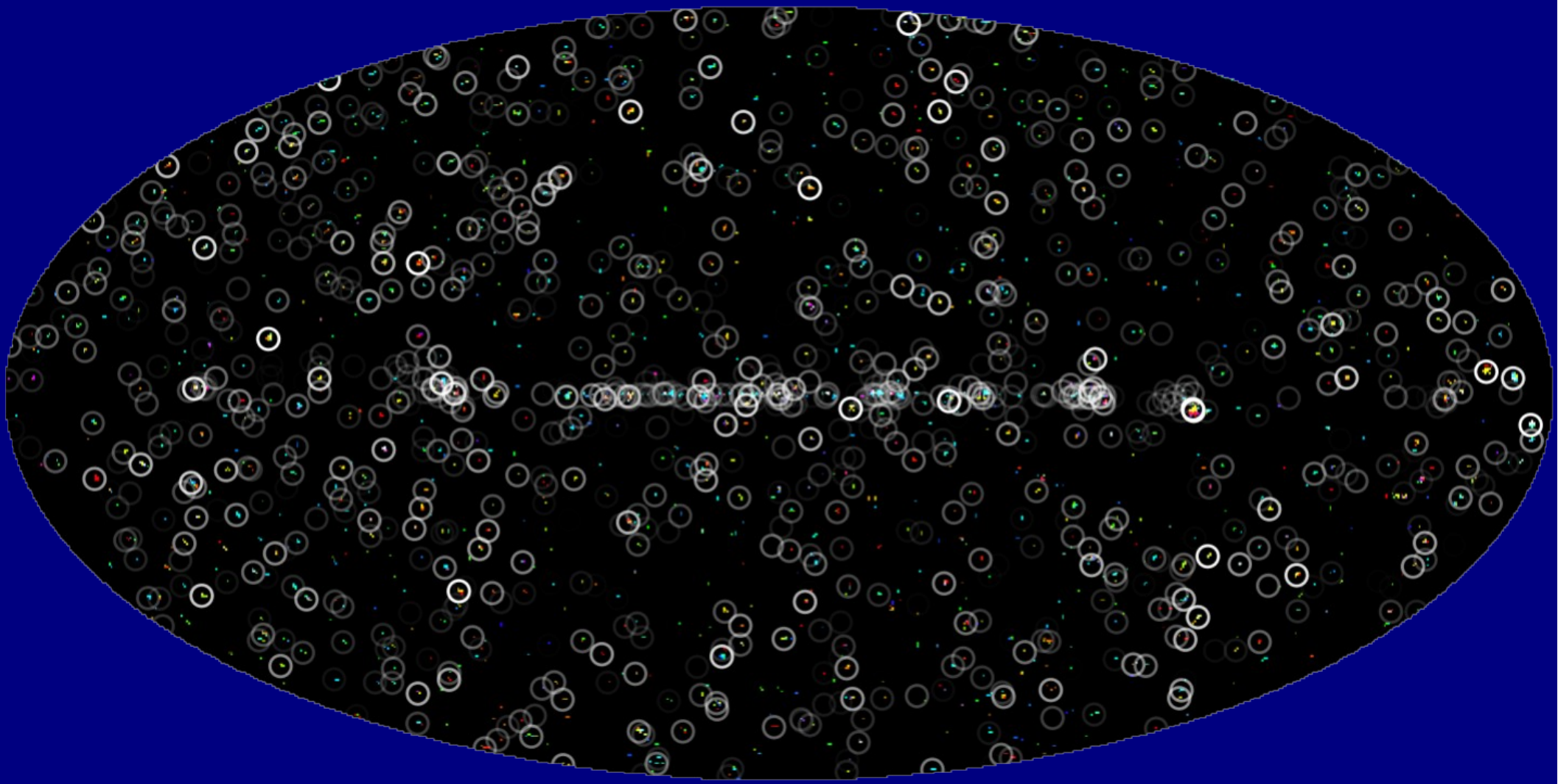

First D³PG[illegible]andidates

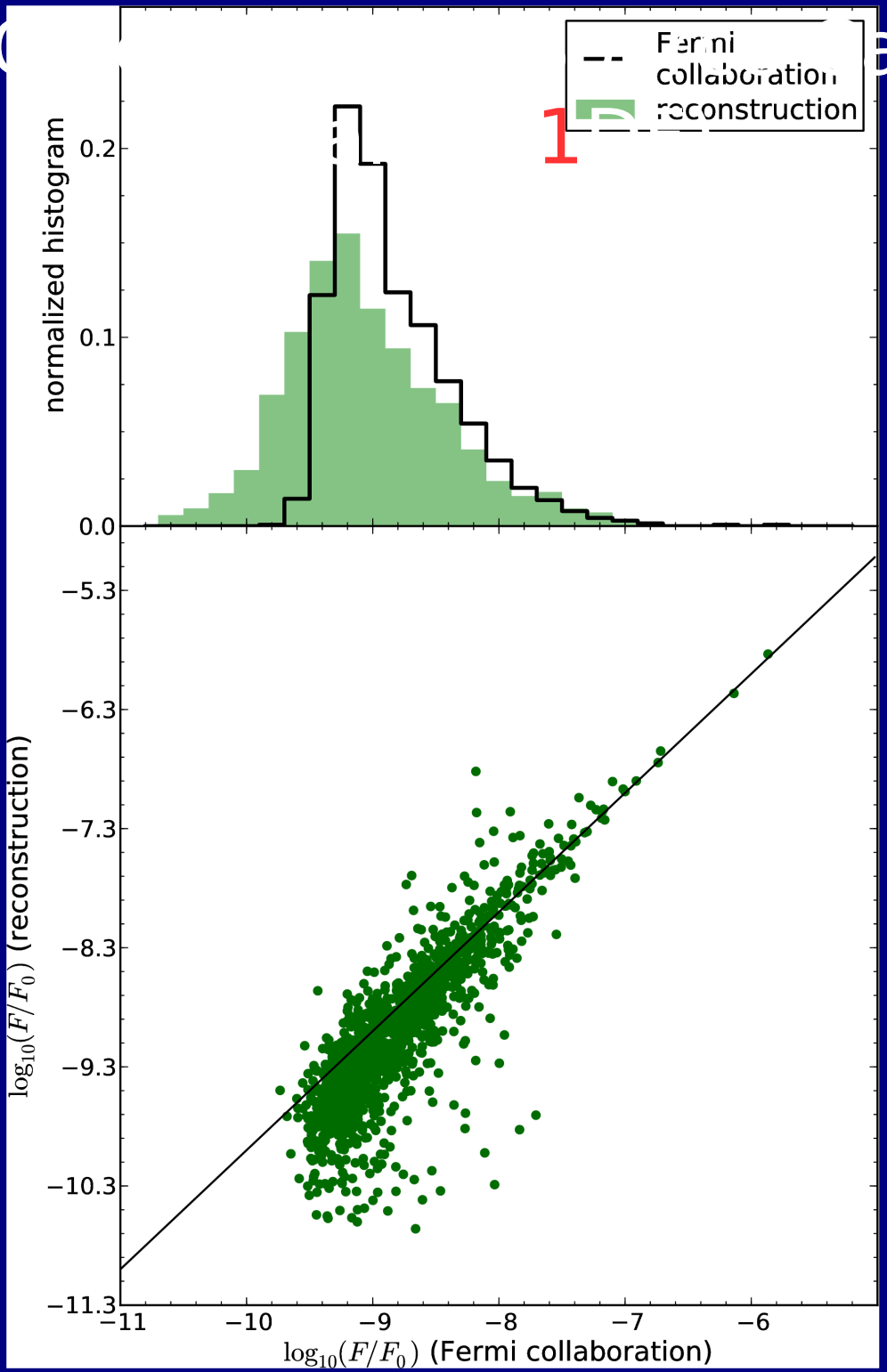

Diffuse gamma-ray sky

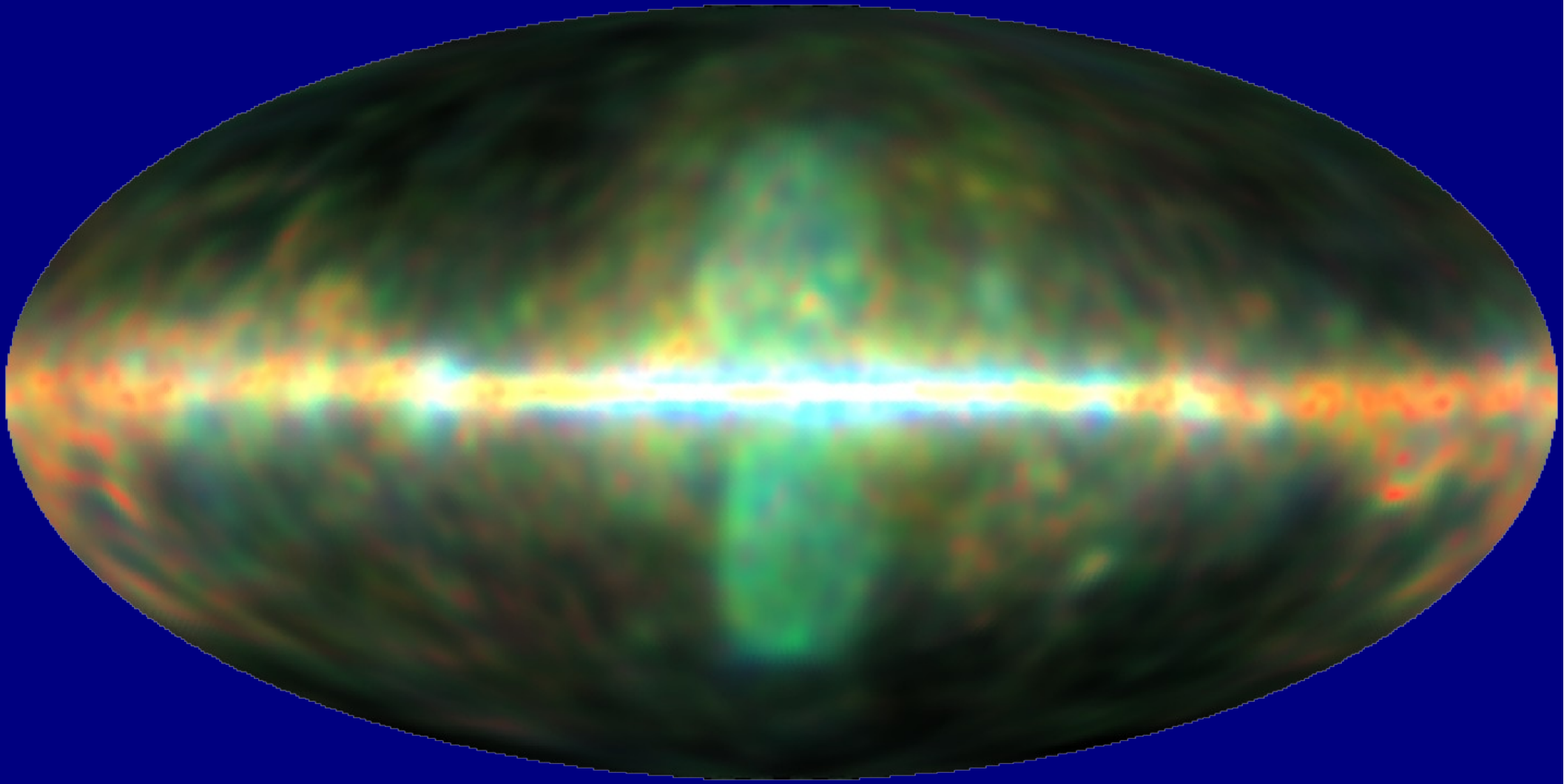

Diffuse gamma-ray sky

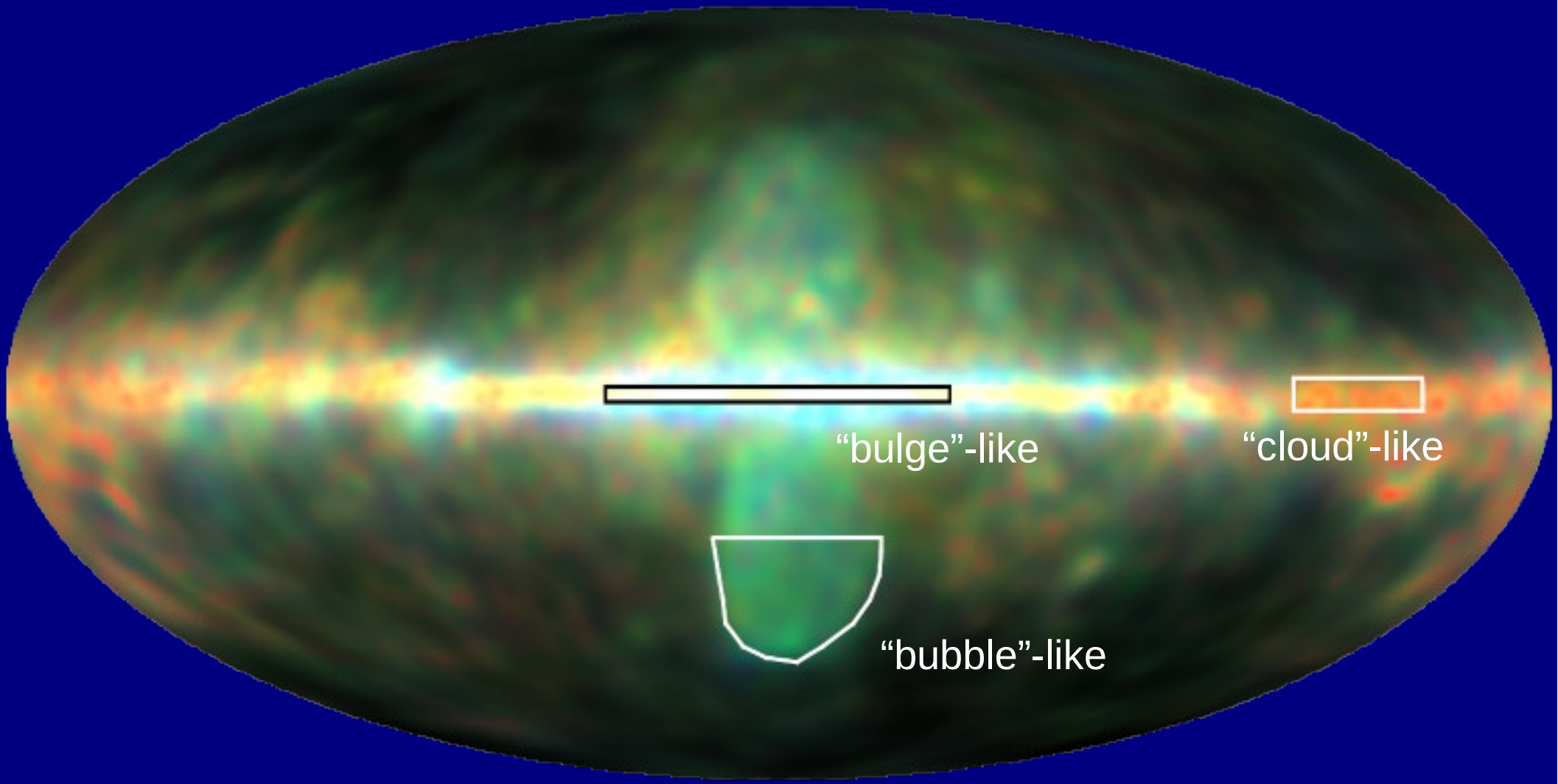

Spectra of diffuse components

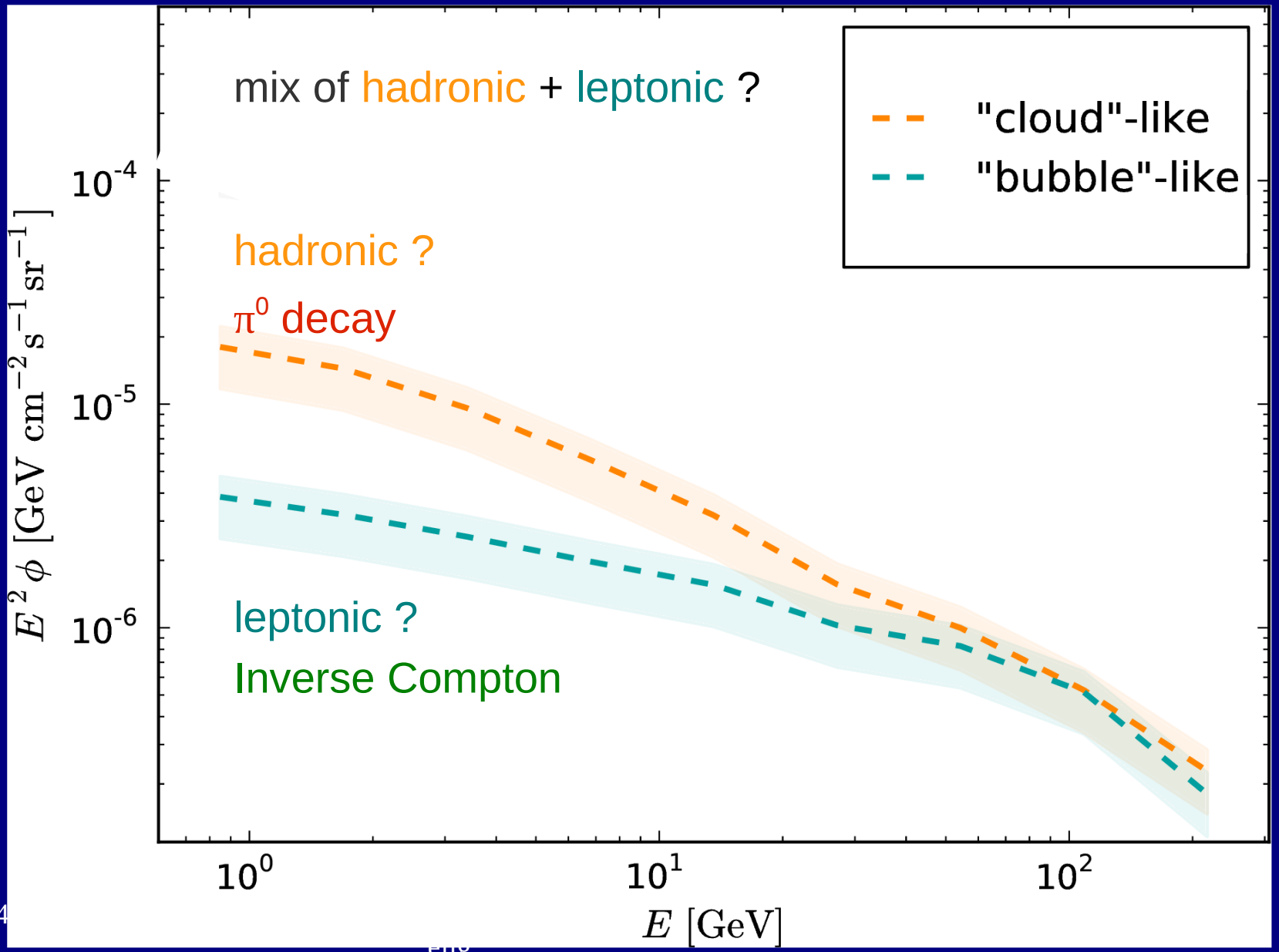

Gamma-ray emitting supernova remnants as the origin of Galactic cosmic rays?

Julia Becker Tjus[a,*], Björn Eichmann[a], Mike Kroll[a], Nils Nierstenhöfer[a]

[a] *Theoretische Physik IV: Plasma-Astroteilchenphysik*
Fakultät für Physik und Astronomie
Ruhr-Universität Bochum
44780 Bochum
Germany

(actually triggered my visit here !)

Use 21 Fermi-LAT SNRs to model proton spectrum.
These are 10% of total active SNRs, assume they are typical.
GALPROP 3D point-source injection mode.
Study proton spectral variations over Galaxy

Not yet secondaries?

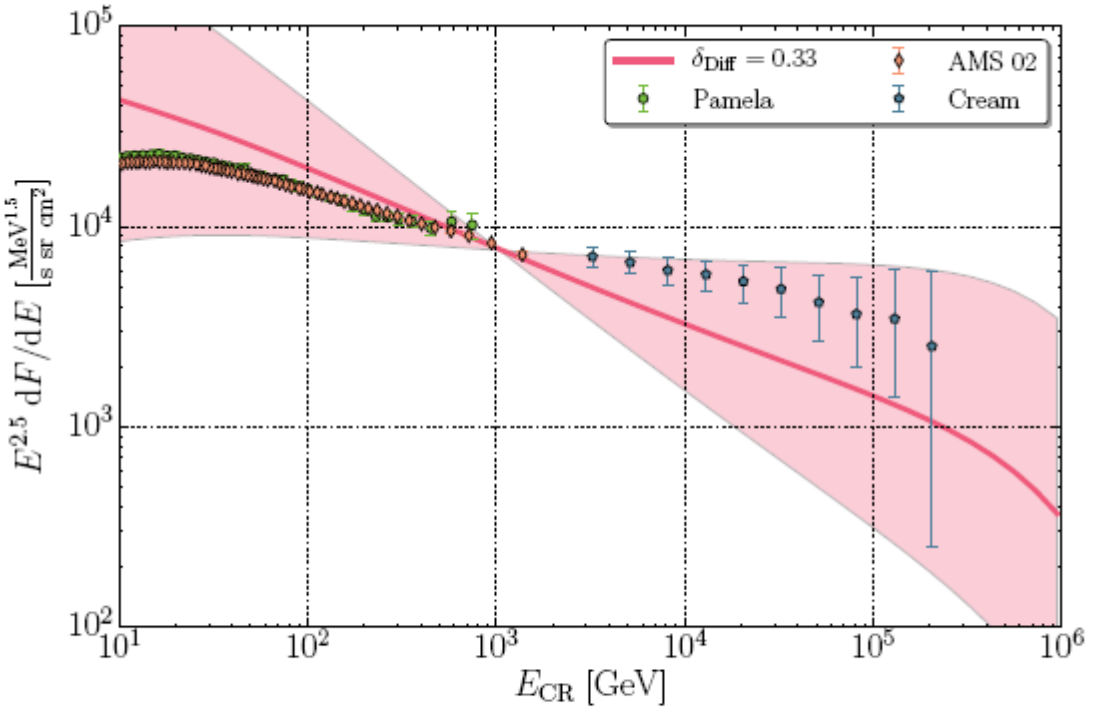

Figure 5: The CR flux in the large galaxy for simulated 20,000 SNRs, with the individual injection parameters taken from [17], considering a 1σ error in the spectral index. The diffusion coefficient has been set to a Kolmogorov-type diffusion, i.e. $D \propto E^{0.33}$. Experimental data taken from CREAM [69], PAMELA [70] and AMS-01 [71].

SNRs : several with claimed 'pion-peak'

But beware, this is at m(π^o) /2 = 67.5 MeV, so Fermi hardly covers it.

NB multiplying by E^2 is good but shifts the peak to higher energies, do not see the 'bump'

May be instead an indication for break in proton spectrum.

Need Fermi extension to lower energies, coming with Pass 8.

Sample spectrum: W44, Cardillo etal 2014. Model proton spectrum has break at 20 GeV.

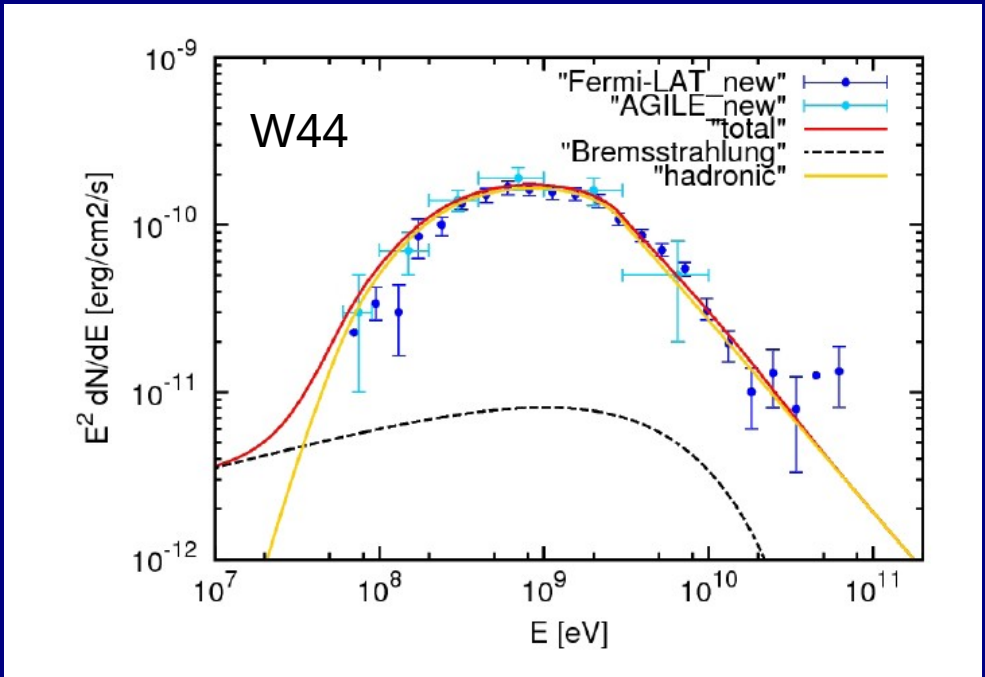

New 25 Jan: Fermi paper on **RCW86**: arXiv:1601.06534
Latest Pass 8 data. Favours a leptonic model

Fermi Bubbles

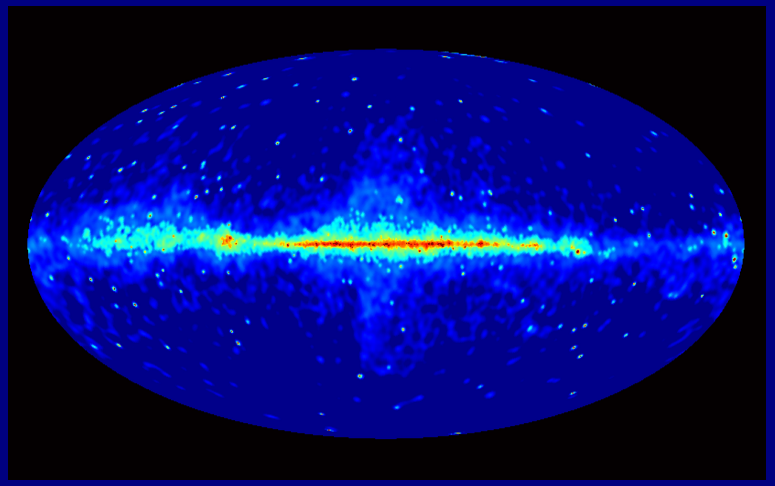

(related to WMAP Haze ?)

Planck haze (arXiv:1208.5483)
Overlaid on Fermi Bubbles

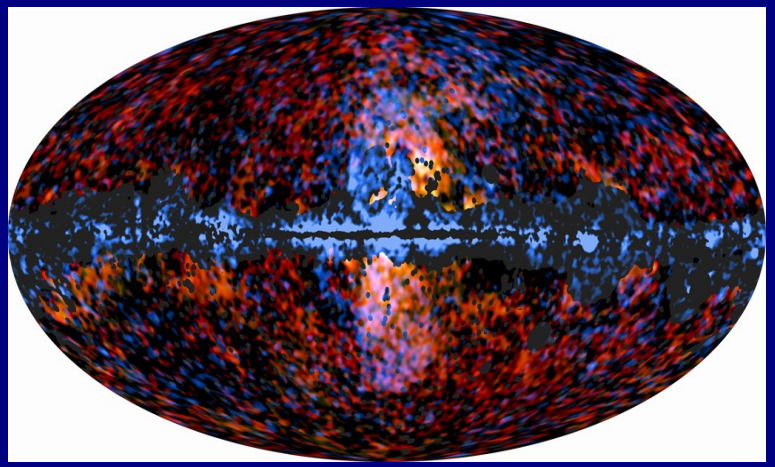

connection to 511 keV line ?

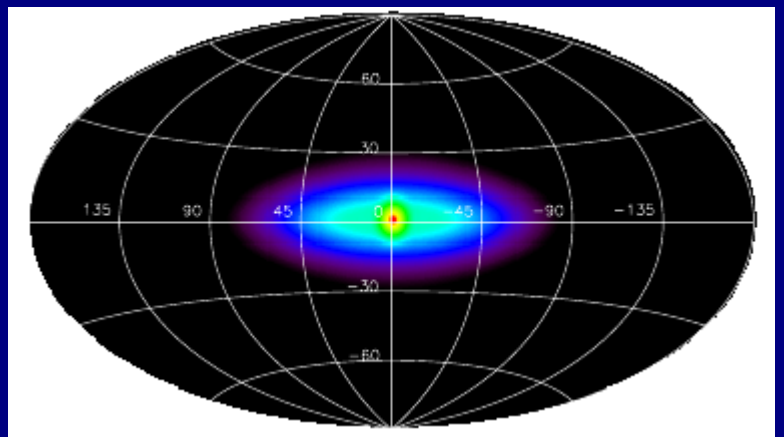

All are -
centred on Galactic Centre
leptonic
unknown origin

The Galbayes collaboration

Free parameters

Propagation

Proton normalization (10^{-9} cm^2 sr^{-1}s^{-1}MeV^{-1})	N_p
Diffusion coefficient[a] (10^{28} cm^2 s^{-1})	D_0
Rigidity power law index	δ
Alfvén speed (km s^{-1})	$v_{\rm Alf}$
Diffusion zone half-height (kpc)	z_h
Rigidity of first injection break (10^4 MV)	ρ_{br}
Nucleus injection index below ρ_{br}	ν_0
Nucleus injection index above ρ_{br}	ν_1
Nucleus injection index above 220 GV	ν_2
Difference between p and heavier inj. indices	δ_ν

Abundances: H, He, C, N, O, Ne, Na, Mg, Al, Si

20 Free parameters!

Results: propagation parameters

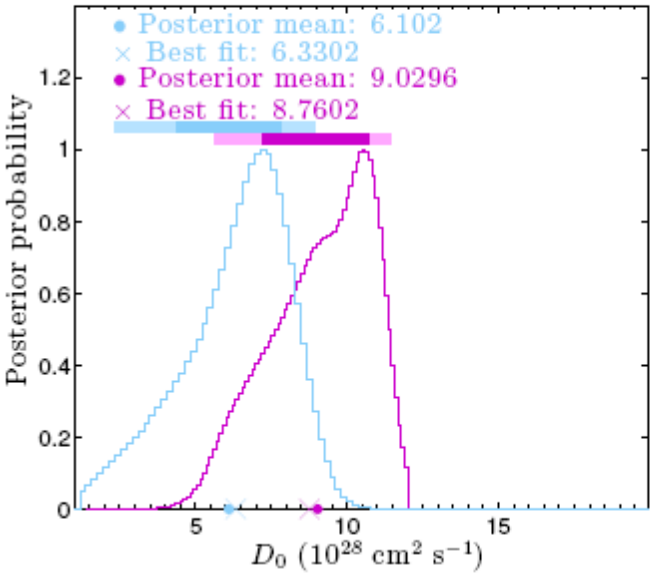

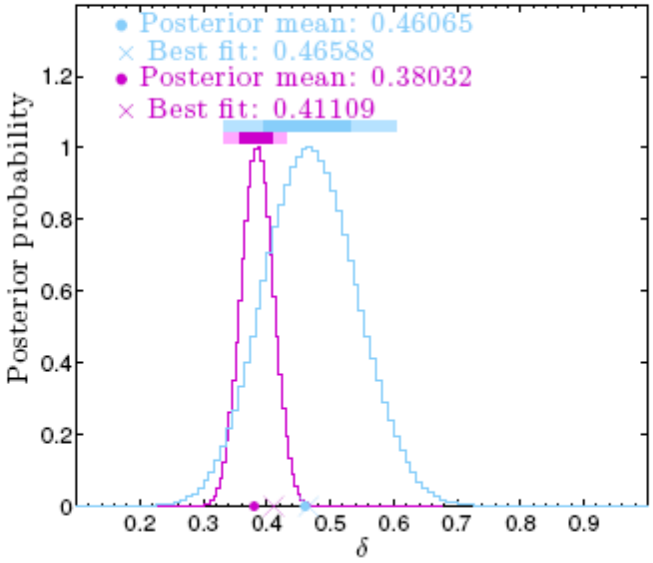

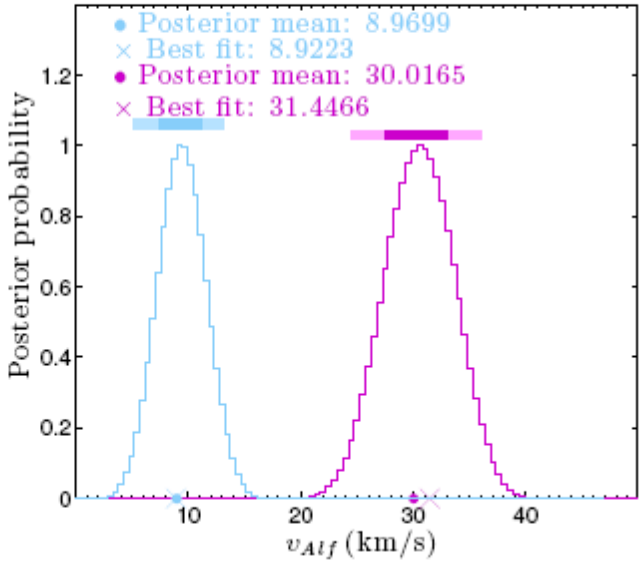

Light (B … Si) elements

$p, \bar{p}, \mathrm{He}$

Electrons, synchrotron and magnetic fields

Planck : Tess Jaffe lead author arXiv:1601:00546

Planck intermediate results. XLII. Large-scale Galactic magnetic fields

Planck Collaboration: R. Adam[64], P. A. R. Ade[76], M. I. R. Alves[84, 8], M. Ashdown[58, 4], J. Aumont[49], C. Baccigalupi[74], A. J. Banday[84, 8], R. B. Barreiro[54], N. Bartolo[25, 55], E. Battaner[86, 87], K. Benabed[50, 83], A. Benoit-Lévy[20, 50, 83], J.-P. Bernard[84, 8], M. Bersanelli[28, 41], P. Bielewicz[70, 8, 74], L. Bonavera[54], J. R. Bond[7], J. Borrill[11, 79], F. R. Bouchet[50, 77], F. Boulanger[49], M. Bucher[1], C. Burigana[40, 26, 42], R. C. Butler[40], E. Calabrese[81], J.-F. Cardoso[63, 1, 50], A. Catalano[64, 61], H. C. Chiang[22, 5], P. R. Christensen[71, 31], L. P. L. Colombo[19, 56], C. Combet[64], F. Couchot[60], B. P. Crill[56, 9], A. Curto[54, 4, 58], F. Cuttaia[40], L. Danese[74], R. J. Davis[57], P. de Bernardis[27], A. de Rosa[40], G. de Zotti[37, 74], J. Delabrouille[1], C. Dickinson[57], J. M. Diego[54], K. Dolag[85, 67], O. Doré[56, 9], A. Ducout[50, 47], X. Dupac[33], F. Elsner[20, 50, 83], T. A. Enßlin[67], H. K. Eriksen[52], K. Ferrière[84, 8], F. Finelli[40, 42], O. Forni[84, 8], M. Frailis[39], A. A. Fraisse[22], E. Franceschi[40], S. Galeotta[39], K. Ganga[1], T. Ghosh[49], M. Giard[84, 8], E. Gjerløw[52], J. González-Nuevo[16, 54], K. M. Górski[56, 89], A. Gregorio[29, 39, 45], A. Gruppuso[40], J. E. Gudmundsson[82, 73, 22], F. K. Hansen[52], D. L. Harrison[51, 58], C. Hernández-Monteagudo[10, 67], D. Herranz[54], S. R. Hildebrandt[56, 9], M. Hobson[4], A. Hornstrup[13], G. Hurier[49], A. H. Jaffe[47], T. R. Jaffe[84, 8*], W. C. Jones[22], M. Juvela[21], E. Keihänen[21], R. Keskitalo[11], T. S. Kisner[66], J. Knoche[67], M. Kunz[14, 49, 2], H. Kurki-Suonio[21, 36], J.-M. Lamarre[61], A. Lasenby[4, 58], M. Lattanzi[26], C. R. Lawrence[56], J. P. Leahy[57], R. Leonardi[6], F. Levrier[61], P. B. Lilje[52], M. Linden-Vørnle[13], M. López-Caniego[33, 54], P. M. Lubin[23], J. F. Macías-Pérez[64], G. Maggio[39], D. Maino[28, 41], N. Mandolesi[40, 26], A. Mangilli[49, 60], M. Maris[39], P. G. Martin[7], S. Masi[27], A. Melchiorri[27, 43], A. Mennella[28, 41], M. Migliaccio[51, 58], M.-A. Miville-Deschênes[49, 7], A. Moneti[50], L. Montier[84, 8], G. Morgante[40], D. Munshi[76], J. A. Murphy[69], P. Naselsky[72, 32], F. Nati[22], P. Natoli[26, 3, 40], H. U. Nørgaard-Nielsen[13], N. Oppermann[7], E. Orlando[88], L. Pagano[27, 43], F. Pajot[49], R. Paladini[48], D. Paoletti[40, 42], F. Pasian[39], L. Perotto[64], V. Pettorino[35], F. Piacentini[27], M. Piat[1], E. Pierpaoli[19], S. Plaszczynski[60], E. Pointecouteau[84, 8], G. Polenta[3, 38], N. Ponthieu[49, 46], G. W. Pratt[62], S. Prunet[50, 83], J.-L. Puget[49], J. P. Rachen[17, 67], M. Reinecke[67], M. Remazeilles[57, 49, 1], C. Renault[64], A. Renzi[30, 44], I. Ristorcelli[84, 8], G. Rocha[56, 9], M. Rossetti[28, 41], G. Roudier[1, 61, 56], J. A. Rubiño-Martín[53, 15], B. Rusholme[48], M. Sandri[40], D. Santos[64], M. Savelainen[21, 36], D. Scott[18], L. D. Spencer[76], V. Stolyarov[4, 80, 59], R. Stompor[1], A. W. Strong[68], R. Sudiwala[76], R. Sunyaev[67, 78], A.-S. Suur-Uski[21, 36], J.-F. Sygnet[50], J. A. Tauber[34], L. Terenzi[75, 40], L. Toffolatti[16, 54, 40], M. Tomasi[28, 41], M. Tristram[60], M. Tucci[14], L. Valenziano[40], J. Valiviita[21, 36], B. Van Tent[65], P. Vielva[54], F. Villa[40], L. A. Wade[56], B. D. Wandelt[50, 83, 24], I. K. Wehus[56, 52], D. Yvon[12], A. Zacchei[39], and A. Zonca[23]

GALPROP Cosmic-ray electrons used for synchrotron emission

Planck comparison with B-field models, Jaffe etal 2015

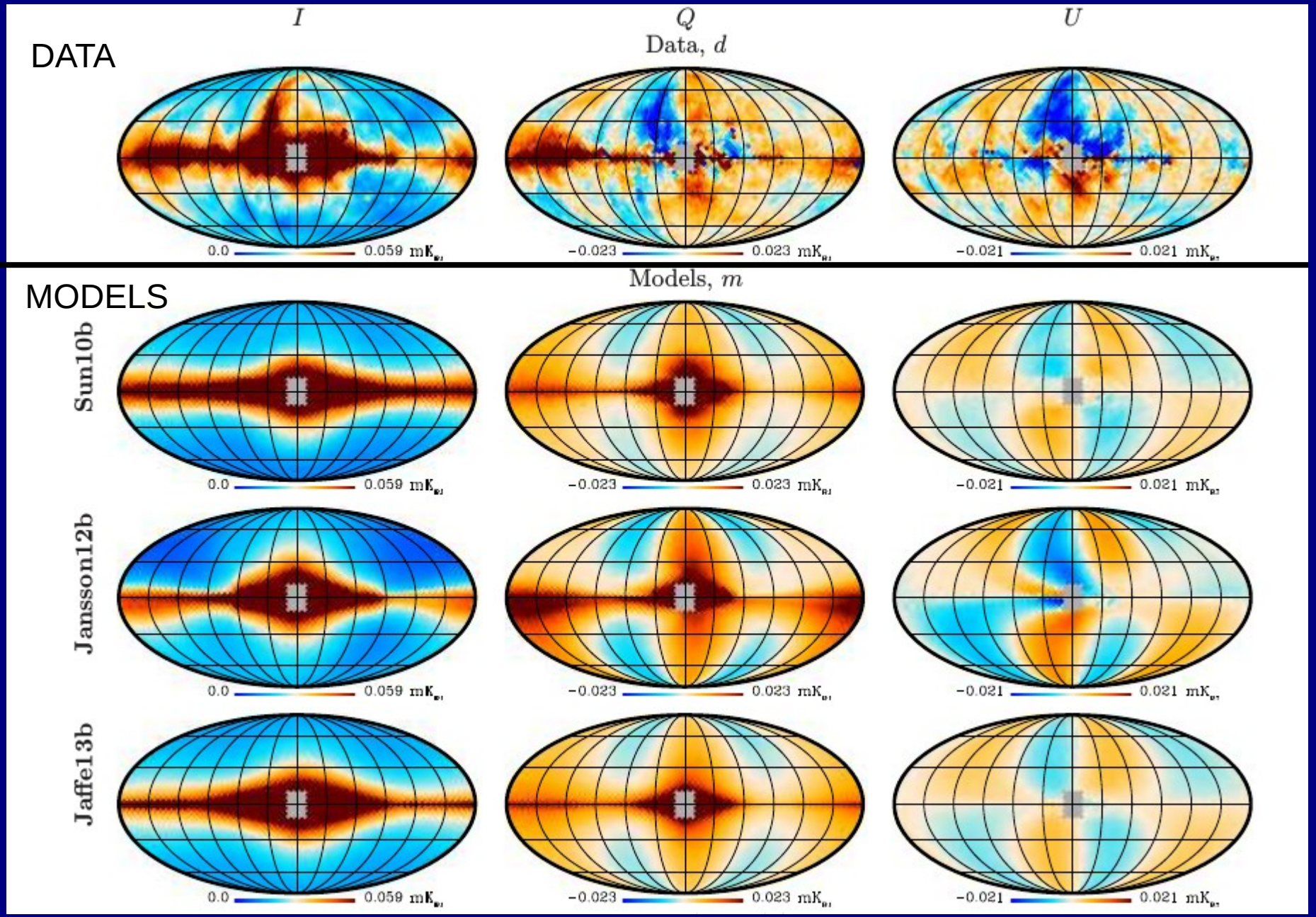

TOTAL Polarized: Stokes Q Stokes U

Hot news:

Hammurabi synchrotron new release from Tess Jaffe (Toulouse)

sourceforge.net/hammurabicode

With GALPROP interface!

Hammurabi = synchrotron package used for Planck etc.
Full Stokes parameters.

Additional to GALPROP features:
Faraday depolarization
Faraday rotation of radio sources
More advances B-field models

GALPROP can compute electrons + positrons
→ good combination.

CHANG-ES Project

JVLA 35 nearby edge-on galaxies
Including familiar ones NGC891, 4631 etc
21 and 6 cm, polarization

Synchrotron halos
Spectral variation, cosmic-ray propagation

Data now public, on-going analysis by collaboration
Followup with GBT, Alma etc

CHANG-ES IV: Radio continuum emission of 35 edge-on galaxies observed with the Karl G. Jansky Very Large Array in D-configuration – Data Release 1

Theresa Wiegert[1], Judith Irwin[2], Arpad Miskolczi[3], Philip Schmidt[4], Silvia Carolina Mora[5], Ancor Damas-Segovia[6], Yelena Stein[7], Jayanne English[8], Richard J. Rand[9], Isaiah Santistevan[10], Rene Walterbos[11], Marita Krause[12], Rainer Beck[13], Ralf-Jürgen Dettmar[14], Amanda Kepley[15], Marek Wezgowiec[16], Q. Daniel Wang[17], George Heald[18], Jiangtao Li[19], Stephen MacGregor[20], Megan Johnson[21], A. W. Strong[22], Amanda DeSouza[23], Troy A. Porter[24]

Composite image of 30 galaxies

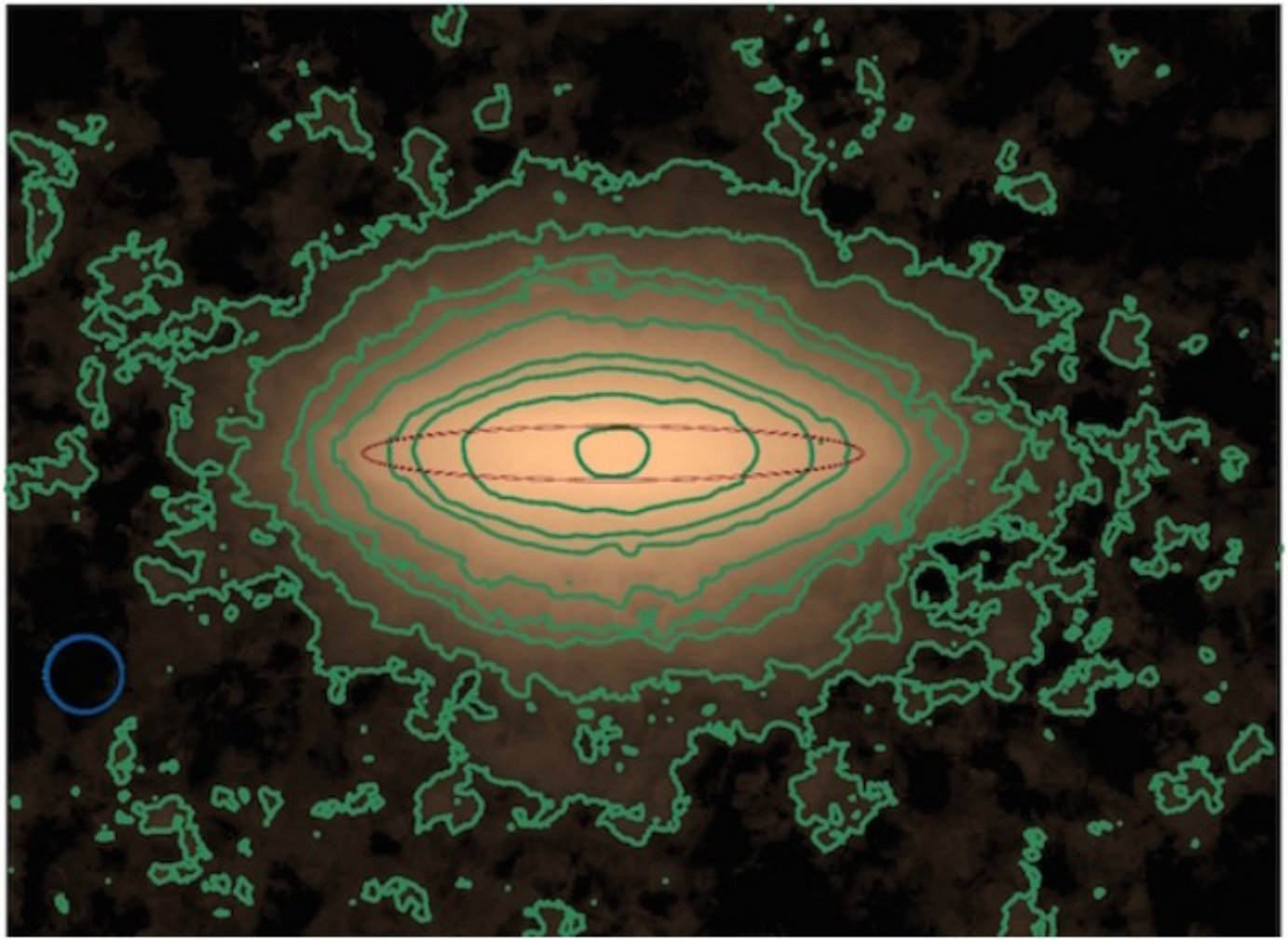

Fig. 6.— The median edge-on spiral galaxy in L-band, made from stacking 30 of the galaxies in Fig. 5. The red ellipse is a sample 22μm contour that corresponds to the scaling of the radio data and thus represents the disk radial extent. The beam shown is the *average* beam of the 30 galaxies.

MNRAS 000, 1–21 (2016) Preprint 15 February 2016 Compiled using MNRAS LATEX style file v3.0

Advective and diffusive cosmic ray transport in galactic haloes

Volker Heesen,[1]* Ralf-Jürgen Dettmar,[2] Marita Krause,[3] Rainer Beck[3] and Yelena Stein[2]
[1]School of Physics and Astronomy, University of Southampton, Southampton SO17 1BJ, UK
[2]Astronomisches Institut der Ruhr-Universität Bochum, Universitätsstr. 150, D-44780 Bochum, Germany
[3]Max-Planck-Institut für Radioastronomie, Auf dem Hügel 69, D-53121 Bonn, Germany

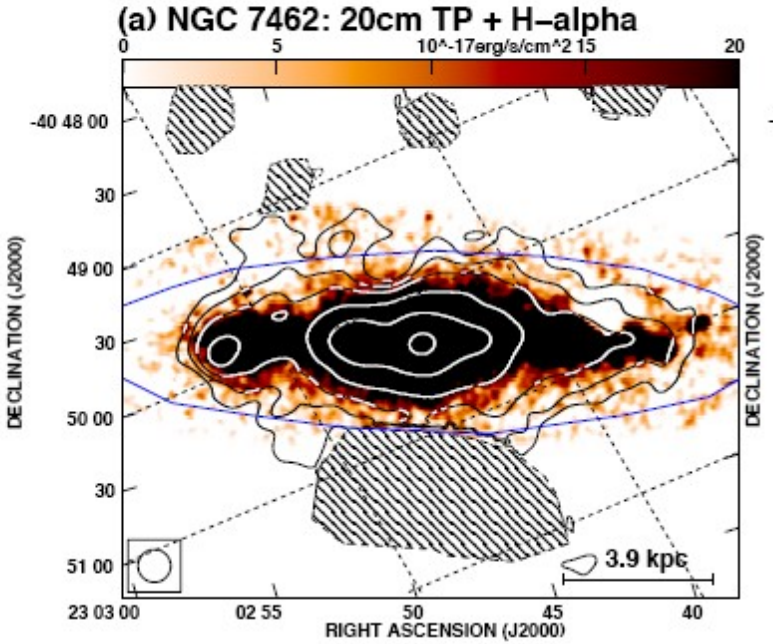

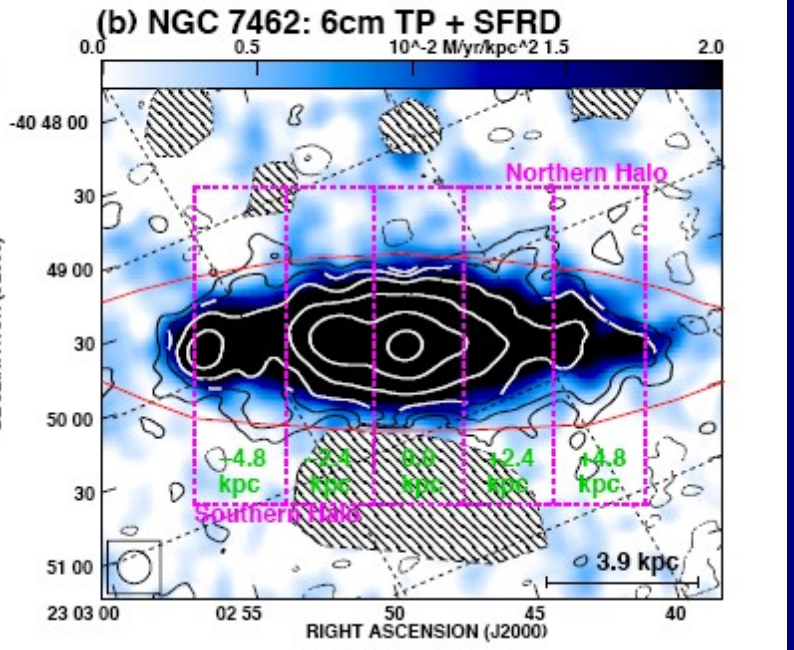

MNRAS 000, 1–21 (2016) Preprint 15 February 2016 Compiled using MNRAS LaTeX style file v3.0

Advective and diffusive cosmic ray transport in galactic haloes

Volker Heesen,[1]* Ralf-Jürgen Dettmar,[2] Marita Krause,[3] Rainer Beck[3] and Yelena Stein[2]

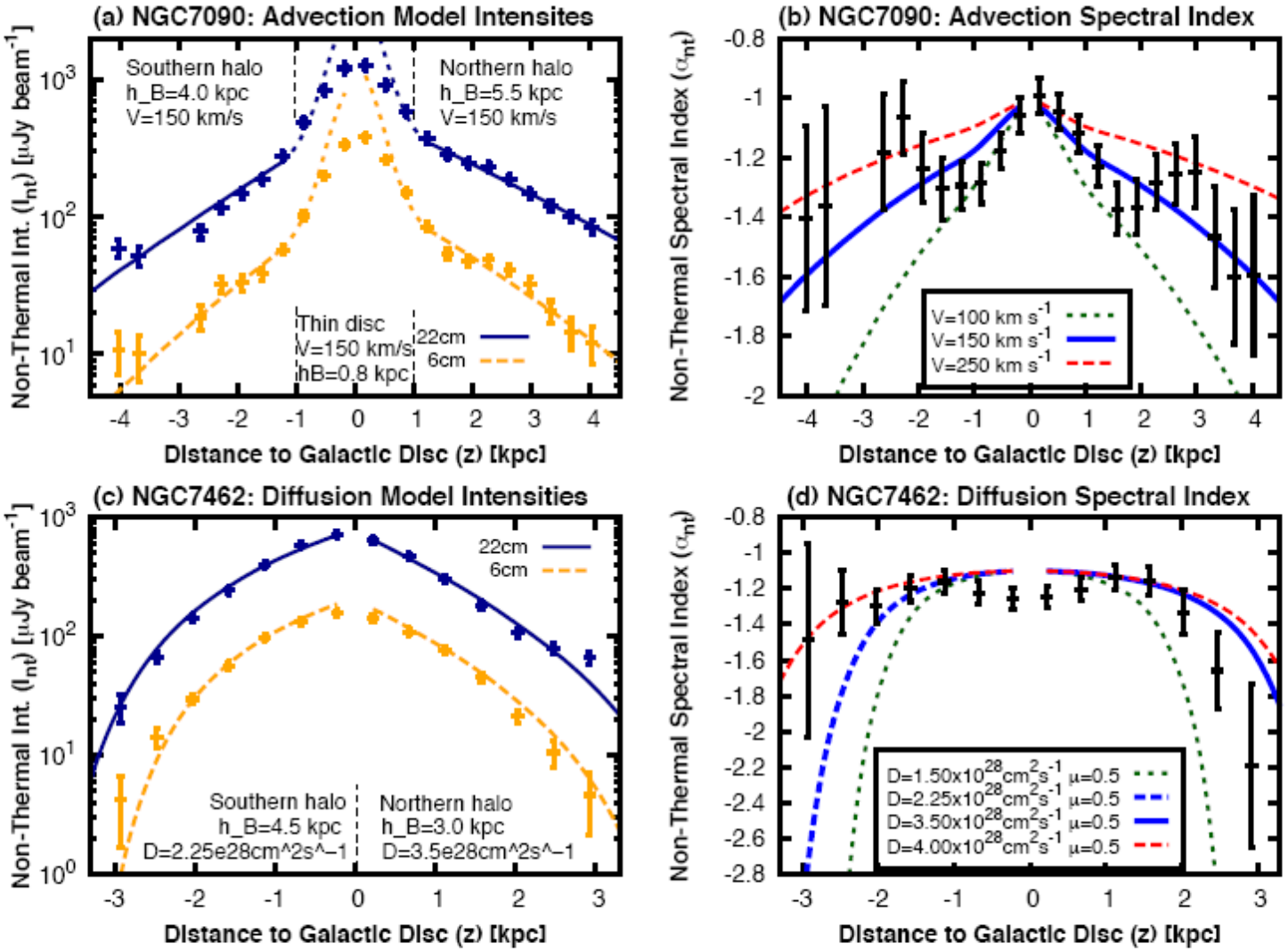

Figure 4. Vertical profiles of the non-thermal radio continuum emission and the non-thermal spectral index in NGC 7090 (averaged between offsets of ±4.25 kpc, top row) and NGC 7462 (averaged between offsets of ±6.0 kpc, bottom row). Negative values of z are for the southern halo, and positive ones are for the northern halo. *Left panels:* modelled profiles from the solution of the 1D cosmic ray transport equations for advection (NGC 7090) and diffusion (NGC 7462) shown as solid, dark-blue (λ22 cm) and as dashed, orange (λ6 cm) lines. The short-dashed lines show the thin disc intensities in NGC 7090, not convolved to the resolution, so that they appear not to fit to the data. *Right panels:* lines show our 1D cosmic ray transport models, with the best-fitting model shown as thick (solid, except in the S halo of NGC 7462) blue line and the error interval indicated by the dashed lines.


That's all Folks!

Producing the cosmic-ray electron spectrum

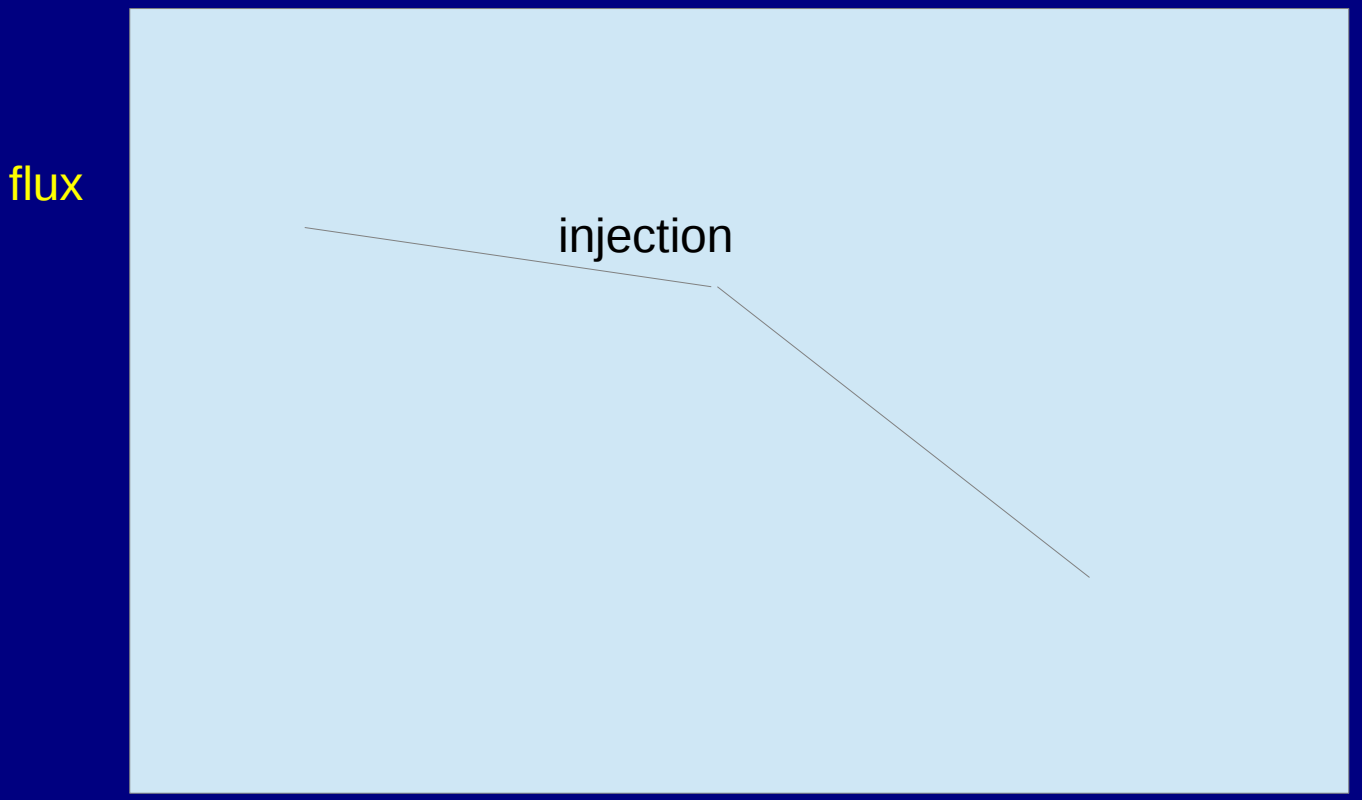

Producing the cosmic-ray electron spectrum

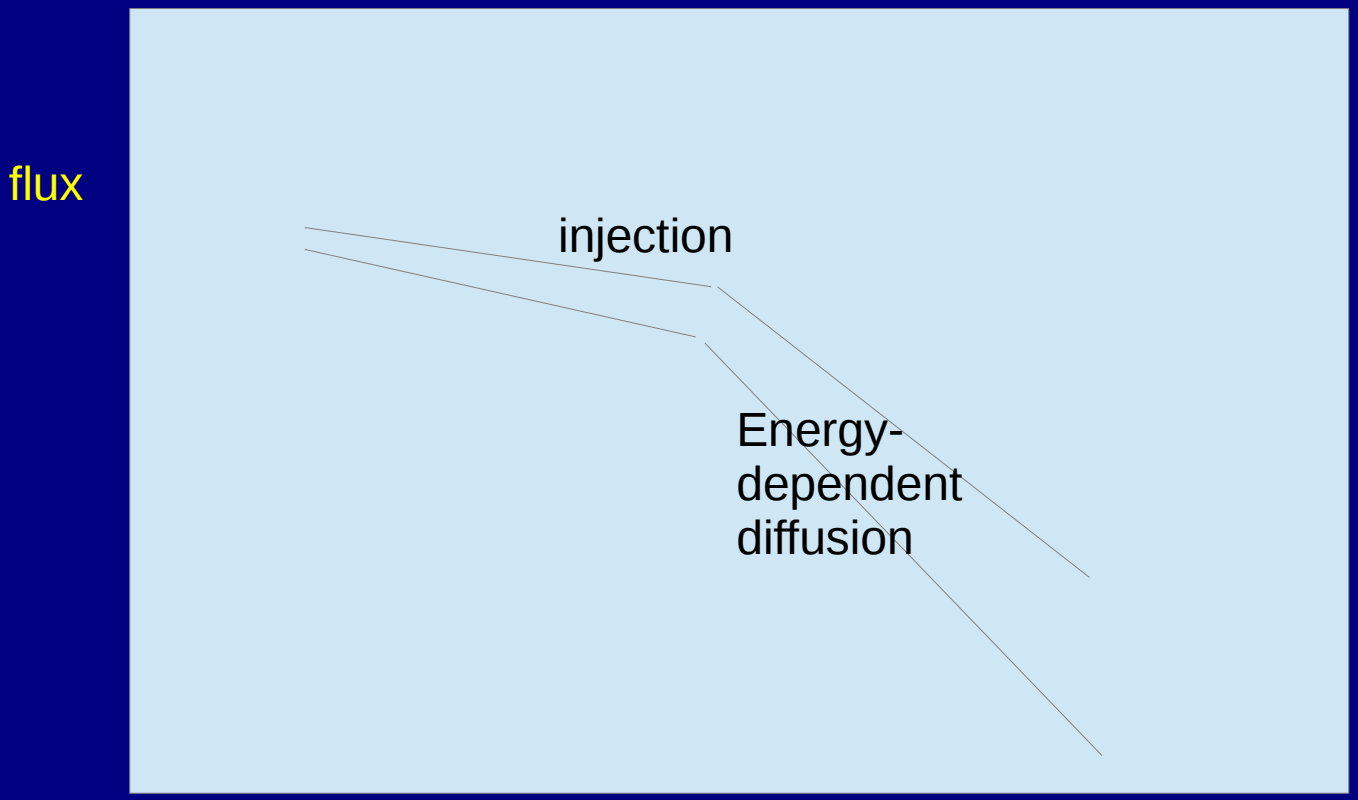

Producing the cosmic-ray electron spectrum

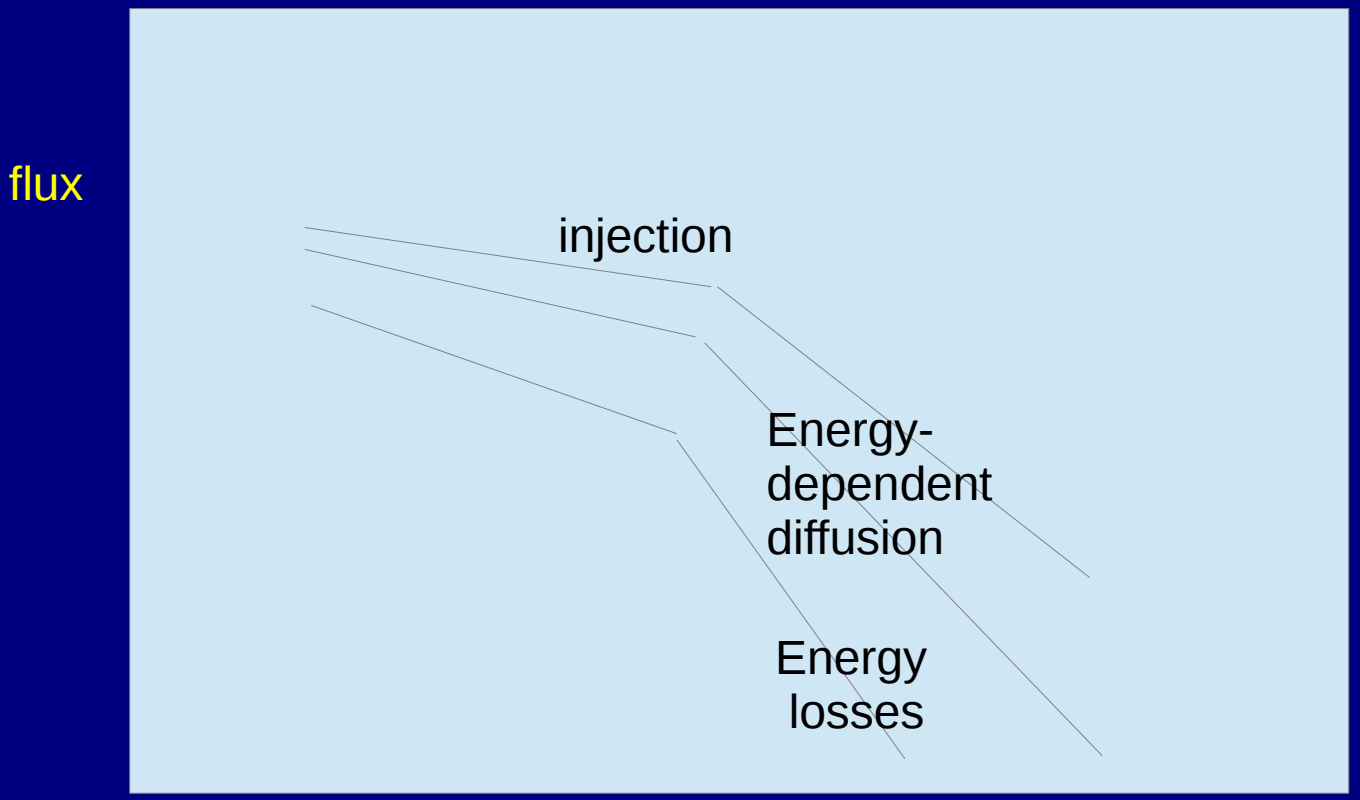

Producing the cosmic-ray electron spectrum

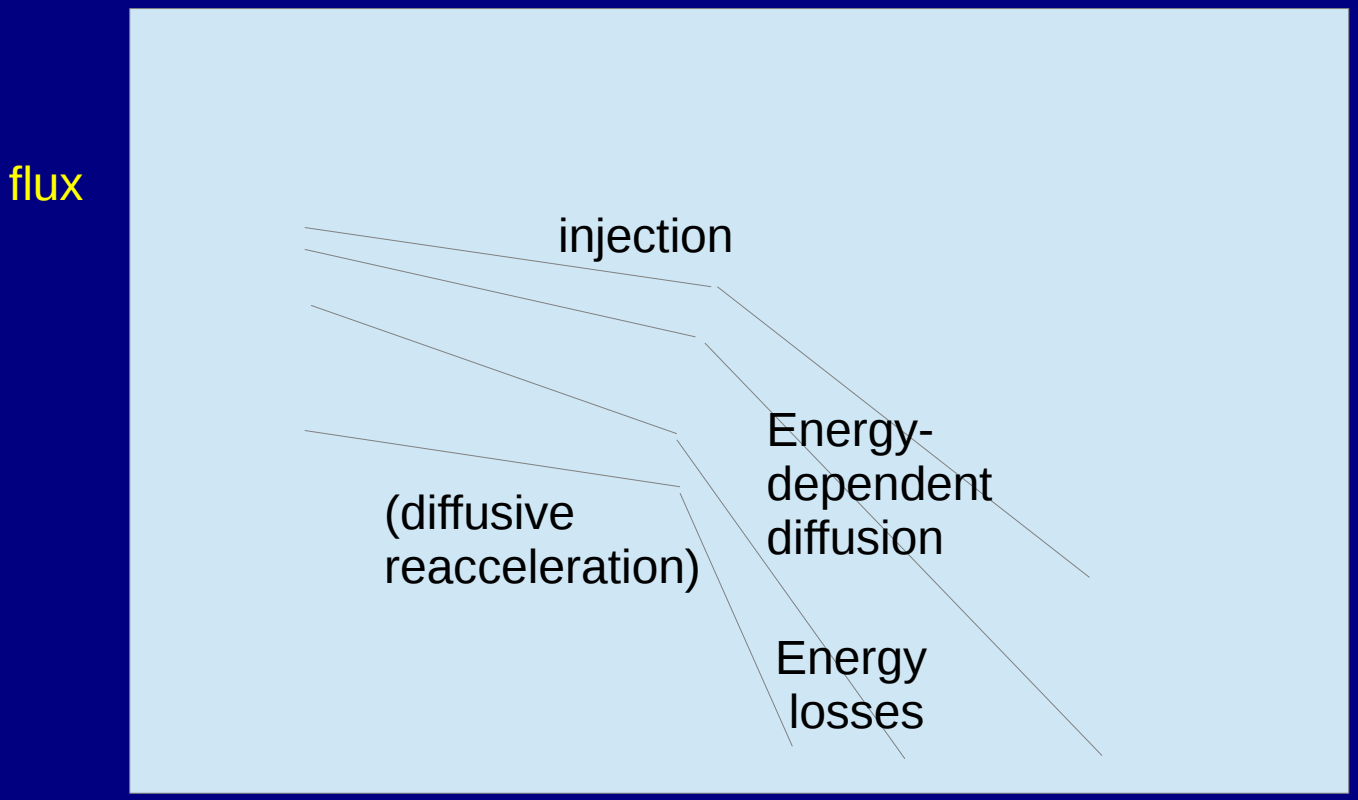

Producing the cosmic-ray electron spectrum

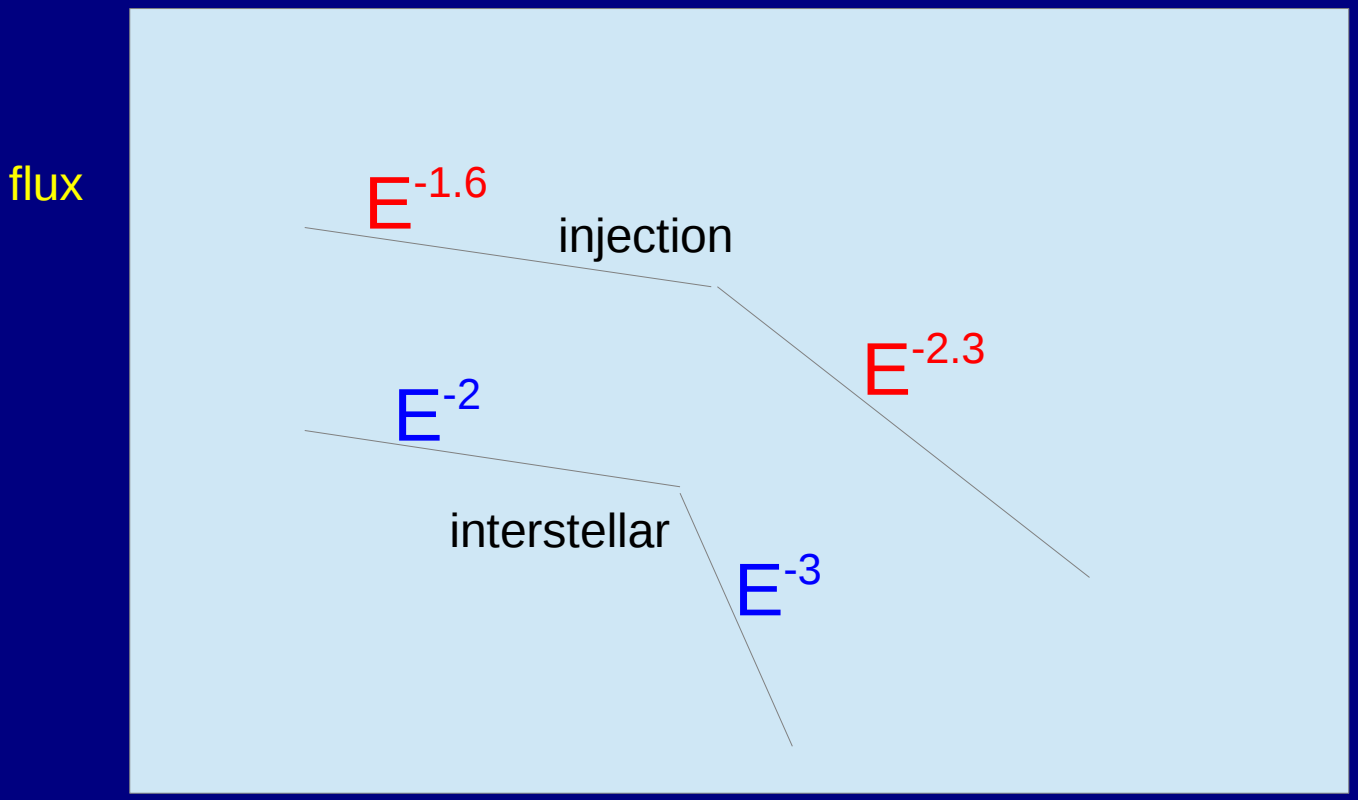

Connecting Synchrotron, Cosmic Rays, and Magnetic Fields in the Plane of the Galaxy

T. R. Jaffe [1,2⋆], A. J. Banday[1,2,3]†, J. P. Leahy[4]‡, S. Leach[5,6]§, A. W. Strong[7]¶

[1] *Université de Toulouse; UPS-OMP; IRAP; Toulouse, France*
[2] *CNRS; IRAP; 9 Av. colonel Roche, BP 44346, F-31028 Toulouse cedex 4, France*
[3] *Max Planck Institute for Astrophysics, Karl-Schwarzschild Str. 1, D-85741 Garching, Germany*
[4] *Jodrell Bank Centre for Astrophysics, School of Physics and Astronomy, The University of Manchester, Oxford Road, Manchester, M13 9PL, United Kingdom*
[5] *SISSA, Astrophysics Sector, via Beirut 2-4, I-34014 Trieste, Italy.*
[6] *INFN, Sezione di Trieste, I-34014 Trieste, Italy.*
[7] *Max-Planck-Institut für Extraterrestrische Physik, Postfach 1312, D-85741 Garching, Germany*

MNRAS 416, 1152 (2011)

Uses RM, polarization, MCMC.
Cosmic-ray electrons from sources + propagation

A&A 534, A54 (2011)
DOI: 10.1051/0004-6361/201116828

Astronomy & Astrophysics

The interstellar cosmic-ray electron spectrum from synchrotron radiation and direct measurements⋆

A. W. Strong[1], E. Orlando[2,1], and T. R. Jaffe[3,4]

[1] Max-Planck-Institut für extraterrestrische Physik, Postfach 1312, 85741 Garching, Germany
e-mail: aws@mpe.mpg.de
[2] W.W. Hansen Experimental Physics Laboratory, Kavli Institute for Particle Astrophysics and Cosmology, Stanford University, Stanford, CA 94305, USA
e-mail: eorlando@stanford.edu
[3] Université de Toulouse; UPS-OMP, IRAP, Toulouse, France
[4] CNRS, IRAP, 9 Av. colonel Roche, BP 44346, 31028 Toulouse Cedex 4, France

Received 4 March 2011 / Accepted 17 August 2011

ABSTRACT

Aims. We exploit synchrotron radiation to constrain the low-energy interstellar electron spectrum, using various radio surveys and connecting with electron data from *Fermi*-LAT and other experiments.
Methods. The GALPROP programme for cosmic-ray propagation, gamma-ray and synchrotron radiation is used. Secondary electrons and positrons are included. Propagation models based on cosmic-ray and gamma-ray data are tested against synchrotron data from 22 MHz to 94 GHz.
Results. The synchrotron data confirm the need for a low-energy break in the cosmic-ray electron injection spectrum. The interstellar spectrum below a few GeV has to be lower than standard models predict, and this suggests less solar modulation than usually assumed. Reacceleration models are more difficult to reconcile with the synchrotron constraints. We show that secondary leptons are important for the interpretation of synchrotron emission. We also consider a cosmic-ray propagation origin for the low-energy break.
Conclusions. Exploiting the complementary information on cosmic rays and synchrotron gives unique and essential constraints on electrons, and has implications for gamma rays. This connection is especially relevant now in view of the ongoing *Planck* and *Fermi* missions.

Following results based on this paper.

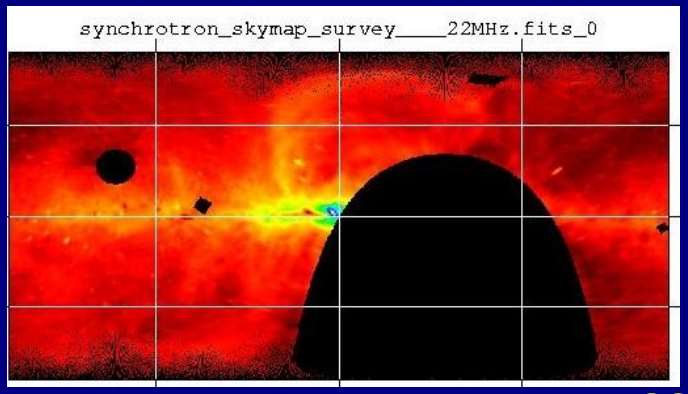

22 MHz

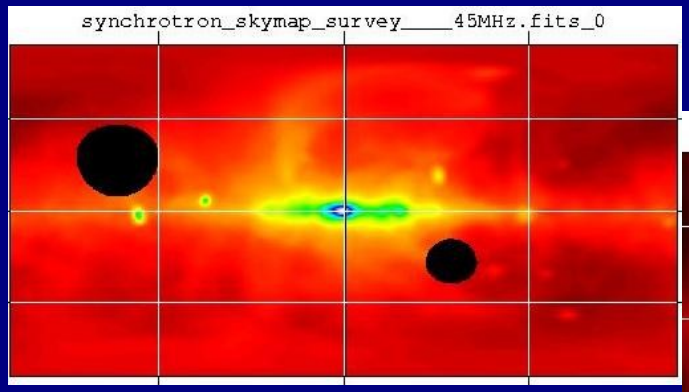

45 MHz

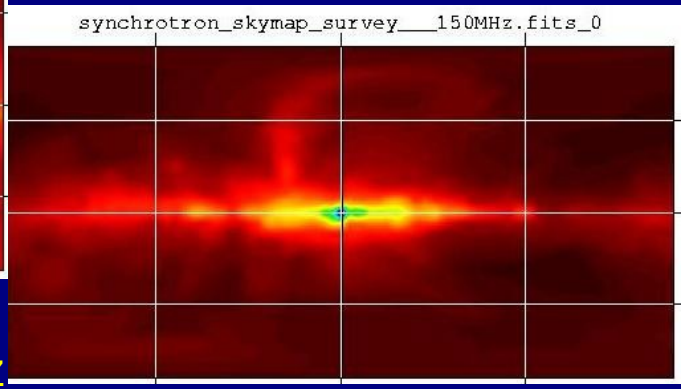

150 MHz

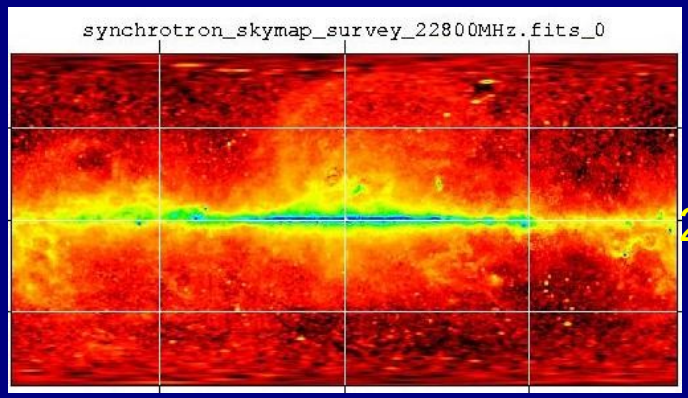

23 GHz

Continuum
sky surveys

408 MHz

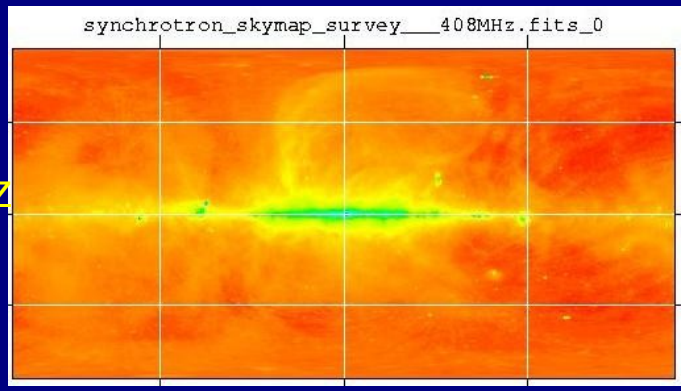

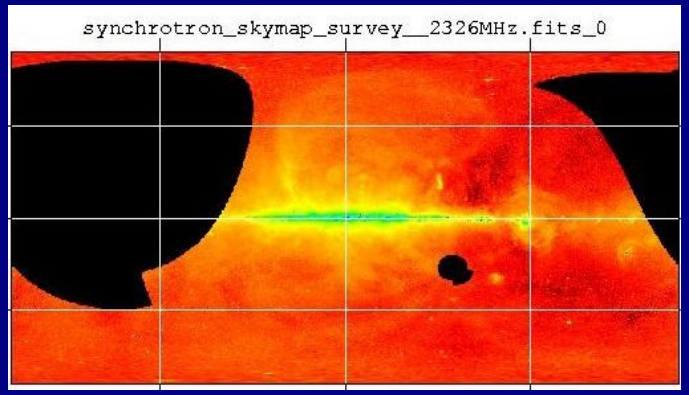

2.3 GHz

820 MHz

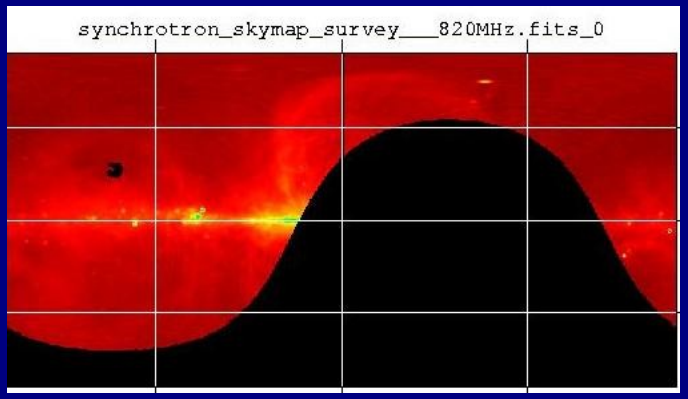

1.4 GHz

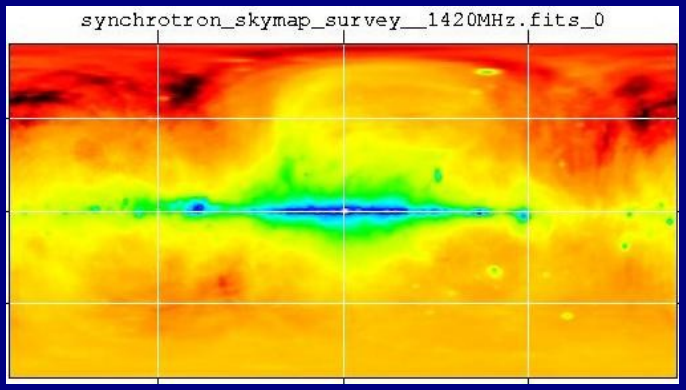

COSMIC RAY ELECTRONS

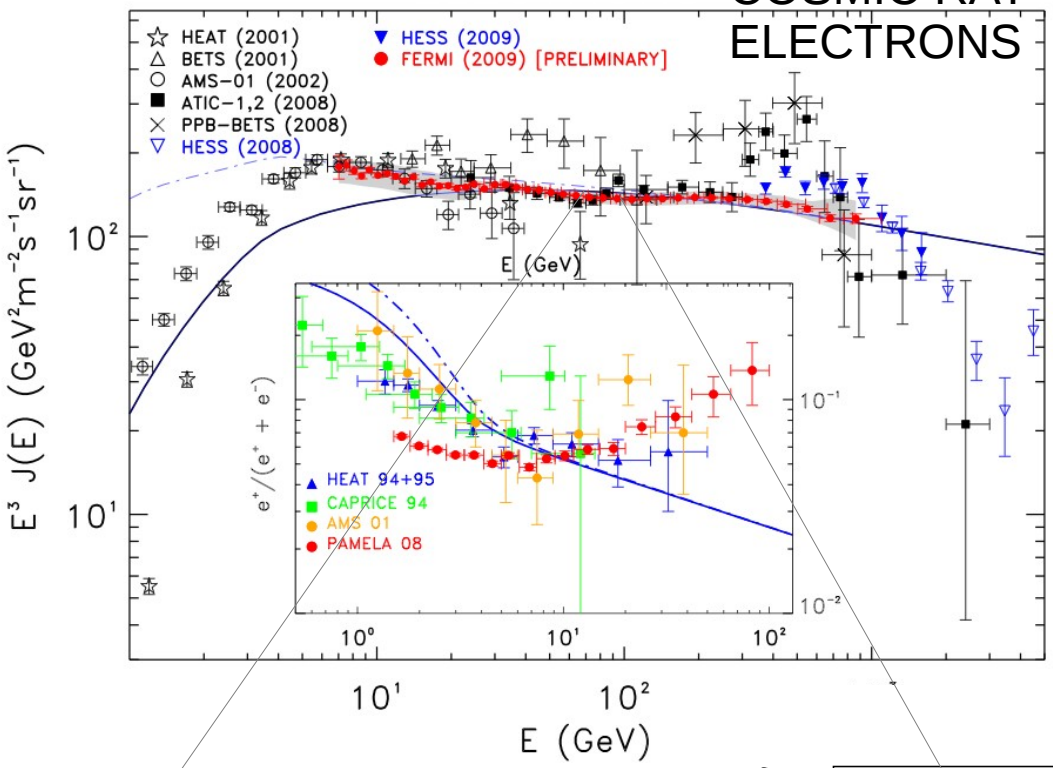

SYNCHROTRON

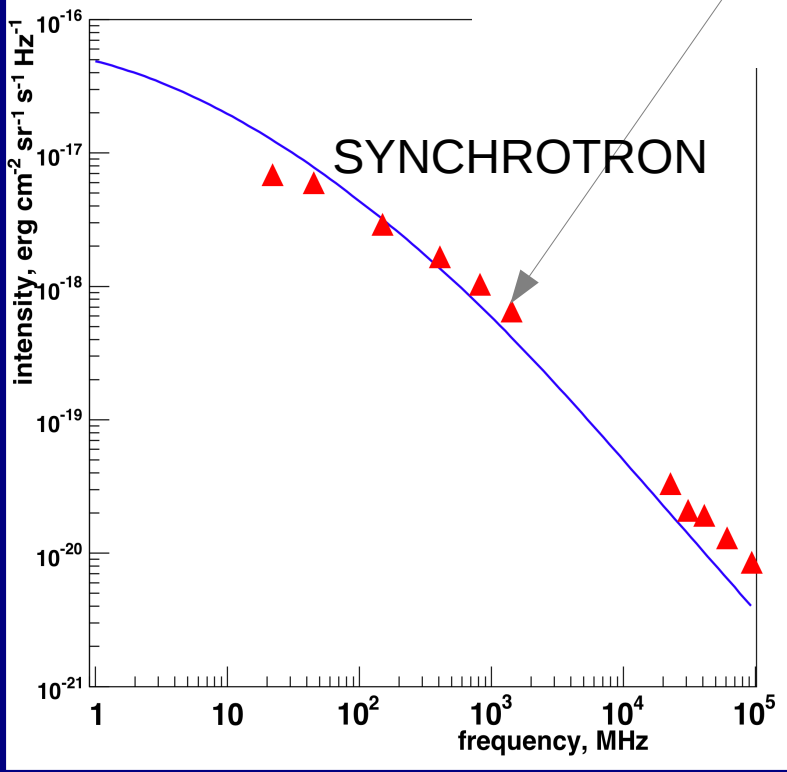

SAME ELECTRONS for RADIO and GAMMA RAYS !

good constraints on models

GAMMA RAYS

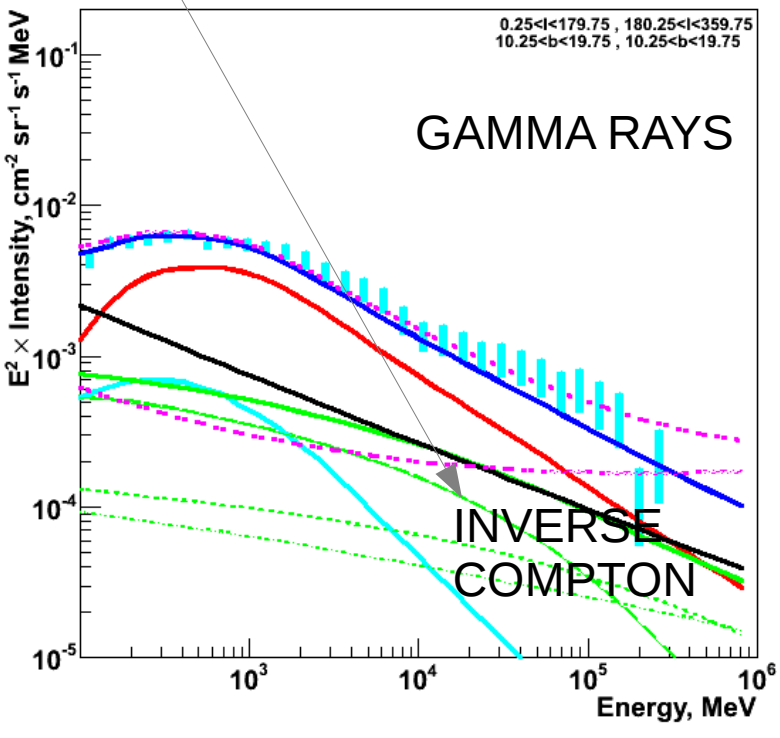

INVERSE COMPTON

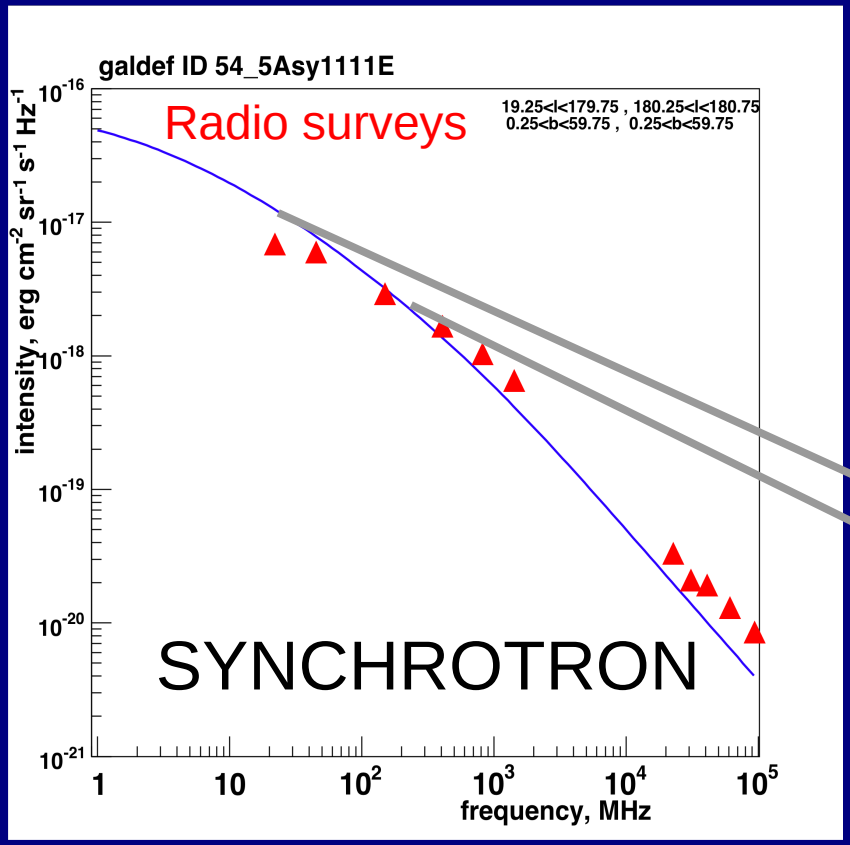

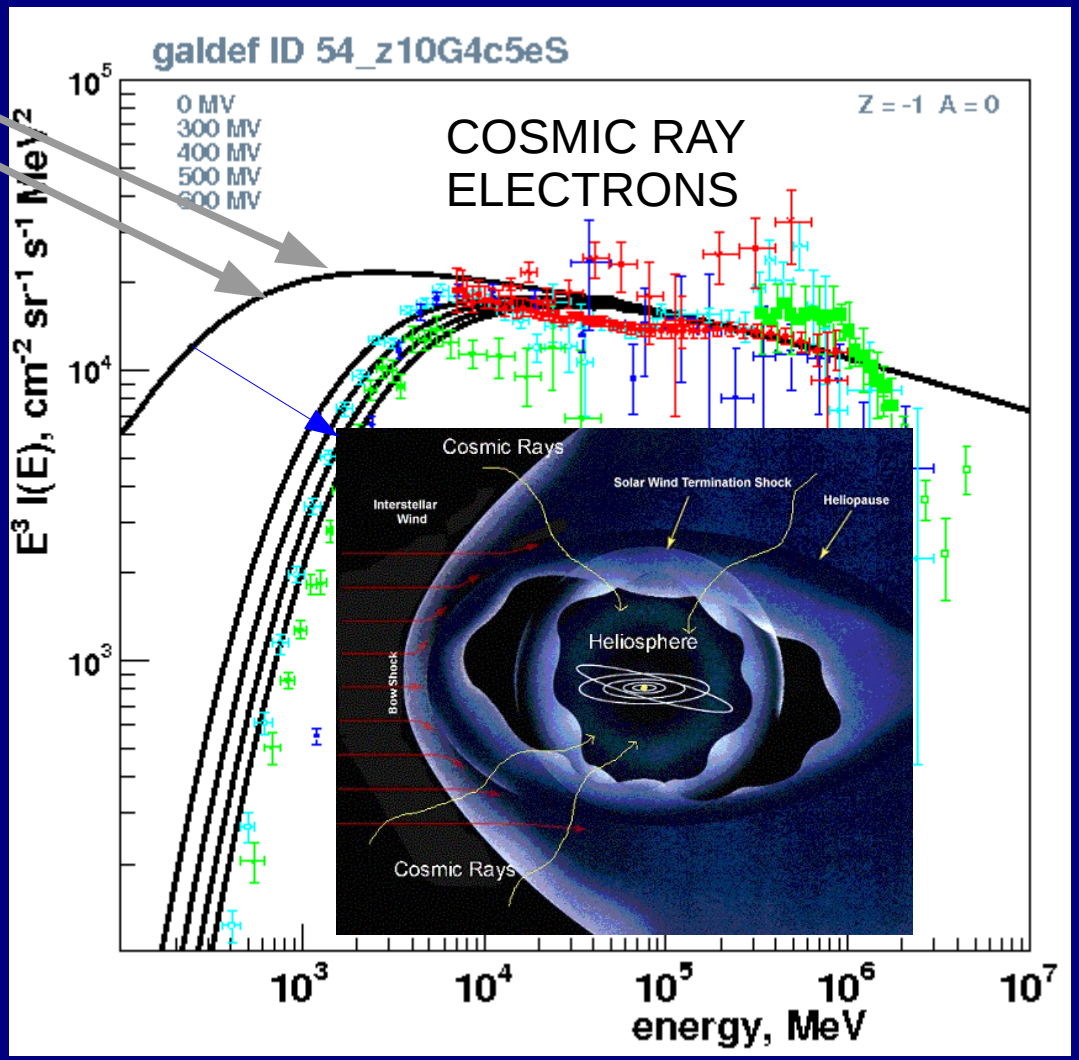

Radio provides essential probe of interstellar electron spectrum at E < few GeV to complement direct measurements and determine solar modulation

Electrons have huge uncertainty due to modulation here

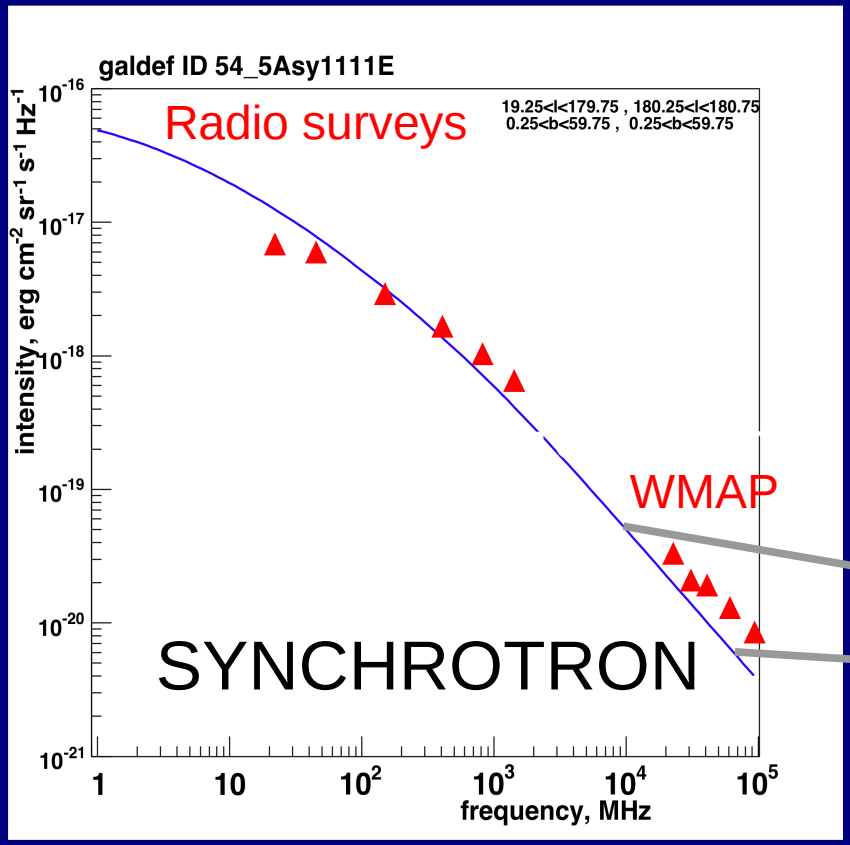

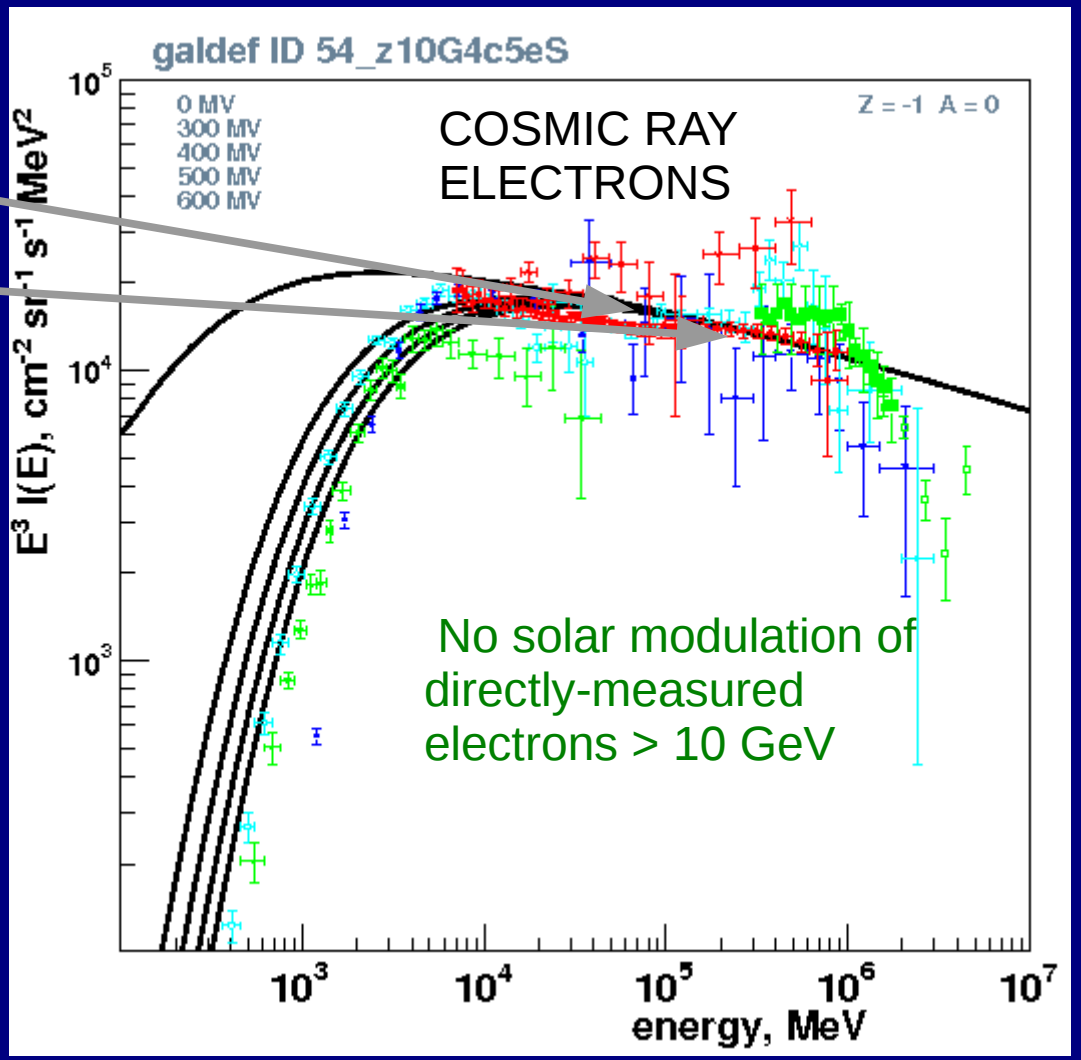

microwaves probe
interstellar electron spectrum
10 - 100 GeV

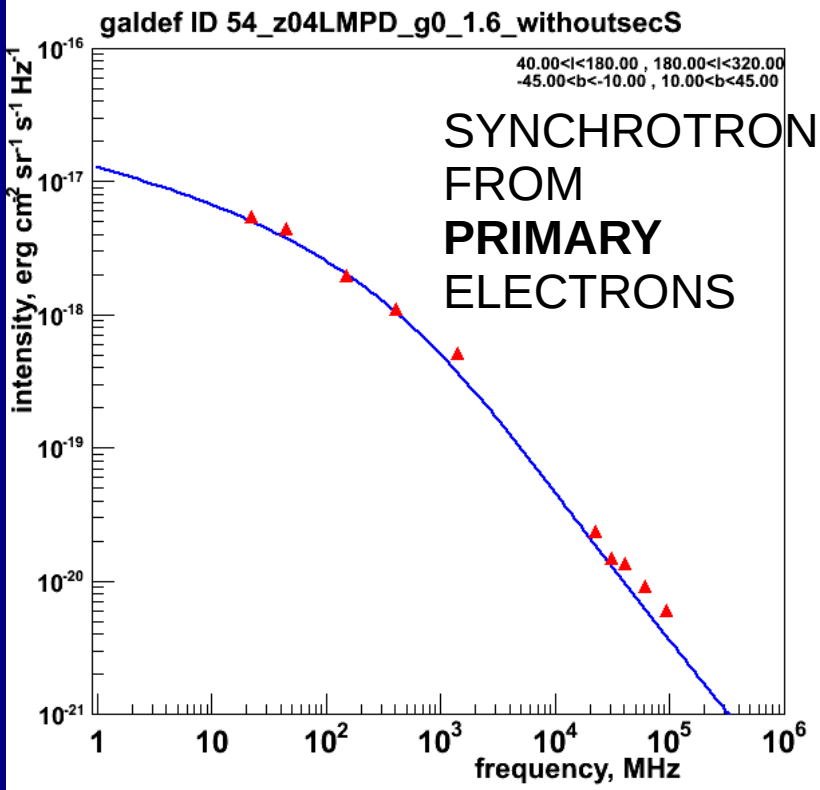

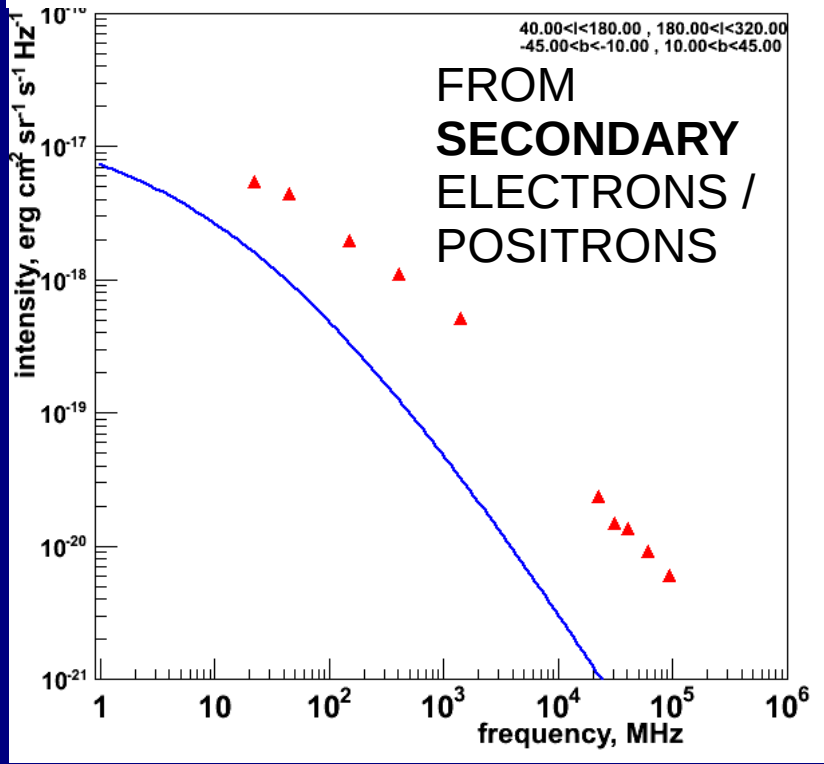

Secondary positrons
(and secondary electrons)
are important for synchrotron !

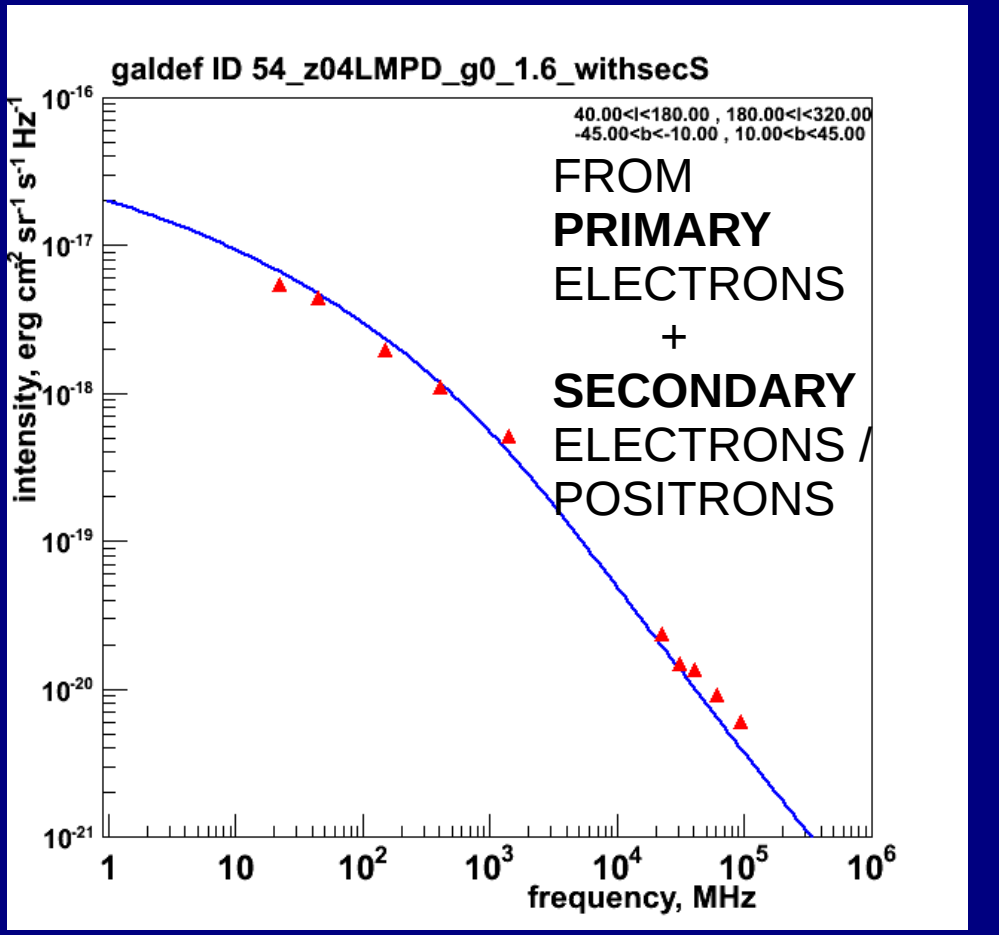

Cosmic-ray electrons

Synchrotron

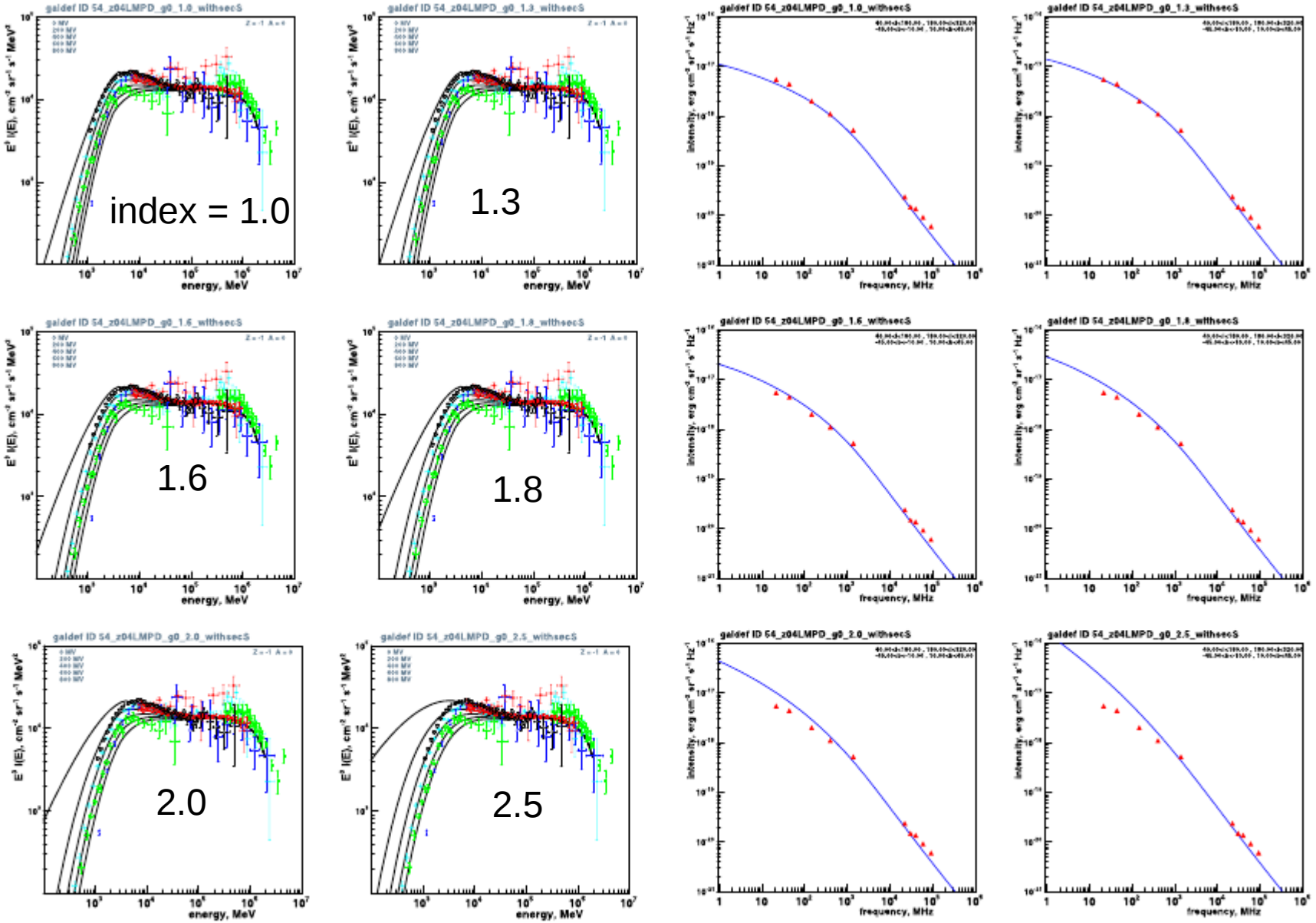

Fig. 4. Electron spectra for pure diffusion model, low-energy electron injection index 1.0, 1.3, 1.6, 1.8, 2.0, 2.5. Modulation Φ = 0, 200, 400, 600, 800 MV. Data as in Fig. 1.

Fig. 5. Synchrotron spectra for pure diffusion model with low-energy electron injection index (*left to right, top to bottom*) 1.0, 1.3, 1.6, 1.8, 2.0, 2.5. Including secondary leptons. Data as in Fig. 2.

Effect of electron injection spectral index

Strong, Orlando & Jaffe, A&A 534, A54 (2011)

Galactic Synchrotron Spectral Index

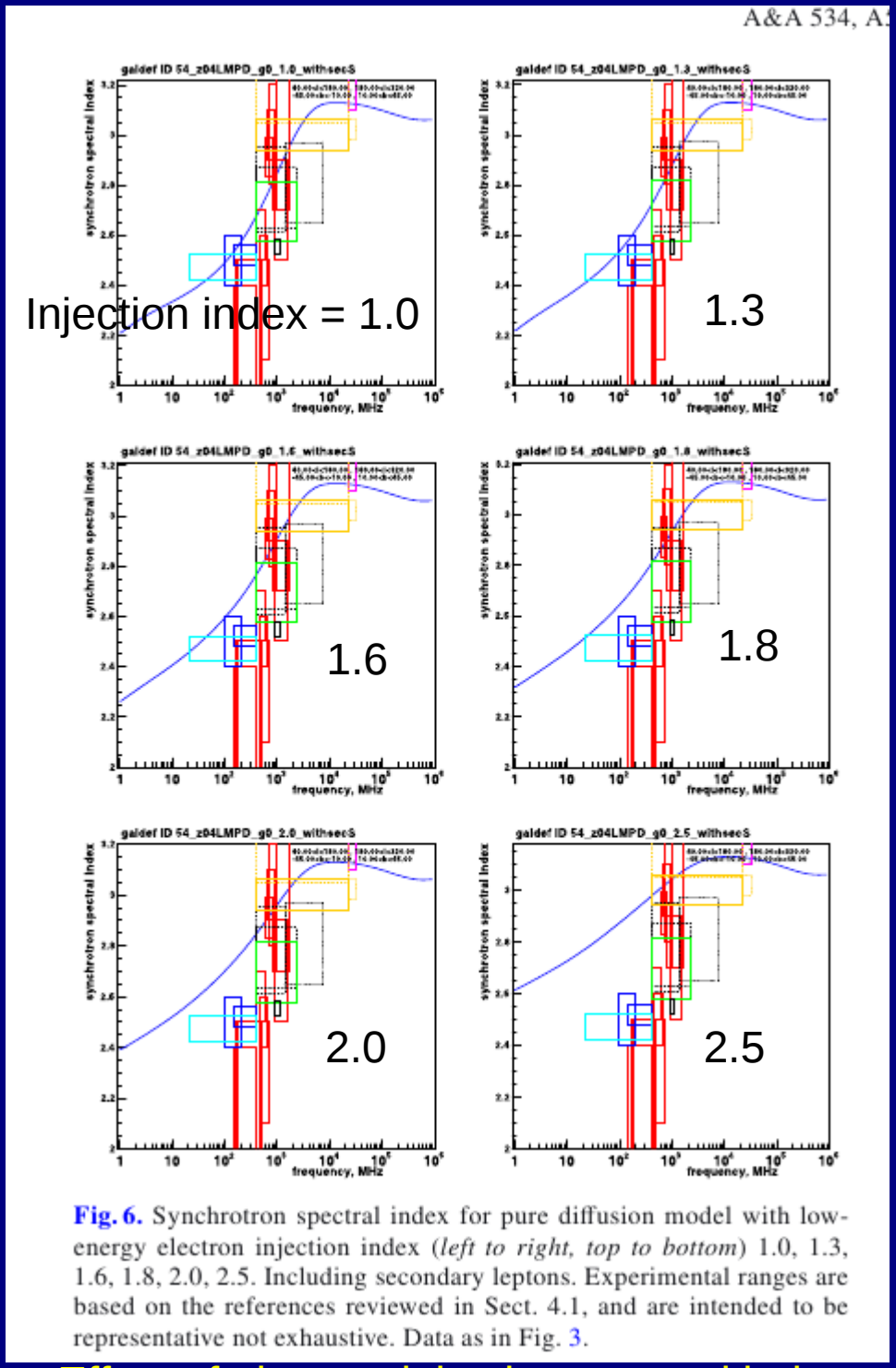

Fig. 6. Synchrotron spectral index for pure diffusion model with low-energy electron injection index (*left to right, top to bottom*) 1.0, 1.3, 1.6, 1.8, 2.0, 2.5. Including secondary leptons. Experimental ranges are based on the references reviewed in Sect. 4.1, and are intended to be representative not exhaustive. Data as in Fig. 3.

Effect of electron injection spectral index

Strong, Orlando & Jaffe (2011)

Galactic Synchrotron Spectral Index

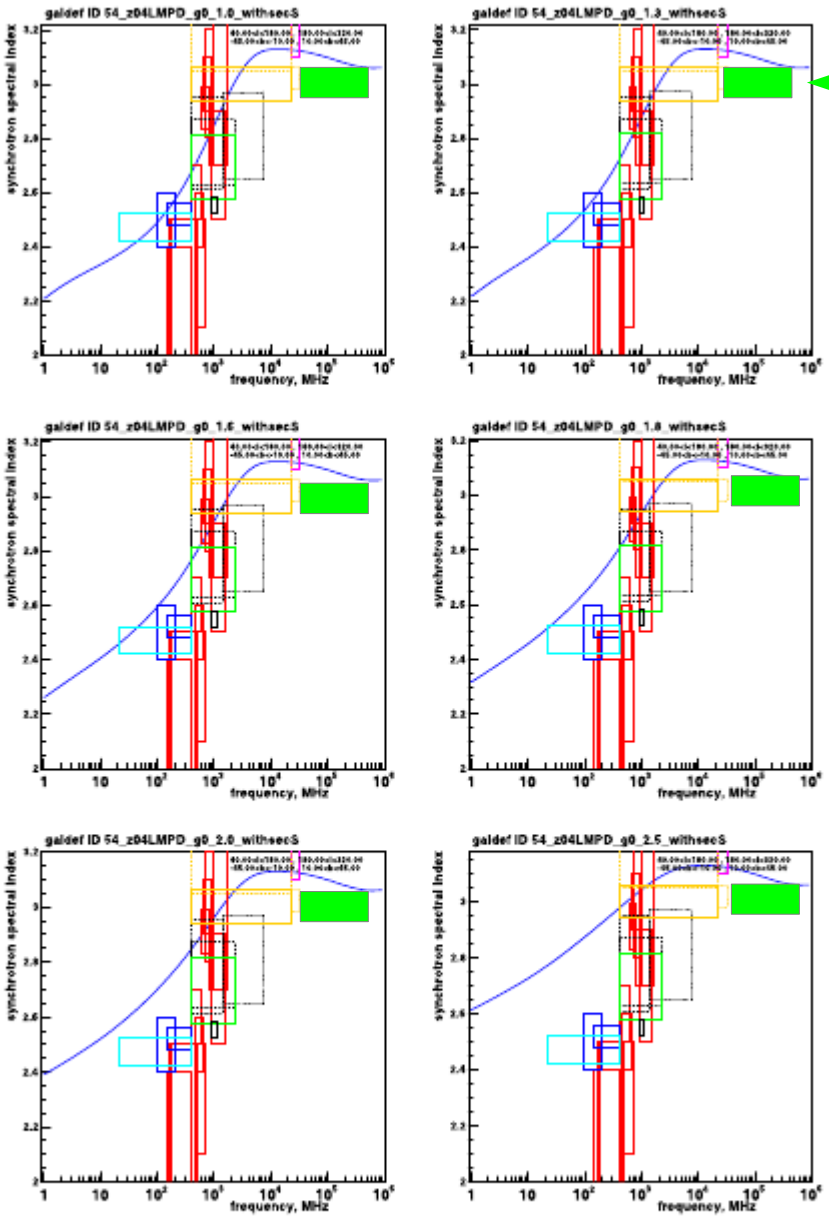

Planck

A&A 536, A21 (2011)

Fig. 6. Synchrotron spectral index for pure diffusion model with low-energy electron injection index (*left to right, top to bottom*) 1.0, 1.3, 1.6, 1.8, 2.0, 2.5. Including secondary leptons. Experimental ranges are based on the references reviewed in Sect. 4.1, and are intended to be representative not exhaustive. Data as in Fig. 3.

Model Synchrotron spectral index

408 MHz – 23 GHz

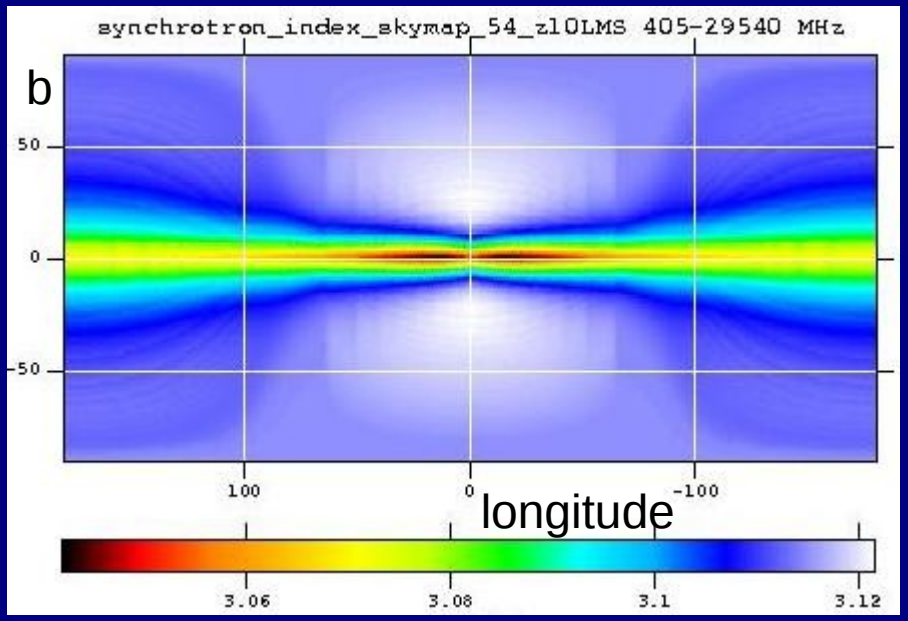

Model predicts small but systematic variations due to propagation effects.

Reality is of course much more complex (Loop I etc not modelled).

The model gives a minimum underlying variation from electron propagation.

Total B (local) =7.5 μG from this analysis

Using high latitudes only, avoiding Loop I etc

Orlando and Strong 2013 (A&A 436, 2127)

What is new :

Polarized synchrotron

Separates regular from random B

Now modelled in GALPROP

B-fields from literature, basic modifications to fit data.

Cosmic-ray electron distribution is a main input from gamma rays.

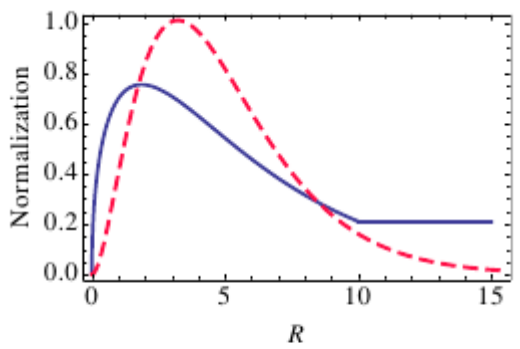

CR source distributions from Strong et al. (2010) (blue line) and pulsar-based Lorimer et al. (2006) (red dashed line). R is the Galactocentric radius in kpc.The distributions are normalized at R= 8.5 kpc.

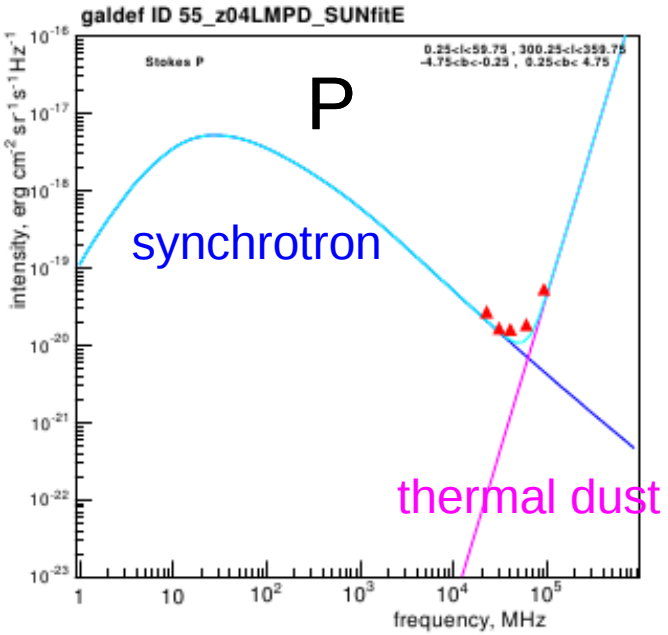

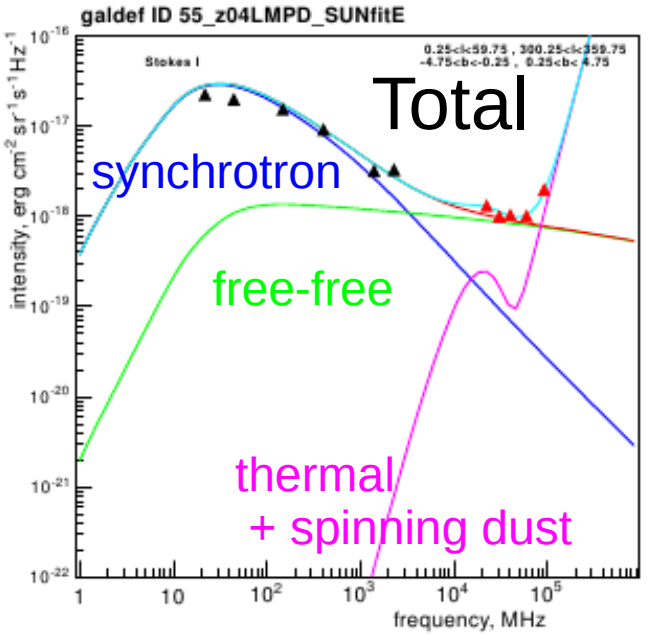

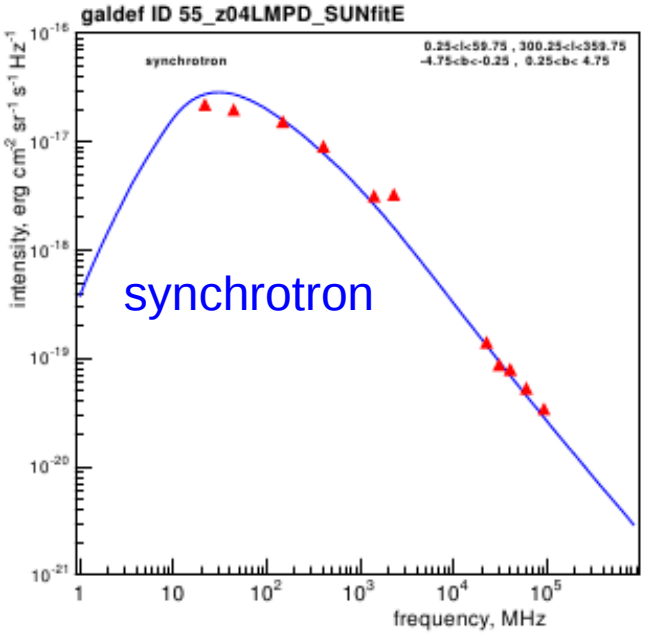

INNER GALAXY

HIGH LATITUDES

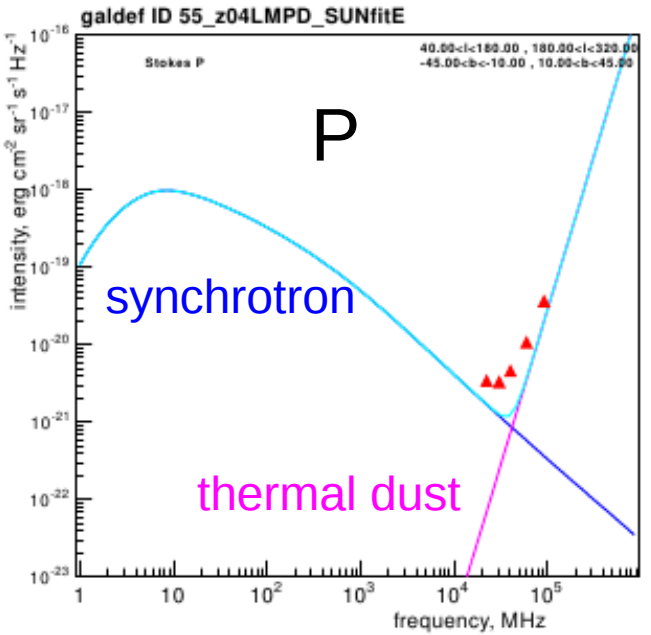

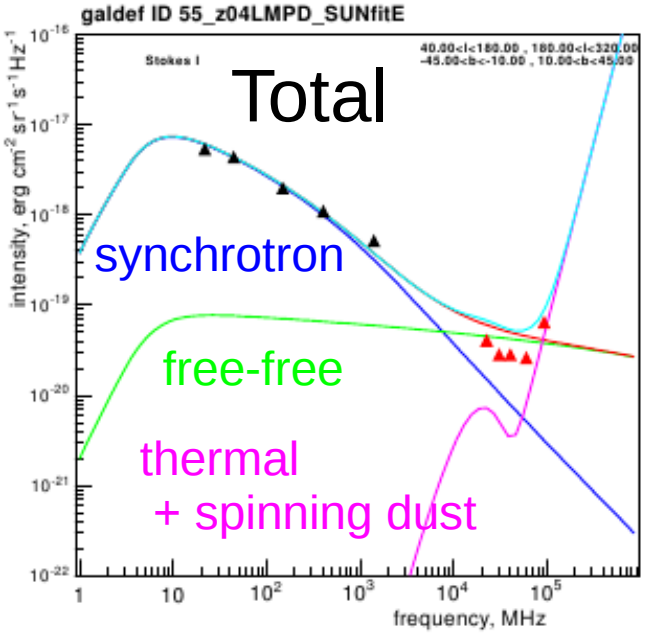

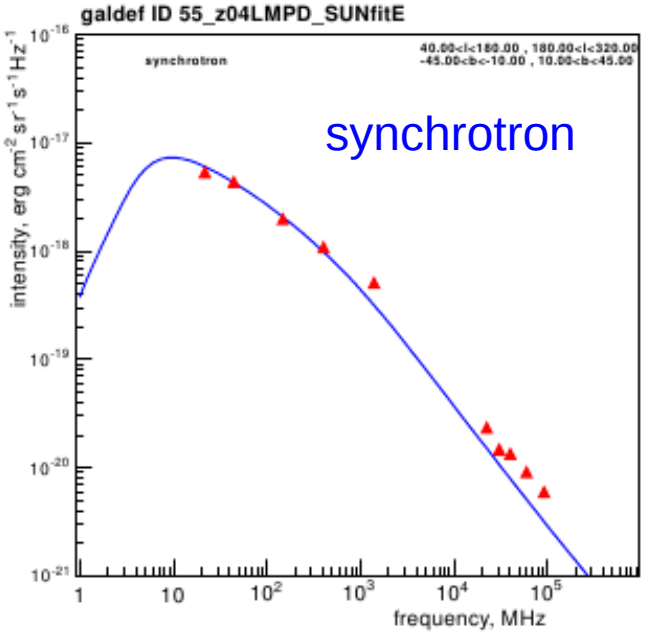

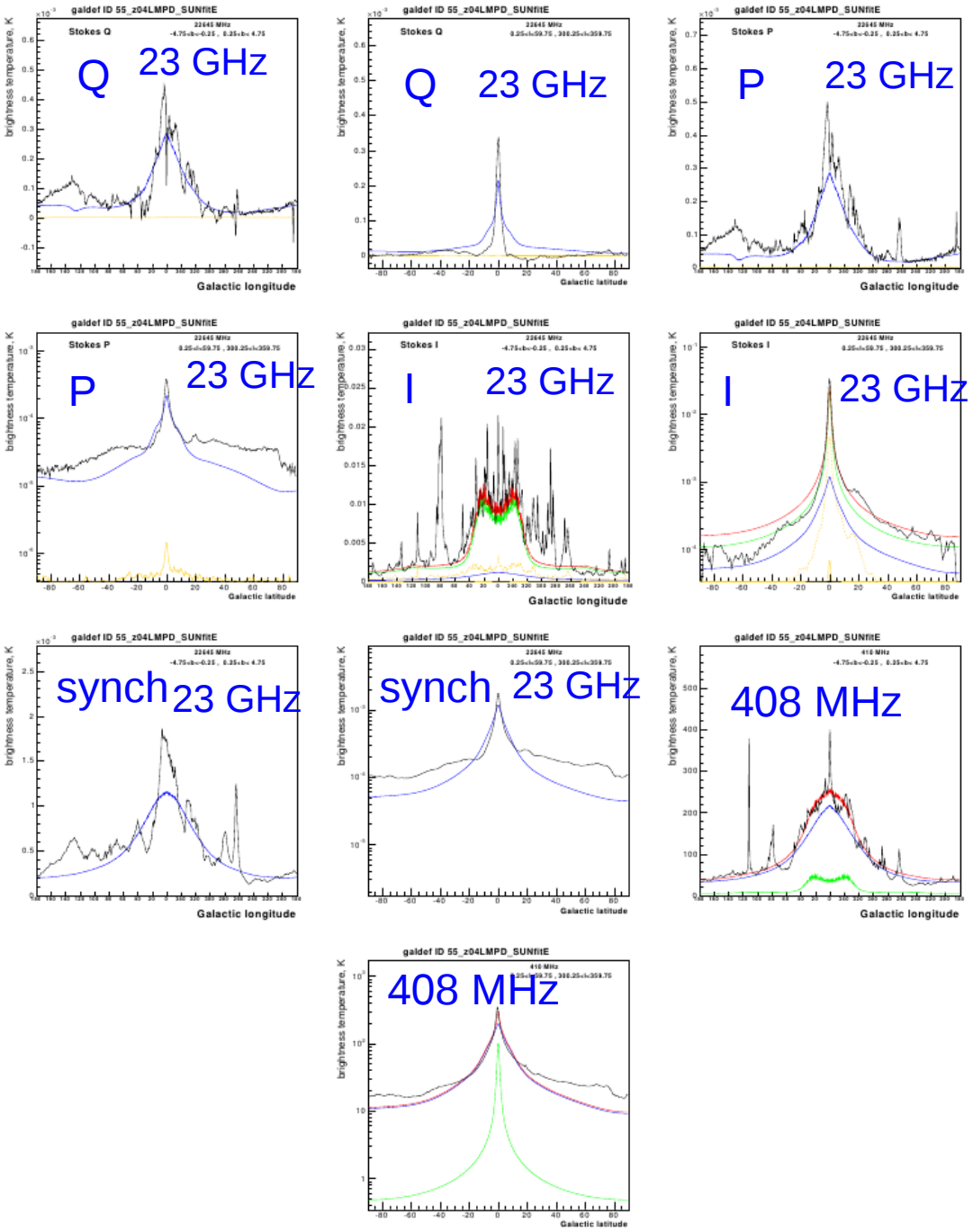

Data: WMAP

Data: Haslam

408 MHz

Using various B-field and cosmic-ray models

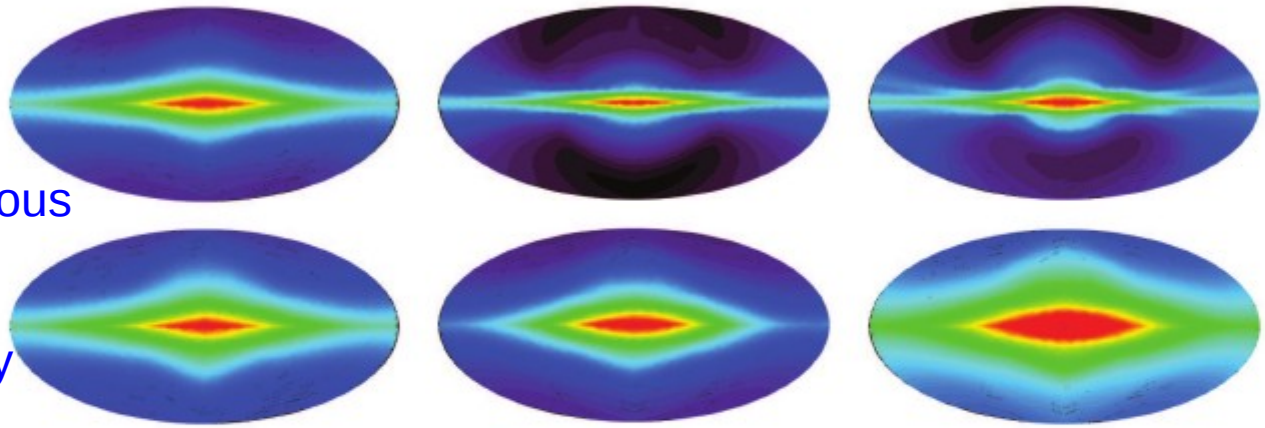

Haslam

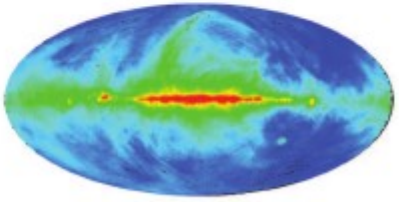

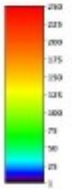

Regular B-field models from Sun etal, Pshirkov et al.
Scaling factor applied.

23 GHz
P

Using various
B-field
and
cosmic-ray
models

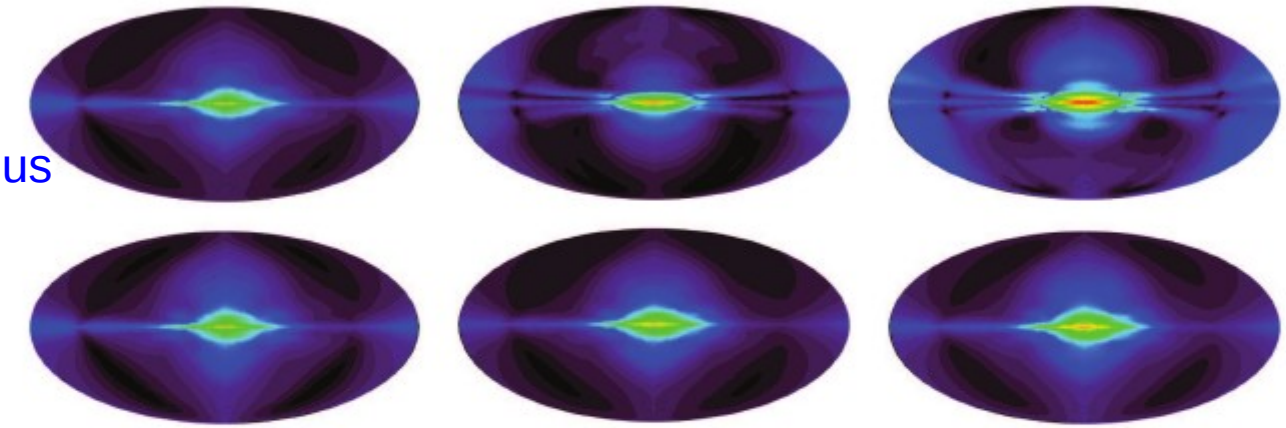

WMAP

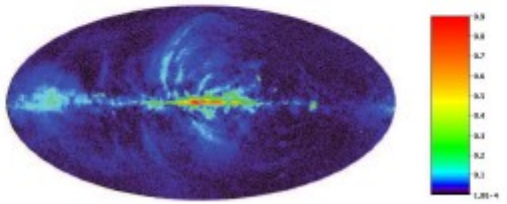

Regular B-field models from Sun et al, Pshirkov et al.
Scaling factor applied.

Illustrative model for 30 GHz Stokes P

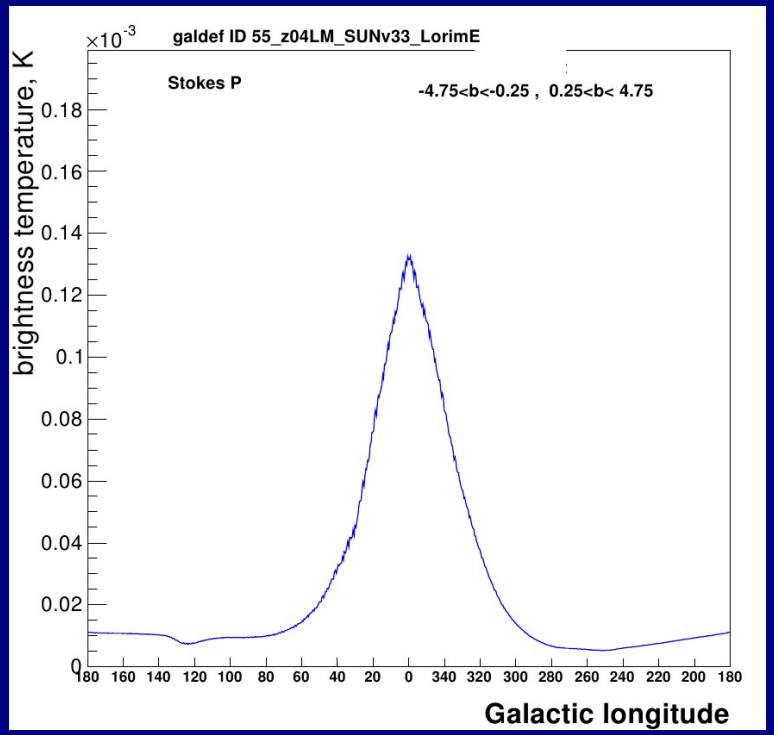

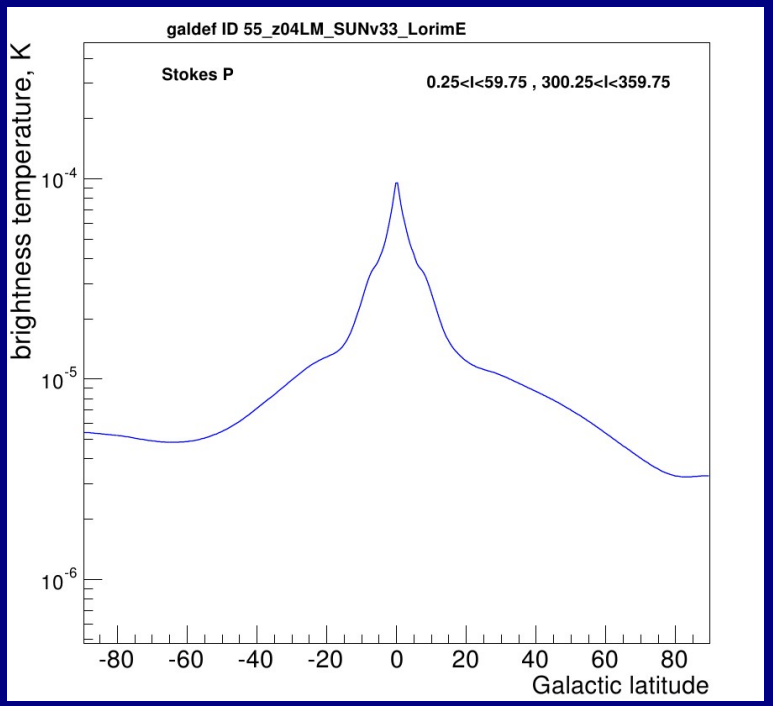

B_reg : Sun et al., scaled
B_rand : double exponential

Cosmic-ray electrons based on gamma rays and locally measured spectrum

Illustrative model for 30 GHz Stokes P

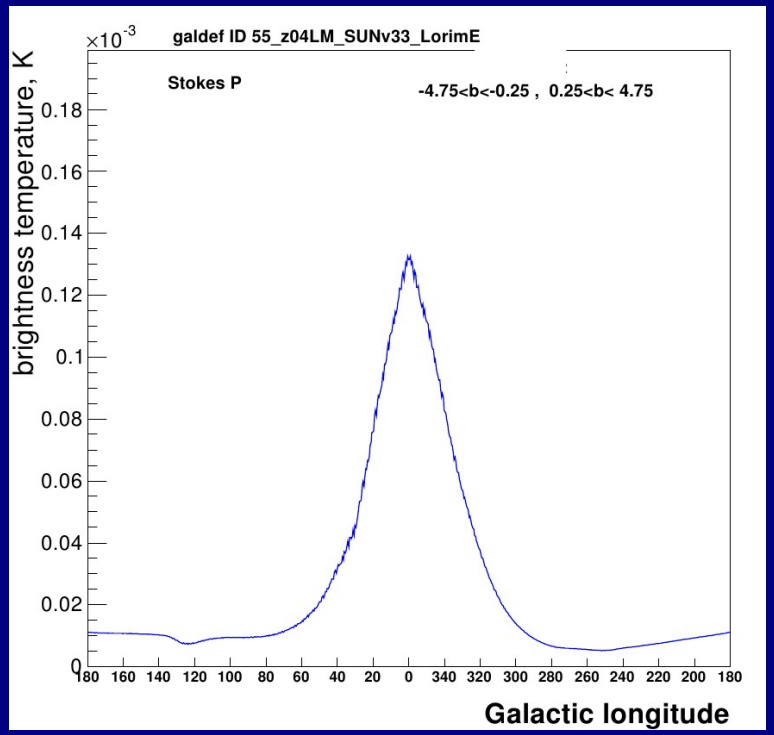

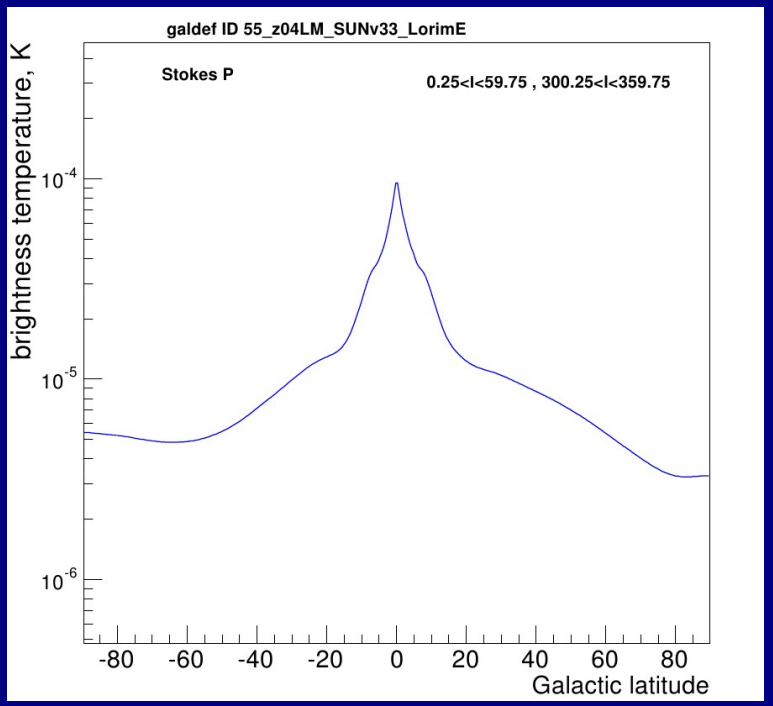

B_reg : Sun et al., scaled
B_rand : double exponential

Cosmic-ray electrons based on gamma rays and locally measured spectrum

Illustrative model for 30 GHz Stokes Q

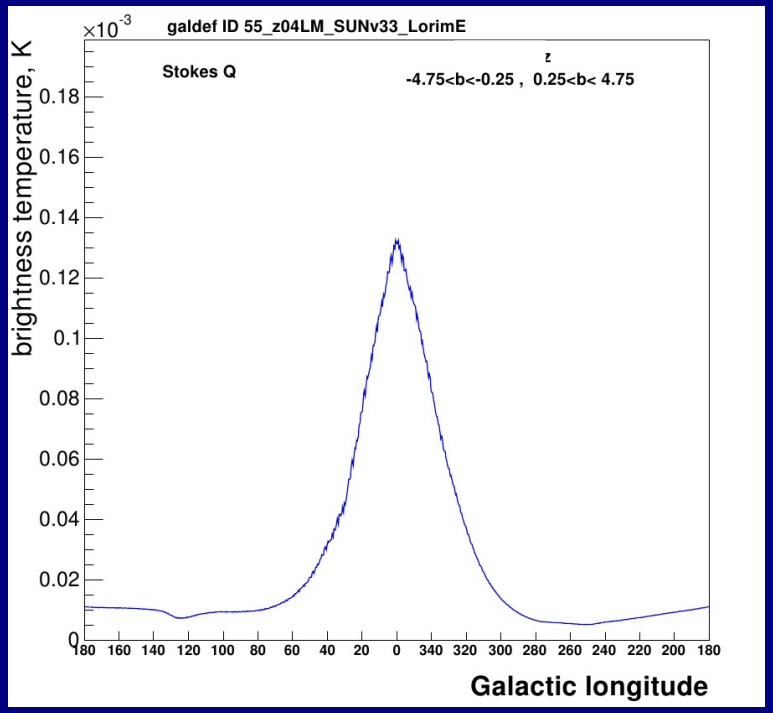

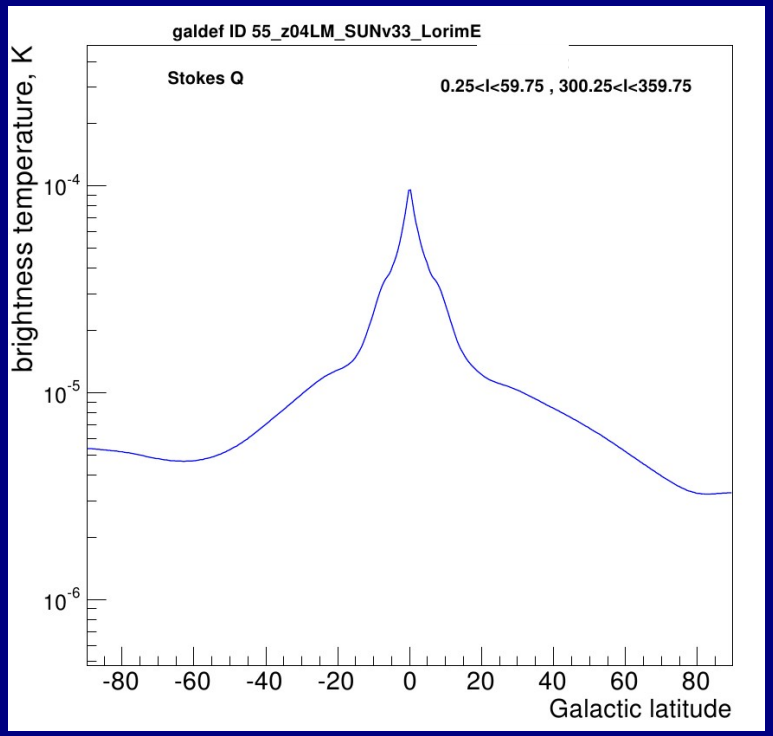

Illustrative model for 30 GHz Stokes I

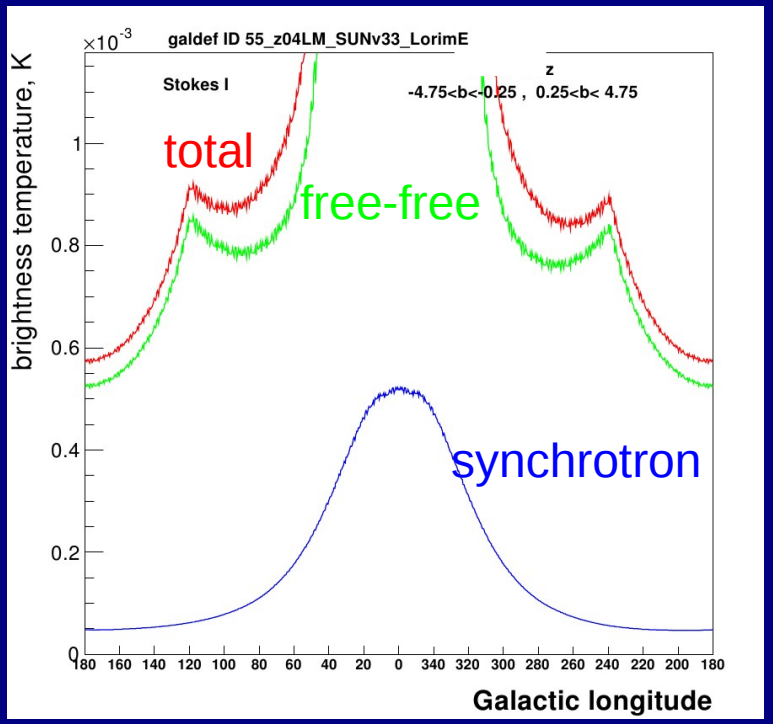

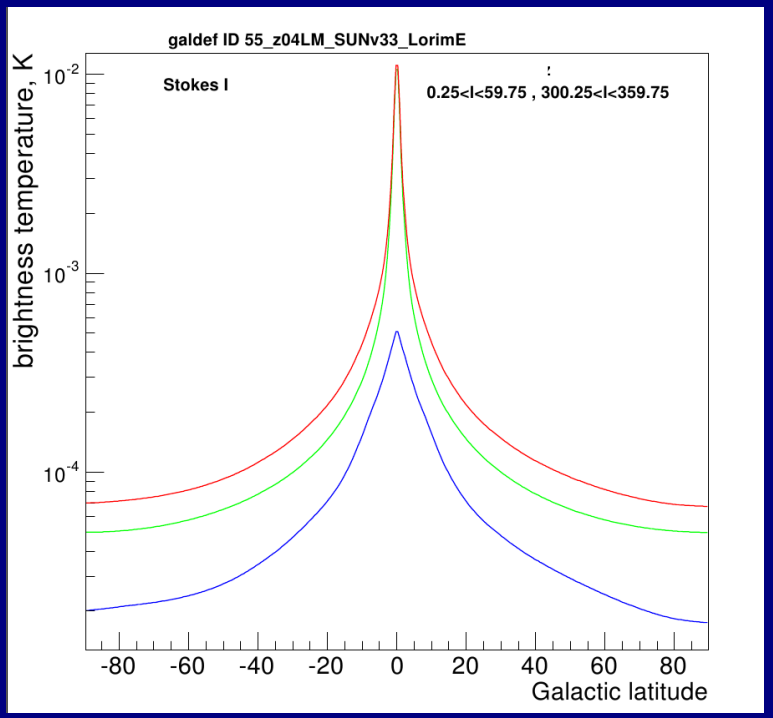

Free-free from NE2001, illustrative

B- field from Orlando & Strong 2013

Using :
  Fermi-LAT cosmic-ray electrons
  408 MHz
  23 GHz WMAP polarized

Local B-field:

Regular : 3-4 μG :
 factor 1.5-2 higher than original models of Sun, Pshirkov
 Attribute to anisotropic field which contributes to synchrotron
 but not to rotation measures.

Random : 6 μG

NOTES on use of GALPROP for synchrotron calculations

1. Computes synchrotron using full formulae and electron + positron spectra.
   no power law or p=-3 approximations (unlike Hammurabi).

2. 3D mode used for B-field and synchrotron.

3. Any B-field model can be incorporated, latest is Jansson & Farrar 2012.

4. Random and regular fields, Stokes Q, U, P, I for any frequencies.

5. No Faraday depolarization (unlike Hammurabi).

6. Only large-scale B, does not attempt Loops and other details.
   No pc-scale random structures (unlike Hammurabi).

7. Electron and positron spectra based on cosmic-ray propagation and locally measured spectra, and synchrotron data, also gamma ray constraints.

8. Updated in public domain, http://sourceforge.net/projects/galprop
   (>500 downloads since start in October 2013).

Positrons: excess above secondary production, probably pulsars.
Need to account for in synchrotron! e.g. for spectral variations measured by Planck and accurate future measurements.
Not yet done.

Synchrotron from molecular clouds

Gamma rays from the heliosphere

Lecture 1 : Basic ideas and relation to astrophysics

Intro: first lecture just about the basics, the physics, second lecture about practical computations.

CR propagation only: *not* CR origin! Only up to 1 TeV, rest covered elsewhere.
Species, nuclei, leptons: standard pics
isotopes, source abundances, reaction chain from Ni down (and >Ni too)
cross-sections, total and partial, K-capture, actinides, radioactive isotopes
LB as basic paradigm
secondaries as probe of propagation because can compute production
secondaries from sources
synchrotron gammas gas tracers
Emissivities → protons
propagation equation, each effect
Reacceleration ala Drury
Anisotropy (not addressed, small up to 1 TeV)
Change to trajectory approach at 10^{15} eV
units momentum KE flux density
Multimessengers
Global galaxy, calorimetry
external galaxies, radio. recognition of halo.
LECR Voyager ionization chemistry (ARAA53) protoplanetary discs
CO destruction
CR becoming mainstream as people realize
MHD winds CR-driven dynamos

RELATE TO OTHER LECTURES:
John Wefel also covers some of these topics including historical perspective .